Analysis of Erythropoietin for Anti-Doping Purposes with a Focus on Hyphenated Techniques

Williams, Samuel Thomas

Awarding institution:
King's College London

Analysis of Erythropoietin for Anti-Doping Purposes with a Focus on Hyphenated Techniques

Sam Williams

Thesis submitted for the degree of Doctor of Philosophy

Supervised by

Professor David Cowan

Dr Mark Parkin

King's College London **2013**

Abstract

To improve detection of the misuse of erythropoietin (EPO) for performance enhancing purposes, this PhD examined ways to improve recovery and preanalysis concentration of EPO from urine. It also looked at ways to enhance the signal in liquid chromatography tandem mass spectrometry of the acidic glycopeptides from digested EPO, and at distinguishing between recombinant EPO and human urinary EPO based on differences in their glycosylation. Due to a shortage of supply of available analytical standards, model glycoproteins were frequently used in place of endogenous EPO.

Immunoextraction with magnetic beads effectively recovered EPO from urine which had been filtered to remove large proteins, but was unsuccessful from unfiltered urine, suggesting more research into the right choice of antibody was needed.

The specific and reversible binding of boronic acids to cis-diol groups found in the glycan groups of glycoproteins was investigated as a device for the selective binding of EPO. Attempts were made to functionalise mesoporous silica for use as a column packing material. Although there was evidence that at least one method of functionalisation was successful, the use of this silica to extract glycoproteins and glycopeptides was not.

Signal enhancement through the introduction of 'superchargers' into LC solvents was investigated. This was effective with small molecules, and also improved detection of sialylated glycopeptides. The results do not fit entirely with current models of how superchargers exert their effect, suggesting they are incomplete.

Finally, the cleavage, digestion and derivatisation of N-glycans to identify bisected and non-bisected structures as a way to discriminate between rEPO and huEPO was examined. Samples were analysed using LC-MS and CE-LIF, and although much of the work was carried out using a model glycoprotein, there is some evidence that the approach may be capable of discriminating between artificial and endogenous EPO at the levels found in anti-doping samples.

Table of Contents

Table of Figures

Table of Tables

Acknowledgements

Firstly, I would like to thank my supervisors, Prof David Cowan and Dr Mark Parkin for their invaluable assistance and advice over the course of my PhD studies. I have also been greatly helped by all the staff of the Drug Control Centre, in particular by Dr Christiaan Bartlett with much of the work on isoelectric focusing gels. I have been similarly aided by the staff of the Mass Spectrometry unit at King's College, especially Dr Anna Caldwell and Prof John Halket. I would also like to thank Prof Norman Smith, Dr Sukhi Bansal and Dr Vincenzo Abbate for listening when I had problems and providing extremely helpful suggestions on ways to move my work forward, and all the other PhD students I have shared offices, coffee and beers with over the past four years. I am also grateful to Dr Jim Thorn and Samuel Fox at Beckman Coulter for going above and beyond the call of duty in trying to help me get data when the thesis submission deadline was nearly upon me.

Special thanks has to go to my girlfriend, Emmeline. Without her love, support and cooking skills I doubt I would have made it to the end of my PhD.

Finally, I would like to thank my sponsors Waters. Their funding made this PhD possible, and their provision of equipment, supplies and advice, especially from Prof Robert Plumb and Paul Rainville, was essential for its success.

Chapter 1: Introduction

1.1 Erythropoietin – a brief history

Erythropoietin (EPO) is a glycoprotein hormone produced principally by the kidney (and in smaller amounts by the liver, spleen, brain, bone marrow and lungs) that regulates red-blood cell production, by binding to receptors on bone marrow cells and initiating an intracellular phosphorylation cascade which stimulates erythropoiesis. It also acts to protect red blood cells and other cell types from apoptosis (Elliott, Pham et al. 2008). Its existence was definitively shown in 1953 by Professor Allan Erslev, who demonstrated significant production of immature red blood cells in rabbits transfused with large amounts of plasma from anaemic rabbits (Erslev 1953).

Attempts to isolate the protein proved problematic. Discussing the isolation of the protein, Goldwasser and Kung wrote in 1968 that to obtain 10 mg of EPO, 3250 L of human urine would be required, or 'about 3 yr's daily collection from a single patient, or one month's collection from 36 patients, which does not seem to be an impossible goal' (Goldwasser and Kung 1968). In 1977, nine years later, they were finally successful in doing so (Miyake, Kung et al. 1977). Their isolation of EPO was carried out from the urine of aplastic anaemia patients, who produce excess amounts of the hormone. Nonetheless, 1500 L of urine was required, and the extraction process involved seven steps, including ion exchange chromatography, ethanol precipitation, gel filtration and adsorption chromatography using hydroxylapatite. The final product had an activity of 70,400 units/mg, and enabled the development of a method for cloning the gene for EPO.

In 1985, a method for the cloning of the human EPO gene and the expression of a cDNA clone in hybrid monkey cells to produce a synthetic product was published in Nature (Jacobs, Shoemaker et al. 1985); later that year a second paper was published (Lin, Suggs et al. 1985), demonstrating the cloning of the human EPO gene and its expression in Chinese hamster ovary (CHO) cells. This technique was patented by Amgen and used to produce their first commercial synthetic EPO product, Epogen, which received its first clinical trial in 1987 (Eschbach, Egrie et al. 1987). Since then, attempts to increase the efficacy of the drug have resulted in the production of other recombinant forms of the hormone including epoietin-beta, or betapoietin (also produced in Chinese hamster ovary cells) and Dynepo (produced in human cell cultures), as well as darbepoetin, commercially called Aranesp or NESP, a similar

erythropoeisis stimulating protein. More recently, since the expiration of the patent on recombinant EPO (rEPO), a number of biosimilar products have been produced in laboratories around the world (Schellekens 2009). Other products which act in a similar fashion include Hypoxia Inducible Factor (HIF) stabilisers, which act to increase endogenous EPO production; MIRCERA (known commonly as CERA), a pegylated beta EPO; and EPO mimetic peptides, such as Hematide, which act in the same way as EPO although they are structurally unrelated.

1.2 EPO – regulation of production

The role of EPO is to maintain red blood cell levels within the normal physiological range, and to restore them after haemorrhage or disease. However, EPO production is regulated entirely by tissue oxygen levels. Low levels of oxygen cause the production of proteins called Hypoxia Inducible Transcription factors (HIFs), which induce the expression of the EPO gene. As a result, athletes can induce the production of greater numbers of red blood cells by training at altitude, where oxygen levels are lower, and an increase in EPO levels has been demonstrated in people moved from sea level to higher altitudes (Faura, Ramos et al. 1969; Abbrecht and Littell 1972). These HIFs are hydroxylated in the presence of oxygen, causing them to be digested by proteosomes, and at the same time reducing their DNA binding capacity, stopping gene expression (Bruegge, Jelkmann et al. 2007). (See Figure 1.1). The levels of EPO found in serum can vary quite widely. One study by Jelkmann and Wiedemann found that the mean EPO level was 6 U/L, but the range was 2 to 25 U/L in 19 serum samples (Jelkmann and Wiedemann 1990).

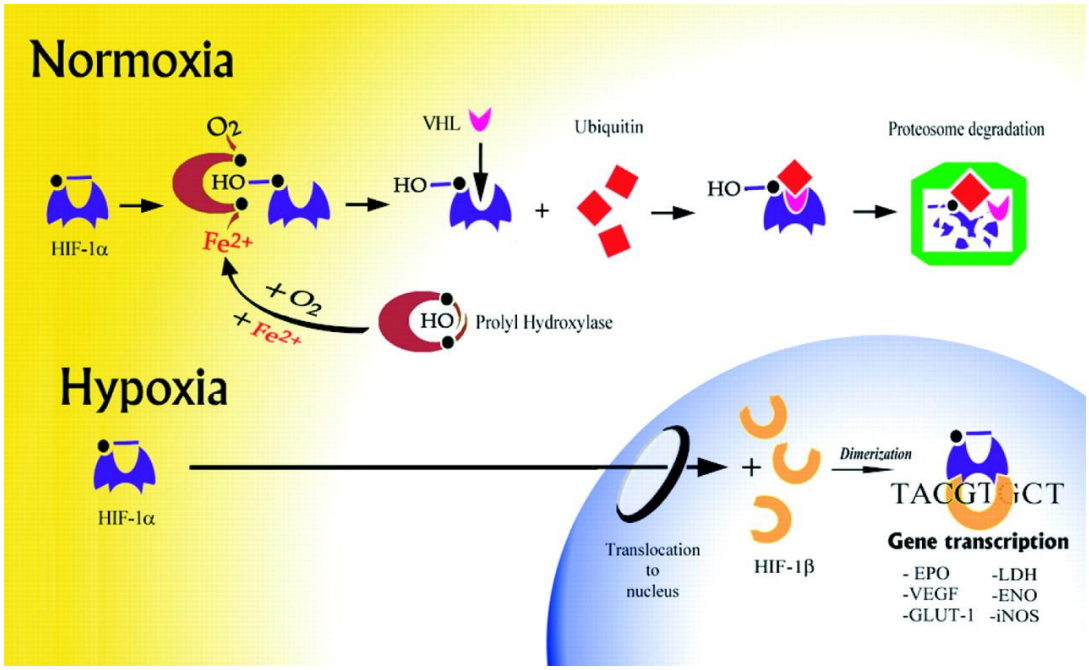

Figure 1.1: Biochemical pathway resulting in EPO production in hypoxic conditions (LaManna, Chavez et al. 2004) (reproduced with permission)

1.3 EPO – binding to receptors and signal transduction

EPO is secreted into the blood stream, and binds to membrane-bound erythropoietin receptors**,** EPO-R, on its target cells (Chang, Sikkema et al. 1974). These are mainly found on the burst-forming units-erythroid (BFU-E) and the colony-forming units-erythroid (CFU-E) cells of the bone marrow (Wu, Liu et al. 1995). The EPO-R is a glycoprotein consisting of 484 amino acids with one N-glycosylation site. This, along with phosphorylation, increases the size of the receptor from 52.6 kDa to about 60 kDa. Two receptor molecules form a homodimer, binding one EPO molecule (Livnah, Stura et al. 1999). Binding induces a conformational change in the two receptor molecules, resulting in tighter binding between them. This in turn activates two Janus kinases (JAK2) on the cytoplasmic region of the receptor, initiating the phosphorylation cascade (Zhao, Dong et al. 2009). The effect of EPO is terminated by the action of the haematopoietic cell phosphatase (HCP) which catalyses JAK2 de-phosphorylation (Klingmuller, Lorenz et al. 1995; Yi, Zhang et al. 1995) On de-phosphorylation, the EPO/EPO-R complex is internalised and degraded by proteosomes and lysosomes (Verdier, Walrafen et al. 2000).

1.4 Pharmacokinetics of EPO

Following intravenous (IV) administration, EPO shows bi-exponential elimination kinetics, with a rapid fall in the first hour, followed by a prolonged and slower loss afterwards. The initial fall is thought to be due to uptake and degradation by cells with EPO-R receptors, and this fits with evidence that the bimodal nature of the elimination is more prominent when small amounts are administered and can be absent when large amounts are given. This suggests that the mechanism of initial elimination is susceptible to saturation (Cheung, Goon et al. 1998; MacDougall, Gray et al. 1999) (see Figure 1.2).

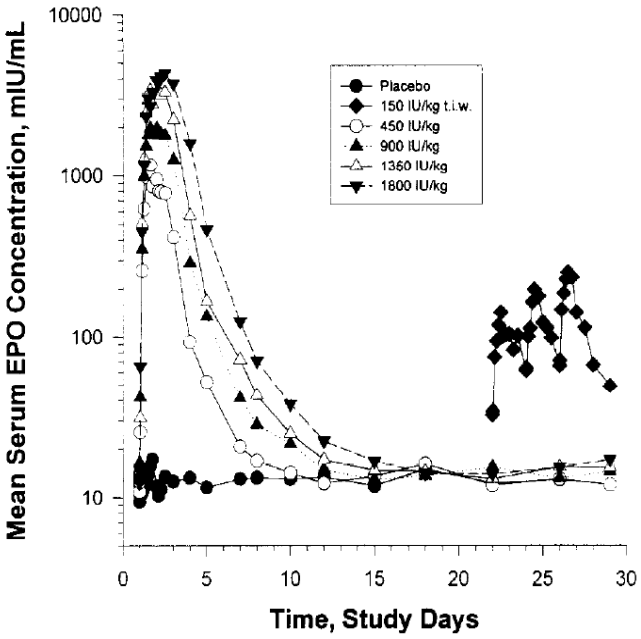

Figure 1.2: Mean serum erythropoietin (EPO) concentration-time profiles (uncorrected for baseline erythropoietin levels) for subjects receiving subcutaneous single- or multiple-dose regimens. From Cheung, Goon et al. 1998; reprinted with permission

The half life of epoetin-alpha and beta is 6-9 hours after IV administration. That of darbepoietin is three to four times longer (25 h) (MacDougall, Gray et al. 1999), while that of CERA is longer still (130-140 h) (Macdougall, Robson et al. 2006). The longer life span of these newer epoetins means that dosing strategies can include fewer administrations, with weekly or even monthly injections. Darbepoietin has also been shown to be more potent in rats and mice, with a single dose of

darbepoietin given to mice once weekly seen to be as effective as the same dose of rEPO given three times a week (Egrie, Dwyer et al. 2003). This effect has not been seen in renal failure patients, however (Jacobs, Frei et al. 2005), where no difference in the effectiveness of darbepoietin compared to epoetin alpha or beta was detected.

1.5 EPO structure

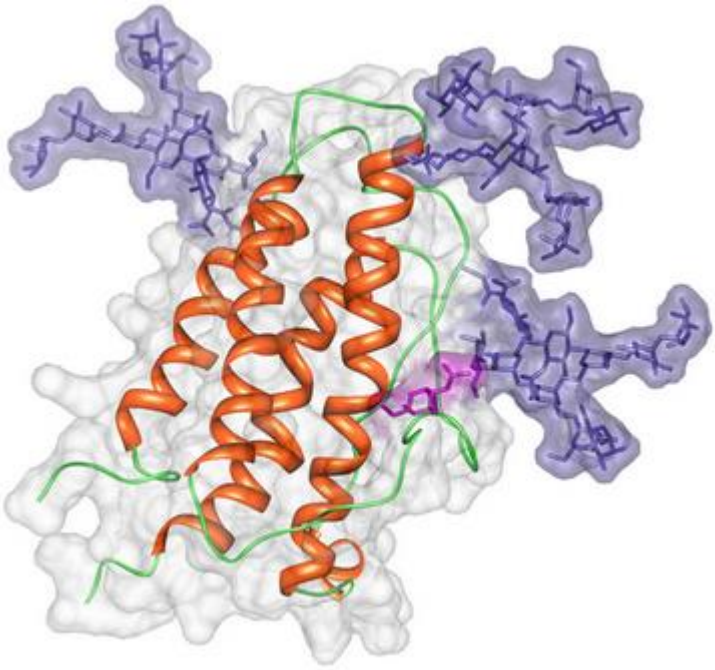

Figure 1.3: Predicted structure of glycosylated human Erythropoietin. Erythropoietin exists as a mixture of glycosylated variants (glycoforms), and glycosylation is known to modulate its biological function. The three high-mannose N-linked oligosaccharides (Man_9 GlcNAc_2) are shown in purple, the single O-linked glycan (alpha-GalNAc) is shown in pink. The structure in the image represents a single glycoform that is the origin from which all others are generated. Figure made by the Woods group using Chimera. Reprinted with permission from http://glycam.ccrc.uga.edu/ccrc/

EPO is a class I cytokine glycoprotein which in its native state consists of four α-helical bundles, creating a hydrophobic core (Figure 1.3). With the exception of darbepoietin, all erythropoietins share the same amino acid sequence (Figure 1.4), with 165 amino acids including three N-glycosylated asparagines (Asn_{24}, Asn_{38} and Asn_{83}) and one O-glycosylated serine (Ser_{126}). The attached carbohydrates are responsible for about 40% of the approximate 30.4 kDa mass of EPO. Darbepoietin

contains an extra two N-linked glycosylation sites (Asn_{30} and Asn_{88}), which appears to extend the drug's serum half-life and *in vivo* biological activity (Egrie and Browne 2001), as mentioned above. They also increase the molecular mass, to about 38.5 kDa. Glycan groups consist of bi, tri and tetra-antennary structures with differing degrees of sialylation and N-acetyl lactosamine repeats. Glycosylation of peptides and proteins, unlike amino acid sequence, is not coded for by DNA and is dependent on cellular conditions, including temperature, pH and physiological levels of biochemicals. As a result, it is not surprising that quantitative and qualitative differences appear to exist in the glycosylation of the different EPO forms, with a greater variation in those found in EPO alpha and beta compared with Dynepo (Llop, Gutierrez-Gallego et al. 2008). There is also evidence that sialic acid variants not produced endogenously in humans (due to a lack of the necessary enzyme) can be detected in preparations of synthetic EPO (Groleau, Desharnais et al. 2008). These differences, and the specific rEPOs in which they are found, will be discussed in greater detail below.

1 APPRLICDSR VLERYLLEAK EAENITTGCA EHCSLNENIT
41 VPDTKVNFYA WKRMEVGQQA VEVWQGLALL SEAVLRGQAL
81 LVNSSQPWEP LQLHVDKAVS GLRSLTTLLR ALGAQKEAIS
121 PPDAASAAPL RTITADTFRK LFRVYSNFLR GKLKLYTGEA
161 CRTGD
Glycosylation sites: ^{24}N, ^{38}N, ^{83}N, and ^{126}S. Disulphide bonds: ^{7}C - ^{161}C, ^{29}C - ^{33}C

Figure 1.4: Amino acid sequence of human EPO; active form cleaved from the 192 amino acid precursor, the full sequence of which is available at http://www.uniprot.org/uniprot/B7ZKK5

The peptide core of the hormone is responsible for its erythropoietic effects, while the presence of the glycan groups seems to be responsible for its in vivo lifespan. Rapid elimination of epoietins appears to be mediated by binding to receptors, which is inversely correlated with the extent of glycosylation (Darling, Kuchibhotla et al. 2002; Elliott, Egrie et al. 2004). This would provide an explanation for the increased half-life of darbepoietin compared to rEPO, as darbepoietin contains two extra glycosylation sites.

The presence of a large number of sialic acid residues also appears to be linked to the longevity of the hormone in the blood, as glycoproteins with exposed galactose residues are rapidly cleared from the blood by binding to asialoglycoprotein receptors on hepatocytes (Fukuda, Sasaki et al. 1989), while rEPO also shows greater binding affinity for EPO-R after desialylation (Takeuchi, Takasaki et al. 1990).

The peptide backbone of CERA is also the same as other epoetins; however, it is modified by reacting the N-terminal amino group or the Є-amino group of any lysine residue with methoxy polyethylene glycol butanoic acid, producing a pegylated form which has a molecular mass of about 60 kDa. As mentioned above, it has a much longer half life than other epoetins, up to 6 times longer than darbepoetin and 20 times longer than Epogen.

1.6 Clinical use of rEPO and potential side effects

Clinically, rEPO is most commonly used to treat patients suffering from anaemia caused by chronic kidney disease. It has also been used to treat anaemia in cancer sufferers caused by chemotherapy and radiotherapy. There is also evidence that erythropoietin could be beneficial in certain neurological disorders, including schizophrenia (Wustenberg, Begemann et al. 2011), depression (Miskowiak, Vinberg et al. 2010) and cerebral malaria (Casals-Pascual, Idro et al. 2008), although to date there have not been any full clinical trials.

Side effects of rEPO include increased blood viscosity, with concomitant increased vascular resistance and the development of hypertension (Raine 1988). Possible reasons for this include elevated red cell mass, neurohormonal system disturbances and direct effects on the vascular smooth muscle (Zhu and Perazella 2006). Long term use of rEPO can also result in pure red cell aplasia, due to the induction of antibodies against the EPO molecule. This in turn causes a virtual absence of erythroid precursors in the bone marrow, and a very low red blood cell count (Casadevall, Eckardt et al. 2005). This is a rare condition, but saw a dramatic increase after 1998. The development of the disease in patients with chronic renal failure receiving rEPO seems to have been associated with subcutaneous administration, and possible reasons could be the use of polysorbate 80 as a stabiliser

or the use of uncoated rubber stoppers on syringes. Subsequent changes to the production method have resulted in a fall again in the number of cases (Wish 2011).
Recent research has also suggested that the use of EPO to treat anaemia may impair disease control with certain cancers (Brian 2003; Henke, Laszig et al. 2003), can result in increased likelihood of venous thromboembolic events (Dicato and Plawny 2010) and that interaction of rEPO with EPO-R in breast tissue may antagonise the effects of chemotherapy (Groner and Hynes 2010).

1.7 Abuse of EPO in sports

Epoetins have been abused in sports because of their potential to improve athletic performance, especially in endurance sports. This was demonstrated in studies which showed improved exercise tolerance in anaemic dialysis patients given rEPO (Muirhead, Keown et al. 2011). The administration of rEPO to healthy human subjects also resulted in an increase in blood haemoglobin concentration and an increase in maximal aerobic power (VO_2max) from 4.52 to 4.88 l min^{-1}, which was the same as resulted from an infusion of the equivalent amount of red blood cells (Ekblom and Berglund 1991). A second study found that administration of rEPO to male athletes resulted in increased VO_2max, and greater time to exhaustion (Birkeland, Stray-Gundersen et al. 2000). These improvements would seem to be advantageous in sporting competitions, although actual athletic performance in terms of time trials was not investigated.
As well as erythropoietic effects, EPO has been shown to depress plasma volume, probably through a down regulation of the rennin–angiotensin–aldosterone axis (Lundby, Thomsen et al. 2007). The relative contribution of a decrease in plasma volume to an increase in arterial oxygen content was calculated to be between 37.9 and 53.9%, suggesting this seems to be as important as erythropoietic effects in increasing circulatory oxygenation.
The use of rEPO has other advantages over autologous blood transfusions (an alternative method also abused for boosting the oxygen carrying capacity of the blood), namely the absence of a need for blood removal, storage, transportation and re-infusion.

The extent to which rEPO is abused is not clear. It is a suspect in the deaths of 20 cyclists in 4 years, while in 1998 a team was ejected from the Tour de France for using the drug, and six other teams withdrew (Eichner 2007). There have been claims that its use is still widespread due to difficulties with testing, and in particular the short time frame for detection. rEPO is difficult to detect 3 days after use, and it has been claimed that if athletes follow a microdosing regime, the use of rEPO may be undetectable 12-18 hours after use, enabling even athletes facing daily testing potentially to escape being caught (Ashenden, Varlet-Marie et al. 2006). Floyd Landis, the 2006 Tour de France winner who was stripped of his title after he tested positive for elevated levels of testosterone, has since claimed that many other riders, including Lance Armstrong, were guilty of abusing EPO. Armstrong denied the claims, and has always tested negative in anti-doping tests, but was recently stripped of his seven Tour de France titles and banned for life from cycling by the U.S. Anti-Doping Agency (USADA).

As a result of both the potential for improved sporting performance and the health risks associated with its use, the International Olympic Committee placed rEPO on its list of banned drugs in 1990.

Recombinant human EPO has also been detected in sporting animals; specifically, it has been detected in urine samples from greyhounds (Bartlett, Clancy et al. 2006), while cases of racing horses testing positive for rEPO or darbepoietin have also been reported (NYDailyNews.com 2008)

1.8 Methods of detecting rEPO use: indirect methods

Initial attempts to counter the use of rEPO were carried out by examining athletes' haematocrits. In 1997, the International Union of Cycling introduced a regulation which banned any male athlete whose haematocrit was more than 50%, and any female athlete whose was more than 47%. However, they have always stated this was done on grounds of safety and that a failed result did not imply rEPO use; as a result, athletes were only banned from competition for two weeks after a failed test.

Attempts to find a serological marker for rEPO meant levels of reticulocytes and macrocytes (production of both of which are increased after rEPO administration) were considered, as were concentrations of soluble transferrin receptor, a protein involved in iron metabolism which influences the production of haemoglobin.

Suggestions that rEPO may have fibrinolytic actions led to proposals to test for its use in urine by the measurement of urine total degradation products. Markedly higher levels of these products were found in 13% of top-level athletes tested by a study; since out-of-competition athletes and a control group of hockey players did not demonstrate similar results, the authors concluded the top-level athletes had taken rEPO (Gareau, Brisson et al. 1995).

For the Olympic Games in Sydney in 2000, two methods were used to test for rEPO. One was an indirect method, based on changes in the haematological profile of blood. Specifically, it examined reticulocyte haematocrit, serum EPO, soluble transferrin receptor, haematocrit and per cent macrocytes. (Parisotto, Gore et al. 2000) Two models were developed, to test for current rEPO use ('ON-model') and previous usage ('OFF-model'). The ON-model was successful at identifying 94-100% of rEPO users during the final 2 weeks of the administration phase, and produced only one false positive from a possible 189. The OFF-model was applied during the wash-out phase and, during the period of 12-21 days after the last rEPO injection, it identified 67-72% of recent users with no false positives.

The indirect method can be further improved by comparing an athlete's haematological profile against their own past history, rather than against values derived from the general population. Studies have suggested that between-individual variation is the largest source of variation in pooled data (Malcovati, Pascutto et al. 2003). An approach has been developed which enables an athlete's baseline profile to be estimated from just one prior blood test, eliminating this variability without imposing undue logistical constraints (Sharpe, Ashenden et al. 2006). Another indirect method uses measurements of haematocrit value, reticulocyte count, soluble transferrin receptor content, and concentration of β-globin mRNA in a multiparametric formula, and was successful in detecting rEPO abuse in 57.5% of the samples examined (Magnani, Corsi et al. 2001).

These indirect methods are relatively successful in detecting rEPO abuse, and have the added advantage that they can also detect other forms of cheating to increase oxygen carrying capacity of the blood, including the use of other epoetins or agents which act in a similar way. The downside is that blood collection is logistically more difficult than urine collection, especially if multiple samples are needed over a period of time to develop a baseline for an individual athlete. It is also necessary to ensure correct pre-analytical procedures are followed, as it has also been

demonstrated that major plasma volume changes, especially those caused by dehydration due to exercise, can markedly affect the soluble transferrin receptor and the haemoglobin concentrations as well as the haematocrit level (Robinson, Saugy et al. 2003).

In 2010 WADA published a guideline (WADA 2010) for the implementation of longitudinal monitoring of athletes' haematological profiles. It says the following markers should be considered for the production of a profile: haematocrit, haemoglobin, red blood cells count, percentage of reticulocyte, reticulocytes count, mean corpuscular volume, mean corpuscular haemoglobin, mean corpuscular haemoglobin concentration and index of stimulation, which was generated by the OFF-model, and is a mathematical function of the haemoglobin and reticulocyte percentage. Samples which are flagged as abnormal with a probability of 99.9% are then considered by a panel of three experts, who will decide if a prohibited substance has been taken, or if further testing is mandated.

1.9 Methods of detecting rEPO use: direct methods

1.9.1 Isoelectric focusing/Immunoblotting

The other process used to test for rEPO was a test on urine, and it is the one which has since been adopted by WADA as its standard method. It depends on detecting differences in the migration of isoforms of EPO on an isoelectric focusing gel, which it is thought is related to the glycan structure of the glycopeptides (Nimtz, Wray et al. 1995; Kawasaki, Haishima et al. 2001). Protein is extracted from urine by repeated ultrafiltration, reducing the sample size from 20 ml to 20 µl. These samples are heated at 80°C for 3 minutes to denature urinary aspartic proteases, then cooled back to room temperature, and supplemented with Tween 80.

Samples are then applied to and separated on polyacrylamide slab gels containing ampholytes 2-4 and 4-6, with isoforms being separated according to their isoelectric point. A Western blot is used to transfer the isoforms to a nitrocellulose membrane. The membrane is incubated in a denaturing DTT buffer, then blocked with nonfat milk in phosphate buffered saline, before being blotted with an anti-EPO antibody (clone AE7A5, murine IgG2A). This is transferred to a separate membrane with a second blot under acidic semi-dry blotting conditions and this membrane blocked

again before being probed with a biotinylated anti-mouse antibody. This is then detected using a streptavidin linked chemiluminescent system (Lasne and de Ceaurriz 2000; Lasne, Martin et al. 2002).

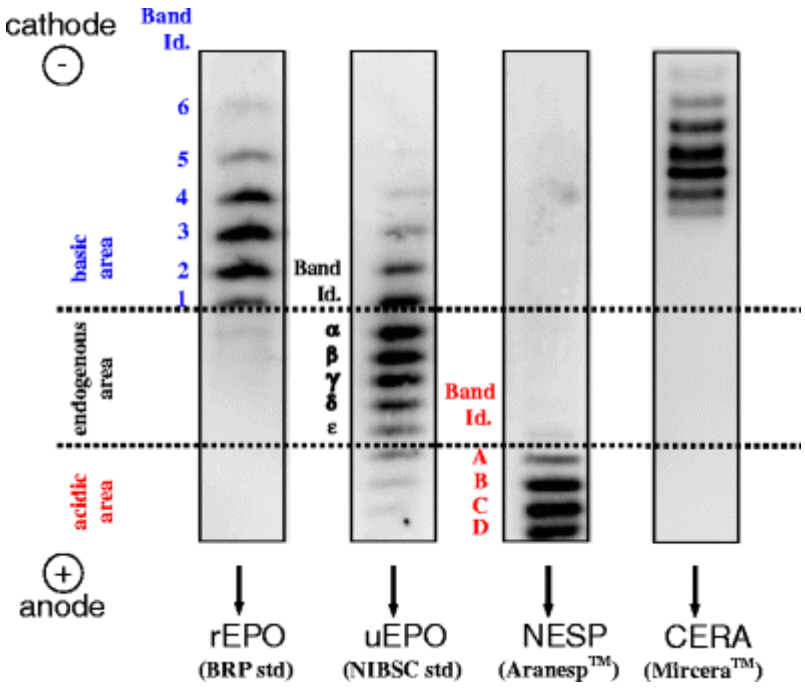

Figure 1.5: Isoelectric focusing/immunoblotting patterns of endogenous and artificial erythropoietins. Reprinted with permission (WADA 2009)

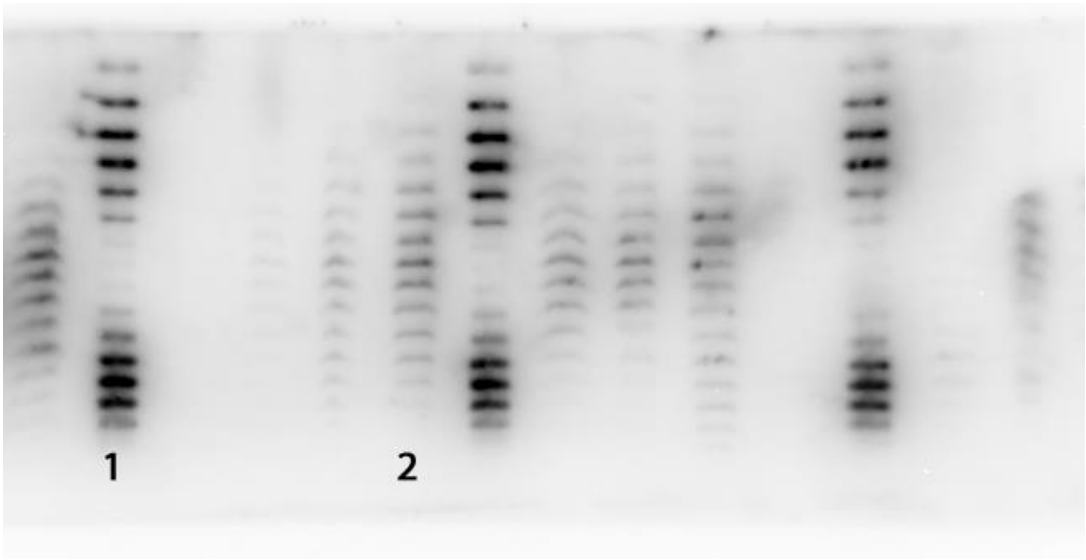

Figure 1.6: Typical IEF gel, showing 1: rEPO (top) and darbepoietin standard and 2. typical pattern of a negative urine sample. Other lanes contain actual anti-doping samples and standards

The isoforms of rEPO are more basic (pI 4.4-5.1) than those of endogenous human urinary EPO (huEPO – pI 3.7-4.7), while those of darbepoietin are more acidic (pI 3.7-4.0)(see Figures 1.5, 1.6) (Delanghe, Bollen et al. 2008).

1.9.2 Definition of a positive result

The WADA definition of a positive result has changed as new EPOs have been developed, with isoform patterns which differed from the original Epoetin-alpha and beta. The current identification criteria state that for a positive declaration of EPO-alpha or beta, in the basic region there must be at least 3 acceptable, consecutive bands assigned as "1", "2", and "3" in the corresponding reference preparation (see Figure 1.5); the 2 most intense bands measured by densitometry must be in the basic area, shall be consecutive and shall be bands "1" and "2" or "2" and "3"; and each of the two most intense bands in the basic area must be more intense (approximately twice or more) than any band in the endogenous area, as measured by densitometry (WADA 2009). For other epoetins, the sum of the intensity of all bands in the basic area must account for approximately 85% or more of the total intensity of the bands in the lane. For darbepoietin, in the acidic area there must be at least 3 acceptable, consecutive bands assigned as "B", "C" and "D" in the corresponding reference preparation, of which C or D must be most intense and must be approximately twice as intense as any endogenous band. For CERA, at least four bands must be present matching those of a reference sample. Band density measurement is carried out using a tailored piece of computer software, called GASepo. Alternative software packages are occasionally used, including AIDA 1D-Evaluation software from Fuji.

1.9.3 Problems with isoelectric focusing/double immunoblotting method

These processes are time consuming, requiring several incubations and blots of membranes, provide a subjective result, and as mentioned above are only effective within a short period of time after administration, potentially as little as 12-18 hours after injection. The requirement to compare band intensities in the different regions of the gel also mean that athletes abusing epoetins who naturally produce more endogenous EPO, or whose EPO production has been stimulated by hypoxia due to

altitude training or strenuous activity, would be more likely to produce a false negative result. This has prompted calls for the intensity requirement, at least in the case of samples positive for darbepoietin, to be scrapped (Lamon, Robinson et al. 2007).

Probably the most significant claims made against the standard method are related to the specificity of the monoclonal antibody used, antibody AE7A5. Khan et al. demonstrated that the antibody could react with other proteins in the pI range 3-5, which they identified as Tamm Horsfall glycoprotein, alpha-antichymotrypsin, alpha-2-thiol proteinase inhibitor and alpha-2-HS glycoprotein (Khan, Grinyer et al. 2005). However, in response it was argued that this cross-reactivity was a result of a different extraction process (precipitation using acetonitrile) which denatures proteins and exposes buried domains, which then bind to the antibody. Under the standard extraction conditions, these domains are not available, and so non-specific binding does not occur (Rabin, Lasne et al. 2006).

Non-specific binding of AE7A5 is also seen with several bacterial proteins, including those from *Escherichia coli*, which is found in human urine and on human skin in the uro–ano–genital region. Furthermore, it reacts with intracellular proteins, which could be released into the urine following urothelial damage. In fact, the generation of the antibody used an antigen which contains an amino acid sequence that occurs in more than 500 human and almost 185 *E.coli* proteins (Franke and Heid 2006).

In 2008, the protein responsible for commonly seen non-EPO bands on gels was identified as zinc-alpha-2-glycoprotein (Reichel 2008). This is abundant in urine, but binding was highly concentration dependent, and so extra bands were only seen in urine samples rich in the protein. Further, they were still outside the interpretative window of the gel, and so should not interfere with results.

It has also been shown that human serum EPO contains isoforms with pIs in the same range as rEPO (Skibeli, Nissen-Lie et al. 2001), prompting suggestions that bleeding into the urine could cause a false positive result. However, by adding an additional immunopurification step using another monoclonal anti human-EPO antibody (clone 9C21D11), a comparison of urine and serum samples was possible using isoelectric focusing (Lasne, Martin et al. 2007). It showed that although urinary profiles are more acidic than those from serum, serum EPO profiles (and, by extension, urinary profiles contaminated with blood) can still be distinguished from

those of rEPO. It also showed that the addition of a further immunopurification step did not affect any bands within the relevant pI window, but only removed proteins found outside it; this demonstrated again the sufficient specificity of the AE7A5 antibody.

1.9.4 Effort urines

One possible cause of false positives with the direct test is post-exercise proteinuria. This has been shown to follow intense (rather than prolonged) exercise, and is of mixed glomerular-tubular type. It appears to be due to increased glomerular permeability, as well as reduced tubular reabsorption of proteins (Poortmans 1985), and it has been reported that it can lead to false positive detection of epoetin-beta in urine samples (Beullens, Delanghe et al. 2006). This has been disputed by Lasne with claims the quality of images obtained was too poor to allow proper interpretation, and counter claims that under the (then) current WADA guidelines, the athlete concerned would have wrongly tested positive (Lasne, Beullens et al. 2006).

A study carried out in 2009 attempted to determine what was responsible for these 'effort profiles' (Lamon, Martin et al. 2009). Seven top cyclists performed periods of intense activity, separated by periods of active recovery. Urine samples were collected at the start of the day, at the start of exercise, half way through and immediately after. Blood samples were also taken, before and after exercise. In all subjects, a clear shift towards more basic pI was observed in urine profiles, although blood profiles remained unchanged (Figure 1.7). Total protein and EPO levels in urine rose 8.5 and 10-fold, while the greatest rise was in retinol-binding protein (RBP), which rose more than 300 times by the end of the exercise. Since the serum profile of EPO does not change, this suggested that effort urine profiles are indeed attributable to changes in kidney permeability or reuptake. The study also noted that despite the shift in patterns, none of the effort urines would have produced a positive result under WADA guidelines, and proposed that RBP levels could be used as a marker in cases where there is doubt.

1.9.5 Active urines

Some urine samples produce profiles with unusual patterns of banding, which appear to be shifted towards the basic region of the gel but which are still noticeably different from those produced by epoetin-alpha or beta. These are thought to be due to bacterial contamination of samples. Lasne reported that the occurrence of shifted profiles was much greater in samples in which bacterial proliferation had occurred (Lasne, 2009). Digestion of human urinary EPO (huEPO), rEPO and darbepoietin with sialidases and sulfatases produced IEF profiles similar to those seen in active urines (Belalcazar, Gutiérrez Gallego et al. 2006). Interestingly, whereas digestion of rEPO with sialidases resulted in proteins which migrated off the end of the gel, digestion of huEPO did not, suggesting that huEPO carries acidic groups other than the sialic acids. Freezing samples directly after collection has been recommended (Lasne 2009), as has the addition of sodium azide as a preservative (Belalcazar, Pascual et al 2005). The procedure for declaring a positive result has also been adjusted, to enable the possibility of active urines to be eliminated. A stability test has been introduced, whereby a sample of the urine is mixed with Complete and Peptstatin A protease inhibitors, adjusted to pH 5.5 using acetate buffer and then incubated overnight with rEPO and NESP. An active urine will result in the bands found in this sample shifting relative to a preparation of rEPO and NESP run simultaneously. (WADA 2009).

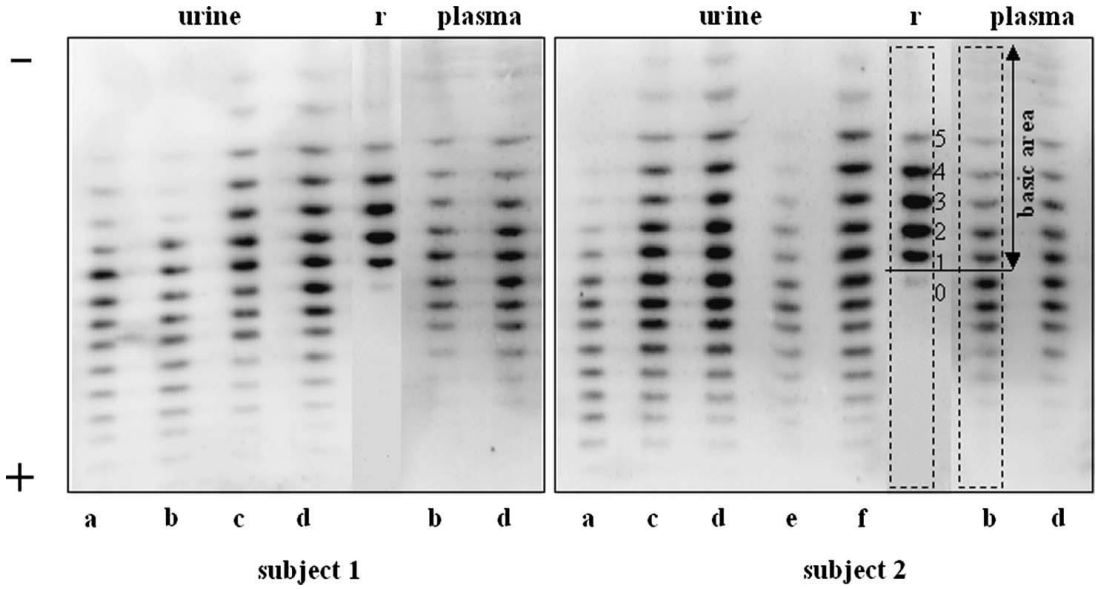

Figure 1.7: IEF patterns of urine and serum EPO from 2 subjects participating in an intense exercise protocol: first morning sample (a), immediately before the warm-up training (b), middle (c), and end of exercise (d) and 3 hours after the end of the morning session (e) and end of the afternoon session (f). Lane r corresponds to BRP. There is an evident shift of the bands toward the cathode induced by exercise. Reprinted with permission from Lamon, Martin et al. 2009

1.9.6 SDS-PAGE

A demonstrable difference exists between huEPO and rEPO, darbepoietin and CERA in terms of molecular mass. This has been exploited to produce a method to distinguish between them using SDS-PAGE. Sodium dodecyl sulfate denatures proteins and wraps around the peptide backbone, in a constant weight ratio of 1.4 g SDS/g of polypeptide. In doing so, it makes negligible the effects of the charged groups on the peptide itself. Thus, when exposed to an electric field, proteins migrate through a polyacrylamide gel at a rate relative only to their molecular size, with smaller proteins migrating faster than large ones. Typical apparent molecular masses for epoetins obtained by SDS-PAGE are listed in Table 1.1. Visualisation of bands follows the same procedure as for IEF and double immunoblotting, above.

Table 1.1: Molecular weights of endogenous and artificial EPOs, as determined by SDS-PAGE (Reichel, Kulovics et al. 2009)

Erythropoietin	Molecular weight (KDa)
Human urinary EPO	34
Erypo	36.9
NeoRecormon	36.6
Dynepo	36.2
Darbepoietin	44.2
MIRCERA	70.2

Because of the various isoforms of EPO, the bands produced by SDS-PAGE are relatively broad. However, this is not true of Dynepo, which produces a narrow band, presumably because of the smaller range of glycosylations found (Llop, Gutiérrez-Gallego et al. 2008). As a result, bracketing suspect samples with Dynepo standards enables a line to be drawn, above which artificial EPOs are found, and below which bands for endogenous EPO lie (Figure 1.8).

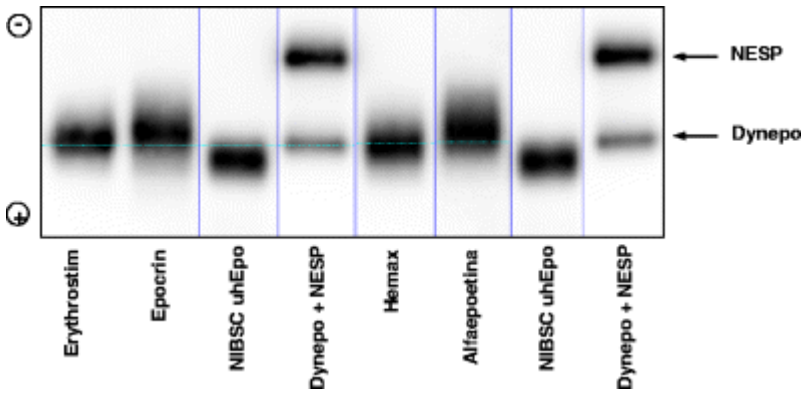

Figure 1.8: SDS-PAGE analysis of EPOs, showing the higher molecular mass of recombinant EPO compared to huEPO (Reichel 2011) – reproduced with permission

One exception to this appears to be Repotin, an epoetin produced in baby hamster kidney cells which appears to have a molecular mass even lower than huEPO. However, on IEF analysis it produced a profile which was even more basic than that of other epoetins tested. (Reichel, Kulovics et al. 2009). SDS-PAGE analysis has been shown to easily distinguish both ‘active’ and ‘effort’ urines. Enzymatic activity in ‘active’ urines is thought to cleave sialic acids, shifting the profile to a more basic (i.e. more rEPO-like) region; with SDS-PAGE, cleavage reduces the molecular mass,

moving the band away from the rEPO region (Reichel, Kulovics et al. 2009). The molecular mass of serum EPO is approximately the same as huEPO; it should not be surprising, then, that effort urines display virtually unchanged profiles (a slight increase in molecular mass only), and that they do not enter into the rEPO region of the gel (Voss, Lüdke et al. 2010).

1.9.7 Sarcosyl-PAGE

MIRCERA excretion in urine is very low, due to its large (60 kDA) molecular size, and as such its presence should be tested for in serum. The human sEPO profile is more basic than the urinary one, complicating profiles derived from blood and analysed using IEF. Unfortunately, SDS-PAGE analysis of samples containing MIRCERA showed reduced sensitivity compared to other epoetins (Reichel, Abzieher et al. 2009). It has been suggested that SDS binds to the PEGylation on MIRCERA, but is incapable of fully solubilising the molecule. As a result, MIRCERA migrates as a broad smeared band. Replacing SDS with Sodium N-lauroyl sarosinate (Sarcosyl), which has enhanced surfactant properties due to containing both carboxylate and amide functional groups, enabled MIRCERA to be resolved into a sharp band, without disturbing the resolution of huEPO and rEPOs.

1.9.8 Capillary zone electrophoresis

Capillary zone electrophoresis (CZE) is a commonly used tool for the separation of glycoprotein isoforms, including those with terminal sialic acids (Kinoshita, Murakami et al. 2000). Several CZE methods have been proposed for the separation of EPO isoforms (Watson and Yao 1993; Yu, Cong et al. 2005; Benavente, Hernández et al. 2007), using either UV absorbance or mass spectrometry as a detection system. Wang et al. used deep UV laser-induced fluorescence detection (deep UV-LIF) combined with an immunomagnetic bead extraction technique and capillary zone electrophoresis (Wang, Dou et al. 2012). They reported high resolution glycoform profiling with improved sensitivity. A further advantage was that the original glycoform distribution was preserved because no fluorescent derivatisation was required. The overall detection sensitivity was 1.5×10^{-8} mol/L, which was two orders of magnitude better than conventional CZE with UV

absorbance detection. This is suitable for pharmaceutical preparations, but is not sensitive enough for the anti-doping analysis of EPO in blood and urine. A method for separating N-linked oligosaccharides, including those derived from rEPO, was described by Ijiri et al. (Ijiri, Todoroki et al. 2011). After derivatisation using rhodamine 110 CE separations were performed using a fused-silica capillary and neutral pH buffer conditions enabling the separation of sialo-oligosaccharides according to the number of sialic acids. A second separation was then performed using the same capillary and acidic pH buffer conditions, enabling the separation of asialo-oligosaccharides according to their sizes. The method gave a limit of detection of maltose of about 10 amol. Structural identification of rEPO glycopeptides was possible, even when starting with just 10 µg of material. Capillary isoelectric focusing methods have also been developed, (Cifuentes, Moreno-Arribas et al. 1999; Lopez-Soto-Yarritu, Díez-Masa et al. 2002), which show good reproducibility and run times of less than 15 minutes; however, sensitivity is poor, with samples often made up at concentrations of 1 mg/mL. As a result, these techniques are suitable to the analysis of pharmaceutical preparations for quality control purposes, but not yet for use in anti-doping efforts (Zhang, Chakraborty et al. 2009). Wang et al. combined a competitive immunoassay with capillary electrophoresis (Wang, Zhang et al. 2009). Recombinant EPO conjugated with horseradish peroxidase (HRP) was incubated with a known amount of anti-EPO antibodies and unconjugated EPO. CE was used to separate the rEPO-HRP from the antibody-rEPO-HRP complex, with silica dioxide nanoparticles used as a pseudostationary phase to improve analyte separation at neutral pH. Measurement of the signal from the two analytes allowed determination of the concentration of unmodifed rEPO in solution. The linear range for EPO was 1.8–158.0 ng/mL and the detection limit was 0.9 ng/mL. The approach was successfully used for the measurement of EPO levels in human sera samples; however, since it could not distinguish between hsEPO and rEPO, it would only be useful as part of a battery of antidoping tools.

1.9.9 Immunoassay

Efforts have been made to develop an immunoassay method for the detection of artificial erythropoietins, which could potentially be faster than testing through IEF or Sarcosyl-PAGE due to the removal of the ultrafiltration or immunoextraction step.

1.9.9.1 CERA: Lamon et al. (Lamon, Giraud et al. 2009) developed a high throughput method for the detection of CERA in serum. Microtitre plates were coated with an anti-EPO antibody, while the detection antibody was a monoclonal anti-PEG antibody labeled with digoxigenin (DIG). After the secondary antibody incubation, an anti-DIG antibody labeled with horseradish peroxidase was bound, and then an ABTS (2,2′-azinobis[3-ethylbenzothiazoline-6-sulfonic acid] diammonium salt) substrate added and the colorimetric reaction produced detected. The lower limit of quantification (LLOQ) of the assay was 30 pg mL^{-1} and the lower limit of quality control (LLQC) 50 pg mL^{-1}. The process is rapid, allowing 70 samples to be processed by an operator per day, and by using a cut off of 100 pg mL^{-1}, the sensitivity of the assay over a 4-week period following 200 μg CERA injection was 80%. The authors recommended that their ELISA method be used to screen samples, which could then be confirmed by either IEF or Sarcosyl-PAGE. They have recently carried out work to compare the three techniques (Leuenberger, Lamon et al.), and have reported that the ELISA technique is more sensitive than IEF; following injection of 200 μg of CERA, the ELISA technique produced positive results until day 20, whereas it was almost undetectable by day 13 using IEF. In contrast, the presence of CERA could also be detected at day 20 through the use of Sarcosyl-PAGE, showing it is a more appropriate method to use when CERA use is suspected.

An alternate method utilised polyethylene glycol precipitation, followed by a commercial homogeneous immunoassay (Van Maerken, Dhondt et al. 2010). Serum samples were incubated with an equal volume of 50% PEG-6000 solution or saline solution, vortexed, centrifuged and the EPO concentration of the supernatant measured using a paramagnetic-particle chemoluminescent immunoassay. The PEGylation of MIRCERA increases its solubility in water, so that the ratio of the measured EPO concentrations was significantly higher in serum samples taken from patients given CERA than in those not given it.

1.9.9.2 rEPO: Mallorqui et al. (Mallorqui, Llop et al. 2010) bound anti-EPO antibodies (clone 9C21D11) to microtitre well plates. Polyvinylpyrrolidone (PVP) was used as a blocking agent, and the serum samples incubated overnight at 4°C, before elution with 0.4 M glycine, 6 M urea, pH 11.0 for analysis by isoelectric

focusing. Alternatively, elution was carried out with 0.7% acetic acid, pH 2.8, and then samples hydrolysed with 0.1 M TFA and derivatised with 7 mM DMB solution. DMB derivatives of sialic acids could then be analysed by reversed-phase capillary-HPLC, allowing the identification of the non-human *N*-glycolyl-neuraminic acid (Neu5Gc), which is present as 1-2% of the sialic content of rEPO and so could provide additional proof of exogenous origin. Whilst carrying out this work, the authors noted that elution from the well plates with acidic solvents resulted in more effective elution of the basic isoforms of EPO. Consequently, they proposed a differential elution method for distinguishing between rEPO and huEPO (Mallorquí, Gutiérrez-Gallego et al. 2010). After incubating ultrafiltered urine samples in the well plates, elution was carried out firstly at pH 2.8; then, a second elution was carried out at pH 11.3. Both elutions were then concentrated through an ultrafilter, diluted with Immulite assay diluent and then analysed using an Immulite 1000. Table 1.2 shows the relative amount eluted in the first elution for different EPO standards.

Table 1.2: Recoveries of erythropoietins in acidic elutions, compared to recovery of huEPO

Erythropoietin	% eluted in acidic elution	Ratio of % eluted to % eluted of huEPO (± s.d)
huEPO	61.7	1
rEPO	86.5	1.34 (±0.125)
Dynepo	89.4	1.40 (±0.018)
Darbepoietin	38.0	0.60 (±0.082)
CERA	96.4	1.51 (±0.011)

Carrying out the same process on blank urine samples produced a ratio of 0.86 (±0.145), suggesting either matrix effects or differences in the endogenous EPO compared to the NIBSC standard. This provides greater certainty when dealing with rEPO or CERA; however, it reduces the discriminatory power of the test for darbepoietin. The authors proposed a cut off ratio of 1.15 for a positive test, and using this comparative analysis of urine samples spiked with rEPO found that analysis by differential elution was slightly more sensitive than analysis of the same samples by the standard IEF approach. The whole process is also much more rapid

than the IEF approach; however, more data is still needed to determine exactly where the cut-off for a positive test should lie.

1.9.9.3 Darbepoietin: Wide et al. were the first to describe an ELISA method for the detection of darbepoetin in human serum (Wide, Wikstrom et al. 2003). Their method was based on an increase in immunoreactivity after treatment with neuramindase. Serum samples were incubated in acetate buffer pH 5.6, either with or without neuraminidase for 1 or 24 hours. EPO activity was then measured using kits from either R&D or medac GmbH. The mean relative increase in immunoactivity of endogenous EPO after enzymatic digestion was 42% with the medac-kit and 117% with R&D-kit. For darbepoetin the equivalent figures were 282% and 231% with 1 h and 299% and 256% with 24 h enzyme incubation, respectively. Both endogenous EPO and rEPO showed similar changes after enzymatic incubation. The method enabled detection of darbepoietin in samples taken 14 days after injection.
Gimenez et al. (Gimenez, de Bolos et al. 2007) developed antibodies that were specific for either EPO or darbepoietin, by synthesising peptides which correspond to the regions of the peptide backbone which are different, coupling these to ovalbumin or keyhole limpet hemocyanin, and using these as antigens. The sera produced was then tested by ELISA against rEPO or darbepoietin. Antibodies raised against EPO (81–95) were able to recognize rHuEPO in its native state, but did not react with darbepoietin in either its native or reduced and alkylated form. In contrast, anti-darbepoietin (86–104) antibodies recognised both darbepoietin and rHuEPO, although rHuEPO was recognised to a lesser extent. Immunopurification using an immobilised darbepoietin (86–91) peptide column isolated the antibodies that specifically recognised the VNET sequence of darbepoietin, enabling QVNETL-specific antibodies to be obtained. These antibodies are able to recognise darbepoietin in ELISA and Western blot assays without binding rEPO. However, to date the ability of these antibodies to discriminate between rEPO and darbepoietin has not been exploited in an anti-doping method.

1.9.9.4 ESAs: A method for the detection of Peginesatide (also known as Hematide) has been described by Leuenberger et al. (Leuenberger, Saugy et al.). Microtitre wells are coated with an anti-PEG monoclonal antibody (clone 1A8); the detection antibody is a biotinylated monoclonal antibody directed against the peginesatide

peptidic moiety (clone 11F9-biotin). Incubation with a streptavidin-horseradish peroxidase conjugate, followed by a TMB substrate produces a colorimetric reaction, which is read at 450 nm, and samples above a predetermined threshold are then analysed by a confirmatory method, using an immuno-precipitation followed by a western blot. Both assays can detect 0.5 ng/mL concentrations of peginesatide in blood samples, enabling detection for up to 10 days after an injection of 0.1 mg/kg.

1.9.9.5 Membrane assisted isoform immunoassay (MAIIA): MAIIA is a technique developed by Maria Lönnberg and Jan Carlsson (Lönnberg and Carlsson 2000), based on separation (by ion-exchange or affinity chromatography) and immunoassay detection of protein isoforms in the same lateral flow, assisted by capillary forces in a membrane device. The method has been applied to the detection of epoetins, using a strip which has a capture zone containing wheat germ agglutin (WGA), illustrated in Figure 1.9. This has been shown to bind to all isoforms of EPO, but shows greater affinity for rEPO isoforms (Franco Fraguas, Carlsson et al. 2008). As a result, it was possible to distinguish between endogenous and artificial EPO by eluting from the lectin using an increasing concentration of the competing sugar, N-acetylglucosamine (GlcNAc). This is exploited in the MAIIA system; following binding to the WGA region, bound EPO is eluted using either a high or low concentration of GlcNAc; this migrates along the membrane to the detection region, which contains an anti-EPO antibody. Visualisation is done using a second anti-EPO antibody labelled with carbon black nanostrings. A scanner then measures the intensity of the obtained grey to black band in the detection zone, which is directly proportional to the amount of bound EPO. Comparison of the results from the two different elutions produces the percentage of migrated isoforms (PMI), the amount eluted at the low concentration expressed as a percentage of the amount eluted at the high concentration. For huEPO, this is around 75%; for rEPOs, it varied from 25.1 to 51.7%; for MIRCERA, it was about 90%, and for darbepoietin it was 7.7% (WADA 2009). To date, this approach has not been validated for use on anti-doping samples.

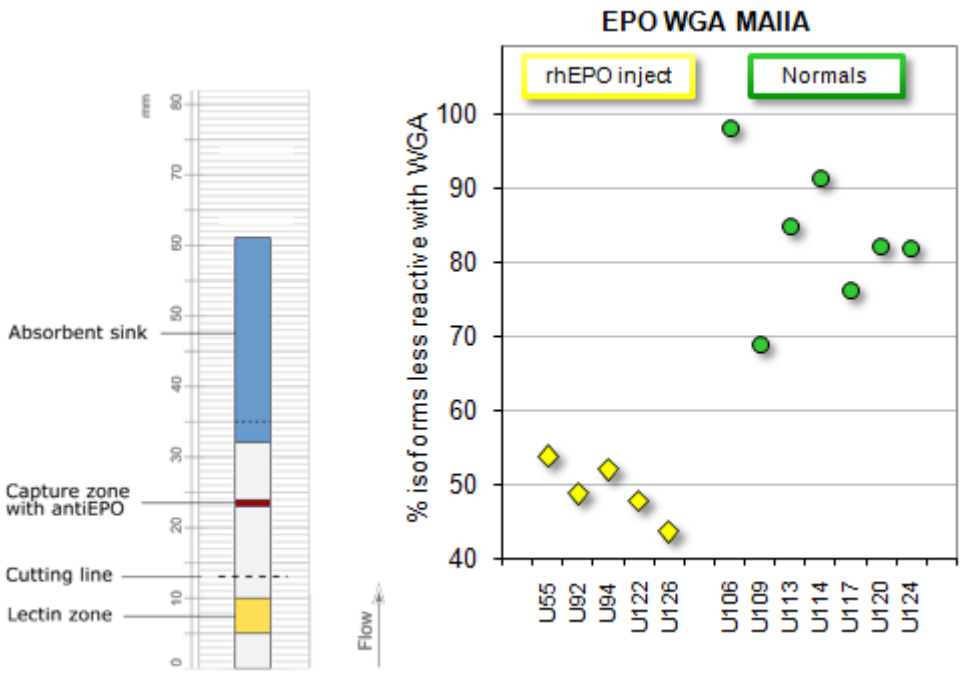

Figure 1.9: Left - EPO WGA MAIIA column. Interaction with the wheat germ agglutinin (WGA) ligands reduces the migration rate for isoforms containing more WGA binding carbohydrate groups. Endogenous isoforms interact less with WGA than recombinant ones, enabling the two to be distinguished (right). Reprinted from http://www.maiiadiagnostics.com/research/epo_doping_test.htm, with permission

1.10 Aptamer-based affinity detection

An alternative to the use of antibodies in affinity-based detection relies on the use of aptamers. These are single stranded DNA or RNA molecules, selected for their binding properties by repeated rounds of *in vitro* selection or Systematic Evolution of Ligands by Exponential Enrichment (SELEX) (Ellington and Szostak 1990; Tuerk and Gold 1990). As well as having binding properties which rival those of antibodies, aptamers possess other significant advantages which antibodies do not: they can be engineered completely in a test tube, are easy to label and are very stable. They have been used for the specific detection of proteins including IgE (German, Buchanan et al. 1998), thrombin (Li, Guo et al. 2008) and ricin (Haes, Giordano et al. 2006). Zhang et al. developed an aptameric molecular beacon (MB) based probe for the detection of rEPO-α in physiological buffer (Zhang, Guo et al. 2009). It involved a fluorescent aptamer and a short complementary quencher sequence, binding to which was disrupted by the specific binding between the

aptamer and rEPO. They reported a linear range of 1–10 nM for the detection of rEPO, and a calculated limit of detection of 0.4 nM. The same authors also developed an aptamer based capillary electrophoresis method with laser-induced fluorescence detection for quantifying rEPO (Shen, Guo et al. 2010). In this method, the complex of aptamer-rEPO and free aptamer can be separated and identified by their migration times. The presence of sodium cations in the sample buffer and running buffer was found to be crucial in stabilising the complex and improving the separation efficiency. They attempted to quantify rEPO-α in physiological buffer, artificial urine and human serum. The linear range for rEPO-α was from 0.2 to 100 nM and the limit of detection was 0.2 nM (i.e. 7.4 ng/mL). Binding experiments using fluorescein isothiocyanate-labeled rEPO-α (F-rEPO-α) and N-deglycosylated F-rEPO-α demonstrated that the glycosylation of rEPO-α was of importance in the specific interaction between it and its aptamer. In comparison, aptamers specific for the peptide backbone of rEPO were isolated by first immobilising rEPO molecules through their glycans on a lectin (Wheat germ agglutin) activated sepharose gel before incubation with an ssDNA library (Zhang, Guo et al. 2010).

1.11 Structural analysis of EPOs

Mass spectrometry is commonly regarded as the gold standard for the identification and detection of biological molecules, due to its sensitivity and specificity. Due to the lack of endogenous, purified material available, there have not been many attempts to determine the structure of the glycans found in huEPO. Takeuchi et al. (Takeuchi, Takasaki et al. 1988) compared huEPO and rEPO produced in Chinese hamster ovary cells. They liberated glycans by hydrazinolysis and separated them by paper electrophoresis, lectin affinity chromatography, and Bio-Gel P-4 column chromatography. They concluded that there were three N-linked sugar chains in each molecule all of which were complex and acidic. The major sugar chains were of fucosylated tetraantennary complex type with and without N-acetyllactosamine repeating units, and small amounts of 2,4- and 2,6-branched triantennary and biantennary sugar chains were detected. Repeat units were particularly prominent in the rEPO, where they were found in 34.5% of glycans, compared to just 7.5% of

the huEPO. Sialic acid linkage in huEPO was of the NeuAc α2 - 6Gal and NeuAc α2 - 3Gal type, while that in rEPO was solely of the NeuAc α2 - 3Gal type.

In the same year, Tsuda et al. (Tsuda, Goto et al. 1988) compared the structures of glycans from EPO from the urine of aplastic anaemic patients, with that of rEPO produced in baby hamster kidney cells. Desialylated glycans were released using N-oligosaccharide glycopeptidase, aminated with a fluorescent reagent and then separated using HPLC. The structure of each oligosaccharide thus isolated was analysed by a combination of sequential exoglycosidase digestion and further HPLC separation with an amide-silica column. They also used high resolution proton nuclear magnetic resonance spectroscopy to analyse the structure of rEPO. They reported significantly different glycan profiles in huEPO isolated from different individuals, whereas different rEPO preparations showed great similarity. They also confirmed Takeuchi's findings, that tetraantennary structures are the most common, and were only able to detect N-acetyllactosamine repeat units in rEPO.

Site-specific glycosylation of huEPO has been investigated using MALDI (Rahbek-Nielsen, Roepstorff et al. 1997). huEPO was reduced, alkylated and digested using Endoproteinase Lys-C, before being separated into fractions using HPLC and a C8 column. Fractions were desialylated using neuraminidase before being spotted using a 4HCCA matrix and analysed using MALDI-TOF mass spectrometry. They concluded that the single O-glycosylation at Ser_{126} consisted of a Hex-HexNAc core with either one or two sialic acids attached. The distribution of bi-, tri- and tetraantennary glycans varied significantly between the three N-glycosylation sites. Those found at Asn_{24} are the most heterogeneous, and biantennary structures are only found here. The glycans at Asn_{38} and Asn_{83} consisted of tri and tetraantennary structures, and all sites were found to contain small amounts of tetraantennary structures with N-acetyllactosamine repeats. These results matched well with those of Takeuchi et al., and with one of the profiles reported by Tsuda et al. However, they differ significantly from another of the profiles recorded by Tsuda; Rahbek-Nielsen et al. have suggested this may be due to the different sources of huEPO, or the purification steps involved.

There has been a great deal more work done in determining the structures of the glycans found in rEPOs, darbepoietin and CERA, since these are more readily available in purer form and in larger amounts.

Rush et al. (Rush, Derby et al. 1995) found that rEPO produced in Chinese hamster ovary cells featured Asn_{24} glycans of mostly biantennary and triantennary forms, with varying levels of Neu5Ac residues that are differentially O-acetylated. As with huEPO, glycans at Asn_{38} and Asn_{83} consisted of tri and tetraantennary structures, with or without N-acetyllactosamine repeating units, with the greater heterogeneity found in Asn_{83} glycans. Di-O-acetylations were also found on glycans at Asn_{83}. The Ser_{126} oligosaccharide is composed of GalGalNAc and either one or two Neu5Ac residues, which also exhibit varying levels of O-acetylation. O-acetylation was predominantly 9-O linked, although O-acetyl groups are known to migrate to other positions when hydrolysed. 52 different N-linked glycan structures were identified in total. Fucosylation of rEPO glycans has been shown to be almost complete on the innermost GlcNAc residues through an α1–6 linkage (Nimtz, Martin et al. 1993). The presence of N-glycolylneuraminic acid has been demonstrated in rEPO from Chinese hamster ovary cells (Hokke, Bergwerff et al. 1990; Hokke, Bergwerff et al. 1995), and in rEPO produced in baby hamster kidney cells (Nimtz, Martin et al. 1993) at about 1-2% of the sialic acids present. Since humans lack the enzyme necessary for the production of N-glycolylneuraminic acid (CMP-Neu5Ac hydroxylase) (Varki 2001), this has been proposed as a method for the identification of rEPO. However, since the presence of Neu5Gc has been demonstrated in fetal tissue and in human carcinomas (Higashi, Hirabayashi et al. 1985), and it has also been suggested that it could be taken up in the diet and incorporated into some glycoproteins (Tangvoranuntakul, Gagneux et al. 2003), other confirmatory steps may still be needed. Derivatisation of sialic acids with 1,2-diamino-4,5-methylenedioxy-benzene (DMB) after immunoaffinity purification of EPO enabled the detection of Neu5Gc in plasma samples taken from athletes suspected of taking rEPO (Mallorquí, Llop et al. 2010). Takegawa et al. (Takegawa, Ito et al. 2008) used capillary zwitterionic-type hydrophilic interaction chromatography (ZIC-HILIC) to separate glycopeptides produced by GluC digestion of rEPO. They found that 105 N-glycopeptides and 8 O-glycopeptides could be detected in a single run of a 150 ng injection (Figures 1.10, 1.11). These included partially acetylated sialic acids, and some which were replaced with N-glycoylneuraminic acid. However, their method involved highly concentrated digests (1 mg/mL), and their mass accuracy was only 0.1 m/z.

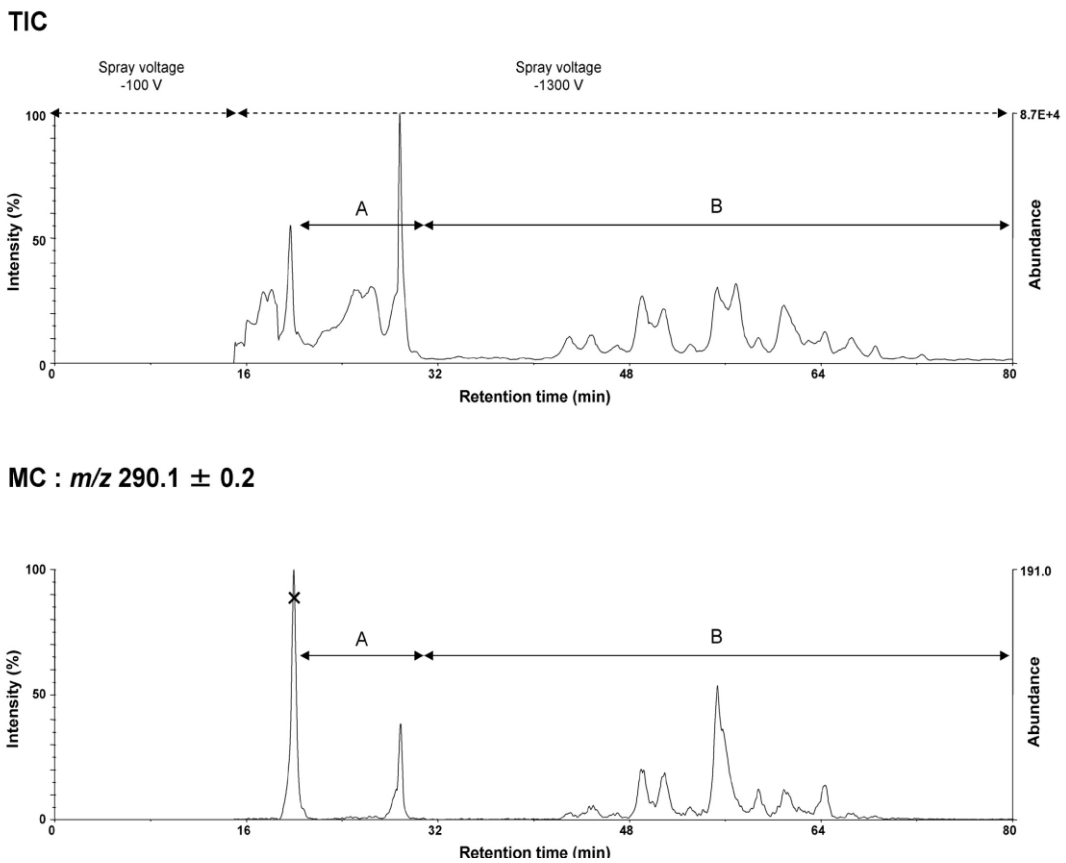

Figure 1.10: ZIC-HILIC separation of glycopeptides from rEPO. TIC and extracted mass chromatogram (MC) of m/z 290.1 corresponding to in-source fragment ions of a sialic acid. From Takegawa, Ito et al. 2008. Reprinted with permission

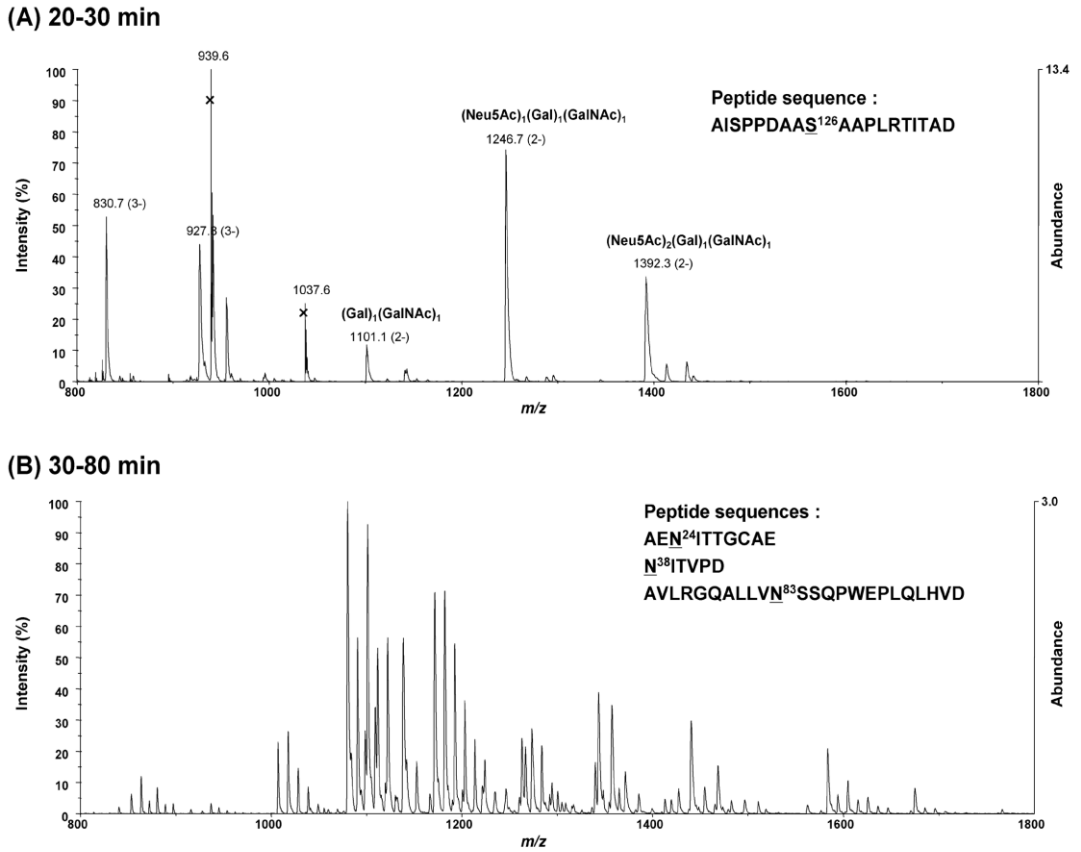

Figure 1.11: MS spectra accumulated in the time periods (A: 20–30 min) and (B: 30-80 min), from the chromatogram in Figure 1.10.

Nanoflow LC-MS/MS has been used to characterise the glycans of rEPO as well, with a view to reducing the limit of detection towards that needed for antidoping analysis. Groleau et al. (Groleau, Desharnais et al. 2008) used Endoproteinase GluC to digest BRP rEPO (mixture of EPO α and EPO β) to give singly glyosylated fragments. Analysis was carried out using the Agilent HPLC-Chip/MS and 6330 ion trap XCT Ultra mass spectrometer. Digested rEPO was injected onto a Zorbax chip with a 40 nL enrichment column and C18 analytical column. Detection and identification of the three most prominent glycoforms of Asn_{24} and Asn_{38} was possible using 100 ng of rEPO after desialylation, at a concentration of 500 μg/mL. Assignment of the glycan structures on these glycopeptides was possible to an extent, with the identification of N-acetyl lactosamine repeat units possible. With the fully sialylated glycopeptides, detection of the three most abundant isoforms of Asn_{24} was possible with 100 ng of material, but identification of repeat units and therefore structural assignment was not. With sialylated material, identification of acetylations on the O-glycopeptide was simplistic. They suggested that this, or the

presence of repeat units on Asn_{24} and Asn_{38}, may be targets for distinguishing between rEPO and huEPO, although huEPO was not available in sufficient quantity for them to try the approach. This remains a problem in developing an antidoping method, and to date further work has not been published by this group.

The differences in glycosylation of different artificial EPOs has been investigated as well. Shahrokh et al. compared the glycosylation of Dynepo, Eprex, NeoRecormon and darbepoietin and found significant differences between them (Shahrokh, Royle et al. 2011). Protein-*N*-glycosidase F was used to remove glycans from the glycoprotein. These were then extracted and fluorescently labelled. They were then separated using HILIC and WAX chromatography, and detected using fluorescence detectors set with excitation and emission wavelengths of 330 and 420 nm respectively. They found that darbepoietin had up to six O-acetyl groups attached to the sialic acids. Eprex and NeoRecormon had only minor amounts of O-acetylation while Dynepo had none. Dynepo, produced in human cell lines, had no Neu5Gc, and contained the lowest amount of disialylated glycans, while darbepoietin contained the highest amount of tetrasialylated glycans. NeoRecormon and Eprex contained more trisialylated, but less tetrasialylated glycans than Dynepo and darbepoietin. The highest amount of tetraantennary glycans was found in Dynepo, as was the lowest amounts of triantennary glycans with a β 1-6-GlcNAc linkage. All the epoetins were found to contain N-acetyl-lactosamine repeat units, although Dynepo had the least. In Dynepo and darbepoietin, these repeat units were mostly found on biantennary glycans, whereas in NeoRecomon and Eprex they were on triantennary glycans. The sLe(x) epitope was only detected in Dynepo. Recent work by Bones et al. (Bones, McLoughlin et al. 2011) used a 2D LC approach, with a shallow weak anion exchange gradient in the first dimension followed by further separation of each obtained peak using a HILIC column. Analysing the European Pharmacopeia Biological Reference Preparation (BRP) 3 erythropoietin standard, a mix of recombinant epoetin alpha and epoetin beta expressed in CHO cells, they found tetra-antennary glycans to be the primary glycosylation on Asn_{24} and $Asn_{83.}$ A novel finding was that up to five poly-*N*-acetyl lactosamine repeats were observed on a tetrasialylated glycan present at Asn_{83}, although this made up less than 0.1% of the total glycan pool. In contrast, biantennary glycans were the major structure detected at Asn_{38}.

Capillary zone electrophoresis coupled with ESI-TOF-MS was used by Balaguer et al. (Balaguer, Demelbauer et al. 2006) to characterise intact rEPO and enzymatically released glycans. Effective separation of glycoforms is necessary to avoid a broad unresolved signal. Balaguer et al. used a novel acrylamide-based capillary coating to suppress electroosmotic flow, and an orthogonal accelerated TOF mass spectrometer for detection. They were able to get baseline resolution of rEPO molecules containing different numbers of sialic acids, and some separation of rEPO molecules containing different numbers of N-acetyl lactosamine repeat units. Analysis of N-glycans released by PNGase digestion identified 19 different glycans, including ones with 5 sialic acids attached, and sulfated glycans. Distinguishing between glycans with repeat units and those with multiple antennae was not possible, due to the single MS method used. As with the previous CZE techniques, the main drawback of this method was the need for highly concentrated (1 mg/mL to 2.5 mg/mL) solutions. Intact mass spectrometry of rEPO was also attempted by Giménez et al., who used CE separation with physically adsorbed capillary coatings from UltraTol™ Pre-Coats on the capillaries, and an ion trap as an analyser (Giménez, Benavente et al. 2008). They were able to identify a total of 17 different glycoforms, including ones with different numbers of sialic acids and different numbers of N-acetyl-lactosamine repeat units. However, a lack of stability and bleeding of the capillary coating caused problems with MS detection, such as a significant loss of sensitivity and the presence of peaks in the mass spectra corresponding to molecular ions from the coating. An orthogonal accelerating time-of-flight mass spectrometer, combined with CE-MS was also used in a paper published by Giménez et al. in 2012 (Giménez, Ramos-Hernan et al. 2012). In this paper, they examined tryptic and Endoproteinase Glu-C digests of rEPO either with or without digests with neuraminidase. Twelve sialoforms corresponding to 5 different glycoforms were detected at Asn_{83}, and they also reported for the first time a sulfated sialoform of this glycopeptide. Different sialoforms were also detected on the O-glycosylation, and an estimate of the different amounts of acetylated sialic acids and N-glycolylneuraminic acid was produced. As previously however, highly concentrated solutions were needed.

If the presence or absence of sialic acid groups was the only difference between isoforms of EPO, then a maximum of 14 isoforms would be detectable using IEF (with the maximum sialylation occurring when three tetraantennary, fully sialylated

N-glycans and one doubly sialylated O-glycan are found). However, as mentioned above, digestion of huEPO with sialidase did not result in a product which was too basic to be detected in the IEF window, suggesting charges are carried elsewhere in the molecule as well. Other structural features of rEPO which have been reported include the presence of mannose-6-phosphate (Nimtz, Wray et al. 1995) and the sulfation of GlcNAc (Kawasaki, Haishima et al. 2001; Balaguer, Demelbauer et al. 2006). Cointe et al. (Cointe, Béliard et al. 2000) attempted to produce a rEPO as close as possible to huEPO, by expressing the EPO gene in a human lymphoblastoid cell line, named RPMI 1788. This resulted in unusual glycosylation patterns: 80% of N-glycans possessed a bisecting GlcNAc residue, 25% bore a second fucose residue which was largely present in a sialyl Le^x motif, and 13% contained more than three LacNAc repeats (up to five per molecule).

Recently, Christian Reichel suggested that there may be a structural difference between all rEPOs and endogenous EPO (Reichel 2011). Sequential digestion of recombinant and huEPO with exoglycosidases and subsequent analysis by SDS-PAGE showed that both responded the same to digestion with *Arthrobacter ureafaciens* α-sialidase and *Steptococcus pneumoniae* β-D-galactosidase. However, further digestion with N-acetyl-β-D-glucosaminidase from *Steptococcus pneumoniae* was partly inhibited in endogenous but not recombinant erythropoietins. Subsequent digestion with Jack bean α-D-mannosidase and *Helix pomatia* β-D-mannosidase led to only very limited further deglycosylation of endogenous EPO, while rEPO glycans continued to be degraded. Reichel proposed that this could be due to tissue specific glycosylation, such as the existence of a bisecting GlcNAc residue in endogenous EPO, sterically hindering the exoglycosidases. IEF analysis of sialidase treated rEPO and huEPO found that it resulted in the disappearance of most isoforms of rEPO, suggesting charge on them lies solely in sialic acid residues. However, with huEPO it resulted in the appearance of more than ten additional basic isoforms, suggesting additional charges (e.g. sulfates) are present. This remained after subsequent deglycosylation with β-D-galactosidase and N-acetyl-β-D-glucosaminidase, suggesting the charges must either be present on the core sugars or on the non-cleavable residues of the glycan arms. The presence of these charges could also be responsible for steric hindrance of the deglycosylating enzymes.

The structures of the component saccharides of EPO glycans are illustrated in Figure 1.12. Summary diagrams of the range of structures found are shown in Figure 1.13 (for N-glycans) and Figure 1.14 (for O-glycans).

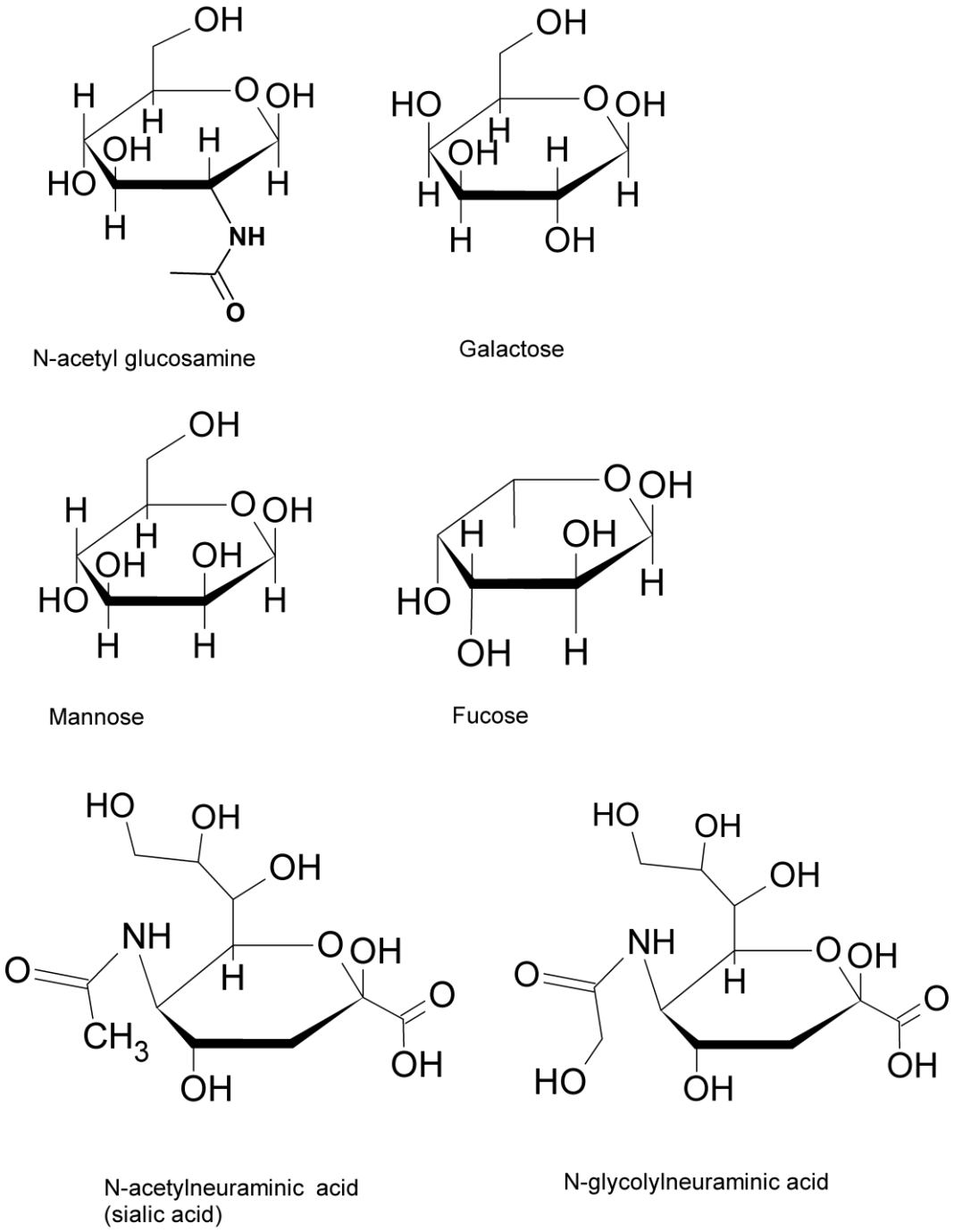

Figure 1.12: Sugars found in rEPO and huEPO glycans

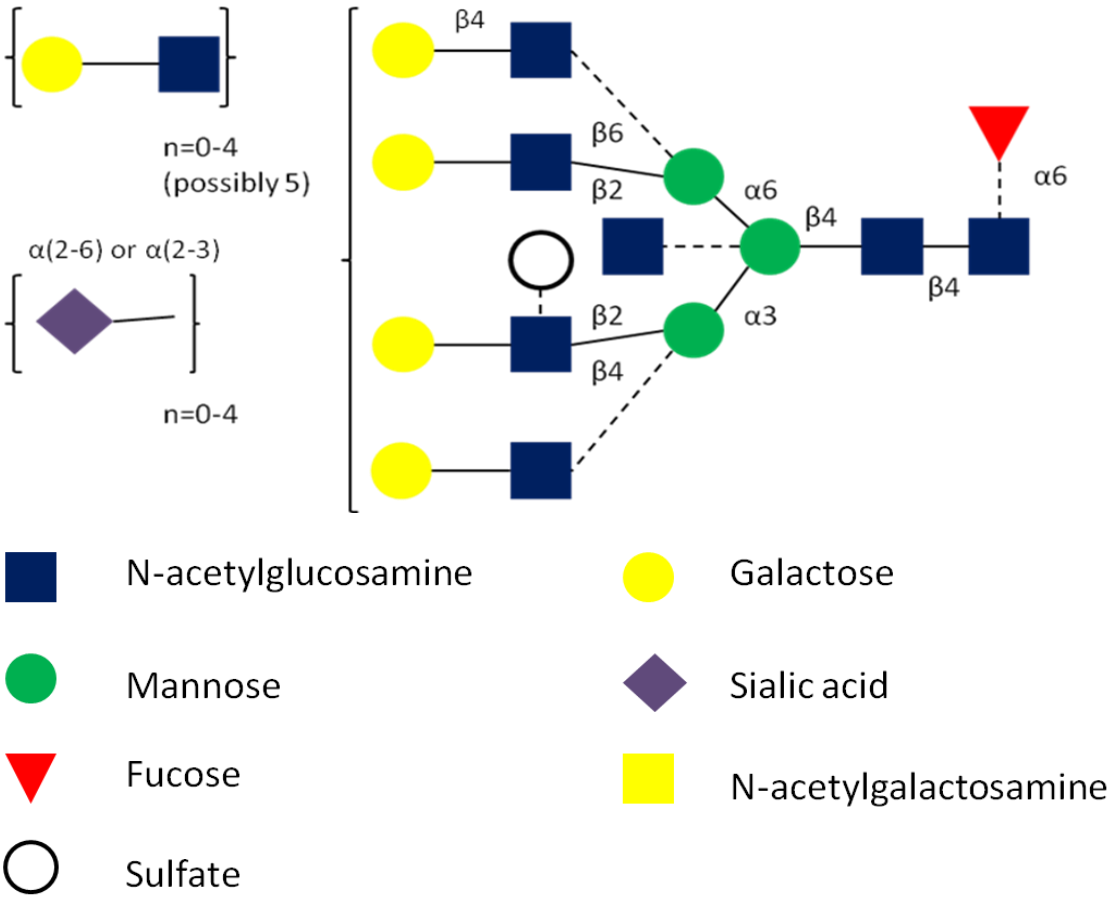

Figure 1.13: Summary diagram of N-glycans found on rEPO and endogenous EPO, including possible positions of sulfate and bisecting N-acetylglucosamine moieties. After Varki et al. (Varki, Cummings et al. 2009)

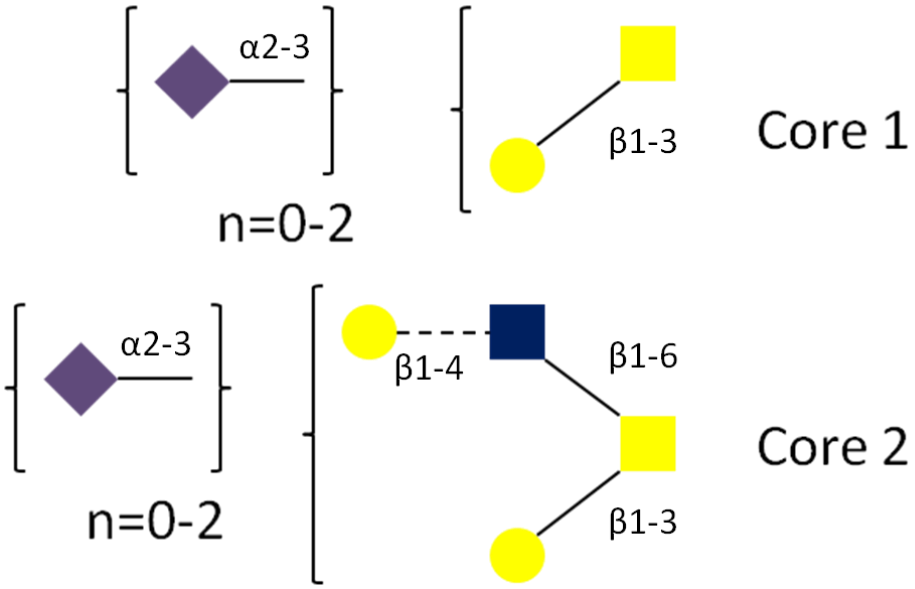

Figure 1.14: O-glycans found on rEPO and endogenous EPO; same key as in Figure 1.13.

1.12 Sample preparation

Extraction of EPO from urine and especially serum faces the same challenge; extraction of EPO, which is present at low concentrations, coupled with the removal of interfering matrix components which may be present at (much) higher concentrations. In serum, the concentration of albumin in particular is in the region of 40 g/L, compared to 50 ng/L for EPO. Ultrafiltration through 30 kDa centrifugal filters is the standard approach for urine samples, as mentioned above, where EPO is typically present at a concentration of about 10 ng/L (Emslie, Howe et al. 1999). However, this does not remove abundant urine proteins, which can cause interference either inside (Khan, Grinyer et al. 2005) or outside (Lasne, Martin et al. 2007) the pI range of EPO. Immunoaffinity approaches can theoretically result in more specific sample clean up. In demonstrating that huEPO and hsEPO profiles are different, Lasne et al. (Lasne, Martin et al. 2007) used an immunoaffinity column to extract EPO from serum, consisting of monoclonal antibody 9C21D11 coupled to an Affi-Gel Hz hydrazide gel. Elution was carried out using a buffer at pH 11, containing 6 M urea, and samples were then subject to ultrafiltration, before being analysed by isoelectric focusing. Paramagnetic beads (Guan, Uboh et al. 2007; Guan,

Uboh et al. 2008) have also been used to extract EPO and darbepoietin from equine plasma, and from human serum (Skibeli, Nissen-Lie et al. 2001). Tosyl activated beads were used to bind polyclonal rabbit anti-EPO antibodies, which were then incubated overnight with samples. Elution was then carried out using a pH 2 buffer containing PEG 6000. As mentioned above, Wang et al. (Wang, Dou et al. 2012) also developed a technique using antibody-functionalised paramagnetic beads. They used Protein A coated beads, functionalised using a rabbit polyclonal antibody, incubated them with the sample for 3.5 hours and eluted using 10 M urea for 2 hours. Although they demonstrated that extraction from albumin-containing pharmaceutical preparations was possible, they were unable to replicate this result in urine samples. After filtering urine through a 50 kDa filter, recovery was improved although still low. They concluded that large molecules were interfering with the antibody binding, and proposed Tamm Horsfall glycoprotein (M_r, 69,000) and alpha-2-thiol proteinase inhibitor (M_r, 72,000) as two possible candidates.

These processes all take a relatively long time; either long incubations are required, or immunoaffinity extraction is followed by ultrafiltration, a lengthy process on its own. Immunoaffinity extraction using these processes is also costly, if beads or columns are disposed of after use. In 2006, Mi et al. (Mi, Wang et al. 2006) produced an immunoaffinity column for extracting EPO from urine, which used polyclonal rabbit antibodies. It had a binding capacity of 2 μg of EPO, and recovery from urine samples was measured at 86 ± 9%. However, elution was carried out with 8 mL of glycine-HCl buffer, so very little preconcentration occurred, and a subsequent lack of IEF data meant that possible isoform selectivity was not addressed. Furthermore, the authors claim the column can be used up to 30 times. However, no data is presented to demonstrate the existence or absence of carryover between extractions. Attempts to repeatedly use extraction materials risks carryover between samples and false positives or negatives as a result.

Validation has however taken place for another kit developed by the producers of the MAIIA method (Lönnberg, Dehnes et al. 2010); this uses disposable anti-EPO monolithic columns for extraction of EPO from blood or urine samples, as an alternative to ultrafiltration or immunoaffinity extraction using ELISA plates. These are much smaller than traditional monoliths, being only 0.15 mm long with a volume of 6 μL, meaning that much less antibody is required and that the columns can be disposable and (relatively) low cost. Each column used in the study had

approximately 20 to 40 µg of anti-EPO (clone 3F6) immobilised on it. Recovery of huEPO was 65 ± 17% (mean ± SD), which compared to a mean of 51% from ultrafiltration, in line with earlier estimations of recovery by this method (Lasne 2002). Mircera recovery is lower (mean of 57%), as the pegylation reduces its affinity for the antibody used; recovery is enhanced by the use of an 'Exposure aid', which presumably partially denatures the molecule and exposes binding sites. Isoform distribution was retained, and background noise was reduced compared to extraction by ultrafiltration (Figure 1.15).

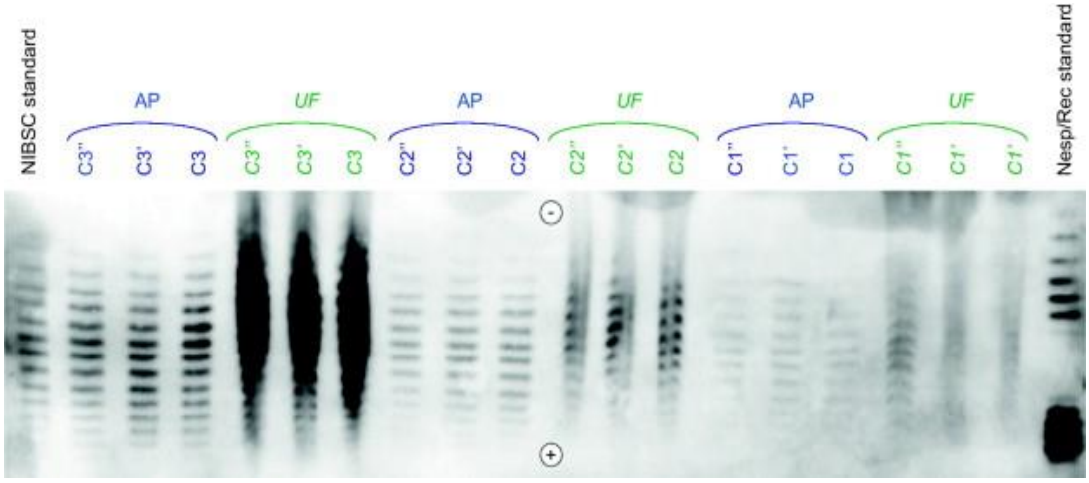

Figure 1.15: IEF (pH 2–6) analysis of isoform distribution for endogenous EPO. Endogenous EPO from a 20 mL urine sample was obtained by either ultrafiltration (UF) or affinity purification using MAIIA cartridges (AP). C1, C2 and C3 represent three different urine samples with an estimated original concentration in urine of 4, 7 and 60 ng EPO/L. Affinity purification of the urine sample removed the background staining and made the interpretation of band intensity, intensity ratio calculation and estimation of position much more reliable. From Lönnberg, Dehnes et al. 2010; reprinted with permission

1.13 Mass spectrometry for anti-doping analysis

To date, no mass spectrometric method has been developed for the detection of artificial EPOs in anti-doping samples from humans. The problem is one of sensitivity; where the artificial and endogenous form share the same peptide backbone, differences are due to the glycosylation patterns found. One key

difference between endogenous and recombinant EPOs appears to be the number of sialic acids detected; these groups are notoriously labile in both MALDI and ESI sources.

However, mass spectrometric methods have been developed for cases where the peptide sequence is not the same for the natural and artificial EPOs being considered, i.e. in humans with the example of darbepoietin, or in animals injected with rEPO. Guan et al. (Guan, Uboh et al. 2007) developed a method to detect the presence of rEPO and darbepoietin in horse plasma. It involved extraction using immunomagnetic beads, digestion by trypsin and then analysis using LC-MS/MS. Two digest peptides, ^{46}VNFYAWK^{52} and ^{144}VYSNFLR^{150} from rEPO and darbepoietin were used for confirmation. The limit of confirmation reported was 0.2 ng/mL, and the limit of detection was 0.1 ng/mL for rEPO and darbepoietin. A modified method was also proposed (Guan, Uboh et al. 2008), which enabled distinction between rEPO and darbepoietin using two different peptides, ^{21}EAENITTGCAEHCSLNENITVPDTK^{45} (T_5) from rEPO and ^{77}GQALLVNSSQVNETLQLHVDK^{97} (T_9) from darbepoietin, produced after digestion with both trypsin and PNGaseF. The limit of identification was 0.1 ng/mL for darbepoietin and 0.2 ng/mL for rEPO in equine plasma, and the limit of detection was 0.05 ng/mL for darbepoietin and 0.1 ng/mL for rEPO. The same approach has also been applied to human plasma (Guan, Uboh et al. 2009), where the limit of detection for darbepoietin was 0.1 ng/mL, and that of identification was 0.2 ng/mL. However, as mentioned above, this method cannot distinguish between rEPO and hsEPO.

Yu et al. produced a slightly modified version, which also involved immunoaffinity extraction using anti-rEPO antibody-coated Dynabeads followed by trypsin digestion (Yu, Ho et al. 2010). They used a nano-flow reversed phase LC system, with a peptide trapping column and a C18 analytical column. Monitoring four transitions in SRM mode for the peptide VNFYAWK for the detection of rEPO, darbepoietin and CERA in equine plasma, they reported limits of detection of 0.1, 0.2 and 1.0 ng/mL, respectively.

The method was further improved (Guan, Uboh et al. 2010) through switching to a different tryptic peptide T_8 (^{54}MEVGQQAVEVWQGLALLSEAVLR^{76}), common to rEPO, darbepoietin and CERA, and extracting analyte from plasma samples that had been pretreated with polyethylene glycol (PEG) 6000, to precipitate plasma proteins.

The limit of identification was 0.5 ng/mL for CERA, 0.2 ng/mL for rEPO, and 0.1 ng/mL for darbepoietin in equine plasma; the limit of detection was 0.3 ng/mL for CERA, 0.1 ng/mL for rEPO, and 0.05 ng/mL for darbepoietin.

1.14 Biosimilars

Since the expiration of the patent on EPO, a number of biosimilar EPOs have been produced as well as a number of cheaper-production "copy" epoetins. It has been estimated that up to 80 such products may already be available in countries with more relaxed pharmaceutical standards (Macdougall and Ashenden 2009). Since the glycosylation of EPO is dependent on the specific cell conditions, these would be expected to show variation in their isoforms from those already available. Park et al. (Park, Park et al. 2009) compared Epogen produced by Amgen with a number of biosimilar products produced in Korea, China and India. They found a high degree of variability of isoforms. Analysis by IEF showed four isoforms to be present in the Epogen samples. Those from rEPOs made by Jia Lin Hao, Ji Mai Xin, and Huan Er Bo, all in China, showed approximately nine isoforms; additionally, the isoform patterns of rEPO from Huan Er Bo differed between samples, demonstrating variability in the manufacturing process. Eporon (from Korea) also contained more isoforms than Epogen, and again differed between batches. Samples from India also showed multiple isoforms. In particular, Zyrop, manufactured in Argentina and sold in India and Wepox, which is manufactured in India, demonstrated a great range of isoforms (Figure 1.16). Similar variability and differences from Epogen has also been described in other Korean rEPOs (Kang, Sang et al. 2010), and in biosimilars from Brazil, South Africa, Ukraine and Russia (Reichel, Kulovics et al. 2009).

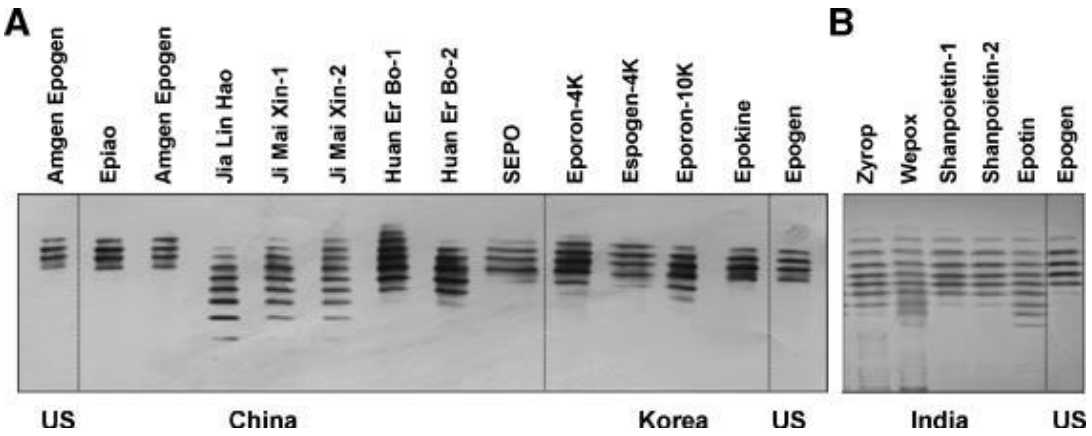

Figure 1.16: IEF/Immunoblotting gel of rEPO samples (A) samples from China (lanes 2–9) and Korea (lanes 10–13) and (B) samples from India (lanes 1–5). Reprinted with permission from Park, Park et al. 2009

1.15 Aim of this PhD

The current methods for identification of the misuse of erythropoietins and related drugs, IEF and SDS/Sarcosyl-PAGE, are both time and labour intensive. The results they produce are subjective, as different gels cannot be compared; it is also suspected that they result in a large number of false negatives, as their lack of specificity means that the criteria for a positive test need to be set more tightly than is perhaps desirable. Alternative methods developed with the intention of tackling this problem either fail to identify all the isoforms, lack sufficient sensitivity to be used in anti-doping tests or have not been validated with real antidoping samples (see Table 1.3 for a summary of the approaches attempted with EPO). The aim of this PhD was to develop a mass spectrometric method for the identification of recombinant EPOs in anti-doping samples. To this end, Chapter 2 details the attempt to develop an immunoaffinity approach to EPO extraction from urine as an alternative to ultrafiltration. Chapter 3 concerns attempts to produce a boronic acid functionalised silica, for the extraction and concentration of rEPO glycopeptides, with a view to using the modified silica in a trapping column. Chapter 4 is about the use of so-called 'superchargers' to improve the signal from compounds which are typically difficult to detect using mass spectrometry, such as acidic glycoproteins; and Chapter 5 considers an approach to distinguish between recombinant and endogenous EPO based on the proposed presence of a bisecting N-acetylglucosamine in glycans from endogenous EPO only.

Table 1.3: Methods used for identifying EPO isoforms/glycopeptides *Lowest EPO concentration used

Analytical method	Limit of detection	EPO type	Separation time	Resolution (glycoforms observed)	Ref.
CZE-deep UV-LIF	0.5 μg/mL	α, BRP, α in injection	25 min	5 for α; 8 for BRP	Wang et al., 2012
CE-LIF	7.4 ng/mL	α, shEPO	9 min	1	Shen et al., 2010
CE-CL	0.9 ng/mL	shEPO	250 s	1	Wang et al., 2009
Gel IEF-CL	3.4 pg/mL	α, uhEPO	2–3 days	4–6 for α; 10–15 for uhEPO	Lasne et al., 2002
SDS-PAGE-CL	20 pg/mL*	α , δ, uhEPO	2-3 days	1	Reichel, Kulovics et al. 2009
2DGE-CL	2.5 pg/mL	BRP, uhEPO	2–3 days	5 for BRP; 6 for urine; 8 for uhEPO-spiked urine	Khan et al, 2005
CZE-ESI-TOF MS	1 mg/mL*	BRP	30 min	64	Balaguer et al., 2006
CE-ESI- IT MS	3 mg/mL* 1 mg/mL	BRP BRP-tryptic digest	45 min 34 min	17 36 glycopeptides	Gimenez et al., 2008 Gimenez et al., 2012
CIEF-UV	1 mg/mL*	BRP	14 min	5	Lopez-Soto-Yarritu, 2002
IA	4 ng/mL	BRP, uhEPO	6 hours	2	Mallorquí, Gutiérrez Gallego et al., 2010
Lectin – IA	2 pg/ sample	α , β, Ω, δ, uhEPO, shEPO	1 hour	2	WADA (Tokyo), 2009
(ZIC-HILIC) HPLC-MS	1 mg/mL*	rEPO – not specified, GluC digest	80 minutes	113 glycopeptides	Takegawa, 2008
Nanoflow ChipLC-ESI-IT MS/MS	500 μg/mL	BRP, GluC digest	30 minutes	17 glycopeptides	Groleau, 2008

1.16 References

Abbrecht, P. H. and J. K. Littell (1972). "Plasma erythropoietin in men and mice during acclimatization to different altitudes." Journal of Applied Physiology **32**(1): 54-58.

Ashenden, M., E. Varlet-Marie, et al. (2006). "The effects of microdose recombinant human erythropoietin regimens in athletes." Haematologica **91**(8): 1143-1144.

Balaguer, E., U. Demelbauer, et al. (2006). "Glycoform characterization of erythropoietin combining glycan and intact protein analysis by capillary electrophoresis – electrospray – time-of-flight mass spectrometry." Electrophoresis **27**(13): 2638-2650.

Bartlett, C., G. J. Clancy, et al. (2006). "Detection of the Administration of Human Erythropoietin (HuEPO) to Canines." Journal of Analytical Toxicology **30**(9): 663-669.

Belalcazar, V., R. Gutiérrez Gallego, et al. (2006). "Assessing the instability of the isoelectric focusing patterns of erythropoietin in urine." Electrophoresis **27**(22): 4387-4395.

Benavente, F., E. Hernández, et al. (2007). "Determination of human erythropoietin by on-line immunoaffinity capillary electrophoresis: a preliminary report." Analytical and Bioanalytical Chemistry **387**(8): 2633-2639.

Beullens, M., J. R. Delanghe, et al. (2006). "False-positive detection of recombinant human erythropoietin in urine following strenuous physical exercise." Blood **107**(12): 4711-4713.

Birkeland, K. I., J. Stray-Gundersen, et al. (2000). "Effect of rhEPO administration on serum levels of sTfR and cycling performance." Medicine & Science in Sports & Exercise **32**(7): 1238-1243.

Bones, J., N. McLoughlin, et al. (2011). "2D-LC Analysis of BRP 3 Erythropoietin N-Glycosylation using Anion Exchange Fractionation and Hydrophilic Interaction UPLC Reveals Long Poly-N-Acetyl Lactosamine Extensions." Analytical Chemistry **83**(11): 4154-4162.

Brian, L.-J. (2003). "Breast cancer trial with erythropoietin terminated unexpectedly." The Lancet Oncology **4**(8): 459-460.

Bruegge, K., W. Jelkmann, et al. (2007). "Hydroxylation of Hypoxia-Inducible Transcription Factors and Chemical Compounds Targeting the HIF-Hydroxylases." Current Medicinal Chemistry **14**(17): 1853-1862.

Casadevall, N., K.-U. Eckardt, et al. (2005). "Epoetin-Induced Autoimmune Pure Red Cell Aplasia." Journal of the American Society of Nephrology **16**(3 suppl 1): S67-S69.

Casals-Pascual, C., R. Idro, et al. (2008). "High levels of erythropoietin are associated with protection against neurological sequelae in African children with cerebral malaria." Proceedings of the National Academy of Sciences of the United States of America **105**(7): 2634-2639.

Chang, S. C. S., D. Sikkema, et al. (1974). "Evidence for an erythropoietin receptor protein on rat bone marrow cells." Biochemical and Biophysical Research Communications **57**(2): 399-405.

Cheung, W. K., B. L. Goon, et al. (1998). "Pharmacokinetics and pharmacodynamics of recombinant human erythropoietin after single and multiple subcutaneous doses to healthy subjects[ast]." Clin Pharmacol Ther **64**(4): 412-423.

Cifuentes, A., M. Ì. a. V. Moreno-Arribas, et al. (1999). "Capillary isoelectric focusing of erythropoietin glycoforms and its comparison with flat-bed isoelectric focusing and capillary zone electrophoresis." Journal of Chromatography A **830**(2): 453-463.

Cointe, D., R. Béliard, et al. (2000). "Unusual N-glycosylation of a recombinant human erythropoietin expressed in a human lymphoblastoid cell line does not alter its biological properties." Glycobiology **10**(5): 511-519.

Darling, R. J., U. Kuchibhotla, et al. (2002). "Glycosylation of Erythropoietin Affects Receptor Binding Kinetics: Role of Electrostatic Interactions." Biochemistry **41**(49): 14524-14531.

Delanghe, J. R., M. Bollen, et al. (2008). "Testing for recombinant erythropoietin." Am J Hematol **83**(3): 237-41.

Dicato, M. and L. Plawny (2010). "Erythropoietin in cancer patients: pros and cons." Current Opinion in Oncology **22**(4): 307-311.

Egrie, J. C. and J. K. Browne (2001). "Development and characterization of novel erythropoiesis stimulating protein (NESP)." Br J Cancer **84 Suppl 1**: 3-10.

Egrie, J. C., E. Dwyer, et al. (2003). "Darbepoetin alfa has a longer circulating half-life and greater in vivo potency than recombinant human erythropoietin." Experimental Hematology **31**(4): 290-299.

Eichner, E. R. (2007). "Blood Doping: Infusions, Erythropoietin and Artificial Blood." Sports Medicine **37**(4-5): 389-391.

Ekblom, B. and B. Berglund (1991). "Effect of erythropoietin administration on mammal aerobic power." Scandinavian Journal of Medicine & Science in Sports **1**(2): 88-93.

Ellington, A. D. and J. W. Szostak (1990). "In vitro selection of RNA molecules that bind specific ligands." Nature **346**(6287): 818-822.

Elliott, S., J. Egrie, et al. (2004). "Control of rHuEPO biological activity: The role of carbohydrate." Experimental Hematology **32**(12): 1146-1155.

Elliott, S., E. Pham, et al. (2008). "Erythropoietins: a common mechanism of action." Exp Hematol **36**(12): 1573-84.

Emslie, K. R., C. Howe, et al. (1999). Measurement of urinary erythropoietin levels in athletes. Proceedings of the Manfred Donike Workshop, 17th Cologne Workshop on Dope Analysis, Recent Advances in Doping Analysis, Vol. 7, Cologne, Sport and Buch Strauss.

Erslev, A. (1953). "Humoral Regulation of Red Cell Production." Blood **8**(4): 349-357.

Eschbach, J. W., J. C. Egrie, et al. (1987). "Correction of the anemia of end-stage renal disease with recombinant human erythropoietin. Results of a combined phase I and II clinical trial." N Engl J Med **316**(2): 73-8.

Faura, J., J. Ramos, et al. (1969). "Effect of Altitude on Erythropoiesis." Blood **33**(5): 668-676.

Franco Fraguas, L., J. Carlsson, et al. (2008). "Lectin affinity chromatography as a tool to differentiate endogenous and recombinant erythropoietins." Journal of Chromatography A **1212**(1-2): 82-88.

Franke, W. W. and H. Heid (2006). "Pitfalls, errors and risks of false-positive results in urinary EPO drug tests." Clinica Chimica Acta **373**(1-2): 189-190.

Fukuda, M., H. Sasaki, et al. (1989). "Survival of recombinant erythropoietin in the circulation: the role of carbohydrates." Blood **73**(1): 84-89.

Gareau, R., G. R. Brisson, et al. (1995). "Total fibrin and fibrinogen degradation products in urine: a possible probe to detect illicit users of the physical-performance enhancer erythropoietin?" Horm Res **44**(4): 189-92.

German, I., D. D. Buchanan, et al. (1998). "Aptamers as Ligands in Affinity Probe Capillary Electrophoresis." Analytical Chemistry **70**(21): 4540-4545.

Giménez, E., F. Benavente, et al. (2008). "Analysis of intact erythropoietin and novel erythropoiesis-stimulating protein by capillary electrophoresis-electrospray-ion trap mass spectrometry." Electrophoresis **29**(10): 2161-2170.

Gimenez, E., C. de Bolos, et al. (2007). "Anti-EPO and anti-NESP antibodies raised against synthetic peptides that reproduce the minimal amino acid sequence differences between EPO and NESP." Analytical and Bioanalytical Chemistry **388**(7): 1531-1538.

Giménez, E., R. Ramos-Hernan, et al. (2012). "Analysis of recombinant human erythropoietin glycopeptides by capillary electrophoresis electrospray–time of flight-mass spectrometry." Analytica Chimica Acta **709**(0): 81-90.

Goldwasser, E. and C. K. H. Kung (1968). "Progress in the purification of Erythropoietin." Annals of the New York Academy of Sciences **149**(1): 49-53.

Groleau, P. E., P. Desharnais, et al. (2008). "Low LC-MS/MS detection of glycopeptides released from pmol levels of recombinant erythropoietin using nanoflow HPLC-chip electrospray ionization." J Mass Spectrom **43**(7): 924-35.

Groner, B. and N. E. Hynes (2010). "Unfavorable Drug Interactions in Targeted Breast Cancer Therapy." Cancer Cell **18**(5): 401-402.

Guan, F., C. E. Uboh, et al. (2007). "LC-MS/MS Method for Confirmation of Recombinant Human Erythropoietin and Darbepoetin α in Equine Plasma." Analytical Chemistry **79**(12): 4627-4635.

Guan, F., C. E. Uboh, et al. (2008). "Differentiation and Identification of Recombinant Human Erythropoietin and Darbepoetin Alfa in Equine Plasma by LCâ^'MS/MS for Doping Control." Analytical Chemistry **80**(10): 3811-3817.

Guan, F., C. E. Uboh, et al. (2009). "Identification of Darbepoetin Alfa in Human Plasma by Liquid Chromatography Coupled to Mass Spectrometry for Doping Control." Int J Sports Med **30**(02): 80,86.

Guan, F., C. E. Uboh, et al. (2010). "Confirmatory Analysis of Continuous Erythropoietin Receptor Activator and Erythropoietin Analogues in Equine Plasma by LC−MS for Doping Control." Analytical Chemistry **82**(21): 9074-9081.

Haes, A. J., B. C. Giordano, et al. (2006). "Aptamer-Based Detection and Quantitative Analysis of Ricin Using Affinity Probe Capillary Electrophoresis." Analytical Chemistry **78**(11): 3758-3764.

Henke, M., R. Laszig, et al. (2003). "Erythropoietin to treat head and neck cancer patients with anaemia undergoing radiotherapy: randomised, double-blind, placebo-controlled trial." The Lancet **362**(9392): 1255-1260.

Higashi, H., Y. Hirabayashi, et al. (1985). "Characterization of N-Glycolylneuraminic Acid-containing Gangliosides as Tumor-associated Hanganutziu-Deicher Antigen in Human Colon Cancer." Cancer Research **45**(8): 3796-3802.

Hokke, C. H., A. A. Bergwerff, et al. (1995). "Structural Analysis of the Sialylated N- and O-Linked Carbohydrate Chains of Recombinant Human Erythropoietin Expressed in Chinese Hamster Ovary Cells." European Journal of Biochemistry **228**(3): 981-1008.

Hokke, C. H., A. A. Bergwerff, et al. (1990). "Sialylated carbohydrate chains of recombinant human glycoproteins expressed in Chinese hamster ovary cells contain traces of N-glycolylneuraminic acid." FEBS Letters **275**(1-2): 9-14.

Ijiri, S., K. Todoroki, et al. (2011). "Highly sensitive capillary electrophoresis analysis of N-linked oligosaccharides in glycoproteins following fluorescence derivatization with rhodamine 110 and laser-induced fluorescence detection." Electrophoresis **32**(24): 3499-3509.

Jacobs, C., D. Frei, et al. (2005). "Results of the European Survey on Anaemia Management 2003 (ESAM 2003): current status of anaemia management in dialysis patients, factors affecting epoetin dosage and changes in anaemia management over the last 5 years." Nephrology Dialysis Transplantation **20**(suppl 3): iii3-iii24.

Jacobs, K., C. Shoemaker, et al. (1985). "Isolation and characterization of genomic and cDNA clones of human erythropoietin." Nature **313**(6005): 806-810.

Jelkmann, W. and G. Wiedemann (1990). "Serum erythropoietin level: Relationships to blood hemoglobin concentration and erythrocytic activity of the bone marrow." Journal of Molecular Medicine **68**(8): 403-407.

Kang, M.-J., M. S. Sang, et al. (2010). Characteristics of IEF Patterns and SDS-PAGE Results of Korean EPO Biosimilars. Seoul, Republic of Korea, Korean Chemical Society.

Kawasaki, N., Y. Haishima, et al. (2001). "Structural analysis of sulfated N-linked oligosaccharides in erythropoietin." Glycobiology **11**(12): 1043-1049.

Khan, A., J. Grinyer, et al. (2005). "New urinary EPO drug testing method using two-dimensional gel electrophoresis." Clinica Chimica Acta **358**(1-2): 119-130.

Kinoshita, M., E. Murakami, et al. (2000). "Comparative studies on the analysis of glycosylation heterogeneity of sialic acid-containing glycoproteins using capillary electrophoresis." Journal of Chromatography A **866**(2): 261-271.

Klingmuller, U., U. Lorenz, et al. (1995). "Specific recruitment of SH-PTP1 to the erythropoietin receptor causes inactivation of JAK2 and termination of proliferative signals." Cell **80**(5): 729-738.

LaManna, J. C., J. C. Chavez, et al. (2004). "Structural and functional adaptation to hypoxia in the rat brain." Journal of Experimental Biology **207**(18): 3163-3169.

Lamon, S., L. Martin, et al. (2009). "Effects of Exercise on the Isoelectric Patterns of Erythropoietin." Clinical Journal of Sport Medicine **19**(4): 311-315.

Lamon, S., N. Robinson, et al. (2007). "Detection window of Darbepoetin-α following one single subcutaneous injection." Clinica Chimica Acta **379**(1-2): 145-149.

Lamon, S. v., S. Giraud, et al. (2009). "A high-throughput test to detect C.E.R.A. doping in blood." Journal of Pharmaceutical and Biomedical Analysis **50**(5): 954-958.

Lasne, F. and J. de Ceaurriz (2000). "Recombinant erythropoietin in urine." Nature **405**(6787): 635-635.

Lasne, F., L. Martin, et al. (2002). "Detection of isoelectric profiles of erythropoietin in urine: differentiation of natural and administered recombinant hormones." Analytical Biochemistry **311**(2): 119-126.

Lasne, F., L. Martin, et al. (2007). "Isoelectric profiles of human erythropoietin are different in serum and urine." International Journal of Biological Macromolecules **41**(3): 354-357.

Lasne, F. o., M. Beullens, et al. (2006). "No doubt about the validity of the urine test for detection of recombinant human erythropoietin." Blood **108**(5): 1778-1780.

Leuenberger, N., S. Lamon, et al. (2011) "How to confirm C.E.R.A. doping in athletes' blood?" Forensic Science International **213**(1-3): 101-103.

Leuenberger, N., J. Saugy, et al. (2011) "Methods for detection and confirmation of Hematide™/peginesatide in anti-doping samples." Forensic Science International **213**(1-3): 15-19.

Li, Y., L. Guo, et al. (2008). "High-sensitive determination of human α-thrombin by its 29-mer aptamer in affinity probe capillary electrophoresis." Electrophoresis **29**(12): 2570-2577.

Lin, F. K., S. Suggs, et al. (1985). "Cloning and expression of the human erythropoietin gene." Proceedings of the National Academy of Sciences **82**(22): 7580-7584.

Livnah, O., E. A. Stura, et al. (1999). "Crystallographic Evidence for Preformed Dimers of Erythropoietin Receptor Before Ligand Activation." Science **283**(5404): 987-990.

Llop, E., R. Gutierrez-Gallego, et al. (2008). "Structural analysis of the glycosylation of gene-activated erythropoietin (epoetin delta, Dynepo)." Anal Biochem **383**(2): 243-54.

Lönnberg, M. and J. Carlsson (2000). "Membrane assisted isoform immunoassay: A rapid method for the separation and determination of protein isoforms in an integrated immunoassay." Journal of Immunological Methods **246**(1-2): 25-36.

Lönnberg, M., Y. Dehnes, et al. (2010). "Rapid affinity purification of erythropoietin from biological samples using disposable monoliths." Journal of Chromatography A **1217**(45): 7031-7037.

Lopez-Soto-Yarritu, P., J. C. Díez-Masa, et al. (2002). "Improved capillary isoelectric focusing method for recombinant erythropoietin analysis." Journal of Chromatography A **968**(1-2): 221-228.

Lundby, C., J. J. Thomsen, et al. (2007). "Erythropoietin treatment elevates haemoglobin concentration by increasing red cell volume and depressing plasma volume." The Journal of Physiology **578**(1): 309-314.

Macdougall, I. C. and M. Ashenden (2009). "Current and Upcoming Erythropoiesis-Stimulating Agents, Iron Products, and Other Novel Anemia Medications." Advances in Chronic Kidney Disease **16**(2): 117-130.

MacDougall, I. C., S. J. Gray, et al. (1999). "Pharmacokinetics of Novel Erythropoiesis Stimulating Protein Compared with Epoetin Alfa in Dialysis Patients." Journal of the American Society of Nephrology **10**(11): 2392-2395.

Macdougall, I. C., R. Robson, et al. (2006). "Pharmacokinetics and Pharmacodynamics of Intravenous and Subcutaneous Continuous Erythropoietin Receptor Activator (C.E.R.A.) in Patients with Chronic Kidney Disease." Clinical Journal of the American Society of Nephrology **1**(6): 1211-1215.

Magnani, M., D. Corsi, et al. (2001). "Identification of Blood Erythroid Markers Useful in Revealing Erythropoietin Abuse in Athletes." Blood Cells, Molecules, and Diseases **27**(3): 559-571.

Malcovati, L., C. Pascutto, et al. (2003). "Hematologic passport for athletes competing in endurance sports: a feasibility study." Haematologica **88**(5): 570-581.

Mallorquí, J., R. Gutiérrez-Gallego, et al. (2010). "New screening protocol for recombinant human erythropoietins based on differential elution after immunoaffinity purification." Journal of Pharmaceutical and Biomedical Analysis **51**(1): 255-259.

Mallorqui, J., E. Llop, et al. (2010). "Purification of erythropoietin from human plasma samples using an immunoaffinity well plate." Journal of Chromatography B-Analytical Technologies in the Biomedical and Life Sciences **878**(23): 2117-2122.

Mi, J., S. Wang, et al. (2006). "Efficient purification and preconcentration of erythropoietin in human urine by reusable immunoaffinity column." Journal of Chromatography B **843**(1): 125-130.

Miskowiak, K. W., M. Vinberg, et al. (2010). "Effects of erythropoietin on depressive symptoms and neurocognitive deficits in depression and bipolar disorder." Trials **11**: 10.

Miyake, T., C. K. Kung, et al. (1977). "Purification of human erythropoietin." Journal of Biological Chemistry **252**(15): 5558-5564.

Muirhead, N., P. A. Keown, et al. (2011). "Dialysis patients treated with Epoetin α show improved exercise tolerance and physical function: A new analysis of the Canadian Erythropoietin Study Group trial." Hemodialysis International **15**(1): 87-94.

Nimtz, M., W. Martin, et al. (1993). "Structures of sialylated oligosaccharides of human erythropoietin expressed in recombinant BHK-21 cells." European Journal of Biochemistry **213**(1): 39-56.

Nimtz, M., V. Wray, et al. (1995). "Identification and structural characterization of a mannose-6-phosphate containing oligomannosidic N-glycan from human erythropoietin secreted by recombinant BHK-21 cells." FEBS Letters **365**(2-3): 203-208.

NYDailyNews.com. (2008). "New Jersey race horses test positive for doping." Retrieved 24 November, 2012, from http://www.nydailynews.com/sports/more-sports/new-jersey-race-horses-test-positive-doping-article-1.326984.

Parisotto, R., C. J. Gore, et al. (2000). "A novel method utilising markers of altered erythropoiesis for the detection of recombinant human erythropoietin abuse in athletes." Haematologica **85**(6): 564-72.

Park, S. S., J. Park, et al. (2009). "Biochemical assessment of erythropoietin products from Asia versus US Epoetin alfa manufactured by Amgen." Journal of Pharmaceutical Sciences **98**(5): 1688-1699.

Poortmans, J. R. (1985). "Postexercise Proteinuria in Humans." JAMA: The Journal of the American Medical Association **253**(2): 236-240.

Rabin, O. P., F. Lasne, et al. (2006). "New urinary EPO drug testing method using two-dimensional gel electrophoresis." Clinica Chimica Acta **373**(1-2): 186-187.

Rahbek-Nielsen, H., P. Roepstorff, et al. (1997). "Glycopeptide profiling of human urinary erythropoietin by matrix-assisted laser desorption/ionization mass spectrometry." Journal of Mass Spectrometry **32**(9): 948-958.

Raine, A. (1988). "Hypertension, Blood Viscosity, and Cardiovascular Morbidity in Renal Failure: Implications of Erythropoietin Therapy." The Lancet **331**(8577): 97-100.

Reichel, C. (2008). "Identification of zinc-alpha-2-glycoprotein binding to clone AE7A5 antihuman EPO antibody by means of nano-HPLC and high-resolution high-mass accuracy ESI-MS/MS." Journal of Mass Spectrometry **43**(7): 916-923.

Reichel, C. (2011). "The overlooked difference between human endogenous and recombinant erythropoietins and its implication for sports drug testing and pharmaceutical drug design." Drug Testing and Analysis **3**(11-12): 883-891.

Reichel, C. (2011). "Recent developments in doping testing for erythropoietin." Analytical and Bioanalytical Chemistry **401**(2): 463-481.

Reichel, C., F. Abzieher, et al. (2009). "Sarcosyl-PAGE: a new method for the detection of MIRCERA- and EPO-doping in blood." Drug Testing and Analysis **1**(11-12): 494-504.

Reichel, C., R. Kulovics, et al. (2009). "SDS-PAGE of recombinant and endogenous erythropoietins: benefits and limitations of the method for application in doping control." Drug Testing and Analysis **1**(1): 43-50.

Robinson, N., M. Saugy, et al. (2003). "Effects of exercise on the secondary blood markers commonly used to suspect erythropoietin doping." Clin Lab **49**(1-2): 57-62.

Rush, R. S., P. L. Derby, et al. (1995). "Microheterogeneity of Erythropoietin Carbohydrate Structure." Analytical Chemistry **67**(8): 1442-1452.

Schellekens, H. (2009). "Assessing the bioequivalence of biosimilars The Retacrit case." Drug Discov Today **14**(9-10): 495-9.

Shahrokh, Z., L. Royle, et al. (2011). "Erythropoietin Produced in a Human Cell Line (Dynepo) Has Significant Differences in Glycosylation Compared with Erythropoietins Produced in CHO Cell Lines." Molecular Pharmaceutics **8**(1): 286-296.

Sharpe, K., M. Ashenden, et al. (2006). "A third generation approach to detect erythropoietin abuse in athletes." Haematologica **91**(3): 356-363.

Shen, R., L. Guo, et al. (2010). "Highly sensitive determination of recombinant human erythropoietin-α in aptamer-based affinity probe capillary

electrophoresis with laser-induced fluorescence detection." Journal of Chromatography A **1217**(35): 5635-5641.

Skibeli, V., G. Nissen-Lie, et al. (2001). "Sugar profiling proves that human serum erythropoietin differs from recombinant human erythropoietin." Blood **98**(13): 3626-3634.

Takegawa, Y., H. Ito, et al. (2008). "Profiling of N and O-glycopeptides of erythropoietin by capillary zwitterionic type of hydrophilic interaction chromatography/electrospray ionization mass spectrometry." Journal of Separation Science **31**(9): 1585-1593.

Takeuchi, M., S. Takasaki, et al. (1988). "Comparative study of the asparagine-linked sugar chains of human erythropoietins purified from urine and the culture medium of recombinant Chinese hamster ovary cells." Journal of Biological Chemistry **263**(8): 3657-3663.

Takeuchi, M., S. Takasaki, et al. (1990). "Role of sugar chains in the in vitro biological activity of human erythropoietin produced in recombinant Chinese hamster ovary cells." Journal of Biological Chemistry **265**(21): 12127-30.

Tangvoranuntakul, P., P. Gagneux, et al. (2003). "Human uptake and incorporation of an immunogenic nonhuman dietary sialic acid." Proceedings of the National Academy of Sciences **100**(21): 12045-12050.

Tsuda, E., M. Goto, et al. (1988). "Comparative structural study of N-linked oligosaccharides of urinary and recombinant erythropoietins." Biochemistry **27**(15): 5646-5654.

Tuerk, C. and L. Gold (1990). "Systematic evolution of ligands by exponential enrichment: RNA ligands to bacteriophage T4 DNA polymerase." Science **249**(4968): 505-510.

Van Maerken, T., A. Dhondt, et al. (2010). "A rapid and simple assay to determine pegylated erythropoietin in human serum." Journal of Applied Physiology **108**(4): 800-803.

Varki, A. (2001). "N-glycolylneuraminic acid deficiency in humans." Biochimie **83**(7): 615-622.

Varki, A., R. Cummings, et al., Eds. (2009). Essentials of Glycobiology. Cold Spring Harbor (NY), Cold Spring Harbor Laboratory Press.

Verdier, F. d. r., P. Walrafen, et al. (2000). "Proteasomes Regulate the Duration of Erythropoietin Receptor Activation by Controlling Down-regulation of Cell Surface Receptors." Journal of Biological Chemistry **275**(24): 18375-18381.

Voss, S., A. Lüdke, et al. (2010). "Effects of High Intensity Exercise on Isoelectric Profiles and SDS-PAGE Mobility of Erythropoietin." Int J Sports Med **31**(06): 367,371.

WADA. (2009). "Harmonization of the method for the identification of recombinant erythropoietins (i.e. epoetins) and analogues (e.g. darbepoetin and methoxypolyethylene glycol-epoetin beta)." Retrieved 05 Jan 2012, from http://www.wada-ama.org/Documents/World_Anti-Doping_Program/WADP-IS-Laboratories/Technical_Documents/WADA_TD2009EPO_Harmonization_of_Method_Identificiation_Recombinant_Erythropoietins_Analogues_EN.pdf.

WADA. (2009). "MAIIA method for EPO detection." Retrieved 05 Jan 2012, from http://www.wada-ama.org/Documents/Science_Medicine/Scientific%20Events/Tokyo_Symposium_2009/WADA_Tokyo_Symposium_Dr.Carlsson-Dr.L%C3%B6nnberg-Dr.Garle.pdf.

WADA. (2010). "Athlete biological passport. Operating guidelines and compilation of required elements." Retrieved 05 Jan 2012, from http://www.wada-ama.org/Documents/Resources/Guidelines/WADA_ABP_OperatingGuidelines_EN_2.1.pdf.

Wang, H., P. Dou, et al. (2012). "Immuno-magnetic beads-based extraction-capillary zone electrophoresis-deep UV laser-induced fluorescence analysis of erythropoietin." Journal of Chromatography A(0).

Wang, W., S. Zhang, et al. (2009). "CE immunoassay with enhanced chemiluminescence detection of erythropoietin using silica dioxide nanoparticles as pseudostationary phase." Electrophoresis **30**(17): 3092-3098.

Watson, E. and F. Yao (1993). "Capillary Electrophoretic Separation of Human Recombinant Erythropoietin (r-HuEPO) Glycoforms." Analytical Biochemistry **210**(2): 389-393.

Wide, L., B. Wikstrom, et al. (2003). "A new principle suggested for detection of darbepoetin-alpha (NESP) doping." Upsala Journal of Medical Sciences **108**(3): 229-238.

Wish, J. B. (2011). "Erythropoiesis-stimulating agents and pure red-cell aplasia: you can't fool Mother Nature." Kidney Int **80**(1): 11-13.

Wu, H., X. Liu, et al. (1995). "Generation of committed erythroid BFU-E and CFU-E progenitors does not require erythropoietin or the erythropoietin receptor." Cell **83**(1): 59-67.

Wustenberg, T., M. Begemann, et al. (2011). "Recombinant human erythropoietin delays loss of gray matter in chronic schizophrenia." Molecular Psychiatry **16**(1): 26-36.

Yi, T., J. Zhang, et al. (1995). "Hematopoietic cell phosphatase associates with erythropoietin (Epo) receptor after Epo-induced receptor tyrosine phosphorylation: identification of potential binding sites." Blood **85**(1): 87-95.

Yu, B., H. Cong, et al. (2005). "Separation and detection of erythropoietin by CE and CE-MS." TrAC Trends in Analytical Chemistry **24**(4): 350-357.

Yu, N., E. Ho, et al. (2010). "Doping control analysis of recombinant human erythropoietin, darbepoetin alfa and methoxy polyethylene glycol-epoetin beta in equine plasma by nano-liquid chromatography–tandem mass spectrometry." Analytical and Bioanalytical Chemistry **396**(7): 2513-2521.

Zhang, J., U. Chakraborty, et al. (2009). "Optimization and qualification of capillary zone electrophoresis method for glycoprotein isoform distribution of erythropoietin for quality control laboratory." Journal of Pharmaceutical and Biomedical Analysis **50**(3): 538-543.

Zhang, Z., L. Guo, et al. (2010). "In vitro lectin-mediated selection and characterization of rHuEPO-α-binding ssDNA aptamers." Bioorganic & Medicinal Chemistry **18**(22): 8016-8025.

Zhang, Z., L. Guo, et al. (2009). "An aptameric molecular beacon-based "Signal-on" approach for rapid determination of rHuEPO-alpha" Talanta **80**(2): 985-990.

Zhao, L., H. Dong, et al. (2009). "A JAK2 Interdomain Linker Relays Epo Receptor Engagement Signals to Kinase Activation." Journal of Biological Chemistry **284**(39): 26988-26998.

Zhu, X. and M. A. Perazella (2006). "Hematology: Issues in the Dialysis Patient: Nonhematologic Complications of Erythropoietin Therapy." Seminars in Dialysis **19**(4): 279-284.

Chapter 2: Extraction of EPO from urine using antibody activated paramagnetic beads

Aim: to use antibody activated paramagnetic beads to extract EPO from urine samples, with greater recovery or in shorter time than the current standard method of ultrafiltration.

2.1 Introduction

Extraction of EPO from urinary samples has generally been performed using ultrafiltration using successive 30 kDa filters. In this way, EPO is retained in the sample, while the sample volume is reduced from 20 mL to about 20 µL, a 1000 fold increase in concentration. This is a time consuming process, requiring multiple centrifugation steps and producing a final sample which will also contain any other large urinary compounds. Their presence means that the extract is often thick and viscous, making it difficult to apply to an isoelectric focusing gel and unsuitable for analysis, for example, by LC-MS. The presence of high amounts of protein in the retentate can also result in distortion of the EPO bands on the IEF gel, while the retention of urinary proteases means that an additional heating and cooling step is required before the samples can be run.

Immunoaffinity extraction uses antibodies to bind analytes of interest specifically. Extraction using an immunoaffinity approach would seem to be a more desirable approach than ultrafiltration, as it could mean the removal of interfering and unwanted proteins and produce a product more amenable to analysis by LC-MS, with or without initial digestion.

Antibody modified extraction columns have been shown to be effective (Mi, Wang et al. 2006). However, they are expensive and time consuming to produce, and the issue of carryover, which would prevent their use in anti-doping work, was not addressed. Extraction from blood using antibody modified paramagnetic beads has been demonstrated (Skibeli, Nissen-Lie et al. 2001). However, these used polyclonal antibodies, and tosyl-activated beads. Tosyl groups will bind to any amino group on the antibody; use of Protein G coated beads should improve antibody orientation (as shown in figure 2.1), potentially improving recovery, whilst correct selection of monoclonal antibody should improve specificity of EPO extraction. Since blood samples are less desirable than urine samples in anti-doping (due to the increased difficulty of collection and the more invasive nature of sampling), the aim of this work was to develop a method for the successful extraction of EPO from urinary

samples using paramagnetic beads (Dynabeads) modified with monoclonal anti-EPO antibodies.

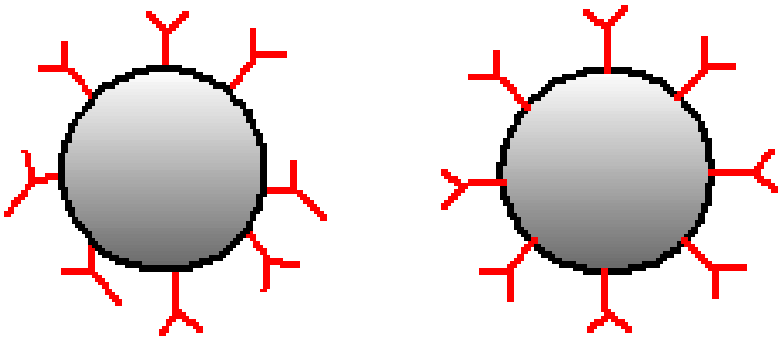

Figure 2.1: Theoretical improved antibody orientation on Protein G coated beads (right) compared with tosylated beads (left)

2.2 Experimental

2.2.1 Materials and equipment

Dynabeads Protein G paramagnetic beads were purchased from Invitrogen (Paisley, UK). Streptavidin coated LodeStar paramagnetic beads were a generous gift from Varian, Inc. (Oxford, UK). Bis(sulfosuccinimidyl) suberate (BS3), Sulfo-NHS-LC-biotin, goat anti-mouse antibodies and HRP-Streptavidin conjugate were bought from Pierce Protein Research Products, a division of Thermo Fisher Scientific. Recombinant EPO standard (88/574) was purchased from NIBSC (Hertfordshire, UK). Eprex rEPO was from Janssen-Cilag (High Wycombe, UK). Complete protease inhibitor was bought from Roche (Welwyn Garden City, UK). Hydrochloric acid and acetonitrile (HPLC gradient grade) were purchased from Fisher Scientific (Loughborough, UK). Formic acid was from VWR International (Pennsylvania, USA). Immulite EPO quantification test kits (Immulite 1000 EPO assay) were purchased from Siemens (Frimley, UK). Anti-EPO antibodies (clones AE7A5 and 9C21D11) were purchased from R&D Systems (Abingdon, UK). Tris was bought from Amersham Biosciences (Buckinghamshire, UK). Trypsin was from Promega (Southampton, UK). Amicon and Microcon centrifugal filters, Steriflip filters, Durapore membranes and Immobilon membranes were from Millipore

(Watford, UK). ChemiGlow West Chemiluminescence Substrate Kit was from ProteinSimple (Ringmer, UK). Non-fat milk powder was from Marvel (St Albans, UK). Servalyt ampholytes were from Serva Electrophoresis (Heidelberg, Germany). Black ink was from Winsor & Newton (London, UK). MAIIA monolithic cartridges were from MAIIA Diagnostics (Uppsala, Sweden). All other chemicals were of analytical grade and were purchased from Sigma Aldrich (Poole, UK).

Quantification of rEPO in samples was carried out using the Immulite immunoassay system.

Separation of Dynabeads was carried out using a magnetic separator from New England Biolabs (Ipswich, Massachusetts, USA).

LC-MS/MS was carried out using a Waters (Manchester, UK) nanoAcquity UPLC system, combined with a Waters Premier Quattro triple-quadrupole mass spectrometer with Waters nanospray source.

2.2.2 Dynabead Protein G preparation

Dynabeads were prepared as in manufacturer's instructions. Briefly, 50 µL was washed twice with 0.1 M phosphate buffer (pH 7.0) with 0.01% Tween 20, (wash and bind, W&B, buffer) each time separating the beads out on a magnet. Ten microlitres (1 mg/mL) anti-EPO AE7A5 was added to 200 µL W&B buffer and this added to the beads. These were incubated at room temperature on a multi-tube vortex for ten minutes then washed using 0.01 M phosphate buffered saline (PBS) twice.

2.2.3 Cross linking of beads

BS3 solution was made up fresh, and incubated for 30 minutes with the modified Dynabeads to cross link antibodies to their surface. Beads were then incubated in 200 µL 50 mM Tris-HCl buffer to quench the reaction, then washed twice more using PBS to produce Dynabeads ready for extraction. Modified and cross linked

beads were stored in PBS with 0.01% Tween 20. Volume used to store beads was the same as the initial volume of beads.

2.2.4 EPO extraction (direct method)

The direct and indirect methods of extraction are illustrated in figure 2.2. For the direct method, 50 µL beads were incubated with 20 mL of 10 mIU/mL aqueous rEPO solution with gentle shaking. Aliquots (250 µL) were taken every half hour, for analysis using Immulite.

2.2.5 EPO extraction (indirect method)

Anti-EPO (10 µg) was incubated with 20 mL of 10 mIU/mL rEPO solution, pH 7.4, 0.01% Tween 20 overnight. Dynabeads Protein G (50 µL) were then added, and the tubes incubated at room temperature with aliquots taken for analysis at 1, 3, 7 and 24 hours and frozen for later analysis with Immulite. A control sample with no addition of beads was run at the same time.

2.2.6 Effect of presence of antibodies on Immulite results

To check if the presence of antibodies to EPO could prevent the Immulite detection of the glycoprotein, 1 mL of 20 mIU/mL rEPO was added to 10 µg anti-EPO, vortexed and a 250 µL sample taken, then incubated on a plate shaker with further samples taken at 2 and 4 hours. The EPO concentration was then compared to that measured in a tube without antibody added.

2.2.7 Biotinylation of antibodies

Ultrapure water (360 µL) was added to 2 mg of sulfo-NHS-LC-biotin. 6.5 µL of solution was immediately added to 200 µg anti-EPO and the mixture placed on ice

for two hours. The solution was then transferred to a 30 kDa Microcon and centrifuged to remove unreacted biotin. The membrane of the filter was then washed with 200 µL PBS and the retentate transferred to a new tube and frozen at -80 ºC.

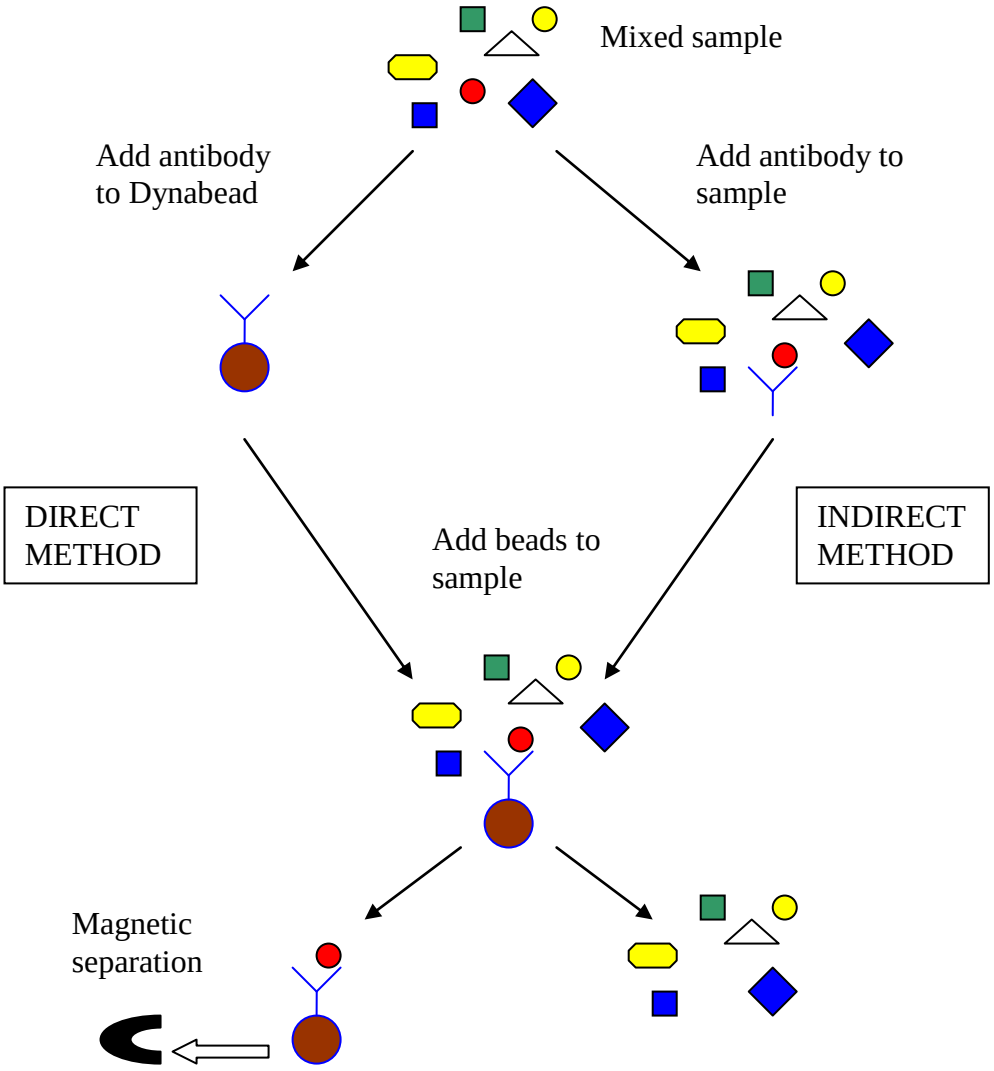

Figure 2.2: Direct and indirect method for extraction of analytes using paramagnetic Protein G coated Dynabeads. The direct method can theoretically allow the reuse of beads, but the indirect method may be better if the concentration of the target analyte is low or the specific affinity is weak.

2.2.8 Steptavidin coated LodeStar bead preparation

LodeStar beads (100 µL) were washed once with tris buffered saline (TBS) then incubated for 1 hour with 10 µL biotinylated anti-EPO. Beads were washed gently three times with 300 µL TBS.

2.2.9 Streptavidin coated LodeStar bead extraction of EPO

1.5 mL of 100 mIU/mL rEPO was added to the beads produced in 2.2.8 and the sample incubated for 21 hours, with 250 µL aliquots taken at intervals and analysed using Immulite. A control sample without beads was incubated and sampled simultaneously. Beads were then washed in 200 µL TBS, transferred to a new tube and 25 µL glycine buffer (pH 2.4) added. The sample was incubated for 2 minutes then magnetically separated and the supernatant added to 225 µL of 1 M Tris-HCl buffer, before being analysed again using Immulite.

2.2.10 Extraction using biotinylated goat anti-mouse antibodies

Lodestar beads (100 µL) were washed as in 2.2.8, then incubated with 10 µL biotinylated goat anti-mouse antibodies in 300 µL TBS for 1 hour at room temperature with shaking. Beads were gently washed three times with TBS, then incubated with mouse anti-EPO (clone AE7A5) for two hours. The beads were then washed gently again with TBS, twice.

rEPO (60 mIU/mL) was made up in 0.01 M PBS, with 0.05% sodium azide as a preservative. Beads were gently washed twice with TBS, then resuspended in 50 µL TBS and added to 1.5 mL of EPO solution. 250 µL aliquots were taken at hourly intervals and frozen overnight, then defrosted and analysed using Immulite. A control sample without beads was run and sampled simultaneously.

2.2.11 Effect of Thimerosal/Complete/Sodium azide

To ensure that breakdown of rEPO in solution by bacteria was minimised, antibacterials were added to the solution. To see if these had any effect on the binding of rEPO to beads, the experiment in 2.2.10 was repeated using 20 mIU/mL rEPO solution, without the addition of any preservative, and with the replacement of sodium azide with 0.05% thimerosal or Complete protease inhibitor (1 tablet dissolved in 50 mL 0.01 PBS).

2.2.12 Effect of heating urine before extraction

To see if binding of AE7A5 antibody to EPO is to domains only exposed after denaturation of the hormone, 20 mL urine samples were buffered with 3.75 M Tris-HCl to approximately pH 7. They were heated at 90 °C for 10 minutes, then allowed to cool, and then incubated with 50 µL Dynabeads made up as in 2.2.2 and 2.2.3 for 30 minutes. Beads were removed using a magnetic separator, and urine samples then analysed using the standard isoelectric focusing/immunoblotting method. Control urine samples were heated then incubated with unmodified Dynabeads, before being analysed in the same way.

2.2.13 Modification of Dynabeads using antibody 9C21D11

Protein G coated Dynabeads were modified in the same way as in 2.2.2 and 2.2.3, using anti-EPO antibody 9C21D11. Recombinant EPO solution (50 mIU/mL) was made up in PBS + 0.02% sodium azide. Fifty microlitres of beads were added to 20 mL of the solution and incubated on a blood spinner for 24 hours, with aliquots taken at intervals, frozen and then analysed using Immulite. A control solution with unmodified beads was analysed at the same time.

2.2.14 Effect of cross linking

Dynabeads modified with antibody 9C21D11 and cross linked as in 2.2.3 were incubated with rEPO solution (50 mIU/mL), made up as in 2.2.13, for 1 hour. An aliquot was then taken and analysed using Immulite. Dynabeads modified with the same antibody but not cross linked were incubated and analysed at the same time.

2.2.15 Necessity of cross-linking

It was hoped that it would be possible to reuse modified Dynabeads more than once. To investigate if cross-linking of antibodies to Dynabeads was necessary, the ability of Dynabeads to bind rEPO after several incubation/wash/elution steps was investigated. Dynabeads were modified as in 2.2.13, and either cross-linked or not. Recombinant EPO solution was made up as in 2.2.13. 50 µL of Dynabeads were added to either 20 mL of rEPO solution, or 20 mL of a PBS + 0.02% sodium azide blank. Samples were incubated for 1 hour at room temperature, with rotation. Aliquots were then taken from the rEPO solution and frozen, before being defrosted and analysed using Immulite. Beads from the blank solution were removed using a magnetic separator, and washed once using 250 µL 0.01 M PBS. Elution was carried out using 50 µL phosphate buffer, pH 2.2, + 0.01% PEG 6000. Beads were incubated for 30 minutes at room temperature with gentle shaking, then removed using a magnetic separator, and washed twice using 250 µL 0.01 M PBS + 0.02 % Tween 20. This process was repeated twice more, so that for both crosslinked and non-crosslinked beads, the efficacy of extraction could be measured after no, one and two elution cycles.

2.2.16 Dynabead extraction from spiked urine samples

Attempts to quantify rEPO spiked into urine samples using Immulite proved unsuccessful, with significant differences in the measured values of repeats of rEPO standards. This occurred despite the use of 3.75 M Tris-HCl, pH 7.4 to ensure urine pH was theoretically suitable and the addition of human serum albumin. As a result,

extraction from urine samples was measured using LC-MS/MS instead. To improve accuracy, endogenous urinary EPO was removed from urine by ultrafiltering it through a 30 kDa filter. Filtered urine was pooled, then measured into 20 mL aliquots.

Table 2.1: Theoretical tryptic fragments of rEPO

Tryptic Fragment	Start-End	Sequence
T1	1-4	APPR
T2	5-10	LICDSR
T3	11-14	VLER
T4	15-20	YLLEAK
T5	21-45	EAENITTGCAEHCSLNENITVPDTK
T6	46-52	VNFYAWK
T7	53-53	R
T8	54-76	MEVGQQAVEVWQGLALLSEAVLR
T9	77-97	GQALLVNSSQPWEPLQLHVDK
T10	98-103	AVSGLR
T11	104-110	SLTTLLR
T12	111-116	ALGAQK
T13	117-131	EAISPPDAASAAPLR
T14	132-139	TITADTFR
T15	140-140	K
T16	141-143	LFR
T17	144-150	VYSNFLR
T18	151-152	GK
T19	153-154	LK
T20	155-162	LYTGEACR
T21	163-165	TGD

Digests of rEPO were carried out by making up standards in 100 mM glycine buffers, pH 1.8 and pH 11. Standards were made up so that 70 µL pH 11 buffer added to 30 µL pH 1.8 buffer gave a neutral (pH 7.4) solution. Standards were made up at 50, 100, 250, 500, 750 and 1000 ng/mL rEPO. Separate pH standards were incubated at room temperature for 30 minutes before being mixed together. Mixed standards or samples were heated at 80 °C for ten minutes, then allowed to cool to room temperature. 10 µL trypsin solution (10 µg/mL, in 50 mM ammonium bicarbonate, pH 7.4) was added and samples were incubated overnight at 37 °C.

Concentration of rEPO was determined by measuring the peak area of three transitions for a peptide from the rEPO digest characteristic of human EPO. The

selected peptide was ^{144}VYSNFLR^{150} (Table 2.1, T17 fragment), chosen because as well as being characteristic of EPO, repeated overnight digests of EPO demonstrated that the fragment was a reliable indicator of total EPO concentration.

Chromatographic separation was carried out using a Waters nanoAcquity Symmetry C18, 180 µm x 20 mm trapping column, and a Waters nanoAcquity BEH C18, 100 µm x 150 mm separation column. Solvent A was ultrapure water, with 0.1% formic acid. Solvent B was acetonitrile with 0.1% formic acid. Samples were moved onto the trapping column by running 99.5% A at 15 µL/min for 1 minute. LC run conditions were: 0.4 µL/min flow rate; 99% A at start, decreasing linearly to 57% A at 20 minutes. Decrease linearly to 20% A at 21 minutes, hold to 25 minutes, raise linearly to 99% A at 26 minutes, hold to 30 minutes. Column temperature was set at 35 °C, sample tray temperature at 4 °C.

Mass spectrometer was operated in positive ionisation SIM mode, for transitions 450.0 → 235.2, 636.4, 799.4. Mass spectrometer conditions were:

Capillary: 3.20 kV, Cone: 32 V, Extractor: 3 V, RF Lens: 0.6 V

Quadrupole 1: Low mass resolution: 14.0, High mass resolution: 14.0,
Ion energy: 0.5

Collision cell: Entrance: -1, Collision: 20, Exit: 2.0

Quadrupole 2: Low mass resolution: 14.0, High mass resolution: 14.0,
Ion energy: 1.0

Mutiplier: 650
Collision gas flow: 0.18 mL/min

Two injections (5 µL) were made for each standard concentration and the mean peak area for each transition measured. These were then summed to give a total area for the three transitions.

Linearity for the standard curve produced by this method was better if the measurements for 50 ng/mL were disregarded. As a result, it was decided to spike samples at a concentration that would produce a solution of concentration 500 ng/mL if recovery was 100%. With 20 mL urine samples, this meant spiking at 2.5 ng/mL, i.e. 50 ng in total.

Four spiked urine samples were incubated with Dynabeads modified as in 2.2.13. 50 µL of Dynabeads were added to 20 mL of urine, which had been ultrafiltered to remove endogenous EPO then spiked with 50 ng Eprex rEPO. Urine had 2 mL of 3.75 M Tris-HCl, pH 7.4 added, with further Tris-HCl added dropwise to ensure urine pH was between 7 and 8. Dynabeads were incubated in urine for 2 hours, then removed using a magnetic separator and washed with 250 µL PBS. The first elution was carried out using 70 µL 100 mM glycine-NaOH, pH 11, for 30 minutes at room temperature with shaking. A second elution was carried out using 30 µL 100 mM glycine-HCl, pH 1.8. The two elutions were mixed, and digestion and LC-MS/MS analysis carried out as above. Standard digests of 100, 500 and 1000 ng/mL rEPO were carried out at the same time. Recovery by Dynabeads was calculated by dividing the observed total peak area of the transitions by the theoretical total peak area of the transitions at 500 ng/mL obtained from the generated standard curve.

2.2.17 Isoform selectivity of Dynabeads extractions

To examine if extraction by Dynabeads modified with antibody 9C21D11 showed selectivity for some isoforms over others, ultrafiltered urine was spiked with either huEPO or rEPO (NIBSC) at a concentration of approximately 1 mIU/mL. 20 mL urine samples were incubated with Dynabeads and elutions carried out as in 2.2.16. After elution and mixing, eluates were dried down under vacuum, then reconstituted in 20 µL 50 mM Tris-HCl, pH 7.4, containing 1% (w/v) bovine serum albumin. Samples were then analysed using the standard isoelectric focusing/immunoblotting procedure, outlined in 1.9.1

2.2.18 Extraction of EPO from unfiltered urine in comparison with MAIIA monolithic cartridges

Extraction of huEPO using Dynabeads was compared to that of identical samples using MAIIA immunoaffinity monolithic cartridges. It has been reported that MAIIA cartridges showed slightly poorer recovery of EPO from urine samples compared to ultrafiltration, but that isoelectric focusing profiles were improved due to reduced background and band distortion (Lönnberg, Dehnes et al. 2010). To examine if the same was true of Dynabeads, two (non-filtered) urine samples were split into three 20 mL aliquots. One was extracted using ultrafiltration, one with MAIIA cartridges and one with Dynabeads. Briefly, ultrafiltration involved addition of Complete protease inhibitor and buffering to approximately pH 7, followed by ultrafiltration through a 30 kDa centrifugal filter, to obtain a final retentate with a volume of 20 to 40 µL. MAIIA extraction involved passing the urine samples through a MAIIA antibody monolithic cartridge, followed by a wash step and elution from the cartridge in 55 µL of elution buffer. Dynabead extraction was carried out as in 2.2.16. Samples were then analysed using the standard isoelectric focusing/immunoblotting procedure.

2.2.19 Extraction of EPO by sequential Dynabeads/ultrafiltration

A single urine sample was split into four 20 mL aliquots, and extracted either by ultrafiltration or with Dynabeads as in 2.2.16. Urine samples extracted using Dynabeads were kept and remaining EPO was extracted using ultrafiltration as in 2.2.18. Samples were then analysed using the standard IEF/Immunoblotting procedure.

2.2.20 Extraction of EPO from buffer, ultrafiltered urine and whole urine

To demonstrate the differing capability of Dynabeads as an extraction process from different matrices, 20 mL solutions of EPO were made up using NIBSC huEPO standard at 1 mIU/mL in either 50 mM Tris-HCl, pH 7.4 or urine which had been

filtered using a 30 kDa filter. Two 20 mL aliquots of a sample of urine were ultrafiltered until their volume was below 200 µL, a 6 µL aliquot taken and made up to 250 µL with 50 mM Tris-HCl, pH 7.4, then their EPO concentrations measured using Immulite. The mean concentration was then used to adjust the concentration of the original urine sample (using ultrafiltered urine) to 1 mIU/mL. All three types of solution were then extracted using Dynabeads as in 2.2.16, and samples analysed using the standard isoelectric focusing/immunoblotting procedure.

2.3 Results

2.3.1 EPO Extraction (direct method)

Table 2.2 Direct Dynabead extraction of rEPO from aqueous solution

Incubation time (minutes)	Mean rEPO concentration (mIU/mL) (n=2)
0	6.0
30	7.4
60	7.2
90	7.3

As can be seen from Table 2.2 above, there was no apparent extraction of rEPO from solution using the direct method, as mean rEPO concentration did not fall over time. If anything, the concentration of EPO in solution appeared to increase post incubation with the beads, although this is likely to be due to a lack of accuracy in the measurement of EPO concentration.

2.3.2 EPO extraction (indirect method)

Table 2.3. Indirect method extraction of rEPO using Dynabeads

Incubation time (hours)	Mean Control rEPO concentration (mIU/mL) (n=2)	Mean Dynabead rEPO concentration (mIU/mL) (n=2)
0[a]	9.7	8.9
0[b]	4.8	4.9
1	5.1	5.2
3	5.2	5.6
7	5.0	5.2
24	4.7	6.1

[a] At start of incubation with anti-EPO antibodies

[b] At start of incubation with Dynabeads

As can be seen from Table 2.3 above, using the indirect method for extraction there was again no extraction of rEPO seen. A fall in EPO concentration in samples incubated with Dynabeads was observed, but this was also seen in the control sample and was therefore likely to be due to degradation of rEPO in the samples, possibly due to bacterial action.

2.3.3 Effect of presence of antibodies on Immulite results

Table 2.4. Effect of the addition of anti-EPO antibodies on apparent Immulite results

Incubation time (hours)	rEPO concentration – control (mIU/mL)	rEPO concentration – antibodies added (mIU/mL)
0	19.6	16.5
2	18.9	16.1
4	18.5	16.1

The addition of antibodies against EPO to a solution of EPO did appear to reduce slightly the apparent level of EPO in solution as measured using Immulite (see Table 2.4) presumably because binding of the Immulite antibodies to EPO was reduced because the initial antibodies either bind all or part of the same epitope, or because they sterically hinder the binding of further antibodies to a different epitope. However, the difference was not large, and would only affect results if an indirect method of extraction was used.

2.3.4 Use of biotinylated goat anti-mouse antibodies

Table 2.5. Extraction using biotinylated goat anti-mouse antibodies

Incubation time (hours)	Mean EPO conc. – control (mIU/mL) (n=2)	Mean EPO conc. - with beads (mIU/mL) (n=2)
0	60.3	60.3
0.25	64.5	62.4
1	60.2	61.6
3	66.2	58.7
5	61.5	61.2
24	66.7	66.8

Again, Table 2.5 shows that no obvious extraction of EPO from solution was seen, with the mean EPO concentrations in both the control and Dynabead incubations remaining approximately the same throughout the incubation. It is possible that there was a decrease in concentration after 3 hours incubation with the beads, and that this was due to binding which later broke down, possibly due to degradation of the antibody. However, the decrease (and therefore the degree of binding of EPO to the beads) was very small from the starting concentration, and within the range that could be expected from measuring the same concentration again.

2.3.5 Extraction using biotinylated anti-EPO

Table 2.6. Extraction of rEPO using biotinylated anti-EPO activated beads

Incubation time (hours)	rEPO concentration (mIU/mL)	
	Control	+ activated beads
0	103	103
0.25	97.0	102
1	101	83.4
3	102	93.2
5	95.0	102
21	102	94.3
Eluate		1.1

Once more, Table 2.6 shows there is no clear pattern of extraction of rEPO from solution. Variability in the concentration detected in the control sample, and in particular its fall and subsequent rise, suggest a degree of error in the accuracy of measurements which could account for changes seen in the sample incubated with activated beads.

2.3.6 Effect of Thimerosal/Complete/Sodium azide on rEPO extraction

Table 2.7. Effect of different preservatives (PRES) on extraction of rEPO using biotinylated goat anti-mouse and mouse anti-EPO antibodies

Incubation time (hours)	rEPO concentration (mIU/mL)						
	No beads/ no PRES	Beads, no PRES	Beads, +SA	No beads, +SA	Beads, +T	No beads, +T	Beads, +C
0	23.1	19.4	20.1	22.4	20.1	22.5	21.5
1	18.7	16.2	20.8	21.9	21.5	20.5	19.4
2	16.5	12.9	20.5	22.6	20.0	19.1	19.2
3	14.6	9.8	19.6	20.7	22.1	20.0	21.0
4	14.1	9.7	20.4	19.4	20.5	20.4	20.4

SA = sodium azide, T = thimerosal, C = Complete solution

Table 2.7 above shows that in the absence of a preservative or beads, there is a fall in the EPO concentration in solution, presumably due to degradation of EPO by microorganisms. There is a similar sized fall when beads are present, which could mean that there is no binding by the beads of EPO, or that any binding is being masked by degradation of the EPO. The use of anti-bacterials and a protease inhibitor demonstrate that when degradation is prevented, there is no apparent binding of EPO to the beads.

2.3.7 Effect of heating urine samples before extraction

Profiles of urine samples heated, then ultrafiltered and analysed by IEF/immunoblotting after incubation with Dynabeads modified with antibody AE7A5 did not differ from those heated then incubated with non-modified Dynabeads. In all, EPO was clearly detected, demonstrating that heating of urine samples did not result in binding of EPO to Dynabeads.

2.3.8 Modification of Dynabeads with antibody 9C21D11

The concentration of rEPO in solution dropped rapidly when incubated with Dynabeads modified with antibody 9C21D11, as shown in Table 2.8 and figure 2.3.

Table 2.8: Effect on rEPO concentration of incubation with Dynabeads modified with antibody 9C21D11

Time (hours)	Mean EPO concentration (mIU/mL) (n=2)	
	Control	Dynabeads
0	52.4	54.0
0.5	47.1	17.5
1	51.6	15.9
2	53.7	15.4
4	50.3	14.6
24	31.9	14.5

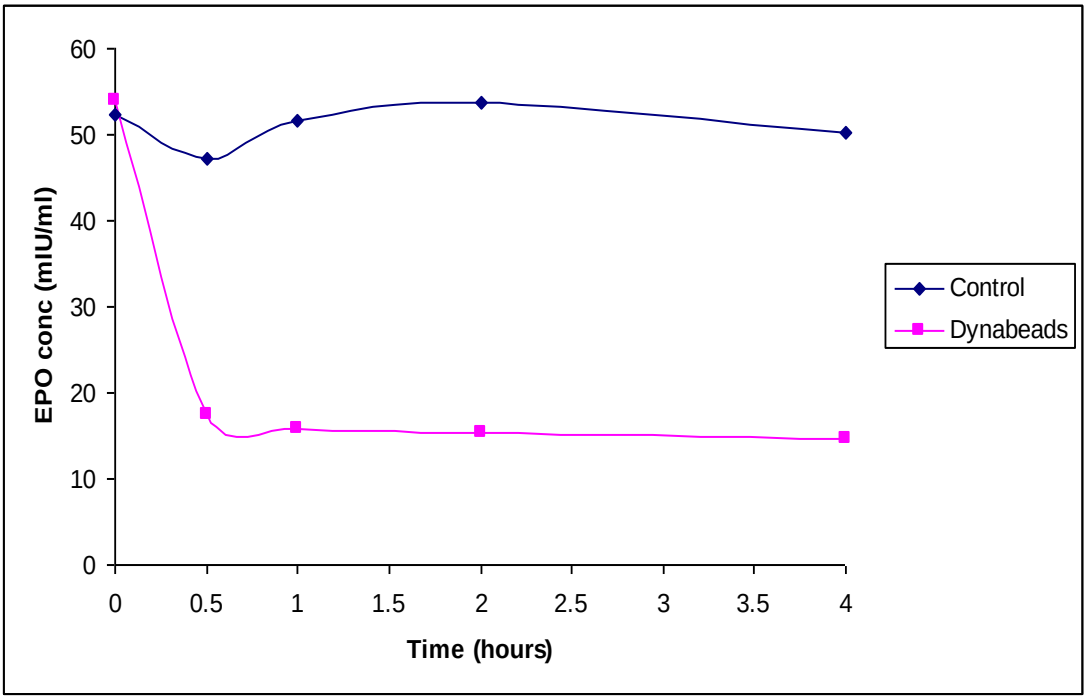

Figure 2.3: Effect on rEPO concentration of incubation with Dynabeads modified with antibody 9C21D11

2.3.9 Effect of crosslinking

As shown in Table 2.9, cross-linking the antibodies to the beads did not affect their ability to bind rEPO.

Table 2.9: Effect of cross-linking antibody-modified Dynabeads on the ability of these beads to bind rEPO

	No beads	AB modified Dynabeads	AB modified and crosslinked Dynabeads
Mean Initial concentration rEPO (mIU/mL) (n=2)	52.6	50.8	50.6
Mean Final concentration rEPO (mIU/mL) (n=2)	51.4	13.7	13.2

2.3.10 Necessity of cross-linking

Initial binding capacity of the Dynabeads was largely unaffected by the cross linking procedure; in Table 2.9, the fall in rEPO concentration was slightly larger with the cross-linked beads; in Table 2.10, the fall was slightly less. However, the binding capacity of the non-cross-linked beads fell off significantly after multiple elution cycles, whereas that of the cross-linked beads remained approximately the same (standard deviation of fall in EPO concentration after incubation of 0.66 for cross-linked beads, compared with 6.81 for non-cross-linked). This, presumably, was due to loss of antibodies from the surface of the beads, with the binding of the Protein G coating to the antibodies being disrupted in the same way as the binding of the antibodies to rEPO would be. This loss is of course prevented when the antibodies are covalently attached.

Table 2.10: Effect of multiple binding/wash/elution cycles on the binding capacity of cross-linked and non-cross-linked Dynabeads

Elution cycles before extraction	Incubation time (hours)	Mean. conc of rEPO (mIU/mL)	
		Cross-linked Dynabeads	Non-cross-linked Dynabeads
0	0	49.0	50.0
0	1	14.8	13.0
1	0	48.9	48.9
1	1	13.4	19.2
2	0	51.9	50.4
2	1	17.2	27.0

2.3.11 Dynabead extraction from spiked urine samples

The spectrum obtained by fragmenting the doubly charged T17 peptide is shown in figure 2.4. From this it was decided to use transitions m/z 450.0 to 236.2 (a_2), 636.4 (y_5) and 799.4 (y_6) in the SIM mode for quantitation.

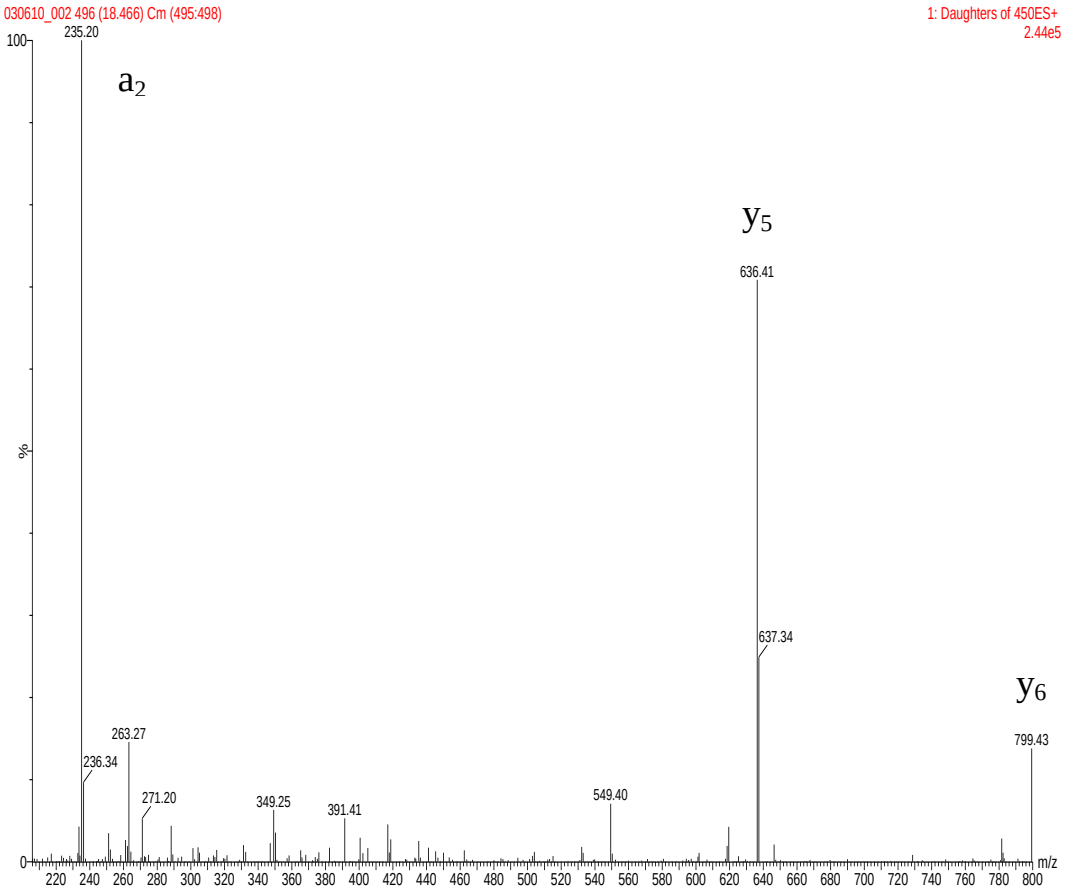

Figure 2.4: Product ion spectrum of the doubly charged tryptic peptide T_{17} (^{144}VYSNFLR ^{150})

The data points generated by measuring the total peak area of this peptide are shown in Figure 2.5. The R^2 value for the linear regression line plotted using all points was 0.9967. If the values for the 50 ng/mL digest were ignored as shown in Figure 2.6, this rose to 0.9974

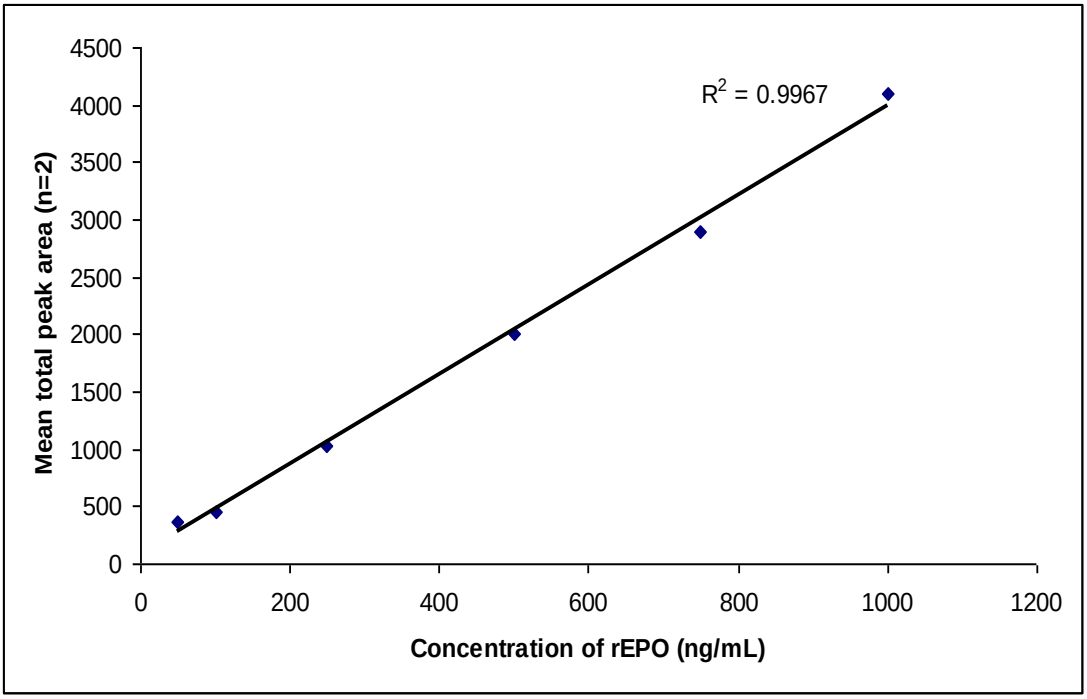

Figure 2.5: Relationship of EPO concentration to total peak area of fragment ions from peptide T17

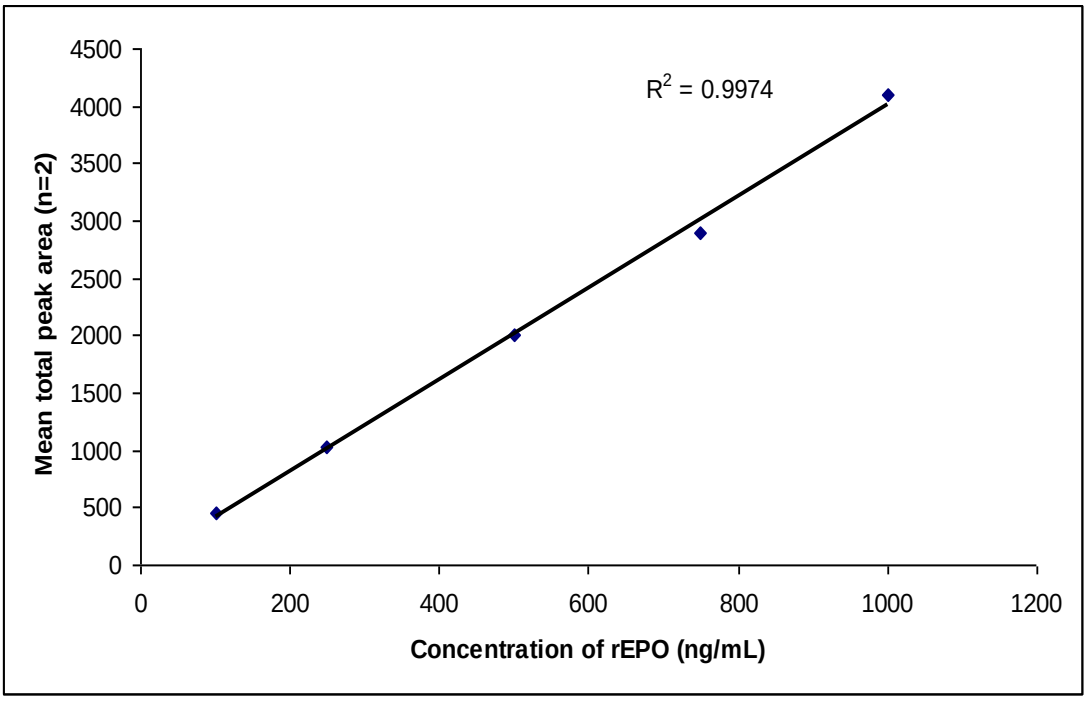

Figure 2.6: Relationship of EPO concentration to total peak area of fragment ions from peptide T17 (50 ng/mL digest excluded)

As a result, it was decided to spike samples such that 100 per cent recovery would give concentrations of 500 ng/mL, and to bracket the samples with standards at 100 and 1000 ng/mL.

Comparison of the measured peak areas from Dynabead extractions with the expected value from standards run at the same time (and digested for the same length of time) gave percentage recovery. Each sample was injected twice, and the mean peak area used.

From the standards run simultaneously, the expected mean peak area for the Dynabead extractions was 2156 (arbitrary units). The obtained values are shown in Table 2.11.

Table 2.11: Recovery of rEPO from urine by Dynabead extraction, as measured by LC-MS/MS

Sample	Mean peak area (observed)	Observed/Expected peak area
1	1854	0.86
2	1186	0.55
3	1897	0.88
4	1035	0.48
	Mean O/E (± s.d.)	0.69 ± 0.21

The mean recovery from Dynabead extractions was 69%. This compares well to extraction by ultrafiltration, which has been reported to be in the region of 50% (Lönnberg, Dehnes et al. 2010) However, the standard deviation is quite large, indicating that the method is not especially robust. The Dynabeads from these extractions were retained and subjected to repeat elutions. These elutions showed the presence of more EPO, unsurprisingly especially from samples 2 and 4 (mean O/E for the two of 18%). This suggests that binding of rEPO to the beads is not the problem, but that elution of rEPO from them is. Carryover is therefore a problem with this method. This could be reduced by repeated elutions (or possibly by eluting

in a larger volume). However, for anti-doping practices, where carryover could potentially result in a false positive result, each batch of magnetic beads would only be able to be used once. Repeated elutions may also improve overall recovery of EPO, but as less EPO would be recovered each time in the same volume of eluent, this would reduce the concentration of EPO in eluate; since sensitivity is a major issue in anti-doping testing, a further concentration step would then be desirable (or necessary), increasing further the time and effort needed by this extraction method.

2.3.12 Isoform selectivity of Dynabeads

The gel obtained by running ultrafiltered samples next to identical Dynabead extracted samples is shown in figure 2.7. There appears to be a slight variation in isoform density between the two samples. However, this is only small, and could be due to experimental variation. Importantly, by both methods both the positive and negative samples would be correctly interpreted.

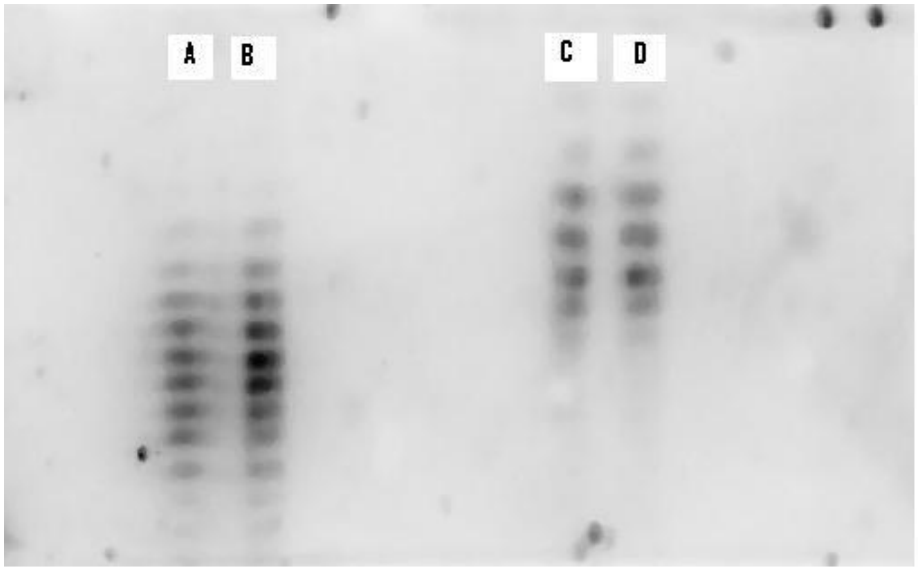

Figure 2.7: Ultrafiltration versus Dynabead extractions of EPO from ultrafiltered and spiked urine. Samples are: A- urine spiked with huEPO, ultrafiltration extraction; B- urine spiked with huEPO, Dynabead extraction; C- urine spiked with rEPO, ultrafiltration extraction; D- urine spiked with rEPO, Dynabead extraction.

2.3.13 Extraction of EPO from unfiltered urine in comparison with MAIIA monolithic cartridges

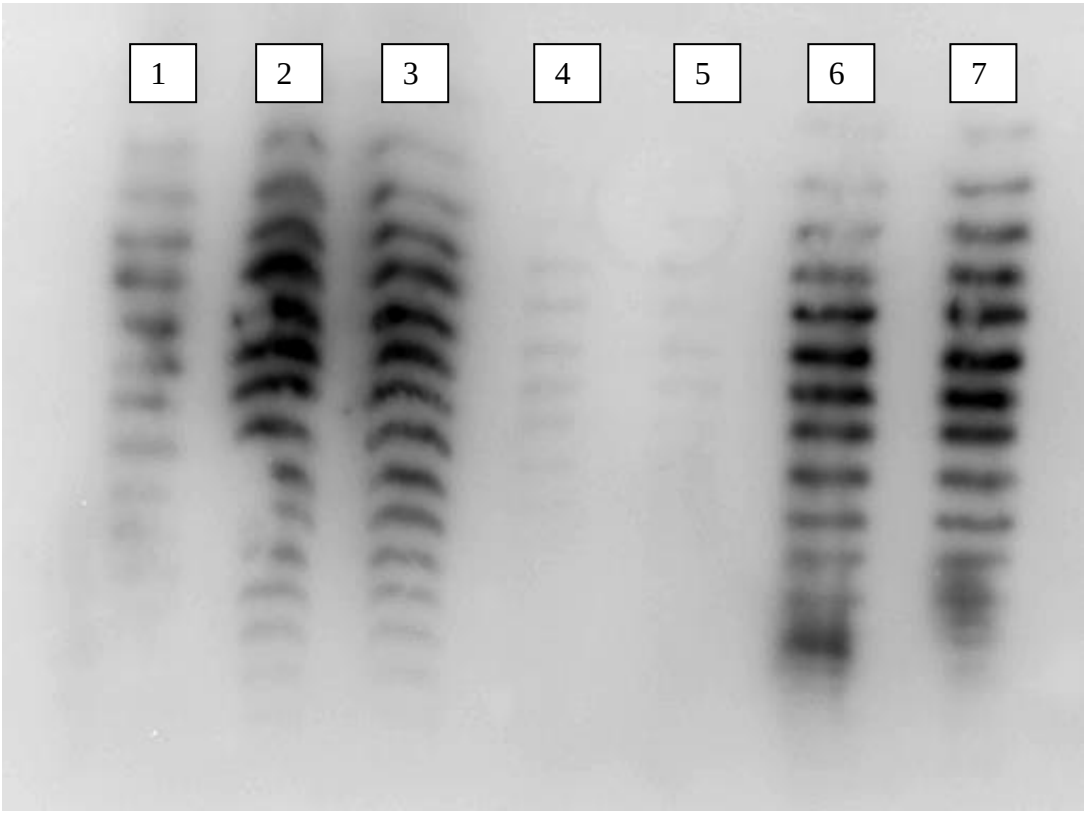

Figure 2.8: IEF gel demonstrating efficacy of extraction of huEPO from urine samples by different methods. Lanes are: 1 - huEPO standard (NIBSC); 2, 3 - extraction by ultrafiltration; 4, 5 - extraction with Dynabeads; 6, 7 - extraction using MAIIA monolithic cartridges.

As shown in figure 2.8, as expected the bands produced by extraction using MAIIA cartridges are clearer, with slightly less background noise and significantly less distortion. There is also no obvious difference in selectivity for isoforms seen between the two methods. However, the extractions carried out using Dynabeads were not successful. Despite the apparent recovery measured using LC-MS/MS being around 70%, similar recovery was not observed in these extractions. This could be due to a difference in the suitability of the elution buffer for analysis by IEF/immunoblotting, but this had not been observed when checking for isoform selectivity in 2.3.12. However, isoform selectivity was checked using spiked, ultrafiltered urine. It is possible that other large compounds (probably proteins)

removed from urine by this same filtration procedure interfere in the binding or elution of EPO to or from Dynabeads.

2.3.14 Extraction of EPO by sequential Dynabeads/ultrafiltration

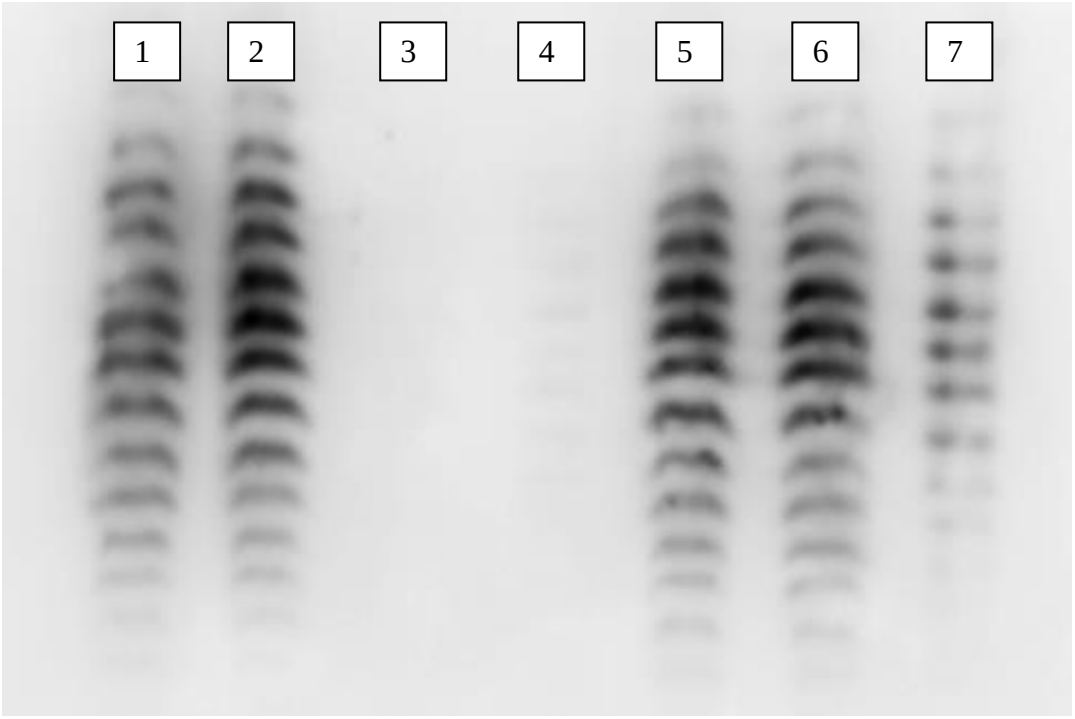

Figure 2.9: IEF gel of urine samples sequentially extracted by ultrafiltration/Dynabeads. From left, lanes are: 1, 2 - Ultrafiltration extraction; 3, 4 - Dynabead extraction; 5, 6 - Dynabead extraction then ultrafiltration; 7- huEPO standard (NIBSC)

Figure 2.9 shows the gel obtained from samples ultrafiltered, extracted with Dynabeads and extracted with Dynabeads and then ultrafiltered. As in 2.3.13, the extractions with Dynabeads were (comparatively) unsuccessful (with very faint bands only being visible). When these samples were then extracted using ultrafiltration, bands similar in intensity to those directly extracted by ultrafiltration were observed. This would indicate that the failure of Dynabeads as an extraction method in 2.3.13 was due to the failure of the beads to bind EPO from whole urine, rather than a failure to elute it from the beads afterwards.

2.3.15 Extraction of EPO from buffer, ultrafiltered urine and whole urine

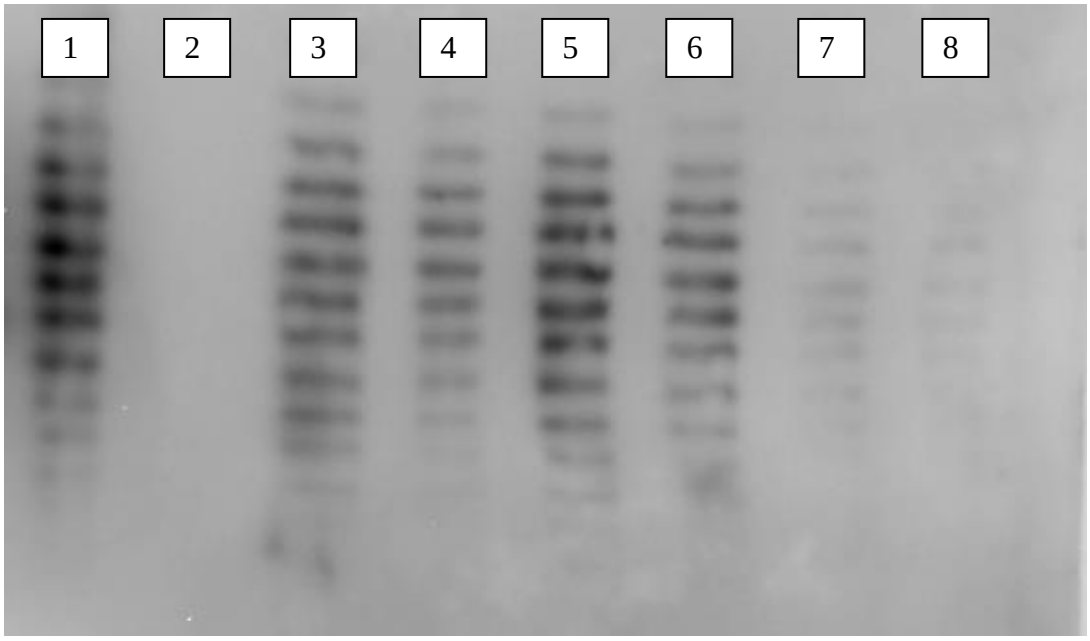

Figure 2.10: Recovery of EPO using Dynabeads from buffer, ultrafiltered urine and whole urine. From left, samples are: 1 - huEPO standard (NIBSC); 2- blank lane; 3, 4 - extraction from buffer; 5, 6 - extraction from ultrafiltered urine; 7, 8 - extraction from whole urine

The difficulty in extracting EPO from whole urine is further illustrated in Figure 2.10. When solutions of EPO are made up at physiological concentrations in a neutral buffer, recovery of EPO is successful. The isoform distribution is the same in the extraction as in the huEPO standard, and the relative intensity of the three most intense bands in the standard compared to the same bands in the extractions suggests a recovery of about 58%. Recovery of EPO from ultrafiltered urine which was then spiked at the same concentration with huEPO was somewhat more than in buffer. Measurement of the three most intense bands this time suggested a recovery of about 80%. It is unclear if this is a 'real' effect, or if as with the mass spectrometric analysis, it suggests a lack of robustness in the extraction method. One explanation may be that ultrafiltration of urine fails to remove all EPO, so that the concentration in the ultrafiltered and spiked urine samples was higher than was thought. Extraction from whole urine adjusted to the same EPO concentration was poor. Bands are only faintly visible on the gel; analysis using GASepo, which can enhance band visibility, suggested a recovery of around 8%.

2.4 Conclusions

Attempts to extract EPO from solution were not successful using the anti-EPO antibody AE7A5, despite this being a key element of the standard IEF/immunoblotting procedure for EPO detection. However, the standard procedure involves the membrane with the EPO attached being incubated in a solution of DTT for one hour, before it is incubated with the antibody. The antibody binds to an epitope in the first 26 residues of the protein, and it is likely that the exposure of this epitope is improved by the breaking of the disulphide bond between the cysteine residues at positions 7 and 161. Attempts to denature EPO by the addition of DTT to urine failed, with the formation of (presumably proteinaceous) solids observed, preventing effective incubation with Dynabeads. Attempts to expose the epitope simply by heating urine previous to extraction were also unsuccessful. This is perhaps not surprising, given the different denaturation mechanisms involved. Furthermore, the standard procedure for extraction of EPO also involves a heating step to denature urinary proteases, which EPO is resistant to, suggesting that attempts to denature EPO in this manner may not be effective. It is also known that AE7A5 binds to other urinary components, especially zinc-alpha-2-glycoprotein. These run at a different pI on an IEF gel, and so do not interfere with EPO detection. However, it is possible that its presence in urine at a comparatively high concentration inhibits binding of EPO to the antibody, and that this was responsible for preventing binding of EPO from urine samples.

Extraction from solution using anti-EPO antibody 9C21D11 was successful in buffer, with relatively rapid falls in EPO concentration when incubated with Dynabeads modified with this antibody. Measurement using LC-MS/MS from ultrafiltered and then spiked urine suggested recovery in the region of 70%, although solutions were made up above physiological concentrations to enable detection within a linear response range. Tryptic digestion of extracts was simple, demonstrating the viability of this extraction process for analysis by alternative methods to IEF/immunoblotting. Analysis of similar samples made up at physiological concentrations demonstrated a lack of isoform selectivity, at least compared to ultrafiltration. However, attempts to extract EPO from whole urine using this method were not successful. Analysis of whole urine samples after incubation with antibody-modified Dynabeads indicated that binding of EPO to the

beads was inhibited in whole urine. This was not seen in ultrafiltered and spiked urine, suggesting that the inhibitory factor is the presence of large (>30 kDa) components. Although the component(s) responsible have not been identified, as mentioned above antibody AE7A5 is known to bind to other urinary proteins; it is quite possible that antibody 9C21D11 also does so, preventing the binding of EPO. Since the binding epitope of 9C21D11 is not known, it is difficult to predict which urinary proteins might affect it.

That this problem is not observed with MAIIA cartridges, which both bind and release EPO rapidly from urine and serum without being excessively affected by the presence of other proteins, demonstrates the importance of obtaining an antibody with optimal binding characteristics. In the case of MAIIA, this antibody is mouse monoclonal antibody 3F6. It is possible that use of this antibody would enable successful extraction of EPO from whole urine samples using modified Dynabeads. Alternatively, a new antibody could be sought, which could in theory have better specificity and more optimal affinity for EPO. However, due to reasons of cost and time, both these approaches are outside the scope of this work at present.

2.6 References:

Lönnberg, M., Y. Dehnes, et al. (2010). "Rapid affinity purification of erythropoietin from biological samples using disposable monoliths." Journal of Chromatography A **1217**(45): 7031-7037.

Mi, J., S. Wang, et al. (2006). "Efficient purification and preconcentration of erythropoietin in human urine by reusable immunoaffinity column." Journal of Chromatography B **843**(1): 125-130.

Skibeli, V., G. Nissen-Lie, et al. (2001). "Sugar profiling proves that human serum erythropoietin differs from recombinant human erythropoietin." Blood **98**(13): 3626-3634.

Chapter 3: The production and comparison of boronic acid functionalised silica and polymeric materials for the extraction of glycopeptides from solution

Aim: To produce boronic acid functionalised silica that could be used to extract and concentrate glycopeptides from solution, with the ultimate intention of improving detection of EPO glycopeptides by LC-MS.

3.1 Introduction

3.1.1 Boronic acid – cis-diol complexes

Boronic acids are alkyl or aryl substituted boric acids, which are capable of reacting with compounds containing cis-diol groups to form reversible covalent complexes (Figure 3.1).

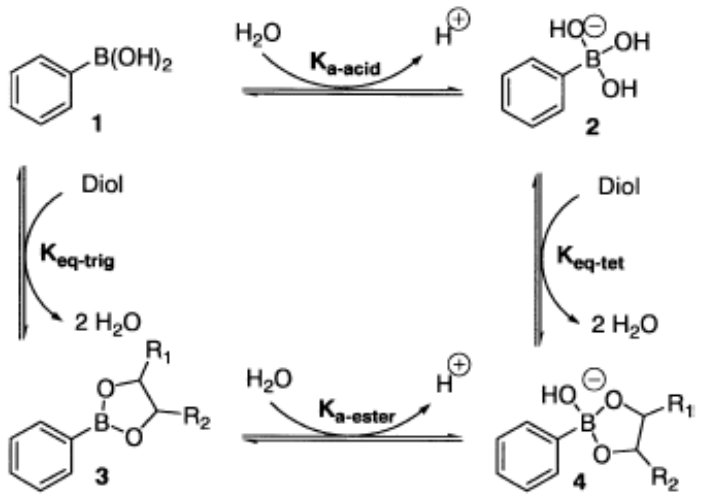

Figure 3.1: Relationship between phenylboronic acid and its diol ester. Due to the involvement of protons, the relationship is pH dependent. Reproduced with permission (Springsteen and Wang 2002)

Cis-diol containing biomolecules make up some of those of most interest to researchers, including glycoproteins, nucleosides and saccharides. The binding of boronic acids to saccharides is affected by the specific sugar involved. In aqueous solution, saccharides exist in different conformations, the open chain structure and the α and β ring forms. Ketohexoses such as fructose or aldopentoses such as ribose can form five-membered (furanose) rings, or six-membered (pyranose) rings. In a process known as ring-flipping, the conformation can change, resulting in axial

substituents becoming equatorial, and vice versa. The binding of boronic acids is affected by this. Reactivity is affected, as axially located OH groups are less electron withdrawing than equatorial OH groups. Furthermore, boron-oxygen bonds are quite short, and so in the absence of rotational freedom of the C-C bonds, boronic ester formation will require the reacting hydroxy groups to have small dihedral angles in a synperiplanar arrangement to ease ring strain.

3.1.2 pH dependence of boronic acid binding

The affinity of boronic acids for cis-diol containing molecules has also been shown to be dependent on the concentration of buffer and importantly highly dependent on the pH of the solution (See tables 3.1 and 3.2) (Springsteen and Wang 2002). In Figure 3.1, an increase in acidity moves the equilibria to the left. As $K_{eq\text{-}tet}$ is much greater than $K_{eq\text{-}trig}$, this leads to greater hydrolysis of the ester bond. For some time it was generally assumed that stronger binding occurred at higher pH. However, Yan et al. (Yan, Springsteen et al. 2004) examined the binding of 25 arylboronic acids with a series of diols at a series of pH values, and demonstrated that the optimal binding pH is not always above the pKa of the boronic acid.

The reversible, pH dependent nature of the binding, combined with the high equilibrium constants of the formation of the boronic esters (for example, the binding of phenylboronic acid with catechol has an equilibrium constant of 830 M^{-1} at pH 7.4) is the reason why the reactions have been used in the construction of sensors for saccharides (Zhao, Fyles et al. 2004; Das, Kim et al. 2011), nucleotide and carbohydrate transporters (Westmark and Smith 1996; Draffin, Duggan et al. 2003) and in binding and separating carbohydrates chromatographically (Adamek, Liu et al. 1992; Liu, Hubbard et al. 1995).

Table 3.1: Association constants (K_{eq}) of the ester formed by saccharides with phenylboronic acid at various pHs, in 0.1 M phosphate buffer. Reproduced with permission (Springsteen and Wang 2002)

pH	K_{eq} (M^{-1}) of the complex with PBA					
	Fructose	Catechol	Glucose	Galactose	Sorbitol	ARS
4.6						190
5.8	4.6	31				990
6.5	29	150	0.84	2.1	47	1200
6.6	35	160				1500
7.0	92	500	2.0	8.4	160	1500
7.4	160	830	4.6		370	1300
7.5	210			17		1100
8.0	310	2900	7.2	38	840	670
8.5	560	3300	11	80	1000	450

Table 3.2: Association constants (K_{eq}) of saccharides with phenylboronic acid at pH 7.4, 0.1 M phosphate buffer. Reproduced with permission (Springsteen and Wang 2002)

Diol	K_{eq} (M^{-1})	Diol	K_{eq} (M^{-1})
Alizarin Red S.	1300	Sialic acid	21
Catechol	830	*cis*-1,2-Cyclopentane diol	20
D-sorbitol	370	Glucoronic acid	16
D-fructose	160	D-galactose	15
D-tagatose	130	D-xylose	14
D-mannitol	120	D-mannose	13
L-sorbose	120	D-glucose	4.6
1,4-Anhydroerythritol	110	Diethyl tartrate	3.7
D-erythronic-γ-lactone	30	Maltose	2.5
L-arabinose	25	Lactose	1.6
D-ribose	24	Sucrose	0.67

3.1.3 Different approaches for glycopeptide/glycoprotein extraction

Recently there has been increasing interest in the use of boronic acid functionalised materials for the capture or separation of larger biomolecules. A quick search of the Web of Science database found 83 papers or patents about boronic acids and glycoproteins published between 2008 and 2012; 54 were published between 2003 and 2007, and 53 were published in all years previously. For oligosaccharides and boronic acids, the equivalent figures were 30, 30 and 14. A number of different

materials with boronic acid functionality have been produced to capture glycoproteins and glycopeptides. Alternatives for the extraction or enrichment of glycosylated molecules are available, but all have drawbacks. Lectin chromatography is most commonly carried out using concanavalin A, but this is only very good for high mannose and hybrid N-glycans, shows less affinity for complex biantennary glycans, and little or no affinity for complex tri and tetra-antennary N-glycans (Cummings and Kornfeld 1982); HILIC chromatography is simple but can also enrich particularly hydrophilic non-glycosylated molecules; and oxidation and hydrazine chemistry is successful but the additional oxidation step increases method time and complexity.

A comparison of three different approaches for glycoprotein/glycopeptide enrichment by SPE (Ozohanics, Turiák et al. 2012), specifically wheat germ agglutinin lectin, phenylboronic acid (PBA) and strong anion exchange, analysed samples by nano-HPLC-MS(MS). Quantification of peptides was based on the sum (or average) intensity of the three most abundant peptide peaks corresponding to a given protein. Quantification of glycopeptides was done in an analogous manner, using the intensity of three product ions (m/z 366.14, 512.19 and 657.23) characteristic of glycopeptides (respectively, the oxonium ions of N-acetyl-lactosamine, fucosyl-N-acetyl-lactosamine and sialyl-N-acetyl-lactosamine). Enrichment at the peptide level was found to be more effective than at that of the protein. It was also found that lectin extraction was disappointing for peptides, but that both anion exchange and PBA Solid Phase Extraction (SPE) materials significantly enriched glycopeptides compared to non-glycosylated peptides. Recovery of glycopeptides was lower (about 50 %) with PBA SPE compared to anion exchange (about 60 % recovery), but the ratio to non-glycosylated peptides was better.

3.1.4 Surface modification with boronic acid

Boronic acid functionality has generally been introduced in two ways; either through the modification of the surface of a material, such as silica or a polymeric material, or through the direct production of polymers from boronic acid containing monomers. The limitation with a flat surface is the lower surface area; however, with

porous materials such as silica or polymeric monoliths, pore size can limit the extent of boronic acid conjugation due to steric and diffusive barriers.

Gold is often used as a structure to which boronic acids can be attached when MALDI is the analysis method, as gold can also adsorb UV laser to help desorption and ionisation of trapped molecules. Tang et al. (Tang, Liu et al. 2009) used gold nanoparticles spotted and sintered onto a steel plate, before being modified with 4-mercaptophenylboronic acid to produce a porous substrate with large surface area. This was capable of selectively binding glycopeptides from solution, which could then be analysed by MALDI after the deposition of 2,5-dihydroxybenzoic acid matrix. The boronic acid functionalised plates exhibited high sensitivity and selectivity to glycopeptides. Furthermore, the enrichment and detection steps were rapid and simple.

On plate enrichment for analysis by MALDI was also demonstrated by Xu et al. (Xu, Zhang et al. 2010). Gold-coated silicon wafers were immersed in 11-mercaptoundecanol (MUD) to produce a MUD monolayer. Hydroxyl groups on the end of the organic chain were converted to carboxylic acids and activated, before being reacted with 3-aminophenylboronic acid. Wafers were immersed in samples to bind glycopeptides, before being analysed using MALDI. Analysis of tryptic digests of three glycoproteins showed that the limit of detection was increased by 93-248 times compared to direct analysis of the digest, while recovery of glycopeptides from tryptic asialofetuin averaged 65.8 %.

Reduction of non-specific adsorption/adhesion to structures on which aminophenylboronic acid (APB) has been immobilised can be obtained through the introduction of a spacer arm between the material and the APB. Jang et al. (Jang, Kim et al. 2009) designed a self-assembled monolayer (SAM)-based MALDI plate, which contained a oligo(ethylene glycol) (OEG) spacer group to reduce the nonspecific adsorption/adhesion, allowing direct detection of glycoproteins after affinity-capture on the plate. The specificity of the APB-functionalised SAMs was demonstrated by the selective capture of model glycoproteins such as RNase B (15 kDa) and transferrin (80 kDa).

Sepharose gel has been activated by binding to it 3-aminophenylboronic acid, and the gel then added to agarose gel on MALDI chips, to produce a high-capacity affinity layer (Gontarev, Shmanai et al. 2007). Calculations show that the maximum amount of a protein that can be immobilised on a flat surface is around 10^{13}

molecules per cm. This corresponds to about 10 ng/mm^2, which is not sufficient for all purposes. The agarose gel has the advantage of porosity, and can bind 1-10 µg/mm^2. The affinity MALDI chips produced were capable of directly and specifically binding glycosylated molecules from samples, allowing their immediate analysis by MALDI mass spectrometry.

Zhang et al. (Zhang, Xu et al. 2009) produced a hybrid material consisting of a silica coated ferrite core with numerous "satellites" of gold nanoparticles with lots of "anchors". The anchors were 3-aminophenylboronic acid molecules, which were attached to the gold surface through long organic chains, to reduce steric hindrance. The grafting of the gold particles to the magnetic core increased the surface area, such that the adsorption capacity of the material was greater than 79 mg/g of material, three times higher than that of commercially available magnetic beads. Extraction of tryptically digested horseradish peroxidase showed that the beads successfully and specifically bound glycosylated peptides and not those without sugars attached. Recovery of glycopeptides from the composite nanoparticles of up to 85.9% was recorded. The nanoparticles could also be used to extract glycoproteins; with intact HRP, recovery of 71.6% was recorded. It was suggested that steric hindrance could be responsible for the reduced recovery compared to glycopeptides.

Aminophenylboronic acid has also been immobilised on magnetic beads for the purposes of direct analysis by MALDI. Lee et al. (Lee, Kim et al. 2005) used carboxylic acid terminated magnetic beads which were activated by a carbodiimide and subsequently reacted with N-hydroxysuccinimide moiety to provide a site for the attachment of aminophenylboronic acid through the amino group. Extraction of glycoproteins was carried out in deionised water, and the same solvent used to wash the magnetic beads several times. Glycoproteins were shown to be significantly enriched by the process, whereas non-glycosylated proteins were not. Since ionisation of glycoproteins using MALDI is suppressed in the presence of non-glycosylated proteins, this resulted in an increase in signal intensity of the glycoproteins.

Magnetic nanoparticles were also produced by Lin et al. (Lin, Zheng et al. 2012) with boronic acid functionality. Amine-functionalised Fe_3O_4 nanoparticles were prepared via a solvothermal method. A homogeneous silica coating was formed by hydrolysis and polycondensation of tetramethyloxysilane (TMOS) and

3-methacryloxypropyl trimethoxysilane (γ-MAPS) on the surface of the nanoparticles, which were then functionalised using vinylphenylboronic acid. Saturation binding of the nanoparticles was 320 mg g^{-1} for the glycosylated protein ovalbumin, 4–7 times higher than the values obtained for the non-glycosylated BSA and Lysozyme, which were 45 and 70 mg g^{-1}, respectively. The binding capacity of mucin, another glycosylated protein, was 2 times less than that of ovalbumin, indicating the effect of steric hindrance due to its larger molecular weight. Extraction of IgG from protein solution showed that both heavy chain and light chain polypeptides were bound by the nanoparticles. However, enrichment of the light chain was greater than that of the (glycosylated) heavy chain, suggesting that disruption of the binding between heavy and light chains was easier than that between the heavy chain and the boronic acid group.

Boronic acid functionalised silica was demonstrated by Li et al. (Li, Zhao et al. 2006). They used γ-glycidoxypropyltrimethoxysilane (GLYMO) to modify silica and introduce an epoxy group. This was then reacted with APB to produce the boronic acid functionalised silica. A similar approach was taken by Xu et al. (Xu, Wu et al. 2008), except that they reacted the GLYMO and APB together first, then reacted the resulting compound with the silica. Xu et al. used mesoporous silica that they manufactured themselves, and reported 2 orders of magnitude improvement in the detection limit of glycopeptides. They also said that the method was applicable to all kinds of glycopeptides regardless of their sizes, structures, and hydrophilicities.

A similar approach was used by Zhang et al. (Zhang, Yao et al. 2011) to produce aminophenylboronic acid (APB) functionalised magnetic mesoporous silica. Magnetic mesoporous silica nanocomposites were first produced. These were reacted with GLYMO in methylbenzene under reflux for 12 hours. The resultant GLYMO-functionalised mesoporous silica nanocomposites were then incubated in chloroform containing APB for 6 h under gentle rotation, to produce the boronic acid functionalised magnetic nanoparticles. The magnetic mesoporous silica nanocomposites were successfully used to selectively enrich glycopeptides. APB functionalised magnetic mesoporous silica also showed high selectivity for glycopeptides in a digest containing a 10-fold excess of bovine serum albumin (BSA) over horseradish peroxidase (HRP).

Recently, boronic acid-functionalised core–shell polymer nanoparticles were successfully synthesised for enriching glycosylated peptides (Qu, Liu et al. 2012).

The nanoparticles were composed of a hydrophilic polymer core manufactured by distillation precipitation polymerisation (DPP) with a boronic acid-functionalised shell. Using the nanoparticles to capture glycopeptides from a tryptic digest of HRP prior to analysis by MALDI-TOF, the authors found that 18 glycopeptides were captured compared to eight glycopeptides enriched by using commercially available 3-aminophenylboronic acid agarose under the same conditions. Glycopeptides could still be selectively isolated by the prepared nanoparticles at concentrations as low as 5 nmol.

3.1.5 Boronic acid solid phase microextraction

Boronate affinity has also been used in solid phase microextraction (SPME) (He, Liu et al. 2009). Here, it was used because the pH dependent change in affinity of boronic acids for compounds containing 1,2 and 1,3 cis-diols allows desorption of bound analytes for analysis by HPLC or CE without harsh conditions such as elevated temperature which may cause degradation of analytes. He et al. electrochemically deposited poly-3-APBA onto a silver wire. Extraction of riboflavin was carried out at pH 9, with elution at pH 3.5. Binding equilibrium was reached after about 30 minutes, although desorption continued to increase up to 60 minutes.

3.1.6 Boronic acid chromatography

Separation phases involving immobilised boronic acids include affinity chromatography supports, where phenylboronic acid is immobilised on dextranes (Hjertén and Li 1990) or co-polymerised with methacrylates (Lei, Liu et al. 2001).
Separation and detection of N-acetylneuraminic acid and N-glycolylneuraminic acid has also been carried out using HPLC coupled to ESI-MS, with separation on a C_{18} column modified using decylboronic acid (Allevi, Femia et al. 2008). This may be of relevance in the detection of rEPO usage, as N-glycolylneuraminic acid is found in rEPO but not endogenous EPO. In this study, the limit of detection was 100 ng/mL, with 2 ng on column. This was whilst using an ion trap as opposed to a triple quadrupole mass spectrometer, and working with a 2.1 mm diameter column. As such it is likely that improvements in sensitivity could be reasonably easily obtained.

Elution was carried out using aqueous formic acid (0.04%). With this weakly acidic mobile phase, other carbohydrates present in the sample were unretained and eluted with the solvent front. Both sialic acids, however, were retained sufficiently to allow baseline separation.

Boronic acid affinity chromatography has also been combined with lectin affinity chromatography (Monzo, Bonn et al. 2007). Agarose beads with bound lectins (Con A or WGA) or bound 3-aminophenylboronic acid were mixed together, packed into spin columns and a protein test mixture added. Binding was carried out using a 50 mM taurine buffer, at pH 8.7. Elution was carried out from the boronic acid functionalised beads using a solution consisting of 50 mM Tris, 0.5 M NaCl, 0.05% NaN3, pH 7.2. Despite the surprisingly high pH of the elution buffer, they were able to successfully elute bound glycopeptides from the boronic acid agarose beads. This was attributed to the high NaCl concentration of the solution, while it has also been reported that the steric configuration of the hydroxy groups in Tris can interfere with binding of glycopeptides to boronic acids (Li, Larsson et al. 2001).

3.1.7 Adjusting the pH of ester formation

The need for a basic pH for conventional phenylboronic acids to bind cis-diols is inconvenient and increases the risk of degradation of labile compounds. Four approaches have been proposed to solve this problem. The first involves the incorporation of a carbonyl or sulfonyl group into the phenyl ring with electron withdrawing effects. Alternatively, an amine group can be incorporated next to the boronic acid, to form an intramolecular boron–nitrogen coordination. Li et al. (Li, Liu et al. 2011) produced a Wulff-type boronate (3-(dimethylaminomethyl)-aniline-4-pinacol boronate) and immobilised it onto a polymeric macroporous monolith. The boronate affinity monolith produced demonstrated enhanced affinity to cis-diol biomolecules such as adenosine at pH as low as 5.5.

Thirdly, the boron-nitrogen coordination can be replaced by a boron-oxygen one. A fourth alternative was proposed by Liu et al. (Ren, Liu et al. 2009), who produced a monolith with a boronic acid and amine group in the same neighbourhood. The amine coordinates with the boronic acid, functioning as a Wulff-type boronic acid, and producing enhanced affinity at neutral pH. Although this monolith exhibited

excellent specificity to small cis-diol containing molecules, it failed to bind glycoproteins, possibly due to steric inhibition.

More recently, Liu et al. (Liu, Ren et al. 2011) produced a sulfonyl substituted boronic acid functionalised monolithic capillary with both a strong boronate affinity at neutral pH and also secondary separation capability to cis-diol biomolecules. As a result, it had two dimensional (2D) separation capability, firstly separating cis-diol compounds from non-cis-diol ones, and then further separating cis-diol compounds according to differential hydrogen bonding interactions with the monolith.

3.1.8 Boronic acid functionalised monolithic materials

Other monolithic materials with boronate functionality have also been produced. Bossi et al. (Bossi, Castelletti et al. 2004) produced polymers from 3-aminophenylboronic acid monomers. This proved capable of separating diastereoisomers of ascorbic acid using capillary zone electrophoresis. Normally, the two diastereoisomers are separated in CZE only in the presence of borate buffer at high molarities (200 mM). The capillaries were also tested for the discrimination of haemoglobin and glycated haemoglobin and showed a fairly high selectivity towards the sugar-modified protein.

Chen et al. (Chen, Lu et al. 2009) manufactured a poly(3-acrylamidophenylboronic acid-co-ethylene dimethacrylate) (AAPBA-co-EDMA) monolith in a 530 mm long capillary by a one-step in situ polymerisation procedure. Extraction of tryptic digests of HRP and mixtures of intact HRP/BSA was carried out. Ten glycopeptides from tryptic HRP peptides were selectively captured, as well as HRP protein from the HRP/BSA mixture, demonstrating both a high extraction capacity and specificity.

Boronate functionalised monolithic capillary columns were also synthesised by in situ free radical polymerisation by Ren et al. (Ren, Liu et al. 2009). They used 4-vinylphenylboronic acid as one of the monomers for the reaction, with ethylene glycol and diethylene glycol as porogens. The column displayed reversed-phase retention due to the hydrophobic nature of the monolith skeleton, requiring high concentrations of acetonitrile in the solvent to avoid this interaction. At pH 8.5, cis-diol containing catechol was completely retained, whereas quinol (without the cis-diol group) was unretained. At pH 2.7, catechol was completely eluted. The presence of a Lewis base such as fluoride aids the formation of the boronic ester. The

fluoride ion has a lone pair of electrons which can form a complex with a boronic acid. This can then form a cyclic ester with a cis-diol group in a less basic media. It has been observed that the presence of fluoride enhances the complexation of saccharides with boronate ions under less basic conditions, facilitating the formation of an anionic ester (Westmark, Valencia et al. 1994; Deore, Yu et al. 2003). Ren et al. found that increasing the concentration of sodium fluoride in their mobile phase increased retention of catechol.

Ren et al. did not look at retention or separation of large molecules such as glycopeptides or glycoproteins using their monolithic column, due to the problems of denaturation caused by the need for a high concentration of organic solvent in the eluent. However, in another paper (Ren, Liu et al. 2009) they synthesised a hydrophilic boronate functionalised polymeric monolithic column by free radical polymerisation through substituting the hydrophobic cross-linker EDMA with a hydrophilic one, N, N-methylenebisacrylamide (MBAA). This significantly reduced the hydrophobicity of the column, enabling retention of the glycosylated proteins HRP and lactoferrin, while non-glycosylated proteins were unretained.

Boronate affinity monoliths have also been produced using metal-organic gels (MOGs) as a porogenic template (Yang, Lin et al. 2011). These proved to be a more convenient method for the formation of macropores in contrast to traditional porogenic methods. HRP and transferrin were selected as model glycoproteins and were completely bound by the boronate monolith at pH 8.5, whereas BSA and Cytochrome C were not. Both HRP and transferrin were eluted after switching to an acidic mobile phase (pH 2.5). The authors also successfully extracted transferrin from a bovine serum sample, demonstrating its application in complex biological samples.

Boronic functionalised materials have also been used as an alternative to Protein A for the specific capture of IgG (Liu, Lu et al. 2012). The easier disruption of boronic acid bonding means that less harsh conditions can be used than with Protein A. The binding of boronic acids should also be to glycan groups located on the Fc region of antibodies, not the important epitope binding region. By locating the boronic acid ligand within mesopores of an optimised size, a monolith was produced such that glycan groups on IgG were able to bind to the boronic acid group while the rest of the antibody was left outside the pore. Other glycoproteins with glycans which could not reach the boronic acid ligand were excluded. Comparison of the binding of

antibodies with other glycoproteins found that all eight tested antibodies were captured by the monolith, whereas only two out of seven non-antibody glycoproteins were retarded. Since the binding affinity between the boronic acid and glycans on the different glycoproteins should have been similar, this demonstrates the importance of correct optimisation of pore size.

The selectivity of polymer-based monoliths is not ideal, due to non-specific adsorption. Hybrid monoliths combine the merits of silica with those of organic polymer monoliths and have gained in popularity recently in the separation field. Lin et al. (Lin, Pang et al. 2011b) described a method for one-pot synthesis of organic–inorganic hybrid affinity monoliths, using hydrolysed tetramethyl orthosilicate (TMOS) and methacryloxypropyltrimethoxysilane (γ-MAPS) as co-precursors and 4-vinylphenylboronic acid (VPBA) as a functionalised organic monomer. The resultant hybrid affinity monoliths specifically bound cis-diol-containing biomolecules and glycoproteins. Extraction of glycoproteins from egg white demonstrated the effectiveness of the hybrid affinity monolith for the specific capture of glycoproteins from complex biological samples.

The same authors (Lin, Pang et al. 2011a) also produced boronic acid functionalised monoliths using VPBA and ethylene dimethacrylate as monomers, with the resultant material demonstrating similar selectivity for glycoproteins.

3.1.9 Choice of approach

Due to the simplicity of the reactions and the availability of materials and equipment, it was decided to attempt to replicate the production of boronic acid functionalised silica as carried out by Xu et al. (Xu, Wu et al. 2008), using commercially available silica. Despite the obvious advantages of using silica (easier control of pore size and simplicity of manufacture), there has been no apparent work in this area since their publication. Their work used their own ‘home-made’ mesoporous silica. Since production of this silica was beyond the scope of this work, it was decided to try and replicate it using commercially available silica. This would have the added advantage of demonstrating that the functionalised material could be easily and cheaply reproduced. The hope was that this would provide a material which could be used to pack a trapping column, helping concentrate glycopeptides from EPO and improve LC-MS. As a comparison, functionalisation with boronic acid groups would

also be carried out on commercially available polymeric beads, and commercially available boronic acid SPE materials would also be tested to examine their ability to bind glycopeptides.

3.2 Experimental

3.2.1 Materials and equipment

All water used was purified using an Elgastat Option 3 water purification unit and had 18.2 MΩ resisitivity. HPLC bulk packing silica (5 μm particle size, 300 Å pore size) was purchased from Varian (Oxford, UK). Azobisisobutyronitrile (AIBN) was purchased from BDH (Leicestershire, UK). Hydrofluoric acid (48%, analytical grade) was purchased from Fisher Scientific (Leicestershire, UK). Trypsin (sequencing grade) was purchased from Promega (Southampton, UK). Horseradish peroxidase (HRP) was a kind gift from Dr. Martyn G. Boutelle, of Imperial College, London. Polymeric beads (PL-CMS) were a gift from Varian. Phenylboronic acid functionalised SPE cartridges (Bond Elut PBA) were purchased from Agilent (Wokingham, UK). All other chemicals were of analytical grade and were purchased from Sigma Aldrich (Poole, UK).

Infrared spectroscopy was carried out using a Perkin-Elmer Spectrum One FTIR Spectrophotometer, with a Durasampler II Diamond ATR attachment.

ICP-MS was carried out using a Perkin-Elmer Elan DRC Plus. Conditions are set out below:

rf power 1.1 kW, frequency 40 MHz
torch Quartz torch using alumina injector tube
plasma Ar flow rate 15 L/min
auxiliary Ar flow rate 0.8 L/min
nebulizer Ar flow rate 0.98 L/min

Nebulizer and Spray Chamber

nebulizer cross-flow type, gemtip type - ruby (argon) & sapphire (sample)
spray chamber Scott Double Pass, room temp.
made of Ryton
solution uptake rate 0.4 mL/min (pumped with peristaltic pump)

Interface

sampling orifice 1.1 mm (made of Pt)
skimming orifice 0.9 mm (made of Pt)

Mass Spectrometer Operating Conditions

Isotope measured ^{11}B, peak hopping mode.

50 sweeps per replicate at 200 ms per sweep.
5 replicates averaged to give the final result, thus sample measurement took ~51 sec.
Background measured in the first sample of the run and subtracted from all other results

A Hypersil Gold C18 column from Thermo Fisher (Loughborough, UK), 200 mm length and 2.1 mm internal diameter with 1.9 µm particles was used for chromatographic separations, except where otherwise specified. LC-MS/MS was carried out using a Thermo Accela HPLC pump and autosampler, and a Thermo LTQ linear ion trap mass spectrometer, again unless otherwise specified.

3.2.2 Production of boronic acid functionalised silica – method one

Silica was modified using the method developed by Xu et al. (Figure 3.2). Fifty milligrams 3-aminophenylboronic acid monohydrate (APB) was dissolved in 20 mL deionised water, and the solution adjusted to pH 9.18 by addition of aqueous NaOH. Forty microlitres of 3-glycidyloxypropyltrimethoxysilane (GLYMO) was added slowly while stirring, with the flask sitting in an ice bath. The flask was then put in a

water bath on a stirrer for 6 hours at 40 ºC. Then, it was returned to an ice bath for five minutes, before a further 40 µL of GLYMO was added, and the flask stirred for 6 more hours at 65 ºC. The resulting solution (boronic acid bonded GLYMO, GA) was transferred to a new vial and kept refrigerated overnight. Twenty milligrams of silica was then weighed into a centrifuge tube, and 5 mL of the solution added to it. This was heated at 75 ºC for two hours, then the tube was centrifuged, the supernatant removed and 5 mL more GA added. This was repeated twice more until all the 20 mL of GA had been used. The resulting silica was washed twice with 3 mL water and twice with 3 mL methanol. It was then resuspended in 100 µL methanol and transferred to a fresh vial before being dried at 30 ºC under nitrogen.

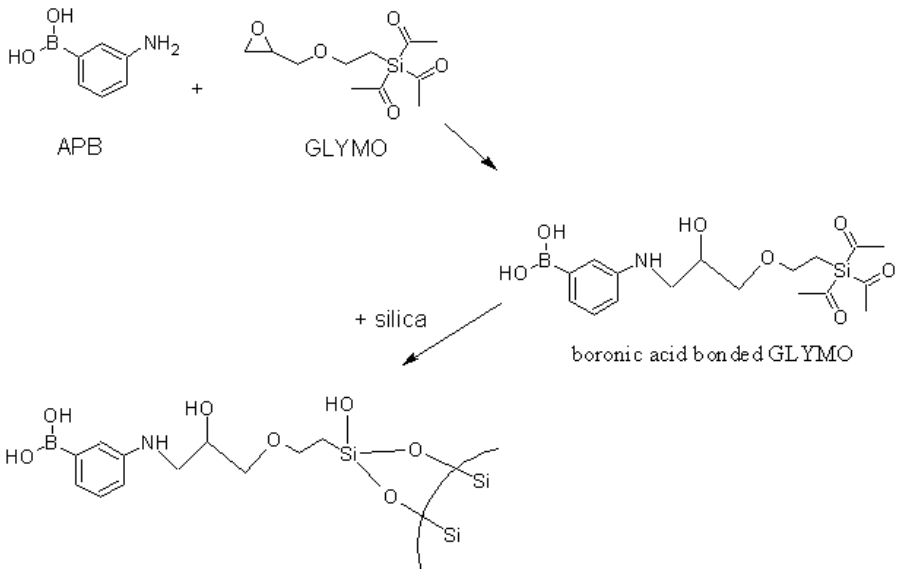

Figure 3.2. Production of phenylboronic acid functionalised silica (method one)

3.2.3 Production of boronic acid functionalised silica – method two

Silica was also modified using the method developed by Li et al. (Li, Zhao et al. 2006) Silica (0.5 g) was dried overnight at 160 °C, then slurried in 20 mL dried dichloromethane. 1 mL GLYMO was added under nitrogen and the mixture stirred and refluxed under nitrogen for 24 hours. The silica was filtered off, washed on a glass filter-funnel with 25 mL of dichloromethane, acetone, dichloromethane and diethyl ether in turn and then dried at 70 °C for 4 hours. 200 mg of APB was dissolved in 20 mL of water and sonicated for ten minutes. The pH of this solution

was adjusted using aqueous NaOH to 7.5 and 0.5 g of the modified silica was added. The mixture was stirred under nitrogen and reflux at 90 °C for 24 hours. The silica was finally filtered off again and washed with 25 mL of water and then methanol.

3.2.4 Production of boronic acid functionalised silica – method three

The third method for modification of silica was similar to that above. The method for reacting silica with GLYMO was the same as in 3.2.3. However, 200 mg of APB was added to 20 mL of chloroform, 0.5 g of silica added to this and the mixture stirred under nitrogen at room temperature for 16 hours, before being washed with methanol, water, and diethyl ether.

3.2.5 IR Spectroscopy of modified silica

Silica was dried overnight at 110 ºC to remove water, which would prevent effective grinding of silica, then ground finely and its total attenuated reflectance measured. As controls, unmodified silica and silica which had been directly reacted with APB instead of GA were used. Spectroscopic analysis was also carried out on silica taken from Bond Elut PBA cartridges.

3.2.6 ICP-MS of modified silica

Mannitol powder was dissolved in 0.1 M HF to obtain a 1% solution and diluted to a 0.1% mannitol solution with water. About 2 mg of silica modified as in 3.2.2 was weighed out accurately to 0.01 mg in a 1 mL polypropylene test tube. The sample was soaked with 0.2 mL of 0.1% mannitol solution to suppress boron volatilisation. Then, 0.1 mL of concentrated HF was added, and the tube tightly capped. The sample was decomposed overnight in an ultrasonic bath until the silica disappeared completely, and the solution subsequently evaporated at 70 °C until dry. Then, 1 mL of 0.5 M HF was added to the dried samples, and the tube agitated in an ultrasonic bath for 30 minutes to recover boron into the HF solution, leaving fluoride deposits. The deposits were removed by centrifuge, 100 µL of the supernatant was made up to 5 mL with water and the resulting solution finally aspirated into the ICP-MS.

A standard curve of boron solutions of concentrations from 10 to 1000 ng mL^{-1} was also produced. This was aspirated into the ICP-MS, along with unknown samples, to enable quantification of samples. The process was also carried out for silica removed from Bond Elut PBA cartridges.

3.2.7 Kinetic study of modification of silica

To see how modification of silica proceeded over time, the procedure (3.2.2) above was followed but samples of 4 mg of silica were modified, for periods from 0 to 10 hours. Samples were then digested as in 3.2.6 and analysed using ICP-MS.

3.2.8 Measurement of epoxide functionalisation of silica produced in 3.2.3 and 3.2.4

To measure to the extent of GLYMO functionalisation of silica by methods 3.2.3 and 3.2.4, silica was reacted with 0.2 N HCl in 1,4-dioxane. This was then titrated against 0.1 M NaOH in methanol to determine how much HCl had reacted with the epoxide groups on the silica.

3.2.9 Boronic acid functionalised silica extraction of glycopeptides from solution

Horseradish peroxidase (HRP) was used as a model glycoprotein. HRP (1 mg) in 50 mM ammonium bicarbonate, pH 7.4 (ABC) was mixed with 20 µg trypsin (50:1 ratio of protein:enzyme) and incubated overnight at 37 ºC. The digest was then diluted down to 100 µg/mL with 95:5 ABC:acetonitrile, and 100 µL added to 10 mg modified silica (which had been conditioned for 30 minutes with 95:5 ABC:acetonitrile). This was incubated for 15 minutes at room temperature with mixing, centrifuged and the supernatant removed. The silica was washed (twice) with 100 µL 95:5 ABC:acetonitrile for 15 minutes, then centrifuged and the supernatant removed again. Elution was carried out by incubating for 30 minutes in 100 µL of 30:70 acetonitrile:water, with 2% formic acid. Samples were centrifuged and the supernatant removed. All samples were dried down under nitrogen and reconstituted in 95:5 water:acetonitrile. The original solution before and after incubation with the silica, the supernatant from the wash steps and the eluent were

all analysed using LC-MS/MS. Extractions were also carried out using unmodified silica as a control. Each extraction was carried out in duplicate.

LC-MS/MS analysis of samples was carried out using the following gradient, with a flow rate of 200 µL/min.

Table 3.3: Gradient used for elution of digest of HRP

Time (mins)	% solvent A	% solvent B
0	95	5
5	95	5
30	20	80
34	20	80
34.5	95	5
40	95	5

10 µL of sample was injected onto the column. The MS conditions were: Sheath gas (nitrogen) flow rate (arbitrary units) 40, auxiliary flow rate 4, sweep gas flow rate 4; spray voltage was 4 kV, capillary temperature 350 ºC, capillary voltage 14 V and tube lens voltage 60 V.

Full scan MS, range 50-2000, and MS/MS scans for theoretical tryptic fragments were carried out. Theoretical masses of peptides were calculated using the PeptideMass characterisation tool, on the ExPASy Proteomics Server website (http://web.expasy.org/peptide_mass)

The three most prominent glycopeptides and non-glycosylated peptides were then selected for quantifying recovery of HRP using boronic acid functionalised silica The peptides were the tryptic fragments with amino acid sequences TPTIFDNK, DTIVNELR and YYVNLEEQK. The 2+ ions for these peptides were detected at m/z 468.5, 480.5 and 593.7 respectively. Glycopeptides were tryptic fragments, SFANSTQTFFNAFVEAMDR, GLIQSDQELFSSPNATDTIPLVR and

LHFHDCFVNGCDASILLDNTTSFR, all of which contained a core-fucosylated and core-xylosylated trimannosyl N-glycan. The 3+ ions for these glycopeptides were detected at m/z 1119.2, 1225.3 and 1299.4 respectively. Four MRM transitions were selected for each glycopeptide/peptide, and the peak area of each summed to give a total peak area for each glycopeptide/peptide. Each sample was injected twice, and the mean peak area recorded. Recovery was calculated as a percentage of peak area in the eluent compared to that in the original digest.

3.2.10 Extraction of mannitol using boronic acid functionalised silica

As a quicker check of the effectiveness of the modified silica at specifically binding cis-diol containing compounds in a pH dependent way, mannitol solution (100 µg/mL) was made up in a range of buffers at different pH. 100 µL of solution was incubated with 10 mg of silica, as detailed in 3.2.9. Samples were then centrifuged and the supernatant removed. Solutions were infused at a rate of 10 µL/min into the mass spectrometer and the average intensity of the signal from the mannitol (molecular ion, sodium adduct) measured over 30 seconds. Unmodified silica was used as a control, and standard curves of mannitol in the relevant buffer used to quantify binding.

3.2.11 Extraction of glycopeptides using Bond Elut PBA silica

Tryptic digests of HRP and fetuin were carried out as in 3.2.9. Solutions of digests were made up at 100 µg/mL in buffers with different pH. Extractions were carried out as in 3.2.9, except using the different buffers in place of ABC, and using silica from the Bond Elut PBA SPE cartridges. Extractions were also carried out using fetuin which had been digested with trypsin after being digested with neuraminidase to remove sialic acids. LC-MS analysis was carried out using a Waters Acquity LC system, connected to a Thermo Exactive Orbitrap mass spectrometer. Peak areas of selected peptides and glycopeptides were measured and recovery measured by comparing the peak areas to those in the original digest. Accurate masses of peptides and glycopeptides were calculated using the PeptideMass characterisation tool and glycan mass calculator (http://web.expasy.org/glycanmass/) on the ExPASy Proteomics Server website. For HRP, the same peptides and glycopeptides were

selected as in 3.2.9. For fetuin, the peptides were HTFSGVASVESSSGEAFHVGK, HTLNQIDSVK and TPIVGQPSIPGGPVR. Their 3+, 2+ and 2+ ions were detected at m/z 707.7, 577.8 and 737.9 respectively. Glycopeptides were RPTGEVYDIEIDTLETTCHVLDPTPLANCSVR with a trisialyated triantennary complex glycan, which was detected as a 4+ ion at m/z 1635.2, and LCPDCPLLAPLNDSR with a trisialyated triantennary complex glycan which was detected as a 3+ ion at m/z 1535.9.

3.2.12 Phenylboronic acid functionalisation of polymeric material

250 mg of 4-aminomethyl phenylboronic acid (HCl salt) was neutralised by reacting with 13.3 mL of 0.1 M NaOH dissolved in methanol. 0.266 g of PL-CMS polymeric beads was suspended in 12 mL of tetrahydrofuran and this added to the APB solution. This was then heated under nitrogen and reflux for 24 hours at 60 °C. The beads were then washed sequentially with 20 mL dichloromethane/acetone/water/tetrahydrofuran, and dried overnight at 40 °C. The reaction is shown in figure 3.3.

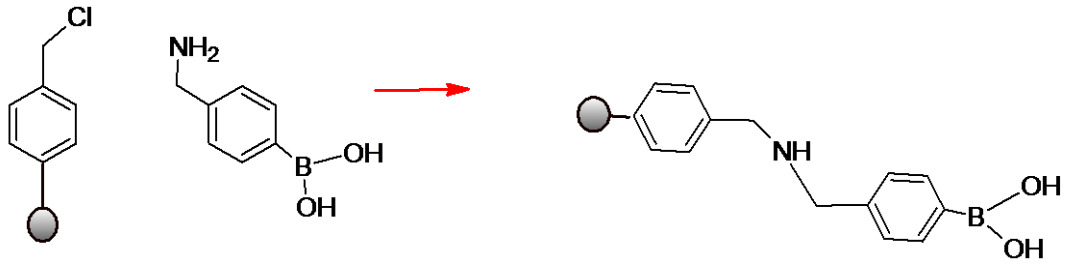

Figure 3.3: Boronic acid functionalisation of polymeric beads

3.2.13 Binding of mannitol by polymeric beads

As a quick check of the extent of functionalisation of the polymeric beads, modified and unmodified beads (about 25 mg, accurately weighed) were incubated with 250 µL of 50 µg/mL mannitol solution (50:50 methanol:50 mM ammonium bicarbonate, pH 7.5) for 30 minutes. Samples were centrifuged and supernatant infused into the LTQ-MS. Intensity of m/z 205 (mannitol Na+ adduct) was averaged

over 1 minute and compared with a standard curve of mannitol. Recovery from the beads was carried out by incubating the beads with 250 µL of either:

1. 50:50 water/methanol + 1 % formic acid, pH 3.4
2. 50:50 water/methanol + 10 % formic acid, pH 3.0
3. 50:50 water/methanol + 1 % TFA, pH 2.2
4. 50:50 water/methanol + 1 % TFA – sample was then dried down under N_2 and reconstituted in 50:50 water/methanol + 0.1 % formic acid

Recovered solutions were then infused into the LTQ-MS.

The effect of pH on mannitol binding to the beads was investigated by repeating the extraction step in buffers at pH 5.0, 6.0 and 8.5. Again, concentration in the solution after incubation was measured by centrifugation and infusion of the supernatant.

3.2.14 Extraction of peptides and glycopeptides using polymeric beads

The experiment in 3.2.9 was repeated, using 25 mg of modified polymeric beads instead of silica. Extraction was carried out using 50:50 water/methanol + 1 % TFA, pH 2.2. Due to the hydrophobic nature of the polymeric beads, extraction from purely aqueous samples was not possible. Solutions were therefore made up in 75:25 water:methanol. All samples were dried down and reconstituted in 95:5 water:acetonitrile, before analysis by LC-MS/MS.

To try to reduce non-specific binding of HRP peptides to the polymeric beads, an attempt was made to block non-specific binding sites with insulin. The HRP extraction was carried out as above; however, beads were incubated for 30 minutes in 1 mg/mL insulin before being incubated with the HRP digest.

3.3 Results and discussion

3.3.1 General discussion

Modification of silica by the first method made a noticeable difference to its appearance, which changed from white to a pale pink. The other two methods, though based on published work, were more problematic. Heating silica at a basic pH in an aqueous solution at 90 °C resulted in much of the sample dissolving. In the third method, the reaction is carried out in chloroform; however, APB was noticeably insoluble in this solvent and suspensions had a marked tendency to separate out over time. Although the APB was added in excess and left to react for a long time, there was no visible sign that the reaction had occurred. This is reflected in the results obtained in experiments using these silicas.

3.3.2. IR-spectroscopy of modified silica

Infrared spectra from unmodified silica, silica that had been incubated directly with APB (control) and fully modified silica produced as in 3.2.2 are shown below (Figure 3.4). The key difference is the appearance of bands in the modified silica at 1348 and 708 cm^{-1} indicating the existence of B-O bonds, not present in the two controls. There are also absorbances at 1572 and 1436 cm^{-1} which can be attributed to C-C bonds in the benzene ring and C-H bonds respectively.

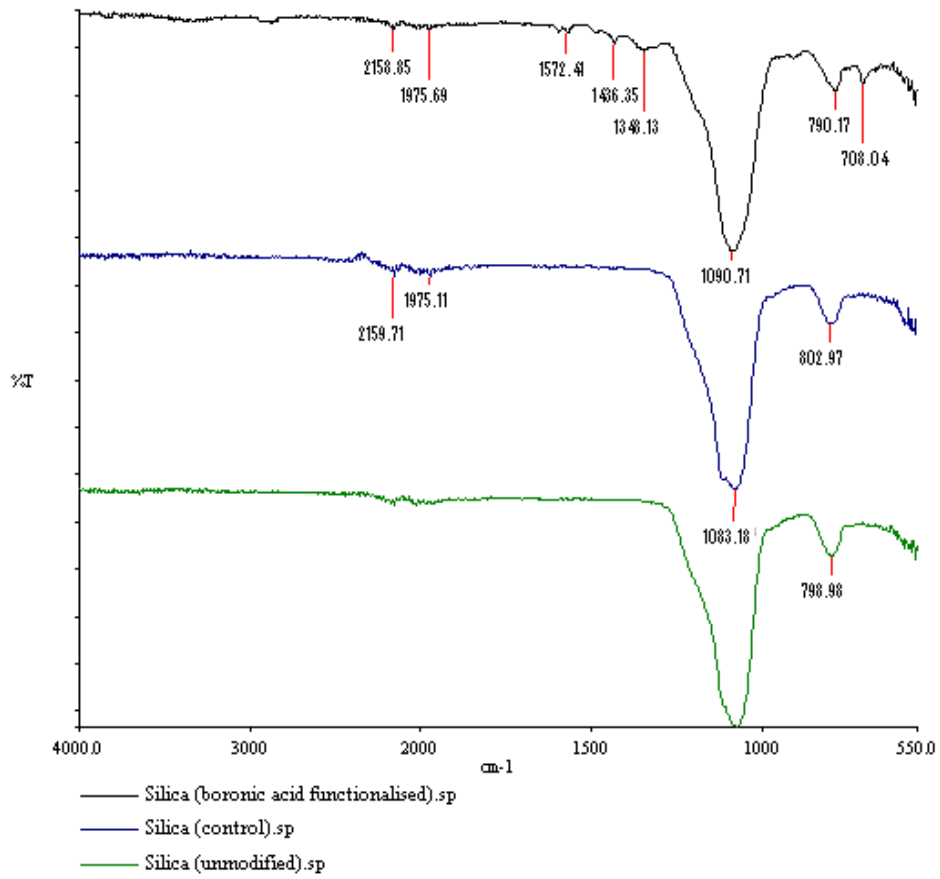

Figure 3.4: Infrared spectra of unmodified, control and boronic acid functionalised silica

Spectra for silica modified by methods two and three showed no difference from the control or unmodified silica, indicating that the functionalisation with phenylboronic acid had not been successful.

The spectrum for Bond Elut PBA silica is shown in figure 3.5. It too shows an absorbance at about 708 cm^{-1} of about a similar intensity.

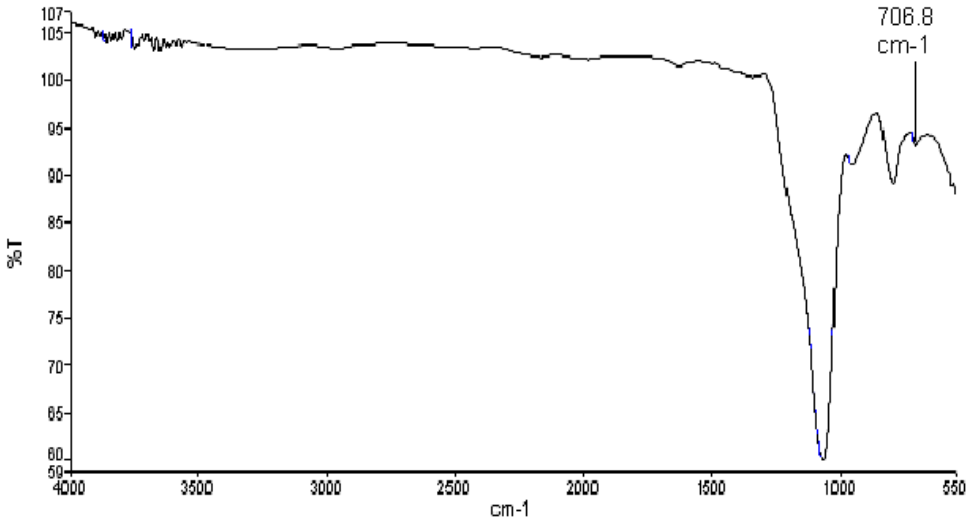

Figure 3.5: FTIR spectrum of Bond Elut PBA silica

3.3.3 ICP-MS of modified silica

Incubation of the silica produced by method 1 with GLYMO-APB for different lengths of time demonstrated an overall increase in boron content of the silica with time, below (Table 3.4, Figure 3.6):

Table 3.4: Effect of increasing reaction time on degree of modification of silica

Modification time (hours)	Boron (µg/mg silica)	Boron (mmol/g silica)
0	0	0
1	4.82	0.44
2	5.78	0.53
3	9.23	0.84
4	8.06	0.73
5	11.75	1.07
6	10.74	0.98
7	11.31	1.03
8	5.64	0.51
9	12.87	1.17
10	13.91	1.26

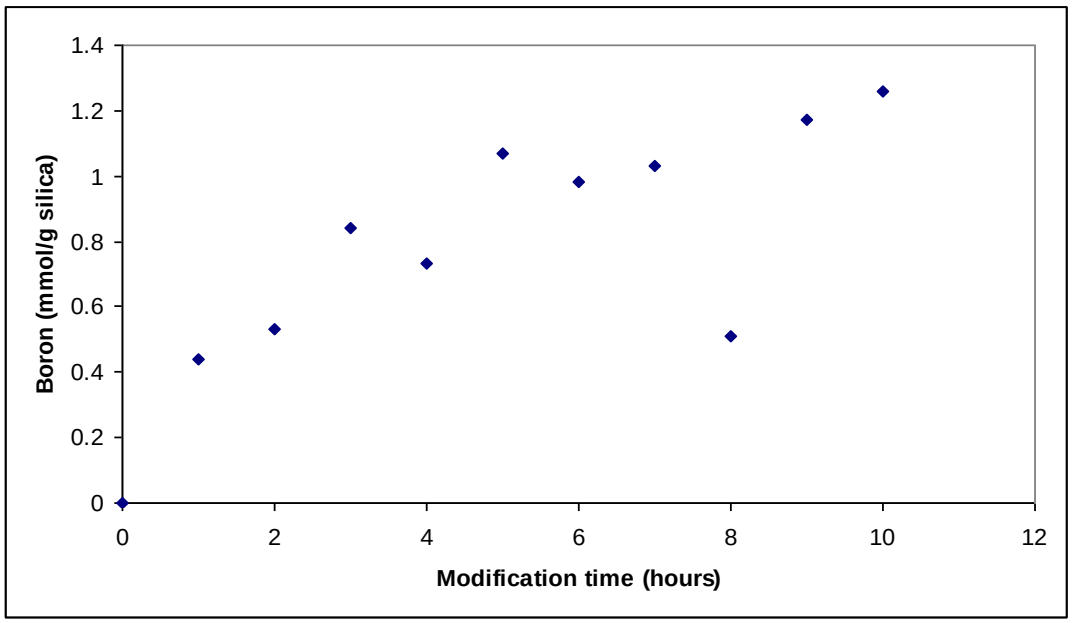

Figure 3.6: Effect of increasing reaction time on degree of modification of silica

The samples were individually incubated with magnetic stirrers. It was noted that these occasionally stuck in position, and it is possible that this is what happened with the sample incubated for 8 hours. It is unfortunate that this time was that used to modify silica in practice. However, if this result is ignored, the other results suggest that an incubation for 8 hours would give a concentration of boronic acid functional groups of about 1 mmol/g silica. ICP-MS of silicas modified by alternate methods was not carried out, due to the difficulties experienced in production of the silica, combined with the lack of positive results from IR spectroscopy and binding experiments with saccharides and glycopeptides. HF digestion of Bond Elut PBA silica produced a value for boron of 4.37 µg/mg of silica, or 0.40 mmol/g of silica. This is significantly lower than that found in the analysis of the modified silica, which perhaps is expected given the much larger particle size of the Agilent material (40 µm compared to 5 µm), and smaller pore size (60 Å compared to 300 Å). Unfortunately, direct measurements of the modified silica were not made, so the exact size of the post-reaction particles is not known. However, it does not seem unreasonable to suggest that the surface area:volume ratio of the modified silica would be larger than that of the Agilent material, given the large difference in their starting sizes.

3.3.4 Measurement of epoxide functionalisation of silica produced in 3.2.3 and 3.2.4

Titration results indicated an epoxide functional group concentration of 0.54 mmol/g silica. This was about half the concentration of boronic acid functional groups detected by the first method, suggesting that the reaction between GLYMO and silica takes place more efficiently in an aqueous solution, presumably because the water speeds up the hydrolysis of the alkoxy groups. Nonetheless, the concentration of epoxide groups detected would still be sufficient to enable efficient binding of glycopeptides and saccharides, if the concentration of epoxide groups translated into the same concentration of phenylboronic acid functional groups.

3.3.5 Boronic acid functionalised silica extraction of glycopeptides from solution

Mean peak areas of peptides and glycopeptides extracted using modified silica are shown in Table 3.5. Mean recovery of peptides was 1.1% with the boronic acid functionalised silica, and 0.1% with the control silica. Mean recovery of glycopeptides was 3.2% with the boronic acid functionalised silica and 0.1% with the control silica. Recovery of both peptides and glycopeptides was better with the modified silica, and best for glycopeptides. However, the recovery was still very poor. The data shows that this was due to a failure of binding rather than elution. Since the ICP-MS data suggests that the total content of boronic acid was not too low, this implied that either the boron detected using ICP-MS was not in a boronic acid group, or that the glycopeptide binding was not taking place for another reason, possibly due to steric hindrance. To examine if this was the case, mannitol binding was examined, as steric hindrance should be much less of a problem for a much smaller molecule.

Table 3.5: Recovery of targeted glycopeptides/peptides pre-incubation with control/boronic acid functionalised silica, post-incubation, from wash solutions and in final elutions

	Mean peak area					
	Peptides			Glycopeptides		
m/z	468.5	480.5	593.7	1119.2	1225.3	1299.4
HRP digest, 100 µg/mL	225000	719000	58600	21400	12400	17300
Control silica, post incubation	222000	578000	40600	21200	12900	35500
Boronic silica, post incubation	225000	515000	40500	16000	7700	21600
Control wash 1	46200	83200	3070	7650	2490	10100
Boronic wash 1	61900	142000	11300	16800	4270	32300
Control wash 2	8380	14200	233	854	306	1370
Boronic wash 2	17600	34900	2380	3840	775	4260
Control elution	678	916	0	80	0	5.5
Boronic elution	4250	6080	242	836	129	789

3.3.6 Extraction of mannitol using boronic acid functionalised silica

The concentration of mannitol in solution before extraction was 100 µg/mL. The concentrations after incubation are shown in Table 3.6.

Table 3.6: Mannitol concentrations after incubation with control or boronic acid functionalised silica

Buffer pH	Mean mannitol concentration post incubation (µg/mL), n=2	
	Boronic acid silica	Unmodified silica
5.0	64.7	49.7
6.0	85.2	84.5
7.0	98.2	84.5
8.0	95.4	94.7
8.8	98.2	96.6

The binding, counter to expectations, appeared to be higher in weakly acidic solutions. However, at all pH values the concentration of mannitol was higher after incubation with boronic acid functionalised silica than with unmodified silica. Only two repeats were carried out for each pH, so it is possible this result is due to noise. However, the results for each set were closely correlated, and for pH 5.0 and 7.0 the results for the boronic and unmodified silica were well separated, implying that the results are real. This would suggest that either the porosity of the silica was significantly reduced by the modification, reducing the surface area available for binding, or that the phenylboronic acid group itself bound the mannitol less strongly than the bare silica. This latter suggestion would go against all the published literature on the subject, so is unlikely to be the case. If the first is true, then binding would also be unlikely using Bond Elut PBA silica, which has a larger particle diameter than the silica being modified. (40 µm compared to 5 µm) and smaller pore size (60 Å compared to 300 Å, before modification). For this reason, extraction using Bond Elut PBA silica was attempted.

3.3.7 Extraction of glycopeptides using Bond Elut PBA silica

Tryptic digests of HRP were extracted first using the Bond Elut PBA silica. Recovery of three peptides (m/z 468.5, 480.5 and 593.7) was measured, as was recovery of three glycopeptides (m/z 1119.2, 1225.3 and 1299.4). Recovery when in

buffers of pH 5.5, 7.0 and 8.5 are shown in table 3.7. Although recovery was reasonable at both pH 7.0 and pH 8.5 for glycopeptides, contrary to expectations it appeared to be better at pH 5.5. Recovery of non-glycosylated peptides was fairly low, although it was higher for the peptide with m/z 468.5.

Table 3.7: Recovery of HRP tryptic peptides and glycopeptides using Bond Elut PBA silica

Buffer pH	Mean % Recovery of Peptide m/z (n=3)			Mean % Recovery of Glycopeptide m/z (n=3)		
	468.5	480.5	593.7	1119.2	1225.3	1299.4
5.5	**37.5**	**9.2**	**13.5**	**96.2**	**76.6**	**88.3**
7.0	**29.4**	**3.1**	**14.6**	**63.4**	**70.1**	**75.6**
8.5	**42.1**	**2.7**	**15.2**	**51.9**	**59.0**	**79.7**

The same process was then repeated using a tryptic digest of fetuin, which contains predominantly sialylated glycopeptides. The results are shown in table 3.8. At neutral and basic pH, recovery of glycopeptides was very low, whereas unexpectedly recovery of non-glycosylated peptides was comparatively high. Recovery of sialylated glycopeptides improved from slightly acidic buffer, but so did recovery of non-glycosylated peptides, so improved recovery could be due to binding of the peptide portion of the molecule, rather than through the cis-diol groups on the glycans.

Table 3.8: Recovery of fetuin tryptic peptides and glycopeptides using Bond Elut PBA silica

Buffer pH	Mean % Recovery of Peptide m/z (n=3)			Mean % Recovery of Glycopeptide m/z (n=3)	
	707.7	577.8	737.9	1535.9	1635.2
5.5	**104.4**	**36.1**	**105.6**	**40.3**	**76.8**
7.0	**69.3**	**18.6**	**73.7**	**0.4**	**2.9**
8.5	**34.6**	**21.6**	**69.6**	**1.2**	**3.8**

To investigate if it was the different binding characteristics of sialic acids which were responsible for altering the way fetuin bound at lower pH, tryptic digests of desialylated fetuin were extracted. The results are shown in table 3.9. Although recovery of glycopeptides improved it was still no better than the recovery of non-glycosylated peptides, and was worse at pH 8.5. Curiously, although the peptide portion of the fetuin should have been unaltered by digestion with neuraminidase, the recovery of the non-glycosylated fragments differed markedly from that observed when fetuin was extracted with sialic acids still attached.

Table 3.9: Recovery of fetuin tryptic peptides and desialylated glycopeptides using Bond Elut PBA silica

Buffer pH	Mean % Recovery of Peptide m/z (n=3)			Mean % Recovery of Glycopeptide m/z (n=3)	
	707.7	577.8	737.9	1244.8	1416.9
5.5	**59.9**	**39.3**	**48.9**	**48.7**	**33.3**
7.0	**55.1**	**29.1**	**68.4**	**60.1**	**34.5**
8.5	**119.2**	**30.4**	**72.4**	**21.6**	**35.4**

3.3.8 Binding of saccharides by polymeric beads

After incubation with unmodified beads, the concentration of the mannitol solution appeared to rise from 25.0 µg/mL to 36.1 µg/mL. After incubation with the modified beads, the concentration of the solution fell to 1.9 µg/mL. However, recovery from the beads was again poor, as shown in table 3.10.

Table 3.10: Recovery of mannitol from modified polymeric beads

Elution method	Mean recovery (%), n=2
50:50 water/methanol + 1% formic acid, pH 3.4	2.9
50:50 water/methanol + 10% formic acid, pH 3.0	1.8
50:50 water/methanol + 1% TFA, pH 2.2	1.0
50:50 water/methanol + 1% TFA – sample was then dried down under N_2 and reconstituted in 50:50 water/methanol + 0.1% formic acid	4.0

The apparent rise in concentration of mannitol when incubated with unmodified beads may be attributable to the hydrophobicity of the beads. A high concentration of organic solvent is required to prevent the beads separating from the solution. It may be that this solvent is forming a layer around the beads, and that the highly hydrophilic mannitol is in turn partitioning into the aqueous fraction of the solvent, resulting in a rise in its concentration in this part. As shown in Table 3.11, there was a small fall in mannitol concentration when the incubation was carried out at pH 5.0. Mannitol solutions are mildly acidic and it may be that when in acidic solutions, mannitol remains protonated and therefore does not partition into the aqueous fraction to the same extent.

Although mannitol concentration had been shown to fall after incubation with the modified beads, recovery was poor. Since the mannitol had been shown to bind effectively to the beads, the problem must lie with the elution. Non-specific binding had not been seen with the unmodified beads, and could not therefore account for the low levels of recovery. However, the low pH values of all the elution buffers suggest that binding other than the expected boronic ester formation (which would be reversed at low pH) was occurring. It is difficult to see what this could have been. This is backed by the data showed in Table 3.11, on mannitol binding at different pH values. This shows that binding across the pH range of 5.0 to 8.5 did not appear to

differ significantly, which it would be expected to if boronic ester formation was responsible for binding.

Table 3.11: Concentration of mannitol solution, originally 25.0 µg/mL, after incubation with polymeric beads in different pH buffers (n=1)

Buffer pH	Concentration of mannitol, post incubation (µg/mL)	
	Modified beads	Unmodified beads
5.0	1.1	23.3
6.0	1.5	32.5
7.5	1.9	36.1
8.5	1.4	36.8

3.3.9 Extraction of peptides and glycopeptides using polymeric beads

Despite the failure of the attempt to recover mannitol from polymeric beads, an attempt was made to extract glycopeptides from tryptically digested HRP. The recovery of peptides and glycopeptides from solution is shown in table 3.12.

Recovery of glycopeptides was again poor. However, unlike the extraction attempts using modified silica, some binding of glycopeptides to the beads was apparent, as seen in the falls in peak area of the glycopeptides with m/z 1119.2 and 1225.3. The concentration of glycopeptides in wash solutions was also low, indicating that they were binding to the modified beads. The low concentrations of (non-glycosylated) peptides after incubation and in wash solutions suggested that non-specific binding of peptides to the beads was a significant problem however, and may be responsible for the binding of glycopeptides as well. This is again also indicated by the poor recovery, which suggests that the binding of the glycopeptides and peptides is not disrupted by the change to an acidic medium, as would be expected if the binding was to a boronic acid group.

Efforts to prevent this non-specific binding by including a pre-incubation step with insulin were not successful at improving recovery of glycopeptides, with results from all stages of the extraction process remaining at similar levels.

Table 3.12: Recovery of targeted glycopeptides/peptides pre-incubation with boronic acid functionalised polymeric beads, post-incubation, from wash solutions and in final elutions.

	Mean peak area					
	Peptides			Glycopeptides		
m/z	468.5	480.5	593.7	1119.2	1225.3	1299.4
HRP digest, 100 µg/mL	204000	687000	76000	22000	15000	15000
Modified beads, post incubation	180000	199000	13800	14600	1460	14600
Modified beads (IB*), post incubation	174000	275000	17600	13000	1750	14500
Modified beads, wash 1	5300	11200	2520	140	646	61
Modified beads (IB) wash 1	6200	12300	3000	190	368	0
Modified beads, wash 2	1620	9110	1510	155	450	0
Modified beads (IB) wash 2	4150	11900	1470	131	277	0
Modified beads, elution	2020	8940	0	208	146	0
Modified beads (IB) elution	2650	10700	0	335	88	0

* insulin blocked

3.4 Conclusions

The experiments attempted in this chapter experienced serious problems. Manufacture of working boronic-acid functionalised silica proved harder than anticipated. By two (published) methods (3.2.3 and 3.2.4), modification of the silica failed comprehensively. Attempts to contact the authors of the methods were also

unsuccessful, but it is difficult to understand how they managed to heat silica at 90 ºC in an alkaline solution, or to react silica with aminophenylboronic acid in chloroform. An attempt by the other method (3.2.2) resulted in silica which, when analysed using FTIR or ICP-MS after HF digestion, appeared to contain high amounts of boron. However, it was distinctly unsuccessful at capturing cis-diol containing molecules, whether large glycopeptides or small saccharides. The failure to bind simple saccharides suggests that it was not lack of porosity that was responsible for the failure of the binding, and leaves only the possibility that the boron detected was not present in a boronic acid group, i.e. that a different, as yet unknown, reaction was taking place to the one expected.

Comparison of the self modified silica with commercially available boronic acid functionalised silica did not serve to clarify the picture. Examination of the Agilent silica detected lower levels of boron than that found in the modified silica. The Agilent material also had a smaller pore size, and larger particle size; nonetheless, at a neutral pH it bound glycopeptides from a solution of a tryptic digest of HRP, and did so more effectively than it bound non-glycosylated peptides. These glycopeptides were also recovered when an acidic eluent was used. However, extraction of these glycopeptides from an acidic buffered solution (pH 5.5) was more effective than extraction from a neutral pH, contrary to expectations. Repeating the experiment using a tryptic digest of fetuin threw up more anomalous results, as at pH 7.0, recovery of glycopeptides was very poor, whereas recovery of non-glycosylated peptides was reasonably high. This was also the case at pH 8.5. At pH 5.5 recovery of glycopeptides was improved, but recovery of non-glycosylated peptides was also improved, suggesting that recovery may not be due to boronic ester formation involving the cis-diol groups.

The formation of such esters between sialic acid and boronic acid has been shown to have a different pH dependence to the majority of cis-diol containing molecules. Specifically, N-acetylneuraminic acid has been shown to continue to bind strongly to phenylboronic acid below neutral pH, and its binding affinity actually increased as pH decreased as far as pH 4 (Otsuka, Uchimura et al. 2003). As a result, the fetuin extraction was repeated, after using neuraminidase to cleave off terminal sialic acids. Although this did increase binding of the glycopeptides at neutral and basic pH, surprisingly it also did the same for peptides, which should have been unaffected by the presence of the enzyme. Perhaps most importantly, recovery of (at least) one of

the non-glycosylated peptides from the digest was higher than recovery of the examined glycopeptides, meaning that even after this modification step the silica was not useful for specifically extracting fetuin glycopeptides.

The confusing picture with the modified and commercially available silica was the reason an attempt was made to modify polymeric beads instead. Initial results showed some promise, with rapid and extensive binding of mannitol from solution, which was not seen with unmodified beads. Recovery, however, was poor. Since incubation with unmodified beads resulted in an apparent rise in the concentration of mannitol (possibly due to partitioning into the aqueous fraction of the incubation buffer), it is unlikely that this poor recovery was due to nonspecific binding of the mannitol to the beads. However, it is not clear what it is due to; again, modification of the beads with a functionality other than the expected boronic acid group could be responsible. This might also explain the problems found when trying to specifically extract glycopeptides from solution using the beads, which bound both glycosylated and non-glycosylated peptides without the desired discrimination.

In summary, attempts to produced boronic acid functionalised materials for the specific extraction and concentration of glycopeptides have not been a success. Neither silica nor polymeric beads were able to do so specifically, despite some evidence that the silica at least had been modified in the intended manner. It is not clear why this is; however, modification with a different boron containing functional group other than the expected boronic acid group cannot be ruled out.

3.5 References

Adamek, V., X.-C. Liu, et al. (1992). "New aliphatic boronate ligands for affinity chromatography." Journal of Chromatography A **625**(2): 91-99.

Allevi, P., E. A. Femia, et al. (2008). "Quantification of N-acetyl- and N-glycolylneuraminic acids by a stable isotope dilution assay using high-performance liquid chromatography-tandem mass spectrometry." Journal of Chromatography A **1212**(1-2): 98-105.

Bossi, A., L. Castelletti, et al. (2004). "Properties of poly-aminophenylboronate coatings in capillary electrophoresis for the selective separation of diastereoisomers and glycoproteins." Journal of Chromatography A **1023**(2): 297-303.

Chen, M., Y. Lu, et al. (2009). "Boronate affinity monolith for highly selective enrichment of glycopeptides and glycoproteins." Analyst **134**(10): 2158-2164.

Cummings, R. D. and S. Kornfeld (1982). "Fractionation of asparagine-linked oligosaccharides by serial lectin-Agarose affinity chromatography. A rapid, sensitive, and specific technique." Journal of Biological Chemistry **257**(19): 11235-40.

Das, D., D.-M. Kim, et al. (2011). "A Glucose Sensor Based on an Aminophenyl Boronic Acid Bonded Conducting Polymer." Electroanalysis **23**(9): 2036-2041.

Deore, B. A., I. Yu, et al. (2003). "A Switchable Self-Doped Polyaniline: Interconversion between Self-Doped and Non-Self-Doped Forms." Journal of the American Chemical Society **126**(1): 52-53.

Draffin, S. P., P. J. Duggan, et al. (2003). "Highly selective lipophilic diboronic acid that transports fructose as the trisdentate 2,3,6-β-d-fructofuranose ester." Tetrahedron **59**(46): 9075-9082.

Gontarev, S., V. Shmanai, et al. (2007). "Application of phenylboronic acid modified hydrogel affinity chips for high-throughput mass spectrometric analysis of glycated proteins." Rapid Communications in Mass Spectrometry **21**(1): 1-6.

He, J., Z. Liu, et al. (2009). "Electrochemically deposited boronate affinity extracting phase for covalent solid phase microextraction of cis-diol biomolecules." Talanta **79**(3): 746-751.

Hjertén, S. and J.-P. Li (1990). "High-performance liquid chromatography of proteins on deformed non-porous agarose beads: Fast boronate affinity chromatography of haemoglobin at neutral pH." Journal of Chromatography A **500**(0): 543-553.

Jang, K. K., Y. H. Kim, et al. (2009). "Method development for direct detection of glycoproteins on aminophenylboronic acid functionalized self-assembled monolayers by matrix-assisted laser desorption/ionization mass spectrometry." Rapid Communications in Mass Spectrometry **23**(22): 3599-3602.

Lee, J. H., Y. Kim, et al. (2005). "Immobilization of Aminophenylboronic Acid on Magnetic Beads for the Direct Determination of Glycoproteins by Matrix Assisted Laser Desorption Ionization Mass Spectrometry." Journal of the American Society for Mass Spectrometry **16**(9): 1456-1460.

Lei, Y., Z. Liu, et al. (2001). "Synthesis of a macroporous hydrophilic ternary copolymer and its application in boronate-affinity separation." Reactive and Functional Polymers **48**(1–3): 159-167.

Li, F., X. Zhao, et al. (2006). "Synthesis of silica-based benzeneboronic acid affinity materials and application as pre-column in coupled-column high-performance liquid chromatography." Analytica Chimica Acta **580**(2): 181-187.

Li, H., Y. Liu, et al. (2011). "A Wulff-type boronate for boronate affinity capture of cis-diol compounds at medium acidic pH condition." Chemical Communications **47**(28): 8169-8171.

Li, Y., E. L. Larsson, et al. (2001). "Shielding of protein-boronate interactions during boronate chromatography of neoglycoproteins." Journal of Chromatography A **909**(2): 137-145.

Lin, Z., J. Pang, et al. (2011b). "One-pot synthesis of an organic-inorganic hybrid affinity monolithic column for specific capture of glycoproteins." Chemical Communications **47**(34): 9675-9677.

Lin, Z., J. Zheng, et al. (2012). "One-pot synthesis of phenylboronic acid-functionalized core-shell magnetic nanoparticles for selective enrichment of glycoproteins." RSC Advances **2**(12): 5062-5065.

Lin, Z. A., J. L. Pang, et al. (2011a). "Preparation and evaluation of a phenylboronate affinity monolith for selective capture of glycoproteins by capillary liquid chromatography." Analyst **136**(16): 3281-3288.

Liu, X.-C., J. L. Hubbard, et al. (1995). "Synthesis and structural investigation of two potential boronate affinity chromatography ligands catechol [2-(diisopropylamino)carbonyl]phenylboronate and catechol [2-(diethylamino)carbonyl, 4-methyl]phenylboronate." Journal of Organometallic Chemistry **493**(1-2): 91-94.

Liu, Y., Y. Lu, et al. (2012). "Restricted access boronate affinity porous monolith as a protein A mimetic for the specific capture of immunoglobulin G." Chemical Science **3**(5): 1467-1471.

Liu, Y., L. Ren, et al. (2011). "A unique boronic acid functionalized monolithic capillary for specific capture, separation and immobilization of cis-diol biomolecules." Chemical Communications **47**(17): 5067-5069.

Monzo, A., G. Bonn, et al. (2007). "Boronic acid–lectin affinity chromatography. 1. Simultaneous glycoprotein binding with selective or combined elution." Analytical and Bioanalytical Chemistry **389**(7): 2097-2102.

Otsuka, H., E. Uchimura, et al. (2003). "Anomalous Binding Profile of Phenylboronic Acid with N-Acetylneuraminic Acid (Neu5Ac) in Aqueous Solution with Varying pH." Journal of the American Chemical Society **125**(12): 3493-3502.

Ozohanics, O., L. Turiák, et al. (2012). "Comparison of glycopeptide/glycoprotein enrichment techniques." Rapid Communications in Mass Spectrometry **26**(2): 215-217.

Qu, Y., J. Liu, et al. (2012). "Boronic Acid Functionalized Core–Shell Polymer Nanoparticles Prepared by Distillation Precipitation Polymerization for Glycopeptide Enrichment." Chemistry – A European Journal **18**(29): 9056-9062.

Ren, L., Y. Liu, et al. (2009). "Synthesis of hydrophilic boronate affinity monolithic capillary for specific capture of glycoproteins by capillary liquid chromatography." Journal of Chromatography A **1216**(47): 8421-8425.

Ren, L., Z. Liu, et al. (2009). "Synthesis and characterization of a new boronate affinity monolithic capillary for specific capture of cis-diol-containing compounds." Journal of Chromatography A **1216**(23): 4768-4774.

Ren, L., Z. Liu, et al. (2009). "Ring-Opening Polymerization with Synergistic Co-monomers: Access to a Boronate-Functionalized Polymeric Monolith for the Specific Capture of cis-Diol-Containing Biomolecules under Neutral Conditions." Angewandte Chemie International Edition **48**(36): 6704-6707.

Springsteen, G. and B. Wang (2002). "A detailed examination of boronic acid-diol complexation." Tetrahedron **58**(26): 5291-5300.

Tang, J., Y. Liu, et al. (2009). "On-plate-selective enrichment of glycopeptides using boronic acid-modified gold nanoparticles for direct MALDI-QIT-TOF MS analysis." Proteomics **9**(22): 5046-5055.

Westmark, P. R. and B. D. Smith (1996). "Boronic acids facilitate the transport of ribonucleosides through lipid bilayers." Journal of Pharmaceutical Sciences **85**(3): 266-269.

Westmark, P. R., L. S. Valencia, et al. (1994). "Influence of eluent anions in boronate affinity chromatography." Journal of Chromatography A **664**(1): 123-128.

Xu, Y., Z. Wu, et al. (2008). "Highly Specific Enrichment of Glycopeptides Using Boronic Acid-Functionalized Mesoporous Silica." Analytical Chemistry **81**(1): 503-508.

Xu, Y., L. Zhang, et al. (2010). "On-plate enrichment of glycopeptides by using boronic acid functionalized gold-coated Si wafer." Proteomics **10**(5): 1079-1086.

Yan, J., G. Springsteen, et al. (2004). "The relationship among pKa, pH, and binding constants in the interactions between boronic acids and diols—it is not as simple as it appears." Tetrahedron **60**(49): 11205-11209.

Yang, F., Z. Lin, et al. (2011). "Synthesis and application of a macroporous boronate affinity monolithic column using a metal-organic gel as a porogenic template for the specific capture of glycoproteins." Journal of Chromatography A **1218**(51): 9194-9201.

Zhang, H., G. Yao, et al. (2011). "Facile Synthesis of Boronic Acid-Functionalized Magnetic Mesoporous Silica Nanocomposites for Highly Specific Enrichment of Glycopeptides." Chinese Journal of Chemistry **29**(4): 835-839.

Zhang, L., Y. Xu, et al. (2009). "Boronic Acid Functionalized Core–Satellite Composite Nanoparticles for Advanced Enrichment of Glycopeptides and Glycoproteins." Chemistry – A European Journal **15**(39): 10158-10166.

Zhao, J., T. M. Fyles, et al. (2004). "Chiral Binol–Bisboronic Acid as Fluorescence Sensor for Sugar Acids." Angewandte Chemie International Edition **43**(26): 3461-3464.

Chapter 4: The use of ‘superchargers’ in mass spectrometry to improve the charging of difficult to detect species including diuretics and glycopeptides

Aim: To investigate the use of different 'superchargers' to improve the charging in electrospray ionisation of species which are difficult to detect in either positive or negative ionisation mode, including diuretics and acidic glycopeptides.

4.1 Introduction

4.1.1 Electrospray ionisation

Electrospray ionisation is a soft ionisation technique for producing gas phase ions from a solution. In liquid chromatography – electrospray ionisation (LC-ESI), a liquid containing ionised analytes flows through a capillary or needle to which a high voltage (typically 1-3 kV) is applied. On leaving the capillary, the stream of liquid is deformed and forms a (Taylor) cone with convex sides and a rounded tip. Above a certain voltage the tip of the cone inverts and produces a jet of liquid. The unstable nature of this jet results in an aerosol spray made up of droplets of solvent containing the charged analyte ions. The solvent evaporates from the droplet until its charge density becomes too great (the Rayleigh limit) and the repulsive forces between the ions cause the original droplet to break up into smaller daughter droplets.
For a spherical droplet, the Rayleigh limit is given by:

$$z_R e = 8\pi(\varepsilon_0 \gamma R^3)^{1/2}$$

where z_R is the unit charge limit, e is the elementary charge, ε_0 is the permittivity of the surrounding medium, γ is the surface tension, and R is the droplet radius.

4.1.2 Mechanism of free ion production

There are two theories of how ions are finally produced in the gas phase, shown in Figure 4.1. The first, originally proposed in 1968 (Dole, Mack et al. 1968), is known as the Charged Residue Model (CRM). It suggested that the subdivision of particles at the Rayleigh limit into smaller particles would continue until droplets are formed containing a single charged analyte particle, which would then enter the gas phase.

An alternative suggestion (the Ion Evaporation Model, or IEM) was put forward by Iribarne and Thomson in 1976 (Iribarne and Thomson 1976). They suggested that before a droplet containing just a single charged analyte is formed, the charge density on its surface would be sufficient to push an ion into the gas phase. As evaporation of solvent continued and droplet size shrank, more and more ions would be pushed into the gas phase.

There is evidence that smaller molecules are ionised by the IEM process, (Gamero-Castaño and Mora 2000; Nguyen and Fenn 2007), whereas larger molecules such as proteins are ionised by the CRM process (Nohmi and Fenn 1992).

4.1.3 Ionisation of small molecules

With electrospray, small molecules tend to produce singly charged ions. The charge on these ions determines whether negative or positive ion mode is suitable for analysis. It in turn is strongly influenced by the choice of solvent and the structure of the analyte in question. Acidic solvents promote protonation, and therefore may be better for positive ion analysis. Conversely, neutral or basic solvents are often used for negative ion analysis. Complicating matters is the fact that such solvents also affect chromatographic retention, so choice of solvent pH may not be quite so straightforward when LC-ESI is used as when a sample is infused into a mass spectrometer. Typically, positive ion mode is used when small molecules contain basic functional groups, whereas negative ion mode is used for molecules with a pronounced acidic nature. This means that compounds containing amino, amide, aldehyde/keto ester or hydroxyl functional groups can be analysed using positive ion ESI, while compounds containing carboxylic acids, hydroxyl/phenol or imide functional groups can be analysed using negative ion ESI.

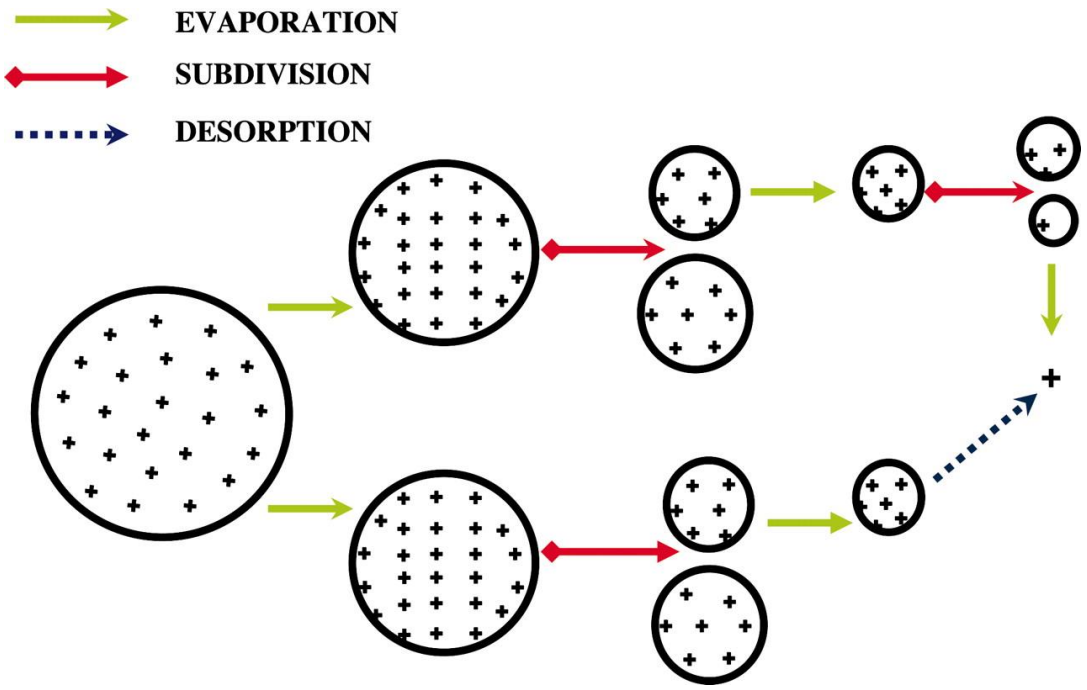

Figure 4.1: Schematic representation of the possible pathways for ion formation from a charged liquid droplet. Upper mechanism is the Charged Residue Model. Bottom mechanism is the Ion Evaporation Model. In the latter model the final ion is produced by desorption, whereas the ion in the former model it is produced by evaporation of solvent from the droplet. (Nguyen and Fenn 2007)

4.1.4 Ionisation of proteins and peptides

Larger molecules such as proteins and peptides tend to form multiply charged species in ESI. This is particularly true of peptides produced by tryptic digestion as they contain an arginine or lysine residue at their C-terminal, as well as an amino group at their N-terminal. A typical spectrum from the ESI of horse myoglobin is shown in figure 4.2. One key detail to note here is that a series of multiply charged species is created, with total charge distributed across the 'multi-charge envelope'. Since mass spectrometers detect ions based not on their mass but on their mass/charge ratio, this has the effect of bringing large molecules into the range where they can be detected by range-limited mass analysers such as triple quadrupoles.

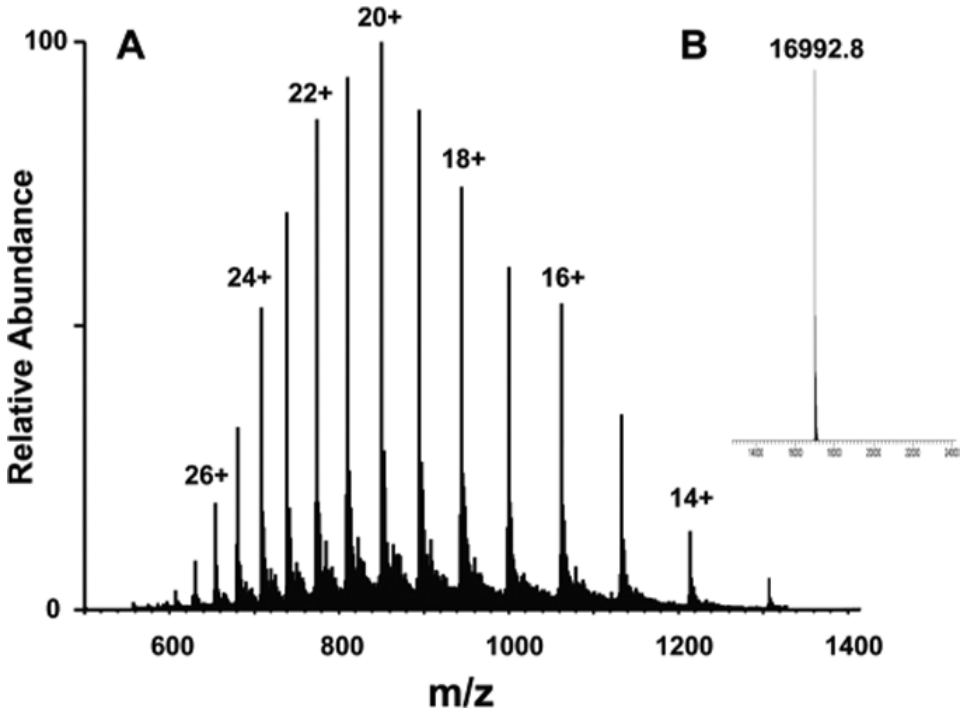

Figure 4.2: ESI mass spectrum from horse myoglobin (A) distribution showing multiple charges (B) spectrum deconvoluted for molecular weight determination (Powell, Razunguzwa et al. 2009)

For Fourier transform mass spectrometers, increased charge also improves signal to noise, mass accuracy and resolution (Hu, Noll et al. 2005).

Under the CRM, the charge on a protein, peptide or other macromolecule is limited by the maximum charge (i.e., the Rayleigh limit) that a droplet of a similar size to the macromolecule can contain before fissioning. Excess charge is lost from a droplet by the expulsion of small electrolyte and solvent ions, until upon desolvation the remaining charge is transferred to the macromolecule. However, this approach fails to quantitatively explain some of the multiple charging observed with macromolecules. Hogan et al (Hogan, Carroll et al. 2008) have proposed that in positive mode for proteins that denature in acidic solutions (or in negative mode for proteins that denature in basic solutions), some of the protein may reside not in the interior of the droplet but at its charged surface. Although the desorption of the entire macromolecule may not be favoured energetically, as desolvation occurs partial desorption of the poorly-solvated charged regions of the protein may occur instead of emission of charge carriers. The macromolecule would then protrude from the

droplet, with the charged segment outside the droplet not contributing to the excess surface charge. This would allow such a protein to carry an overall charge greater than that of the Rayleigh limit of the droplet.

4.1.5 Improving charging on molecules by derivatisation

From the above information it should be clear that increasing the number of charged molecules of an analyte in solution is desirable, as it should increase the signal from that analyte in the mass spectrometer. Increasing the number of charges on a molecule can also improve signal if movement to the gas phase is through the IEM process, as multiply charged ions would be more repelled by surrounding ions of the same polarity, and therefore be more likely to be pushed out of the droplet. A non-polar region is preferable within the analyte, as non-polar ions prefer the air-solvent interface and reside at the droplet surface, meaning they more readily enter the gas phase (Cech and Enke 2000). When tandem mass spectrometry is being used, a move to a higher charge distribution is also desirable, as fragmentation efficiency is better for more highly charged species (Smith, Loa et al. 1990). Finally, it may be desirable to carry out mass spectrometric analysis in a different mode to that optimal for the compound in question, for instance when multiple compounds are being analysed at once and switching between polarities is not possible. All these situations can be addressed by chemical derivatisation of the original compound.

An example of this is the way that molecules containing carboxylic acids have been derivatised to enable their detection in positive ion mode. Butanolic HCl derivatisation produces butyl esters which give a characteristic product ion due to the loss of C_4H_8 in CID, and this approach has been used to measure levels of methylmalonic acid, a marker for defective vitamin B_{12} metabolism (Schmedes and Brandslund 2006). Similarly, sialic acids are frequently derivatised with l,2-diamino-4,5-methylenedioxy-benzene (DMB) to improve detection in positive ion mode (whilst simultaneously introducing a fluorophore). (Morimoto, Nakano et al. 2001). Peptides have also been derivatised to improve their detectability through a variety of methods.

4.1.6 Improving charging through superchargers

The downsides of improving charging through derivatisation are the added time and effort involved, the inevitable in-method losses and the likelihood of reduced signal if multiple derivatives are possible. An alternative that has been found to improve charging on peptides is the introduction into the solvent, either pre- or post-column, of so-called 'superchargers', some of which are pictured in figure 4.3.

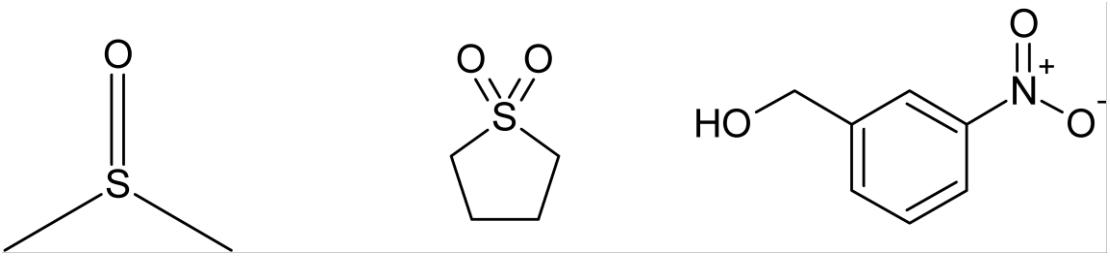

Figure 4.3: Structures of 'superchargers'. From left, dimethyl sulfoxide, sulfolane and *m*-nitrobenzyl alcohol

The effect of these low volatility, high surface-tension compounds, was first reported in a series of papers by Iavarone and Williams (Iavarone, Jurchen et al. 2000; Iavarone, Jurchen et al. 2001; Iavarone and Williams 2002; Iavarone and Williams 2003; Iavarone and Williams 2003b). They found that the addition of glycerol or *m*-nitrobenzyl alcohol (*m*-NBA) to samples being electrosprayed resulted in highly charged protein and peptide ions, with both the maximum charge state detected and the average charge state increased. They also found that the overall base peak abundance was not affected, meaning that the change in charge distribution was not simply due to suppression of lower charge states. The fact that the increase in charging occurred with small (4-mer) peptides suggested that conformational changes are not responsible.

Despite the increase in charge for peptides and proteins, Iavarone and Williams found that when *m*-NBA was added to aqueous solutions of dendrimers, the average charge state, highest charge state and most common charge state were all reduced. The reverse was true for methanolic solutions of dendrimers. Investigation of the effect on solutions of diaminoalkanes to eliminate the possibility of conformational effects produced the same result

A number of different compounds have been found to act as superchargers. The most commonly used are *m*-NBA, dimethylsulfoxide (DMSO) and tetramethylene sulfone (sulfolane), but others which have been shown to have an effect include benzyl alcohol, *m*-nitroacetophenone, *m*-nitrobenzonitrile, *o*-NBA, *p*-NBA, *m*-nitrophenyl ethanol and *m*-(trifluoromethyl)-benzyl alcohol (Lomeli, Peng et al. 2010). These compounds all display low solution-phase basicities and relatively low gas-phase basicities, and are less volatile than water.

The effects of superchargers on chromatographic retention and resolution have also been examined. Valeja et al. (Valeja, Tipton et al. 2010) found that the addition of *m*-NBA and DMSO to LC solvents reduced retention time for intact proteins on a C_{18} column, and the addition of DMSO also improved chromatographic separation.

In comparison, Kjeldsen et al. (Kjeldsen, Giessing et al. 2007), found that the addition of *m*-NBA to LC solvents increased the average charge state of tryptic peptides, resulting in improved fragmentation efficiency when fragmentation was carried out using electron-transfer dissociation (ETD). It also reduced the retention time of the peptides on a reversed-phase column, and at the same time increased peak width and reduced peak height marginally. The extent to which peptide charge increased in the presence of *m*-NBA varied significantly (mean plus standard deviation of 0.25 ± 0.15). This did not appear to be related to peptide length, pI or hydrophobicity. They also examined the effect of *m*-NBA on phosphopeptides. Without *m*-NBA, only one of the nine phosphopeptides examined had a charge state of 3+ or greater; with 0.1% *m*-NBA in the LC solvent, six phosphopeptides were charged to that extent.

Xie et al. (Xie, Shen et al. 2012) demonstrated that superchargers could be used to improve proteomic analysis. Specifically, they showed that the addition of *m*-NBA to LC solvent resulted in an increase in signal intensity for a complex sample of tryptic peptides from a digest of the AMJ2 cell line. When fragmented using ETD, the addition of *m*-NBA also resulted in an increased success rate of identifications using pFind and X!Tandem algorithms.

Meyer and Komives (Meyer and A. Komives 2012) found a similar result. Using a mobile phase with 5% DMSO added and sequencing by both CID and ETD, they found significantly improved peptide identification. However, according to Meyer and Komives, the increase in identifications was not due to supercharging, which was greater when 0.1% *m*-NBA was used, and not observed when 5% DMSO was an

additive. They attributed the improved MS/MS efficiency with the DMSO modified mobile phase to charge state coalescence.

4.1.7 Superchargers mode of action

There has been significant discussion about the exact mode of action of superchargers. Originally, it was thought that denaturation of proteins and large peptides caused by the presence of the superchargers exposed more sites for charging and reduced Coulombic repulsion between the sites. However, evidence that the same charge enhancement is seen with small peptides means this is unlikely to be the sole reason. Iavarone et al. (Iavarone and Williams 2002) said that it appeared to be related to the increased surface tension in electrospray droplets. This, they argued, meant that a higher surface charge density was needed before the Rayleigh limit would be reached, and this in turn would mean peptide and protein ions with higher charges would be found at the droplet surface. This is backed up by the work with dendrimers, where the addition of *m*-NBA to aqueous solutions (lowering the surface tension) reduced the charge, whereas addition of *m*-NBA to methanolic solutions (raising the surface tension) increased the charge. However, Lomeli at al. (Lomeli, Yin et al. 2009) found that addition of *m*-NBA to solutions of proteins in 20 mM ammonium acetate, pH 6.8, also resulted in modest increases in the maximum and average charge. The precise importance of surface tension has also been questioned by Šamalikova and Grandori, who demonstrated that charge state distributions of proteins are not altered by changes in surface tension (Šamalikova and Grandori 2003; Šamalikova and Grandori 2005), although their method meant it was difficult to separate the effect of reducing surface tension from the effect of changing protein conformation. They also found that DMSO increased the average and maximum charge on myoglobin and cytochrome c when acetic or formic acid was used to acidify the solution, but puzzlingly not when HCl was used.

Miladinović et al. (Miladinović, Fornelli et al. 2012) demonstrated that supercharging of proteins and a peptide (substance P) was possible using a dual-sprayer ESI microchip to introduce the supercharging reagent directly into the Taylor cone. This showed that the supercharging process only requires a short period of interaction between the supercharger and the analyte, estimated at less than 1–2 ms when low flow rate ESI conditions are utilised. They also observed that although

both sulfolane and *m*-NBA increased average charge, DMSO resulted in a reduction in average charge.

Sterling and Williams (Sterling and Williams 2009) found that the increased charging of proteins including myoglobin in aqueous solutions caused by the addition of *m*-NBA was mirrored by the effect of heating the solution as it was electrosprayed. They argue that surface tension cannot be responsible for the increase in charging, as *m*-NBA has a lower surface tension than water. Instead, they suggest that because of its lower volatility electrospray droplets become increasingly enriched in *m*-NBA, but that because of the lower vapour pressure of *m*-NBA, the rate of evaporative cooling of the droplet will be lower. As a result, droplets containing *m*-NBA will be at an elevated temperature and have a longer lifetime than those containing just water. This will induce conformational changes in the proteins in the droplets, enabling greater charging. This explanation does not, however, account for the increase in charging seen on small peptides or already denatured proteins.

The higher charge state ions produced from aqueous solutions when sulfolane or *m*-NBA are present have higher collision cross sections measured using ion mobility, consistent with increased protein denaturation (Sterling, Daly et al. 2010; Sterling and Williams 2010).

Evidence that conformational state is important was also provided by Sterling et al. in another paper (Sterling, Cassou et al. 2011). They showed that reduction and alkylation of cytochrome c and ubiquitin did not affect the maximum or average charge states of the proteins in ESI in the absence of *m*-NBA but that, when *m*-NBA was present, charging increased with decreasing numbers of crosslinks. Similarly, addition of *m*-NBA to native RNAse A solutions increased average and maximum charge, but addition to reduced and alkylated RNAse A resulted in a decrease in charge, attributed to the reduced surface tension of the electrospray droplets caused by the addition of the *m*-NBA.

Sterling et al. also used travelling-wave ion mobility-mass spectrometry to investigate the effects of superchargers on the solution- and gas-phase structures of two protein complexes. (Sterling, Kintzer et al. 2012) They found that low concentrations of *m*-NBA effectively increase the charge of concanavalin A dimers and tetramers, but that higher concentrations cause solution-phase dissociation of the dimers and up to a ~22% increase in the collision cross section (CCS) of the

tetramers. They also found that the anthrax toxin octamer, in the presence of 0.8% *m*-NBA, dissociated to an extent which could not be attributed to Coulombic destabilisation in the gas phase as a result of higher charging. They concluded that the supercharging of large protein complexes is the result of conformational changes induced by enrichment of the supercharging reagent in electrospray droplets.

The same group in another study (Sterling, Prell et al. 2011) found that the presence of low concentrations of DMSO reduced the charge on hen egg white lysozyme and equine myoglobin, but that significant increases in charge occurred at higher concentrations. They also found that, at low concentration, DMSO caused a compaction of these proteins but that unfolding took place at concentrations of ~63% and ~43% DMSO for lysozyme and myoglobin, respectively. This is much higher than the concentration in the solvent, suggesting that droplets become concentrated in the electrospray due to preferential evaporation of water. Using evidence of conformational changes obtained using near-UV circular dichroism and solution phase hydrogen/deuterium exchange mass spectrometry, Sterling argued that this increase in concentration causes denaturation of proteins and is largely responsible for the supercharging effect.

Certainly, the change in supercharging effect with increasing concentration is difficult to explain if proton transfer reactivity is responsible. Calculated proton affinities for sulfolane, *m*-NBA and DMSO are shown in Table 4.1. They show that all three display greater proton affinity and gas-phase basicity (GB) than water. As such, if proton transfer reactivity is important, although proton transfer could occur spontaneously from DMSO, sulfolane or *m*-NBA to analytes with lower GB values, such transfer should actually be enhanced when only water is present.

In summary, it would appear that there are different mechanisms responsible for the effects of superchargers in ESI, dependent on the size and type of analyte being examined (as there are for ionisation itself). For proteins and large peptides, superchargers exert their effect as they become concentrated in electrospray droplets, acting as chemical denaturants; in solutions high in organic solvents, they also increase surface tension and reduce evaporative cooling, so that thermal denaturation also occurs. Reduced Coulombic repulsion and increased availability of chargeable sites then result in increased charge.

Table 4.1 : Proton affinity (PA) and gas-phase basicity (GB) for water, acetonitrile and superchargers

	PA (kJ/mol)	GB (kJ/mol)
Water	697	660
Acetonitrile	779	748
Sulfolane	830	801
DMSO	884	853
m-NBA	834	800

For small molecules or larger ones which are incapable of conformational change, any increase in charging appears to be down to increased surface tension, enabling the surface of the droplet to carry greater charge without undergoing Rayleigh limit fission. This then results in greater production of analyte ions, via the IEM mechanism.

There are still some results which do not appear to fit this pattern, however; specifically, the results of Kjeldsen et al., that the addition of *m*-NBA increased the charging on tryptic peptides and phosphopeptides. These are large molecules, but ones which would not be expected to display significant conformational changes to expose more charging sites. However, consideration of the problem using Hogan's theory (mentioned in 4.1.4) that peptides can partially protrude from electrospray droplets could explain this phenomenon. Thus, electrospray droplets with a high organic starting concentration and containing a supercharger would become enriched in the supercharger as water evaporates from the droplet, resulting in droplets with higher surface tension than are found when the supercharger is not present. This results in a greater potential charge on the droplet surface, which can be transferred to the protruding portion of the peptide. Then, when the final ion is produced by the CRM, it carries a higher charge than if the supercharger had not been present. This proposed mechanism is shown in figure 4.4.

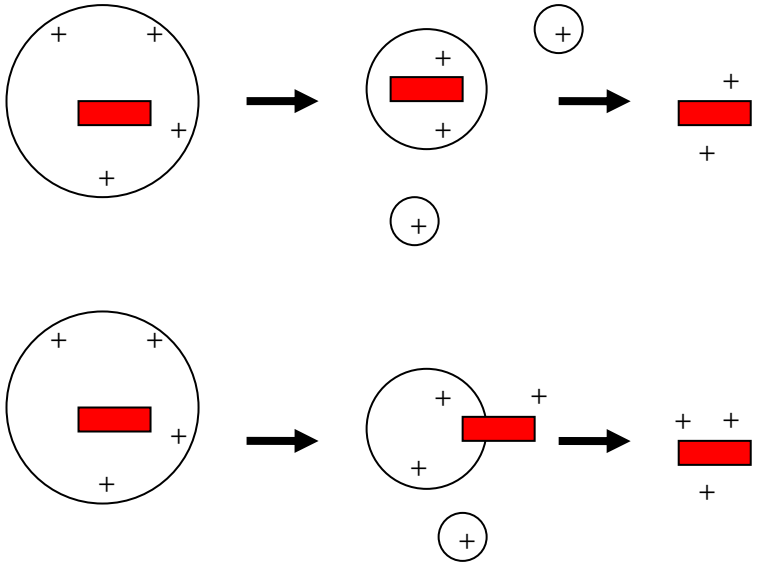

Figure 4.4: Possible mechanism of supercharging of peptides. Top, without supercharger, ion formation by CRM follows loss of charge from droplet in daughter droplets. Bottom, with supercharger, ion formation by CRM follows charge movement onto parts of peptide located outside the droplet.

4.1.8 Switching ionisation mode

The exact mode, or modes, by which superchargers exert their effects on peptides is unknown. However, for small molecules it may be that it at least partially depends on the organic content of the solvent when an analyte enters the electrospray. It may be that for compounds that elute in higher organic concentrations, the charging on droplets, and hence on the analytes themselves, can be improved by the addition of superchargers. A possible application of this would be to enable better detection of small molecules which are only well ionised in one ionisation mode, when the mass spectrometer is operating in the other ionisation mode. This could be useful when rapidly switching ionisation mode is not possible.

Superchargers have also been shown to improve the charging on acidic phosphopeptides, which do not usually ionise well in positive ion mode. It is not unreasonable to suggest that the same may be true of acidic glycopeptides, which can suffer from a similar problem. This has a specific application in nanoflow LC-MS, when dealing with large acidic glycopeptides and using a triple quadrupole mass analyser. As these molecules can be difficult to ionise effectively in positive

ionisation mode, their m/z can lie outside the range of the instrument. In negative ionisation mode, it can be extremely difficult to obtain a stable spray when using nanoflow LC, especially if a gradient elution is being used. However, the use of superchargers to increase charge distribution for these molecules may allow their detection at lower concentrations in positive ion mode, whilst using a triple quadrupole mass spectrometer.

4.2 Experimental

4.2.1 Materials and equipment

All water used was purified using an Elgastat Option 3 water purification unit and had 18.2 MΩ resisitivity. Trypsin (sequencing grade) was purchased from Promega (Southampton, UK). Bendroflumethiazide, canrenone, clopamide and etacrynic acid were from the European Pharmacopeia (Strasbourg). Bumetanide was from Leo Pharma (Buckinghamshire, UK). Chlorothiazide, furosemide, metolazone were from Sanofi-Aventis (Frankfurt, Germany). Xipamide was from Lacer (Barcelona, Spain). Mefruside was from Bayer (Brussels, Belgium). Triamterene was from Smith Kline Beecham (Brentford, UK). All other chemicals were of analytical grade and were purchased from Sigma Aldrich (Poole, UK).

A Hypersil Gold C18 column from Thermo Fisher (Loughborough, UK), 200 mm length and 2.1 mm internal diameter with 1.9 µm particles was used for chromatographic separations.

LC-MS(MS) was carried out using either a Waters Acquity UPLC system and Thermo Exactive Orbitrap mass spectrometer, or a Thermo Accela HPLC pump and autosampler and Thermo LTQ linear ion trap mass spectrometer, as specified.

4.2.2. Effect of superchargers on detection in positive/negative ionisation mode of diuretics

A 1 µg/mL solution of the following diuretics was made up (in 95:5 water:acetonitrile): Acetazolamide; Bendroflumethiazide; Chlorothiazide; Bumetanide; Canrenone; Furosemide; Amiloride; Mefruside; Chlorthalidone; Pemoline; Clopamide; Metolazone; Xipamide; Triamterene; Hydrochlorthiazide; Etacrynic acid (see figure 4.5 for structures).

The mixture was separated and analysed by LC-MS using the Exactive Orbitrap mass spectrometer. Mass spectrometer conditions were (positive/negative ion mode): Sheath gas flow 60/70 arbitrary units (a.u.); auxillary gas flow 10 a.u.; Spray voltage 4.5/3.0 kV; Capillary temperature 250 °C; Capillary voltage 52.5/-95.0 V; Tube lens voltage 135/-145 V; Skimmer voltage 20/-32 V; Heater temperature 300 °C. Scans were carried out between 100 and 500 m/z.

The LC starting conditions were 95% Solvent A, 5% Solvent B, and the gradient changed linearly to 57% Solvent A, 43% Solvent B at 15 minutes, then linearly to 20% Solvent A, 80% Solvent B at 20 minutes. Solvent A was water with 0.1% formic acid and 1% of either sulfolane or dimethyl sulfoxide, or 0.1% *m*-NBA (v/v). *m*-NBA concentration was lower than that of sulfolane or DMSO, as at higher concentrations of *m*-NBA back pressure had been observed to rise excessively. Solvent B was acetonitrile with the same additives.

Five microlitres of solution was injected onto the column for each run. Each analysis was carried out five times in positive and five in negative mode, and the mean peak heights and signal:noise ratios of the extracted ion chromatograms (3 ppm tolerance) generated for each diuretic were measured.

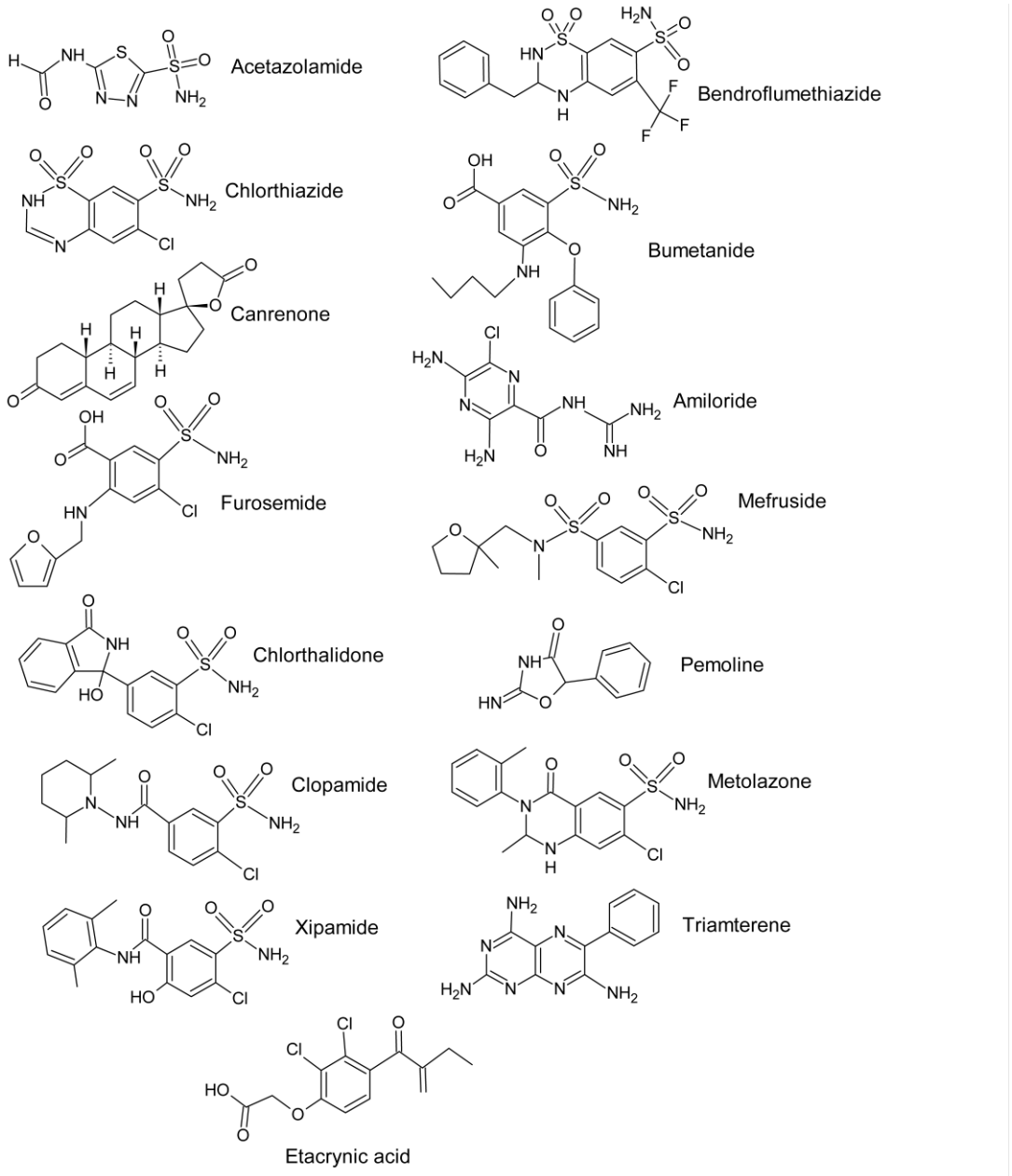

Figure 4.5: Structures of diuretics used in superchargers experiments

Analysis of the same diuretic mixture was also carried out using an isocratic elution (30% A for 45 minutes, other method details the same) to see if differences between the responses of diuretics was due to the solvent make up at the time of elution. Each isocratic analysis was carried out twice with each of the different supercharger additives.

As mentioned in 4.1.7, it has been proposed that some of the effects of superchargers could be due to resultant increased heating of electrospray droplets. To see if the two

had similar effects on the signal from diuretics, the gradient elution method was repeated using water with 0.1% formic acid as solvent A, but with the capillary temperature/heater temperature in the HESI source at 250/300 °C, 300/350 °C, 350/400 °C and 400/450 °C. Each analysis was carried out twice.

4.2.3 Effect of superchargers on detection in positive/negative ionisation mode of glycopeptides

Fetuin was denatured, alkylated and digested using the following procedure: ≈1 mg of protein was weighed out and dissolved in 100 µL 8M urea/50 mM ammonium bicarbonate (ABC) solution, and incubated at room temperature. After 3 hours, 4 µL of 500 mM dithiothreitol was added, and the solution then incubated at 37 °C for 2 hours. The solution was then removed from the incubator, 4 µL of 500 mM iodoacetic acid added and the solution incubated for 30 minutes at room temperature in the dark. 50 mM ABC was added to make the volume up to 950 µL. Trypsin was dissolved to give a 200 µg/mL solution, and 50 µL added to the fetuin solution, to give a protein:enzyme ratio of 100:1. The sample was left overnight at 37 °C, and the reaction stopped by the addition of 4 µL formic acid. Tryptically digested fetuin was then diluted to a concentration of 1 µg/mL (approximately 20 pmol/mL) for analysis by LC-MS.

Recombinant EPO was digested in a similar manner. A vial of rEPO (Epiao, 2,000 IU) was filtered through a 10 kDa Microcon and washed 3 times with 500 µL of 50 mM ABC. It was then recovered and made up to 100 µL with 8M urea/50 mM ammonium bicarbonate (ABC) solution, after which the same digest process was followed as with fetuin.

Acidic glycopeptides were separated and analysed using LC-MS using the Exactive Orbitrap mass spectrometer. Mass spectrometer conditions were (positive/negative ion mode): Sheath gas flow 60 arbitrary units (a.u.); auxillary gas flow 10 a.u.; Spray voltage 4.0/3.0 kV; Capillary temperature 250 °C; Capillary voltage 92.5/-95.0 V; Tube lens voltage 165/-145 V; Skimmer voltage 44/-32 V; Heater temperature 300 °C. Scans were carried out between 200 and 2,500 m/z. The LC starting conditions were 95% Solvent A, 5% Solvent B, and the gradient changed

linearly to 57% Solvent A, 43% Solvent B at 40 minutes. Solvents and analysis methods were the same as in 4.2.2 for the different glycopeptides, except that scans were carried out between 250 and 4,000 m/z.

Automatic peak detection was carried out using Thermo Excalibur software, using the following settings -

Baseline window (number of scans over which to look for a local minima): 40

Area noise factor (noise level multiplier used to determine peak edge after location of possible peak): 5

Peak noise factor (noise level multiplier used to determine potential peak signal threshold): 10

Min peak width: 3 scans

INCOS noise algorithm used to determine noise level

4.3 Results and discussion

4.3.1 Effect of superchargers on detection in positive/negative ionisation mode of diuretics

Addition of superchargers to LC solvents at the concentrations tested slightly affected retention time, though only to a small extent. Peak width was not noticeably affected by the presence of superchargers.

One way analysis of variance was carried out (using Minitab 15) to compare the peak heights of the diuretics with different superchargers in positive ionisation mode, and separately in negative ionisation mode. Dunnett's test was used to see if the data obtained using superchargers was statistically significant at the 5% confidence level from that obtained without superchargers in the LC solvents. Those results which were statistically significant are written in bold in tables 4.2 and 4.3.

A number of observations are possible. Firstly, the presence of sulfolane, dimethylsulfoxide or *m*-NBA affects the peak height of several of the diuretics. These effects were generally significant, especially in positive ion mode and especially for sulfolane and *m*-NBA. However, this is not one way, with some peak

heights increased and others decreased for all of the superchargers. Peak heights in both positive and negative mode are affected. Also, the effect of the superchargers does not change simply with retention time, as may be expected if the effect was solely due to the change caused in the surface tension of the electrospray droplets.

In positive ion mode, after the addition of sulfolane, seven diuretics gave an increased signal (amiloride, acetazolamide, triamterene, pemoline, clopamide, metolazone and bumetanide). Eight compounds gave reduced signal (chlorthiazide, chlorthalidone, furosemide, mefruside, bendroflumethiazide, xipamide, etacrynic acid and canrenone).

With the addition of dimethyl sulfoxide, only the signals from amiloride, pemoline, triamterene and clopamide are increased; all other diuretics display a reduced signal in the presence of the supercharger, except metolazone, which is not significantly affected.

The addition of *m*-NBA to the LC solvents resulted in significantly decreased signal in positive ion mode only from chlorthiazide, while a significant increase was seen for acetazolamide, triamterene, chlorthalidone, clopamide, metolazone, furosemide, mefruside, bendroflumethiazide, bumetanide and etacrynic acid. Signal from the other diuretics was not significantly different.

The use of sulfolane to increase charging appeared to be slightly more effective in negative ionisation mode. Canrenone and triamterene were not detected in negative ionisation mode, with or without superchargers present. However, for all the other compounds signal was significantly increased in the presence of sulfolane; it was significantly increased with eight compounds in the presence of DMSO (amiloride, acetazolamide, chlorthiazide, pemoline, chlorthalidone, clopamide, mefruside and xipamide) and significantly decreased with none. For *m*-NBA, decreases were seen with metolazone and mefruside, while the signal from all other compounds was significantly increased.

Unfortunately, there is no single treatment that enhances signal for all diuretics either in a signal ionisation mode, or if the ionisation mode is switched. However, if

canrenone is excluded and switching is possible, the addition of sulfolane to LC solvent would increase signal from the remaining diuretics by between 1.16 (metolazone) and 7.60 (pemoline) times.

Table 4.2 Ratios of mean peak heights of diuretics with superchargers added to solvents to those measured without superchargers. Positive ion mode. Figures in bold are statistically significant.

Compound	Mean peak height ratio (Sulfolane) +ve	Mean peak height ratio (DMSO) +ve	Mean peak height ratio (*m*-NBA) +ve
Amiloride	**2.40**	**1.92**	1.48
Acetazolamide	**3.05**	**0.06**	**1.55**
Chlorthiazide	**0.07**	**0.02**	**0.81**
Triamterene	**2.75**	**3.91**	**1.49**
Pemoline	**7.60**	**2.87**	2.21
Chlorthalidone	**0.46**	**0.01**	**3.30**
Clopamide	**1.99**	**2.04**	**6.88**
Metolazone	**1.70**	1.03	**3.66**
Furosemide	**0.58**	**0.03**	**2.36**
Mefruside	**0.04**	**0.06**	**1.45**
Bendroflumethiazide	**0.32**	**0.31**	**1.58**
Xipamide	**0.10**	**0.08**	0.84
Bumetanide	**1.81**	**0.03**	**1.89**
Etacrynic acid	**0.0**	**0.0**	**3.70**
Canrenone	**0.50**	**0.0**	1.15

Table 4.3 Ratios of mean peak heights of diuretics with superchargers added to solvents to those measured without superchargers. Negative ion mode. Figures in bold are statistically significant.

Compound	Mean peak height ratio (Sulfolane) -ve	Mean peak height ratio (DMSO) -ve	Mean peak height ratio (*m*-NBA) -ve
Amiloride	**4.14**	**1.55**	**1.32**
Acetazolamide	**3.96**	**2.38**	**1.49**
Chlorthiazide	**6.83**	**1.64**	**2.73**
Triamterene	ND	ND	ND
Pemoline	**3.67**	**1.72**	**2.75**
Chlorthalidone	**1.92**	**1.25**	**1.52**
Clopamide	**2.62**	**1.65**	**1.63**
Metolazone	**1.16**	1.04	**0.58**
Furosemide	**6.11**	1.24	**4.56**
Mefruside	**1.73**	**1.13**	**0.77**
Bendroflumethiazide	**1.51**	0.97	**1.25**
Xipamide	**3.48**	**1.16**	**2.56**
Bumetanide	**3.88**	0.80	**2.62**
Etacrynic acid	**4.91**	1.42	**9.78**
Canrenone	ND	ND	ND

It is not immediately clear why the interaction with sulfolane, dimethyl sulfoxide or *m*-NBA has the effects seen. There is no obvious pattern relating the effect of the superchargers on individual diuretics in positive and negative ionisation mode, with increases and decreases in signal not clearly linked. Examination of the polarity of the compounds did not suggest any reason why some should produce an increased signal, while for others the signal decreased. Similarly, attempts to correlate partition coefficient, isoelectric point or molecular polarisability with peak height ratios for sulfolane, DMSO or *m*-NBA were also unsuccessful. R-squared values for these data sets are shown in Table 4.4, and demonstrate the lack of an obvious link between these characteristics and the effects of superchargers.

Table 4.4 Coefficient of determination (R^2) values demonstrating lack of correlation between physical characteristics of diuretics and effects of superchargers (measured by mean peak height ratios) on diuretic peak heights

Physical characteristic	Sulfolane	DMSO	*m*-NBA
Log P	0.1250	0.0635	0.0589
pI	0.1309	0.3761	0.0176
MP	0.3849	0.1333	0.0282

4.3.2 Effect on changing HESI source temperatures on diuretic peak height

One possible explanation is related to the thermal stability of the compounds involved. Sterling et al. (Sterling, Daly et al. 2010) suggested that the presence of low vapour pressure superchargers during electrospray ionisation results in the preferential enrichment of aqueous droplets in these reagents as evaporation occurs. Evaporative cooling will occur less after the droplets are substantially enriched in the low volatility supercharging reagent, resulting in droplets of a higher temperature. They suggested that this higher temperature may cause destabilisation or denaturation of the protein complex. With small molecules however, gas phase ion production may occur by the ion evaporation model, first proposed by Iribarne and Thomson in 1976 (Iribarne and Thomson 1976). This proposes that charged droplets would have at their surface charged particles, and that the resulting field would become so strong that it would push ions into the gas phase. In this model, multiply charged ions would be more likely to escape, while the likelihood of ions escaping would also be increased by an increase in droplet temperature.

This would suggest that thermal effects may be partially responsible for the effects of superchargers on the peak height of diuretics, with those that are thermally labile decomposing in the electrospray when superchargers are present, resulting in reduced peak height, while those that are not thermally labile are increasingly transferred into the gas phase with a resulting increase in peak height.

To examine this possibility, LC-MS analysis of diuretics was carried out with the capillary and HESI gas heated to different temperatures. However, the results showed that there is no obvious link between the effect of increasing temperature and the effect of the presence of superchargers. Examination of the mass spectra obtained across the diuretics peaks told a similar story. Increasing fragmentation is seen with increasing capillary and HESI gas temperature but this is not mirrored in the spectra obtained in the presence of superchargers. Of course, it is possible that the effect of heating the capillary and gas in the HESI source does not adequately model the effect of heating from superchargers, but it is not unreasonable to expect some correlation if it is an important factor.

4.3.3. Effect of isocratic elution on supercharger effects on diuretics

The other proposed way in which superchargers exert their effect on proteins is through increasing surface tension in electrospray droplets containing high amounts of organic solvents. To see if this was an influencing factor in the effect of superchargers on diuretics, isocratic elutions were carried out, with and without superchargers in the LC solvent. If, as predicted, superchargers exert their effect by changing the surface tension of electrospray droplets, then differences in these effects should be seen with an isocratic elution.

There is some evidence that this is the case with sulfolane. Although the differences are small, twelve of the 15 compounds examined behaved as predicted. With DMSO this was true for six compounds. With *m*-NBA, ten compounds behaved as predicted. For this latter supercharger then, the role of surface tension is perhaps less clear cut, while for DMSO it is ambiguous at best.

The difference between the effects of superchargers in positive and negative ion mode also provides evidence that surface tension and droplet temperature are not the only ways in which superchargers exert their effects, as both of these would be expected to be altered in the same way in positive and negative ionisation mode. The effect of the presence of superchargers on negative ionisation could be due to their greater proton affinity and gas phase basicity than water and acetonitrile, allowing

them to accept protons more readily from the analytes and increasing analyte negative ion formation.

4.3.4. Effect of superchargers on detection in positive/negative ionisation mode of glycopeptides

Glycopeptides were identified by looking for fragment ions corresponding to diagnostic sugar oxonium ions of m/z 292, 366 and 657 (Neu5Ac, Hex-HexNAc, and Neu5Ac-Hex-HexNac). Total ion chromatograms and extracted ion chromatograms for these oxonium ions, with and without superchargers are shown in figures 4.6-4.9. Peaks were automatically detected by the software based on its peak-picking algorithm, and were investigated for the presence of glycopeptides when peaks were automatically detected in the EICs of all three oxonium ions. The number of peaks detected by the software increased with the addition of either m-NBA or sulfolane. In particular, the addition of m-NBA resulted in the detection of a large peak at approximately 37.2 minutes which was not picked up in the other chromatograms.

The way in which the presence of superchargers affects charging can be seen by comparing the mass spectra from the peaks at approximately 17.2 (when the eluent was highly aqueous) and 47.5 minutes (when it was mostly organic). The positive mass spectra from these peaks are shown in figure 4.10 and 4.11. The negative mass spectra are shown in figure 4.12 and 4.13.

The positive ion spectra from the peaks at 17.2 minutes show very little difference between the charge states of the ions with or without superchargers in the LC solvents. The main ions detected are at m/z 1438.2, 1535.3 and 1632.3. This corresponds to the triply charged tryptic fragment containing the N-glycosylation at Asn-156. The ions are glycopeptides with triantennary glycans with two, three or four sialic acid residues, although given the tendency of sialic acids to be lost in electrospray, it is not certain if all these are present originally or are formed by fragmentation in the electrospray. There is no great difference in the charge distributions, although there is a slightly greater abundance of the quadruply charged

ion at m/z 1151.7 when sulfolane was used. The overall intensity of the signal was also increased when sulfolane and DMSO were used.

A different picture is seen with the positive ion spectra from 47.5 minutes. With this peak, the spectrum obtained without superchargers is again dominated by triply charged ions, including ones at m/z 1960.9, 1741.8, and 1863.8. The 1741.8 is an Asn-176 glycopeptide with a biantennary structure and two sialic acids. The 1960.9 could be either the Asn-176, triantennary with three sialic acids, or the Asn-99, biantennary with two sialic acids. Similarly, the 1863.8 ion could be either the Asn-176 triantennary with two sialic acids, or Asn-99, biantennary with one sialic acid.

With the addition of superchargers, the charge distribution shifts. The addition of sulfolane results in an increase in the abundance of the quadruply charged ions at m/z 1308.4, 1470.9, 1543.7 and 1635.2. These are from tryptic glycopeptides containing the Asn-99 glycosylation site. The increase in charge is not as great with DMSO; however, this results in a more condensed charge distribution, with a corresponding increase in signal intensity.

The addition of *m*-NBA did not result in an obvious move to higher charge states. Rather, it appears to have resulted in a reduction in the intensity of the signal from the m/z 1960.9 ion only.

A different result is also obtained when negative ion mode was used. Examination of the spectra from the peak at 17.2 minutes show that without superchargers, the spectrum is dominated by the triply charged m/z 1533.3 ion, corresponding to the Asn-156 glycopeptide, triantennary with three sialic acid residues. There is also a small amount of the same glycopeptide with four sialic acids (m/z 1630.3) but not an ion at m/z 1436.3, suggesting that the small amount of that glycopeptide found in positive ion mode was formed by fragmentation.

When DMSO is added, there is little change in the spectrum in negative ion mode. However, both the addition of sulfolane and *m*-NBA result in increased charge, with a shift with sulfolane to the quadruply charged m/z 1149.7 ion, and a shift with *m*-NBA to both quadruply charged m/z 1149.7 and 1222.7 as well as to the quintuply charged m/z 979.9 ion.

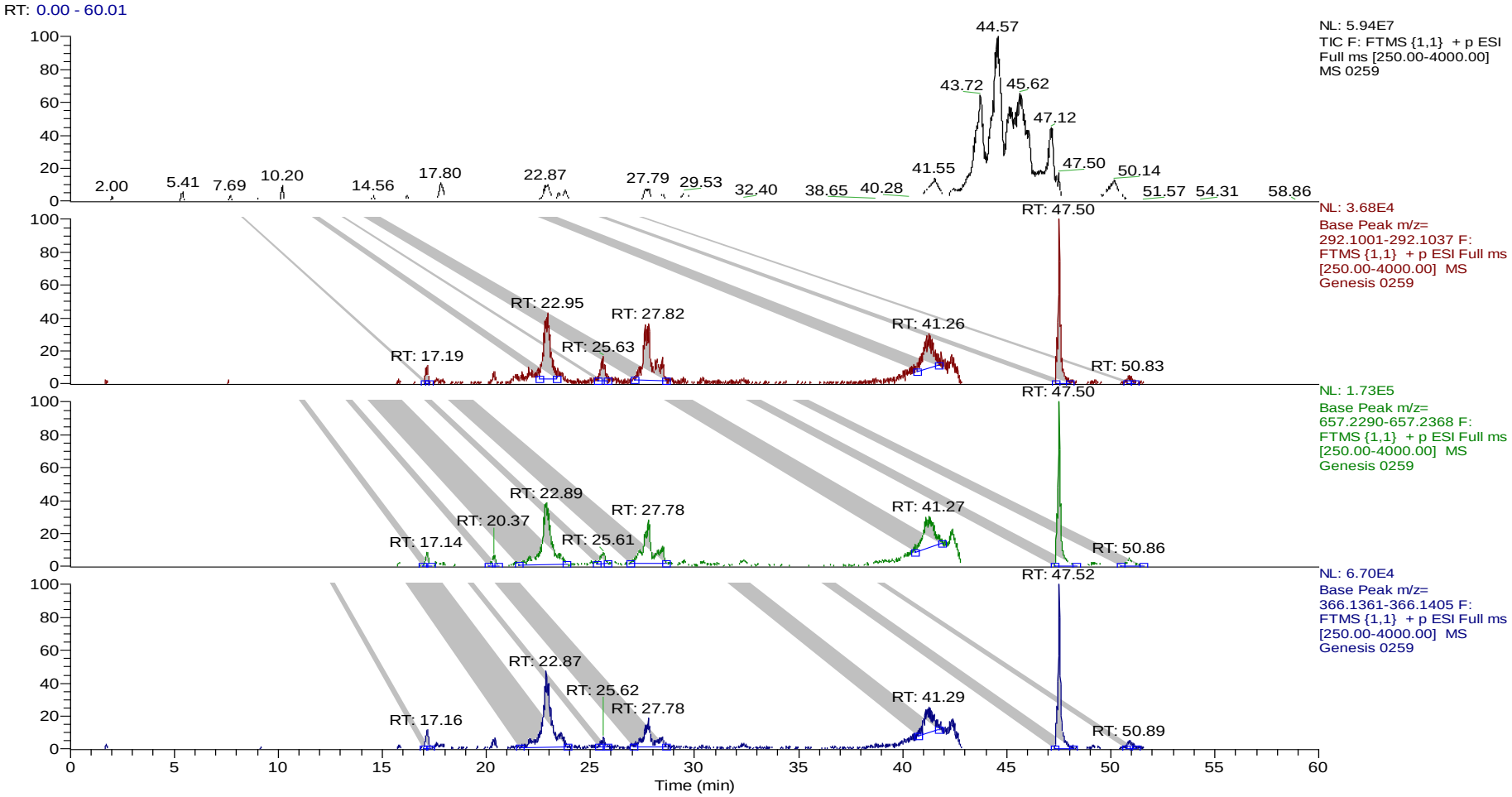

Figure 4.6: (from top) Fetuin tryptic digest. Total ion chromatogram and extracted ion chromatograms for m/z 292.1019, 657.2329 and 366.1383. No superchargers in solvents

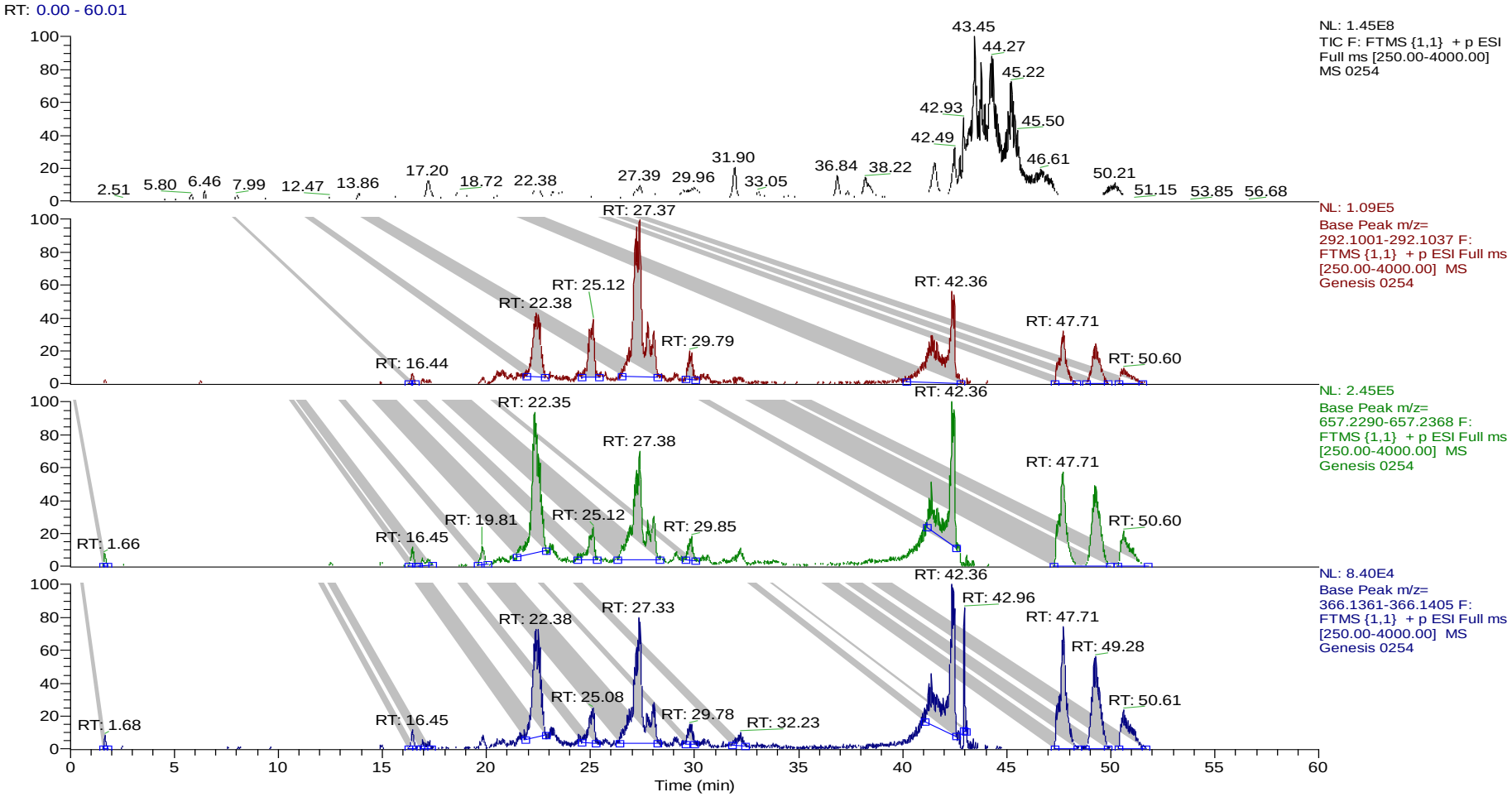

Figure 4.7: (from top) Fetuin tryptic digest. Total ion chromatogram and extracted ion chromatograms for m/z 292.1019, 657.2329 and 366.1383. 1% sulfolane in solvents

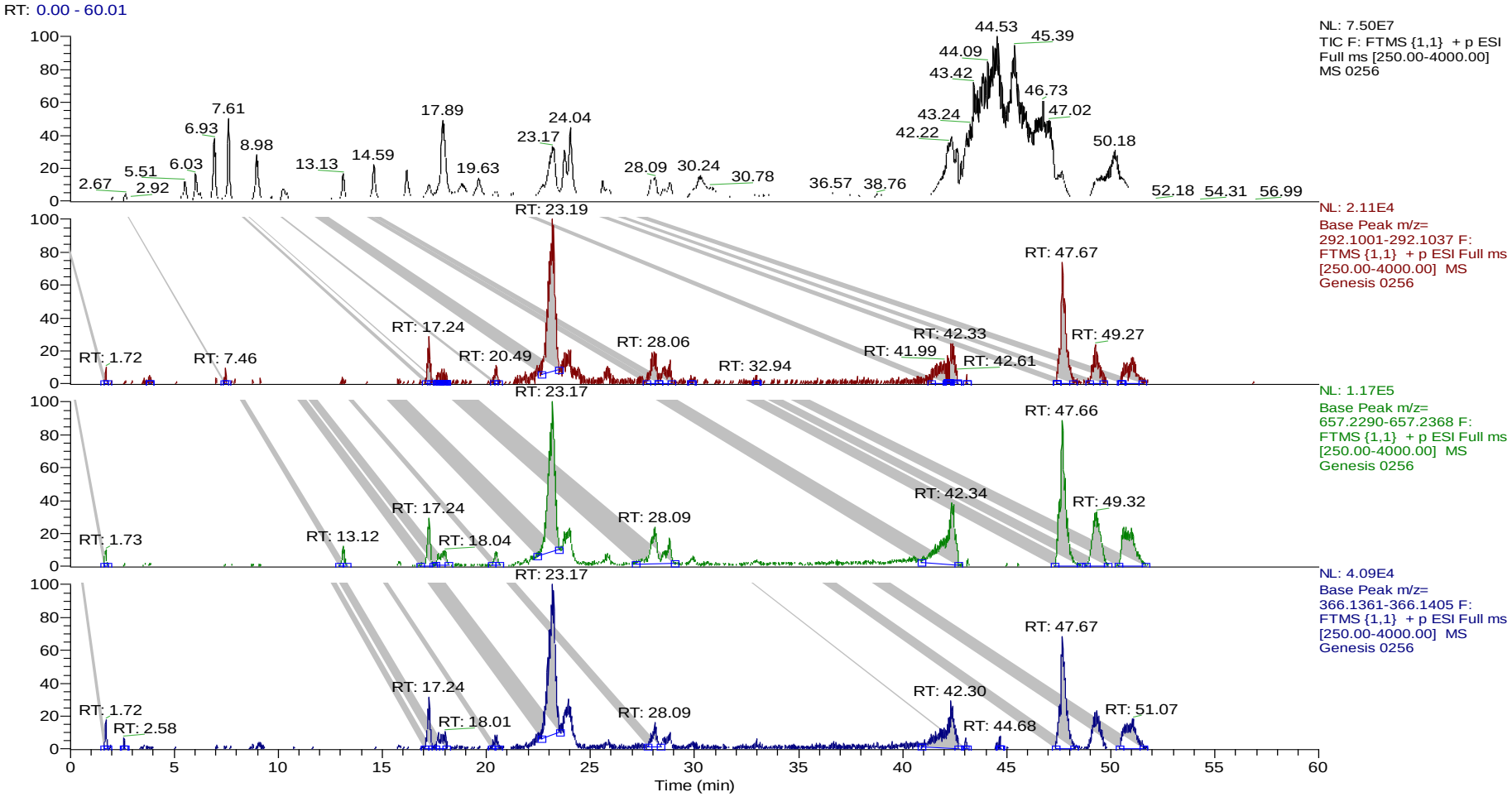

Figure 4.8: (from top) Fetuin tryptic digest. Total ion chromatogram and extracted ion chromatograms for m/z 292.1019, 657.2329 and 366.1383. 1% DMSO in solvents

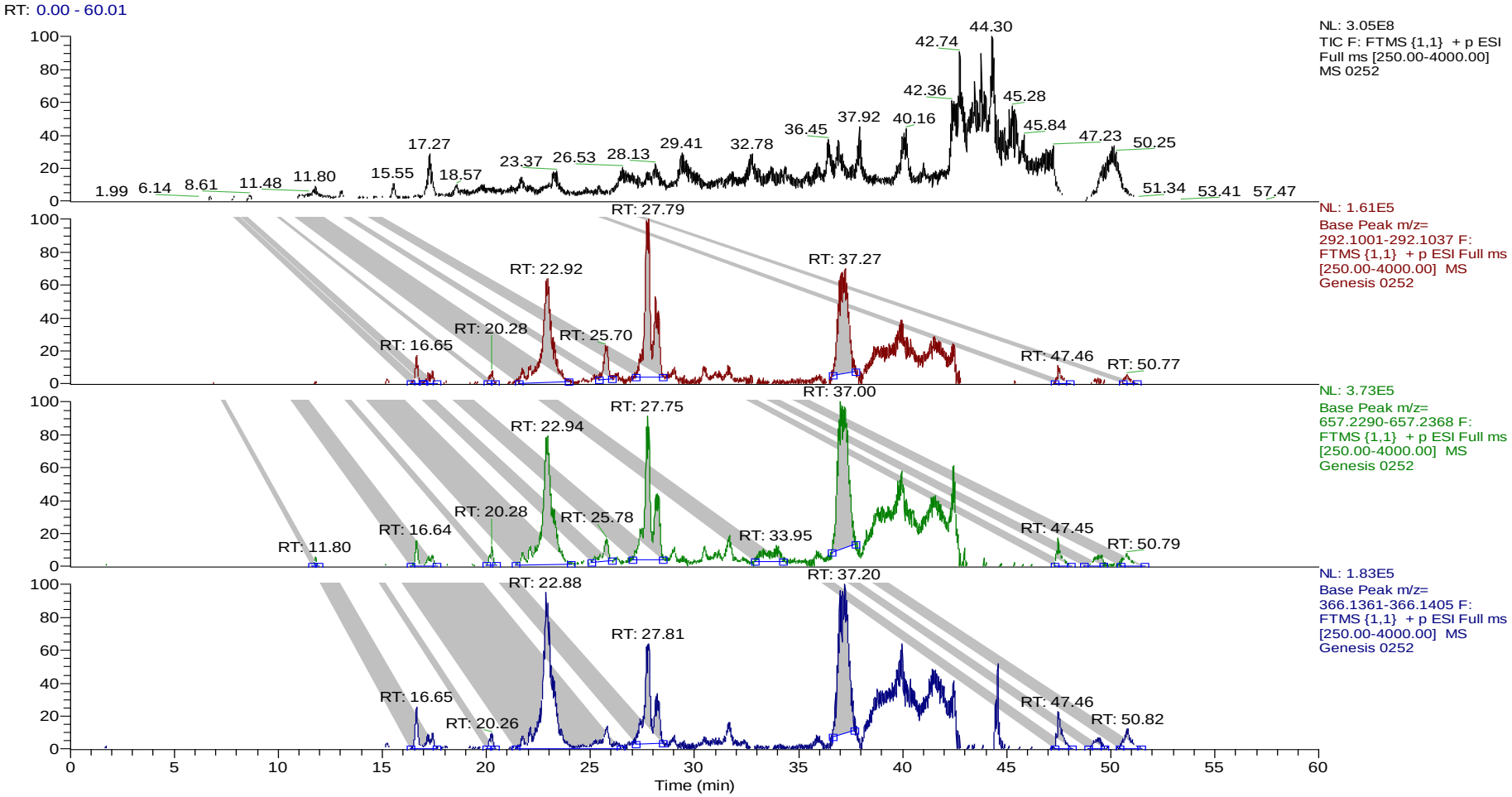

Figure 4.9: (from top) Fetuin tryptic digest. Total ion chromatogram and extracted ion chromatograms for m/z 292.1019, 657.2329 and 366.1383. 0.1% *m*-NBA in solvents

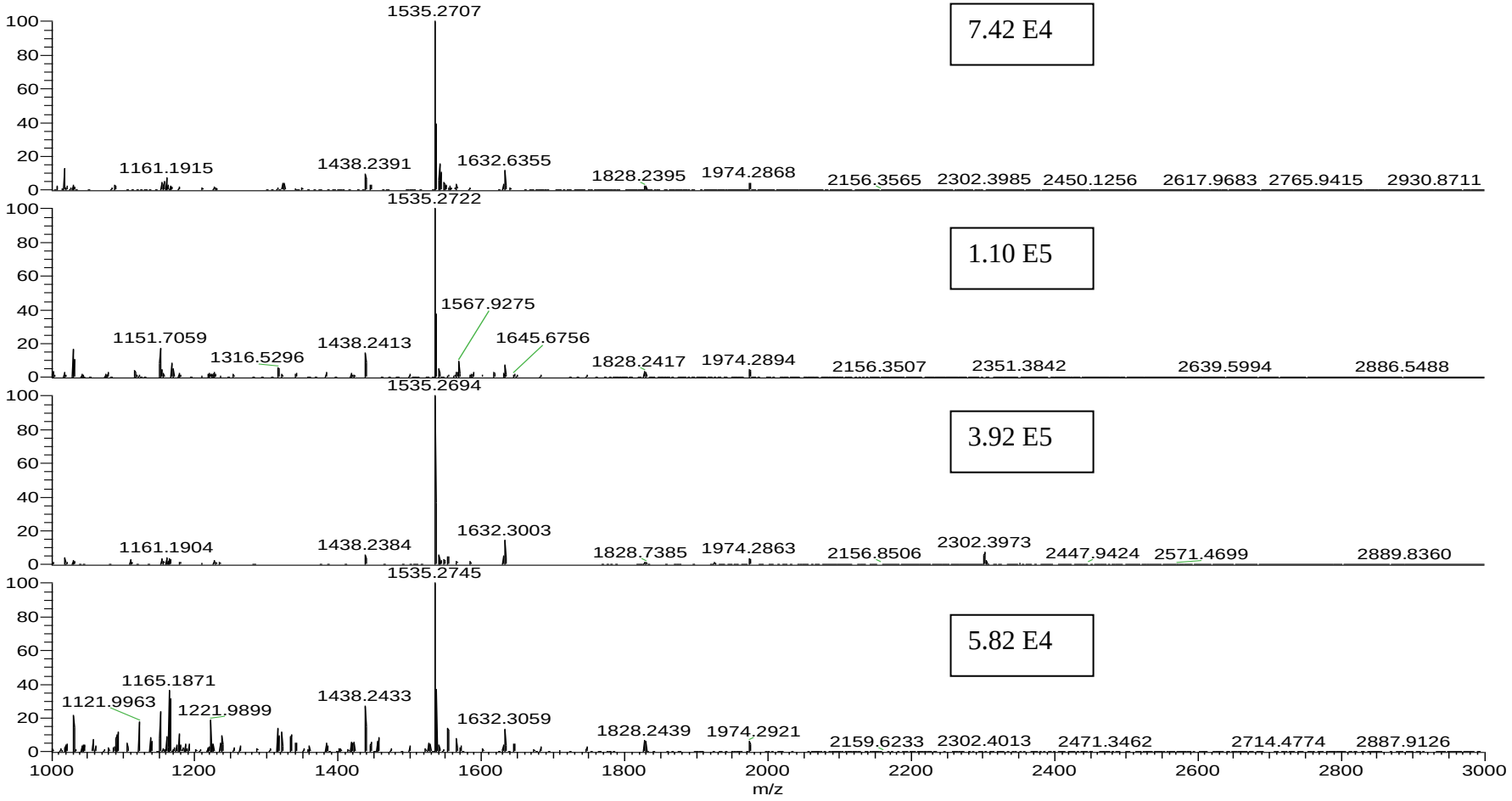

Figure 4.10: Positive ion mass spectra from 17.10 to 17.35 minutes. From top – no superchargers; 1% sulfolane; 1% DMSO; 0.1% *m*-NBA. Inset numbers are base ion intensity

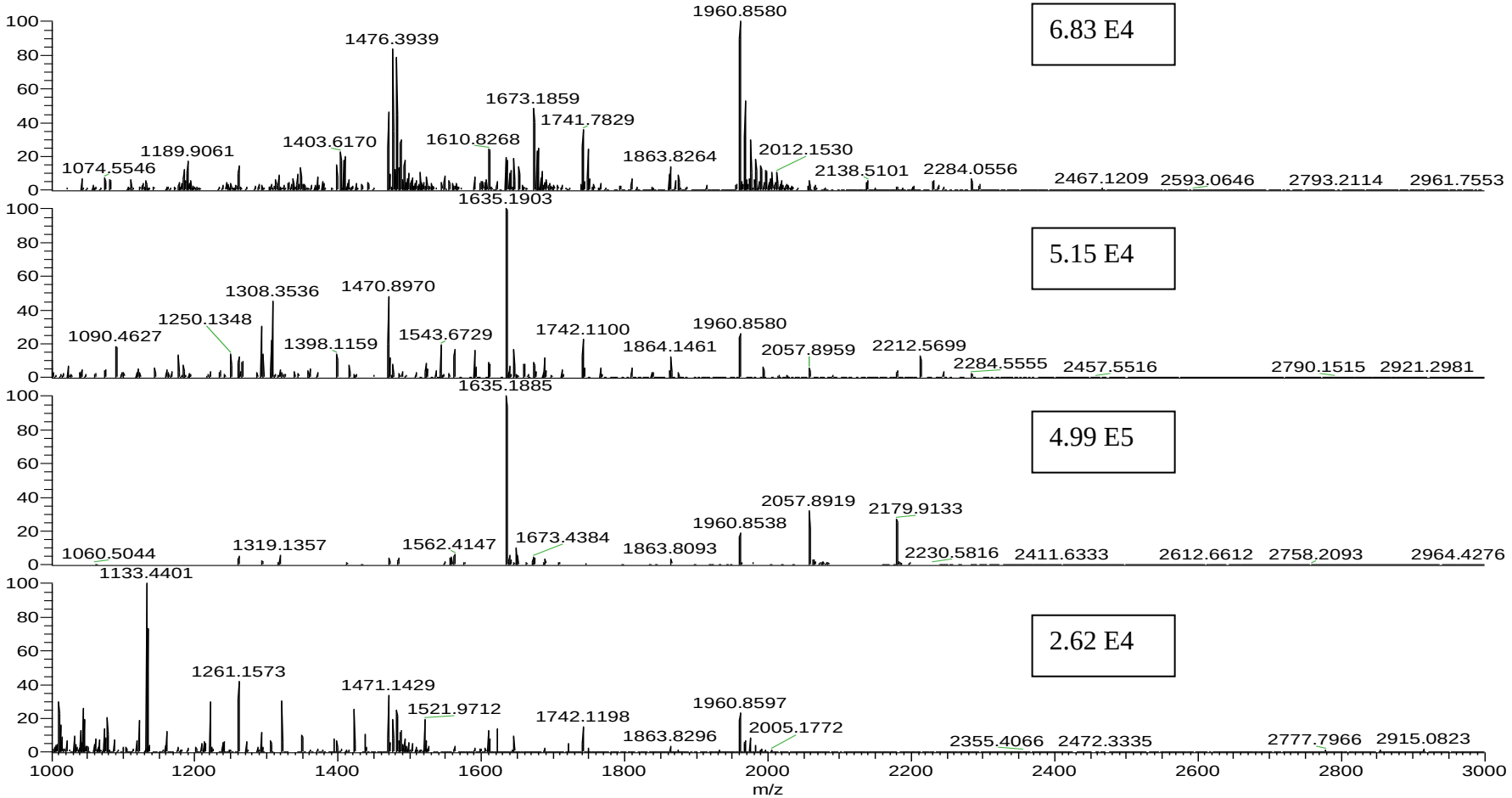

Figure 4.11: Positive ion mass spectra from 47.40 to 47.75 minutes. From top – no superchargers; 1% sulfolane; 1% DMSO; 0.1% *m*-NBA. Inset numbers are base ion intensity

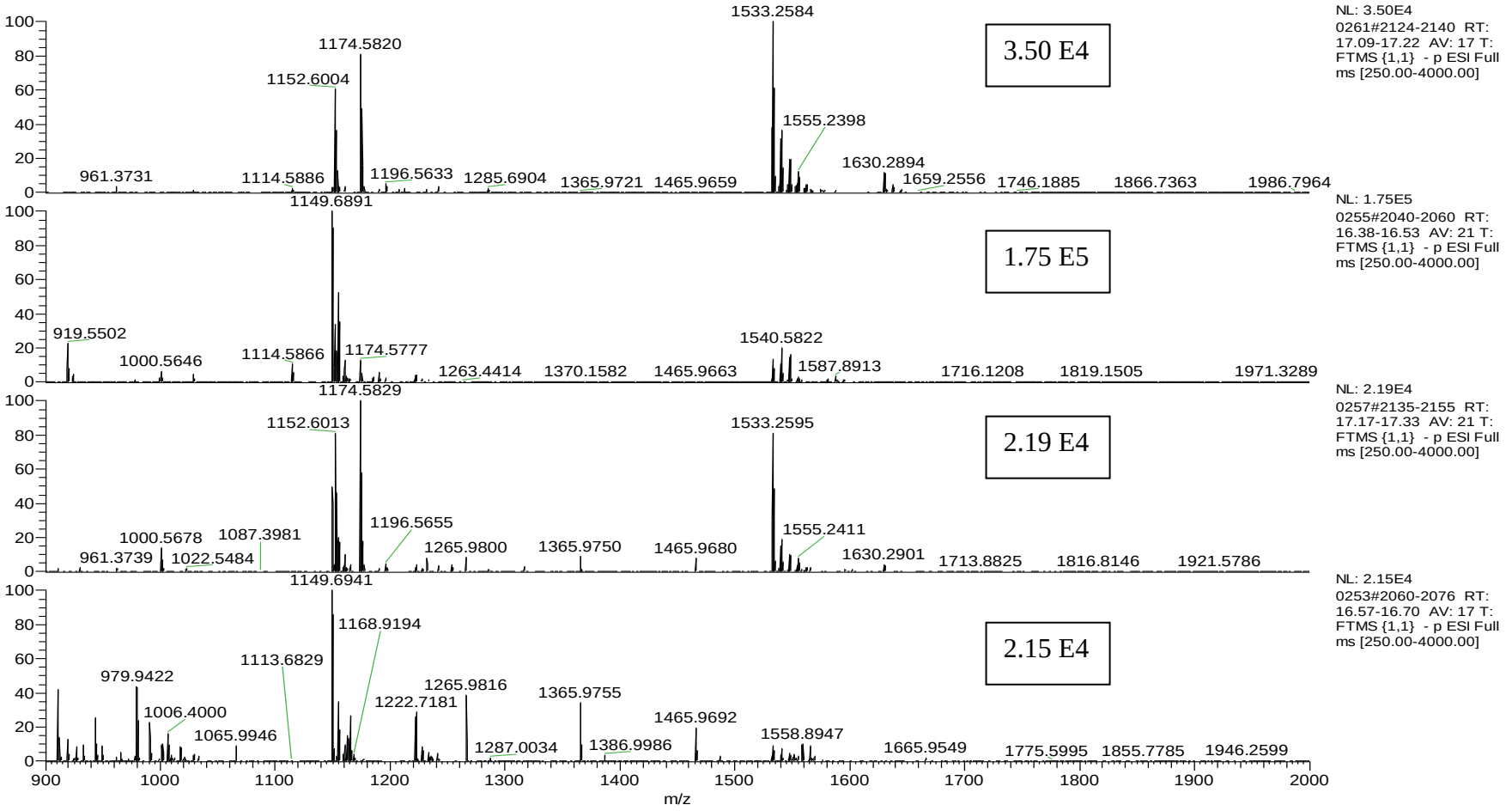

Figure 4.12: Negative ion mass spectra from 17.10 to 17.35 minutes. From top – no superchargers; 1% sulfolane; 1% DMSO; 0.1% *m*-NBA. Inset numbers are base ion intensity

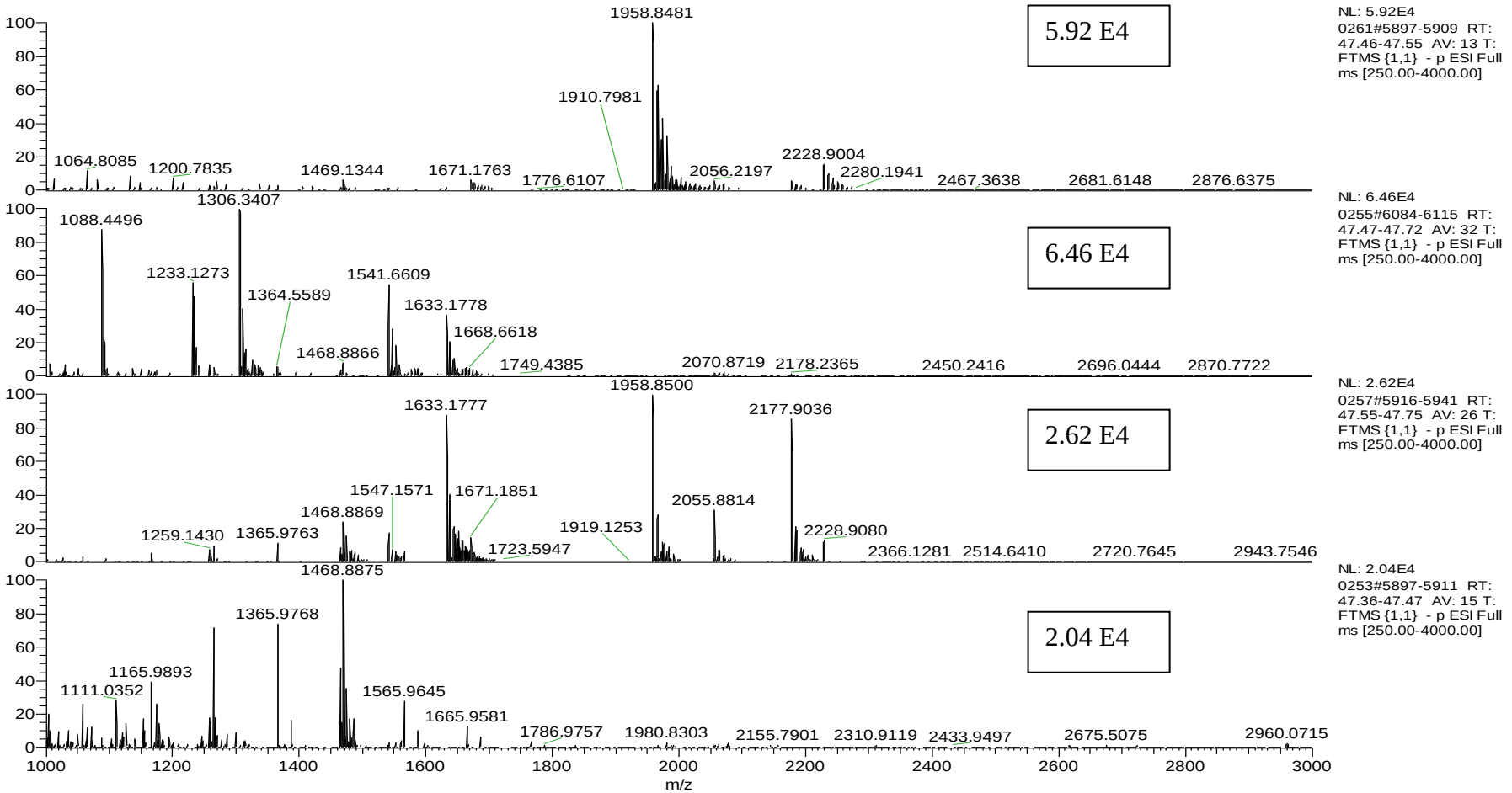

Figure 4.13: Negative ion mass spectra from 47.40 to 47.75 minutes. From top – no superchargers; 1% sulfolane; 1% DMSO; 0.1% *m*-NBA. Inset numbers are base ion intensity

With the peak at 47.5 minutes, a similar pattern is observed. Without superchargers, the spectrum is dominated by the (3+) m/z 1958.8 ion. The addition of sulfolane causes an increase in charge, with a shift to ions at m/z of 1088.8 (5+), 1233.1 (5+), 1306.3 (5+), 1541.7 (4+) and 1633.2 (4+). The addition of DMSO causes a smaller increase in charge, and also allows the ion at m/z 2177.9 to be detected, whereas it was not when superchargers were not used. The addition of *m*-NBA to the LC solvent does not have a huge effect on charging either. Although the distribution moves so that the predominant ion is that of m/z 1468.9, signal intensity also falls, so this shift is caused more by a drop in the intensity of the 1958.8 ion than an increase in more highly charged species.

Peaks detected automatically by the peak picking software in all three of the extracted ion chromatograms for oxonium ions were analysed, and the detected glycopeptides are listed in tables 4.5 and 4.6. They show that the total number of glycopeptides automatically detected increased when superchargers were used compared to when they were absent, except when DMSO was used in negative ion mode. This is particularly true for glycosylations at the Asn-99 site, none of which were automatically detected when superchargers were not present, but at least one variation of which was detected in the presence of all three superchargers. The improvement in detection can be attributed directly to an increase in average charge. Detection of expected glycopeptides of known mass can obviously be more effectively and sensitively carried out by searching for that specific mass. However, when it is desirable to identify all the glycan variants present, identification of peaks by the detection of oxonium ions from in-source fragmentation is a common approach. Since fragmentation efficiency is increased as charge increases, an increase in charge (as is seen in the presence of superchargers) has the added effect of increasing the detection of oxonium ions. This, in turn, results in more glycopeptide peaks being automatically detected.

Table 4.5 Fetuin N-glycans detected in positive ionisation mode, with and without superchargers present. Notation indicates antennae number and sialic acid residues

N-glycan site	Glycans detected with			
	No supercharger	Sulfolane	DMSO	*m*-NBA
99	None detected	Bi-3S	Bi-2S, Bi-3S, Tri-2S, Tri-3S	Bi-1S, Bi-2S, Bi-3S, Tri-3S, Tri-4S
156	Bi-1S, Bi-2S, Tri-2S, Tri-3S, Tri-4S	Bi-2S, Tri-2S, Tri-3S, Tri-4S	Bi-1S, Bi-2S, Tri-2S, Tri-3S, Tri-4S	Bi-1S, Bi-2S, Bi-3S, Tri-2S, Tri-3S, Tri-4S
176	Tri-3S	Bi-2S, Tri-2S, Tri-3S, Tri-4S	None detected	Bi-1S, Tri-3S, Tri-4S

Table 4.6 Fetuin N-glycans detected in negative ionisation mode, with and without superchargers present. Notation indicates antennae number and sialic acid residues

N-glycan site	Glycans detected with			
	No supercharger	Sulfolane	DMSO	*m*-NBA
99	None detected	None detected	Bi-2S	Bi-1S, Bi-3S, Tri-3S, Tri-4S
156	Tri-3S, Tri-4S	Tri-3S, Tri-4S	Tri-3S, Tri-4S	Tri-3S, Tri-4S
176	Tri-3S	Bi-2S, Tri-3S, Tri-4S	None detected	Tri-3S, Tri-4S

The greatest number of glycan variants was detected when 0.1% *m*-NBA was added to the LC solvent. The biggest difference between detection without superchargers present and with *m*-NBA present is seen with glycosylations at Asn-176 and Asn-99. These are the later eluting glycopeptides, which would fit with *m*-NBA exerting its effect through increasing the surface tension on electrospray droplets. This also fits with the proposal that glycopeptides are partially desorbed from electrospray droplets before ionisation, as this would be most likely when glycopeptides have a hydrophobic portion which would sit at the surface of the droplet. Such glycopeptides, due to their increased hydrophobic nature, would also elute later in the chromatographic conditions used here. The validity

of this could be examined using isocratic elution conditions, but time was not available for this.

It is still not clear what causes the differences in the effects of the different superchargers. Although the addition of *m*-NBA improved the detection of all glycopeptides, the addition of DMSO and sulfolane reduced the detection of at least one glycopeptide. Further work to investigate this could be useful, and would involve isocratic elutions to remove the influence of changing solvent concentrations. It may also be useful to examine how mixtures of superchargers influence charging and signal from these compounds, as there appear to be qualitative and not just quantitative differences in their effects.

Somewhat different results were obtained when the same approach was taken with tryptically digested rEPO. The digest results in four glycosylated peptides; one containing the O-glycan, one with the N-glycan at Asn_{83} and one containing the two N-glycans at Asn_{24} and Asn_{38}. The complexity of the latter glycopeptide meant that it was not examined in these experiments. O-glycans were better identified when analysed with sulfolane in the LC solvent than when it was absent. Figure 4.14 shows the EIC obtained for m/z 1207.748, the disialylated O-glycan, with and without sulfolane present in the LC solvent. The peak intensity of the O-glycan with the sulfolane present is much higher than the peak intensity without it. A similar effect is seen in the EIC of m/z 1062.119, the O-glycan with a single sialic acid attached (Figure 4.15). Again the peak with the sulfolane in the LC solvent is about 5 times higher than the peak without superchargers present.

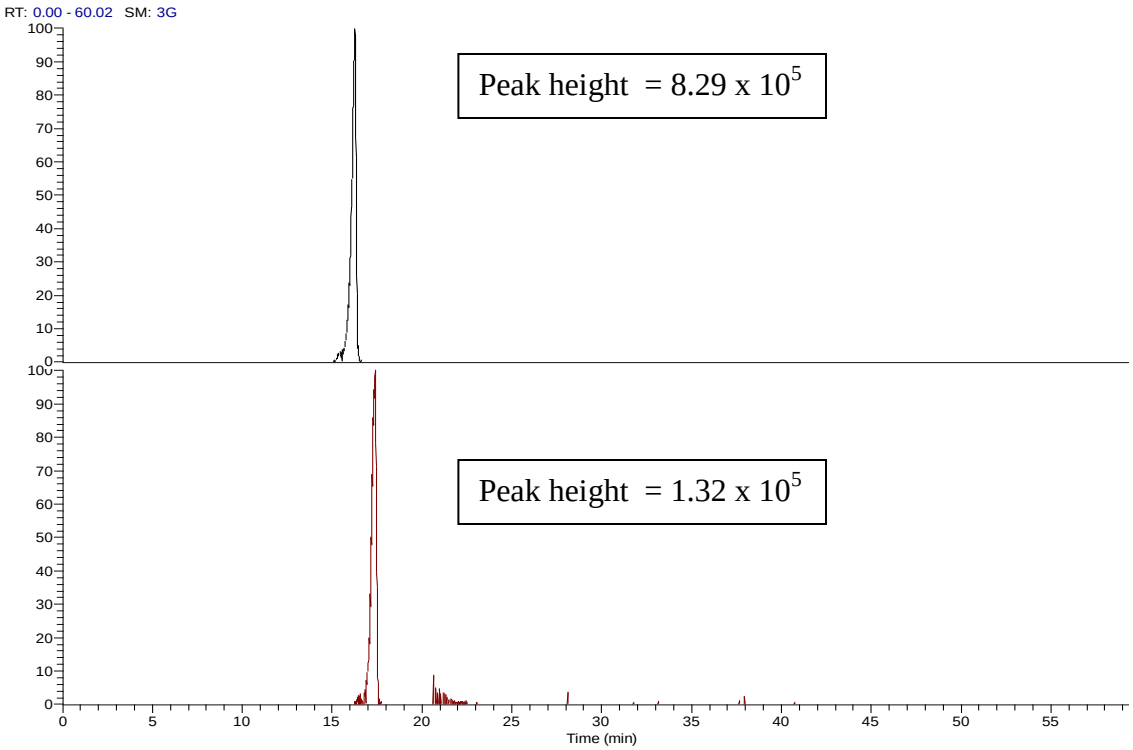

Figure 4.14: EIC for m/z 1207.748, glycopeptide containing disialylated O-glycan. Top, with 1% sulfolane in LC solvent; bottom, no supercharger added.

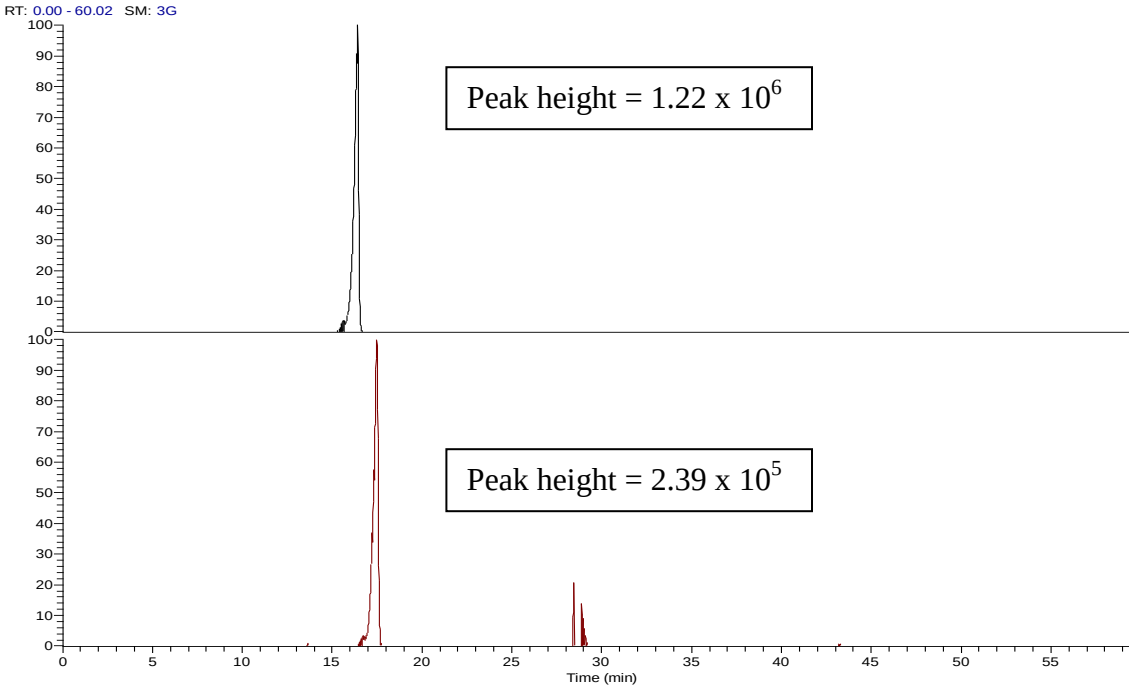

Figure 4.15: EIC for m/z 1062.119, glycopeptide containing singly sialylated O-glycan. Top, with 1% sulfolane in LC solvent; bottom, no supercharger added

This is a different effect to that demonstrated with fetuin, and shows that the use of superchargers can increase the peak height of acidic glycopeptides, as well as improving the ability to identify glycopeptide peaks. This latter approach was also taken with rEPO. Table 4.7 shows the peaks identified with and without the various superchargers present. As mentioned earlier, the increased acetylation of sialic acids and the presence of N-glycolyl neuraminic acid in rEPO have both been suggested as possible methods to distinguish between rEPO and huEPO. In these experiments, however, only one glycan containing an acetylated sialic acid residue was detected, and none were detected containing any Neu5Gc. It is not known if this is due to the specific rEPO chosen, or if the sensitivity of the approach was too poor to detect these glycoforms, but it is a weakness in the approach for anti-doping purposes.

Unlike with fetuin, the greatest increase in peak identification was seen with sulfolane, whereas the other superchargers did not have such a strong effect. Again, it is not clear what causes the difference between the effects of the different superchargers, or why they should have different effects on different glycopeptides. The clear improvement in glycopeptide detection when they are used, however, suggests that this may be something worth further investigation.

Table 4.7 rEPO glycans detected in positive ionisation mode, with and without superchargers present. Notation indicates antennae number (*n*A), N-acetyl lactosamine repeat units (*n*R), N-acetylneuraminic acid residues and acetylations (*n*S(*n*)), and N-glycolylneuraminic acid residues (*n*G)

Glycan site	Glycans detected with			
	No supercharger	Sulfolane	DMSO	*m*-NBA
126 (O-glycan)	0A0R1S(0)0G 0A0R2S(0)0G	0A0R1S(0)0G 0A0R2S(0)0G	0A0R1S(0)0G 0A0R2S(0)0G	0A0R1S(0)0G 0A0R2S(0)0G
83 (N-glycan)	3A0R3S(0)0G 4A0R4S(0)0G	3A0R3S(0)0G 4A0R3S(0)0G 4A0R4S(0)0G 4A0R4S(1)0G 4A1R4S(0)0G 4A2R4S(0)0G	3A0R3S(0)0G 4A0R4S(0)0G 4A0R4S(1)0G	3A0R3S(0)0G 4A0R4S(0)0G 4A0R4S(1)0G

4.4 Conclusions

The addition of sulfolane, DMSO or *m*-NBA to LC solvents did not significantly affect the retention time or peak width of diuretics. However, they did affect the peak height of these compounds. In particular, sulfolane enhanced signal in negative ionisation mode. It is not clear what this effect is due to. Proposals that superchargers exert their effect through effects on electrospray droplet surface tension and temperature were examined, but the two did not appear to be directly correlated with peak height. This is not to say that they have no effect, however. It is possible that they are relevant in determining response, but any effects are likely to be complex and multifactorial, involving (potentially) surface tension, evaporative cooling of electrospray droplets, ionisation mode and electrospray current, and the effects of the superchargers on analyte ionisation. Despite this lack of clarity however, it appears that the addition of superchargers to LC solvents for the analysis of small molecules can result in (analyte-specific) signal enhancement, with very little additional cost or effort.

The analysis by LC-MS of glycopeptides from a tryptic digest of fetuin using LC solvents containing superchargers showed that the average charge state of acidic glycopeptides was increased in the presence of superchargers, although the extent to which this was true varied through the elution. The extent to which it occurred varied also with supercharger, but it was found that the addition of *m*-NBA to LC solvents increased the number of glycopeptides detected when peaks were automatically detected by searching for fragments corresponding to oxonium ions, diagnostic for glycopeptides, as a direct result of the increase in average charge caused by the presence of the supercharger.

With a similar analysis of rEPO, similar effects were seen, except that the most effective supercharger was sulfolane. Its addition to the LC solvent resulted in six N-glycans being detected at Asn_{83} compared to two N-glycans detected in its absence. The addition of sulfolane was also observed to increase the peak height of individual glycopeptides in EICs. Conformational changes, which have been suggested as responsible for the effect of superchargers on protein charging, are less likely to be responsible for their effects on

glycopeptides due to their smaller size. It is not clear what the effect is due to, although surface tension effects may play a part, and more work is needed to elucidate the mechanism involved. As with small molecules, however, it seems that the use of superchargers could be a simple and effective way to improve acidic glycopeptide detection in LC-MS.

4.5 References

Cech, N. B. and C. G. Enke (2000). "Relating electrospray ionization response to nonpolar character of small peptides." Anal Chem **72**(13): 2717-23.

Dole, M., L. L. Mack, et al. (1968). "Molecular Beams of Macroions." The Journal of Chemical Physics **49**(5): 2240-2249.

Gamero-Castaño, M. and J. F. d. l. Mora (2000). "Kinetics of small ion evaporation from the charge and mass distribution of multiply charged clusters in electrosprays." Journal of Mass Spectrometry **35**(7): 790-803.

Hogan, C. J., J. A. Carroll, et al. (2008). "Combined Charged Residue-Field Emission Model of Macromolecular Electrospray Ionization." Analytical Chemistry **81**(1): 369-377.

Hu, Q., R. J. Noll, et al. (2005). "The Orbitrap: a new mass spectrometer." Journal of Mass Spectrometry **40**(4): 430-443.

Iavarone, A., J. Jurchen, et al. (2000). "Effects of solvent on the maximum charge state and charge state distribution of protein ions produced by electrospray ionization." Journal of the American Society for Mass Spectrometry **11**(11): 976-985.

Iavarone, A. T., J. C. Jurchen, et al. (2001). "Supercharged Protein and Peptide Ions Formed by Electrospray Ionization." Analytical Chemistry **73**(7): 1455-1460.

Iavarone, A. T. and E. R. Williams (2002). "Supercharging in electrospray ionization: effects on signal and charge." International Journal of Mass Spectrometry **219**(1): 63-72.

Iavarone, A. T. and E. R. Williams (2003). "Collisionally Activated Dissociation of Supercharged Proteins Formed by Electrospray Ionization." Analytical Chemistry **75**(17): 4525-4533.

Iavarone, A. T. and E. R. Williams (2003b). "Mechanism of Charging and Supercharging Molecules in Electrospray Ionization." Journal of the American Chemical Society **125**(8): 2319-2327.

Iribarne, J. V. and B. A. Thomson (1976). "On the evaporation of small ions from charged droplets." The Journal of Chemical Physics **64**(6): 2287-2294.

Kjeldsen, F., A. M. B. Giessing, et al. (2007). "Peptide Sequencing and Characterization of Post-Translational Modifications by Enhanced Ion-Charging and Liquid Chromatography Electron-Transfer Dissociation Tandem Mass Spectrometry." Analytical Chemistry **79**(24): 9243-9252.

Lomeli, S., I. Peng, et al. (2010). "New reagents for increasing ESI multiple charging of proteins and protein complexes." Journal of the American Society for Mass Spectrometry **21**(1): 127-131.

Lomeli, S., S. Yin, et al. (2009). "Increasing charge while preserving noncovalent protein complexes for ESI-MS." Journal of the American Society for Mass Spectrometry **20**(4): 593-596.

Meyer, J. and E. A. Komives (2012). "Charge State Coalescence During Electrospray Ionization Improves Peptide Identification by Tandem Mass Spectrometry." Journal of The American Society for Mass Spectrometry **23**(8): 1390-1399.

Miladinović, S. M., L. Fornelli, et al. (2012). "In-Spray Supercharging of Peptides and Proteins in Electrospray Ionization Mass Spectrometry." Analytical Chemistry **84**(11): 4647-4651.

Morimoto, N., M. Nakano, et al. (2001). "Specific distribution of sialic acids in animal tissues as examined by LC-ESI-MS after derivatization with 1,2-diamino-4,5-methylenedioxybenzene." Anal Chem **73**(22): 5422-8.

Nguyen, S. and J. B. Fenn (2007). "Gas-phase ions of solute species from charged droplets of solutions." Proceedings of the National Academy of Sciences **104**(4): 1111-1117.

Nohmi, T. and J. B. Fenn (1992). "Electrospray mass spectrometry of poly(ethylene glycols) with molecular weights up to five million." Journal of the American Chemical Society **114**(9): 3241-3246.

Powell, M. J., T. T. Razunguzwa, et al. (2009). "A Novel Chip-based Electroelution System for Rapid and Efficient Recovery of Intact Proteins from Polyacylamide Gels." BioTechniques **46**(5): 373-374.

Šamalikova, M. and R. Grandori (2003). "Protein Charge-State Distributions in Electrospray-Ionization Mass Spectrometry Do Not Appear To Be Limited by the Surface Tension of the Solvent." Journal of the American Chemical Society **125**(44): 13352-13353.

Šamalikova, M. and R. Grandori (2005). "Testing the role of solvent surface tension in protein ionization by electrospray." Journal of Mass Spectrometry **40**(4): 503-510.

Schmedes, A. and I. Brandslund (2006). "Analysis of Methylmalonic Acid in Plasma by Liquid Chromatography-Tandem Mass Spectrometry." Clinical Chemistry **52**(4): 754-757.

Smith, R., J. Loa, et al. (1990). "Collisional activation and collision-activated dissociation of large multiply charged polypeptides and proteins produced by electrospray ionization." Journal of the American Society for Mass Spectrometry **1**(1): 53-65.

Sterling, H., M. Daly, et al. (2010). "Effects of supercharging reagents on noncovalent complex structure in electrospray ionization from aqueous solutions." Journal of The American Society for Mass Spectrometry **21**(10): 1762-1774.

Sterling, H., A. Kintzer, et al. (2012). "Supercharging Protein Complexes from Aqueous Solution Disrupts their Native Conformations." Journal of The American Society for Mass Spectrometry **23**(2): 191-200.

Sterling, H., J. Prell, et al. (2011). "Protein Conformation and Supercharging with DMSO from Aqueous Solution." Journal of The American Society for Mass Spectrometry **22**(7): 1178-1186.

Sterling, H. and E. Williams (2009). "Origin of supercharging in electrospray ionization of noncovalent complexes from aqueous solution." Journal of the American Society for Mass Spectrometry **20**(10): 1933-1943.

Sterling, H. J., C. A. Cassou, et al. (2011). "The role of conformational flexibility on protein supercharging in native electrospray ionization." Physical Chemistry Chemical Physics **13**(41): 18288-18296.

Sterling, H. J. and E. R. Williams (2010). "Real-Time Hydrogen/Deuterium Exchange Kinetics via Supercharged Electrospray Ionization Tandem Mass Spectrometry." Analytical Chemistry **82**(21): 9050-9057.

Valeja, S. G., J. D. Tipton, et al. (2010). "New Reagents for Enhanced Liquid Chromatographic Separation and Charging of Intact Protein Ions for Electrospray Ionization Mass Spectrometry." Analytical Chemistry **82**(17): 7515-7519.

Xie, L.-Q., C.-P. Shen, et al. (2012). "Improved proteomic analysis pipeline for LC-ETD-MS/MS using charge enhancing methods." Molecular BioSystems **8**(10): 2692-2698.

Chapter 5: Cleavage, digestion and derivatisation of N-glycans to identify bisected and non-bisected structures as a way to discriminate between recombinant and endogenous erythropoietin

Aim: To develop a method that would allow discrimination between endogenous and recombinant erythropoietin, based on the absence in rEPO of N-glycans containing bisecting N-acetyl glucosamine residues, with CE-LIF or LC-MS/MS as the detection mechanism.

5.1 Introduction

5.1.1 The N-glycan structures of rEPO and huEPO

The structures found in the glycan groups on rEPO and huEPO were discussed in the introduction (1.10), and are shown in figure 5.1. To reiterate, they are bi-, tri- and tetra-antennary structures with differing degrees of sialylation and N-acetyl lactosamine repeats. They are nearly all core fucosylated. The glycans of rEPO tend to be less acidic than those of huEPO, probably due to their content of fewer sialic acid residues, although it is not certain that this is the sole reason. The glycan groups on rEPO contain more N-acetyl lactosamine repeat units than those of huEPO, and tend to contain more tri- and tetra-antennary structures, explaining its greater molecular weight.

Christian Reichel has recently proposed (Reichel 2011) that there is a fundamental qualitative difference between endogenous human EPO and rEPO. He has suggested that endogenous EPO contains a bisecting N-acetyl glucosamine (GlcNAc) moiety not found in any rEPO. This difference could provide a target for discrimination between the artificial and naturally occurring glycoproteins.

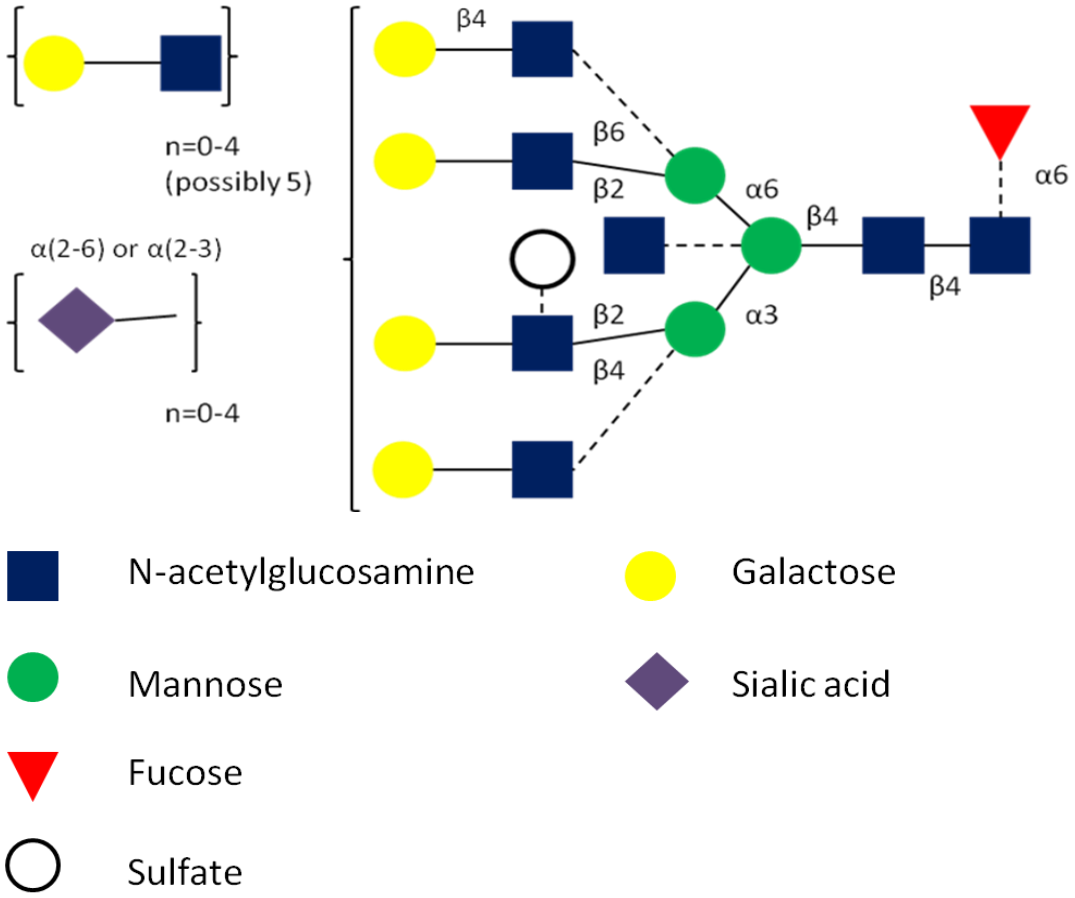

Figure 5.1: Summary diagram of N-glycans found on rEPO and endogenous EPO, including possible positions of sulfate and bisecting N-acetylglucosamine moieties. After Varki et al. (Varki, Cummings et al. 2009)

5.1.2 Exoglycosidase digestion of EPO N-glycans

Detection of this difference when glycans are intact is difficult, as the difference is small, meaning that separation (by LC, CE, or gel electrophoresis) is not easy while identification of positional isomers through (single stage) mass spectrometry is not possible. Differential binding of the different glycans to lectins may provide a route towards discrimination, but Reichel also demonstrated that the presence or absence of the bisecting GlcNAc can be key in affecting exoglycosidase digestion.

Figure 5.2 shows the effect of sequential exoglycosidase digestion on the size of rEPO and huEPO, as measured by SDS-PAGE. As expected, rEPO starts off larger and

treatment with sialidase reduces the size of both rEPO and huEPO, although the decrease is greater for huEPO, due its greater sialic acid content. Addition of β-galactosidase resulted in further decreases in size for both, although this time the drop was greatest for rEPO, possibly because of its greater number of highly branched glycans. After digestion with sialidase, β-galactosidase and β-N-acetylglucosaminidase, however, the huEPO product was larger; this, it was proposed, is because the β-N-acetylglucosaminidase is sterically hindered by the presence of the bisecting GlcNAc in huEPO, preventing full digestion back to the (fucosylated) pentasaccharide core.

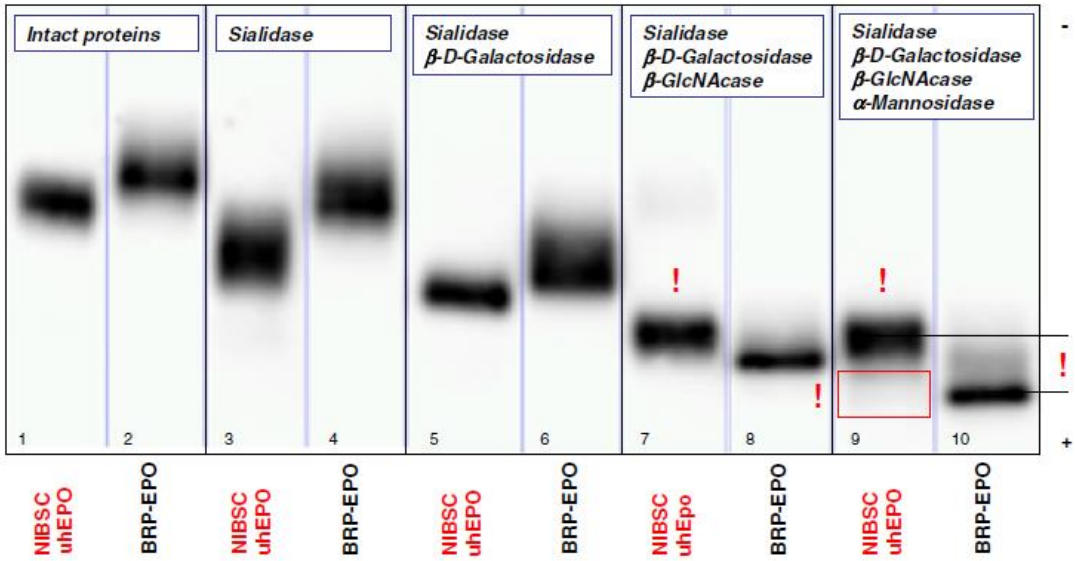

Figure 5.2 Effect of digestion of rEPO and huEPO with different exoglycosidase combinations. Digestion with β-N-acetylglucosaminidase and α-mannosidase did not have the same effect on huEPO as it did on rEPO, possibly because of enzymatic inhibition due to the presence of a bisecting GlcNAc on huEPO (from Reichel 2011)

Backing for this proposal is provided by the further addition of α-mannosidase to the digestion enzyme mix. Since the mannose residues cannot be cleaved with the GlcNAc residues in place, this had little effect on huEPO. However, the mannose residues on rEPO were cleaved, resulting in a further decrease in the size of the artificial form.

5.1.3 Ovine IgG as a model for huEPO

The only commercially available standard for human urinary EPO, that available from the National Institute for Biological Standards and Controls (NIBSC), is currently in very short supply. As of November 8 2012, their website carried a message stating 'Users should be aware that stocks of this standard are running low and it is unlikely to be possible to replace it.' (NIBSC 2012). Even when they are in stock, vials of the standard contain only 10 IU (approximately 100 ng).

However, other glycoproteins exist with similar glycan structures to that purported to be found on huEPO. In particular, a study by Raju et al. (Raju, Briggs et al. 2000) found the glycosylation found in the CH2 domain of the heavy chain of the Fc region of ovine IgG was predominantly bi-antennary, as shown in figure 5.3. Although there are variations in the glycans found, 74.8 % of the glycans found in positive ion mode MALDI were fucosylated, and 97.3 % of those detected in negative mode. They also found that 66.5 % of those detected in positive ion mode contained a bisecting GlcNAc residue, and 60.1 % of those detected in negative ion mode. This suggests that ovine IgG glycans could be an appropriate and readily available model for those from huEPO.

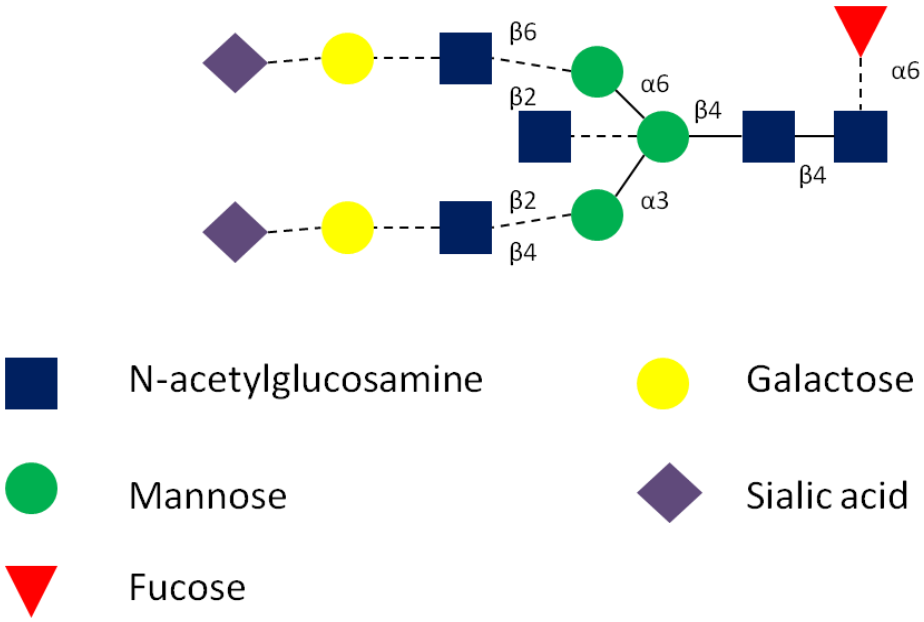

Figure 5.3: Basic structures of glycans found on ovine IgG. Structures found can include fewer sialic acid, galactose, N-acetyl glucosamine and fucose residues, as indicated by dotted lines. Minor amounts of high mannose glycans are also found.

5.1.4 Capillary electrophoresis-mass spectrometry analysis of glycans

Mass spectrometry can provide structural information on glycans released from glycoproteins, but cannot discriminate between structural isomers without multiple order mass spectrometry (MS^n), not possible at the levels at which glycoproteins are typically found. Separation of isomers using an alternative technique prior to analysis by mass spectrometry is therefore required. This has been demonstrated using high-pH anion-exchange chromatography, hydrophilic interaction chromatography and GC (Galuska, Geyer et al. 2012).

However, HILIC separations are generally very time consuming and only provide partial resolution of isomers, although this problem has been somewhat addressed recently by the development of micro- and nanofluidic HILIC approaches (Staples, Bowman et al. 2009; Huang, Shi et al. 2011). Graphitized carbon as a stationary phase has also been shown to be highly selective, allowing resolution of positional isomers of permethylated

glycans (Costell, Contado-Miller et al. 2007), and linkage (Pabst, Bondili et al. 2007) and positional isomers (Pabst, Grass et al. 2012) of native glycans.

Improved resolution is obtained using high performance anion-exchange chromatography with pulsed amperometric detection (Townsend, Hardy et al. 1989), but this too suffers from long analysis time, poor reproducibility and low sensitivity (Lee 1996). Although more recently the approach has been used to carry out analysis of monosaccharides in short time frames (Hurum and Rohrer 2011; Zhang, Khan et al. 2012), it has not yet been fully explored for the analysis of larger oligosaccharides or intact N-glycans.

Analysis of glycans using GC, meanwhile, firstly requires extensive and time consuming derivatisation.

Excellent resolution of similar glycans has been achieved using capillary electrophoresis, with capillary zone electrophoresis (Boucher, Kane et al. 2012) and capillary gel electrophoresis (Guttman and Pritchett 1995; Guttman, Chen et al. 1996) producing the best separation efficiency and resolution of isomeric glycans.

This efficient resolution of isomers means that coupling of CE to MS theoretically provides a powerful technique for the identification of all the glycans present in a complex mixture, such as may be found in a glycoprotein digest.

However, this coupling is not without its complications. These include the proper grounding of the CE electrical circuit, the fact that CE flow rates are of the order of 1-100 nL/min, compared to 200 µL/min or more with traditional LC flow rates, and the need for volatile electrolytes in the CE buffer to enable stable spray formation. Nanoelectrospray systems have meant that flow rates are no longer such a problem; however, much of the CE separation work being done is carried out in buffers which are unsuitable for analysis using ESI-MS. More recent studies demonstrated the use of CE-LIF-MS for the successful analysis of APTS-labelled glycans from monoclonal antibodies (Gennaro and Salas-Solano 2008) and APTS-labelled human milk oligosaccharides (Albrecht, Schols et al. 2010), but studies suffered from the limited comparability of detector traces, due to the differences in analyte response in the different detectors and the physical distance between the detectors. These problems have also been partially addressed recently (Huhn, Ruhaak et al. 2012).

5.1.5 Capillary electrophoresis – laser induced fluorescence (CE-LIF) for separation and detection of oligosaccharides

Analysis of glycans using CE-LIF was first demonstrated in 1991 using 3-(4-carboxybenzoyl)-2-quinolinecarboxaldehyde (CBQCA) as a fluorescent labelling compound (Liu, Shirota et al. 1991). The technique allowed the detection of N-glycans derived from fetuin at subattomole levels.

Chen and Evangelista (Chen and Evangelista 1998) demonstrated the cleavage of N-glycans from glycoproteins using PNGase F, before derivatisation with 8-aminopyrene-1,3,6-trisulfonate (APTS) under mild reductive amination conditions to minimize the cleavage of sialic acid and fucose residues. APTS derivatised sugars have an absorbance maximum at 455 nm with significant amount of absorption at 488 nm, while APTS itself has an absorbance maximum at 424 nm with a relatively low absorptivity at 488 nm. Excitation with a 488 nm argon-ion laser causes APTS-sugar complexes to fluoresce with significantly higher intensity, (em λ_{max} = 512 nm) than the APTS emission (em λ_{max} = 501 nm). Chen and Evangelista demonstrated that this derivatisation, combined with separation using capillary electrophoresis, was suitable for producing profiles of the N-glycans from glycoproteins including fetuin, kallikrein and rEPO. However, the profile obtained for rEPO was unsurprisingly very complex, and analysis was only carried out using 50 μg/mL solutions.

More recently, Ijiri et al. (Ijiri, Todoroki et al. 2011) demonstrated that CE-LIF could be used for the analysis of N-glycans after derivatisation with rhodamine 110. They performed a separation in a fused silica capillary using a neutral buffer to separate acidic glycans by the number of sialic acids present, and a second separation using an acidic buffer which separated asialo-oligosaccharides according to their size.

Rhodamine 110 was used as a fluorescent derivatising agent on the grounds that it has a large fluorescence quantum yield (0.92), a high molar extinction coefficient (92,000 $cm^{-1} M^{-1}$), and an absorption maximum wavelength very close to 488 nm.

The approach was used to profile N-glycans released from rEPO. Solutions were made up using 10 μg of rEPO in a volume of 3 mL. Although the sialylated glycans could not

be fully separated, they migrated in the order of their charge-to-mass ratio in the electropherogram and were also influenced by their branching pattern. Desialylated glycans were well separated using a 150 mM phosphate buffer (pH 2.5), migrating in the order of their charge-to-mass ratio in the electropherogram.

5.1.6 Digestion, derivatisation and detection of N-glycans from rEPO and huEPO.

The suggested difference between rEPO and huEPO could provide a target for discriminating between the two. Exoglycosidase digestion of the N-glycans should, in theory, produce core glycans with different structures. However, due to vagaries in the effectiveness of enzymes, it is necessary to have a method capable of distinguishing between glycans that contain a bisecting GlcNAc and their structural isomers. Because of the excellent resolution of CE it was decided that this approach would be tried, with derivatisation with a fluorophore allowing highly sensitive LIF as a detection method, as well as an LC-MS approach.

5.2 Experimental

5.2.1 Materials and equipment

All water used was purified using an Elgastat Option 3 water purification unit and had 18.2 MΩ resisitivity. β-N-acetylglucosaminidase and β-galactosidase were purchased from New England Biolabs UK (Hitchin, UK). Human urinary erythropoietin standard (67/343) was purchased from the National Institute for Biological Standards and Controls (Hertfordshire, UK). Recombinant EPO Epiao (α-erythropoietin) was from Shenyang Sunshine Pharmaceutical Co (Shenyang, China). Reference standard rEPO (BRP-EPO batch 3) was purchased from the European Directorate for the Quality of Medicines (Strasbourg, France). Aminopyrene trisulfonic acid (APTS) was purchased from Invitrogen (Inchinnan, UK). Glycan standards were purchased from Europa Bioproducts (Cambridgeshire, UK). CE-LIF equipment and materials were from Beckman Coulter (High Wycombe, UK). Centrifugal filters were purchased from

Millipore (Watford, UK). Kits for the extraction of EPO using monolithic cartridges were purchased from MAIIA Diagnostics (Uppsala, Sweden). All other chemicals and products were purchased from Sigma Aldrich (Poole, UK).

A Hypersil Gold C18 column from Thermo Fisher (Loughborough, UK), 200 mm length and 2.1 mm internal diameter with 1.9 μm particles was used for chromatographic separations.

Chromatography was carried out using either a Waters Acquity UPLC system, a Thermo Accela HPLC pump and autosampler, or a Thermo UltiMate 3000 UHPLC pump and autosampler. The first two were used with a Thermo Exactive Orbitrap mass spectrometer, while the latter was used with a Thermo Q-Exactive Orbitrap mass spectrometer.

5.2.2 N-glycan cleavage and exoglycosidase digestion

One vial of Epiao, containing 2000 IU of EPO (approximately 20 μg) was spun through an Ultra-10 Amicon centrifugal filter (10 kDa nominal cut off) at 14,000 g for 10 minutes. The solution was then made up to 500 μL with 50 mM ammonium bicarbonate, pH 7.6 (ABC), and the process repeated twice more. The final retentate was recovered by inverting the filter and spinning for five minutes at 2,000 g. The retentate was recovered into a low-bind microfuge tube and made up to 50 μL with ABC.

Ovine IgG was dissolved in ABC and adjusted to 120 μg in 50 μL ABC, to give an approximately equal molar concentration of glycans as in the rEPO solution.

To each solution, 5 μL of PNGase solution (2.5 IU, in ABC) was added. Samples were briefly vortexed, then incubated at 37 °C for 24 hours.

Samples were dried down under nitrogen, then to each tube was added:

- 0.5 μL bovine serum albumin solution (10 mg/mL)

- 10 μL (100 mIU) Neuraminidase from *Clostridium perfringens (C. welchii)* in 10 mM phosphate buffer (pH 5.5)
- 2 μL (16 IU) β1-4 galactosidase solution
- 2 μL (8 IU) β-N-acetylglucosaminidase solution
- 30.5 μL water
- 5 μL G4 buffer (50 mM sodium citrate, pH 6.0, 100 mM NaCl)

Samples were briefly vortexed, then incubated at 37 °C for 24 hours. An additional 5 μL of sialidase, 1 μL β1-4 galactosidase of and 1 μL of β-N-acetylglucosaminidase solution was then added, and samples incubated for either 12 hours or 20 hours.

The progress of the digest over time was also examined. To do this, 50 μL solutions of IgG and rEPO were made up in ABC at 2 μg/mL (100 ng total). Purified glycan standard NGA2FB containing a bisecting N-acetylglucosamine residue (see Figure 5.4) was also made up in ABC at 1 μg/mL.

To each solution, 5 μL of PNGase solution (2.5 IU, in ABC) was added. Samples were briefly vortexed, then incubated at 37 °C for 24 hours.

Samples were dried down under nitrogen, then to each tube was added:

- 0.5 μL bovine serum albumin solution (10 mg/mL)
- 10 μL (100 mIU) Neuraminidase from *Clostridium perfringens (C. welchii)* in 10 mM phosphate buffer (pH 5.5)
- 2 μL (16 IU) β1-4 galactosidase solution
- 2 μL (8 IU) β-N-acetylglucosaminidase solution
- 50.5 μL water
- 5 μL G4 buffer (50 mM sodium citrate, pH 6.0, 100 mM NaCl)

Aliquots of the digests (10 μL) were taken at 0, 1, 3, 6, 12 and 24 hours. These were frozen at -80 °C, then recovered and derivatised with Rhodamine 110 as in 5.2.4 below.

A vial of huEPO standard (10 IU, approximately 100 ng) was also dissolved in ABC and digested in the same way as these latter samples of IgG and rEPO, but it was digested for the full 24 hours, then the whole digest was recovered and derivatised with Rhodamine 110 as below.

Purified standards of glycans NGA2F and M3N2F (see Figure 5.4) were derivatised with Rhodamine 110, as in 5.2.4 below.

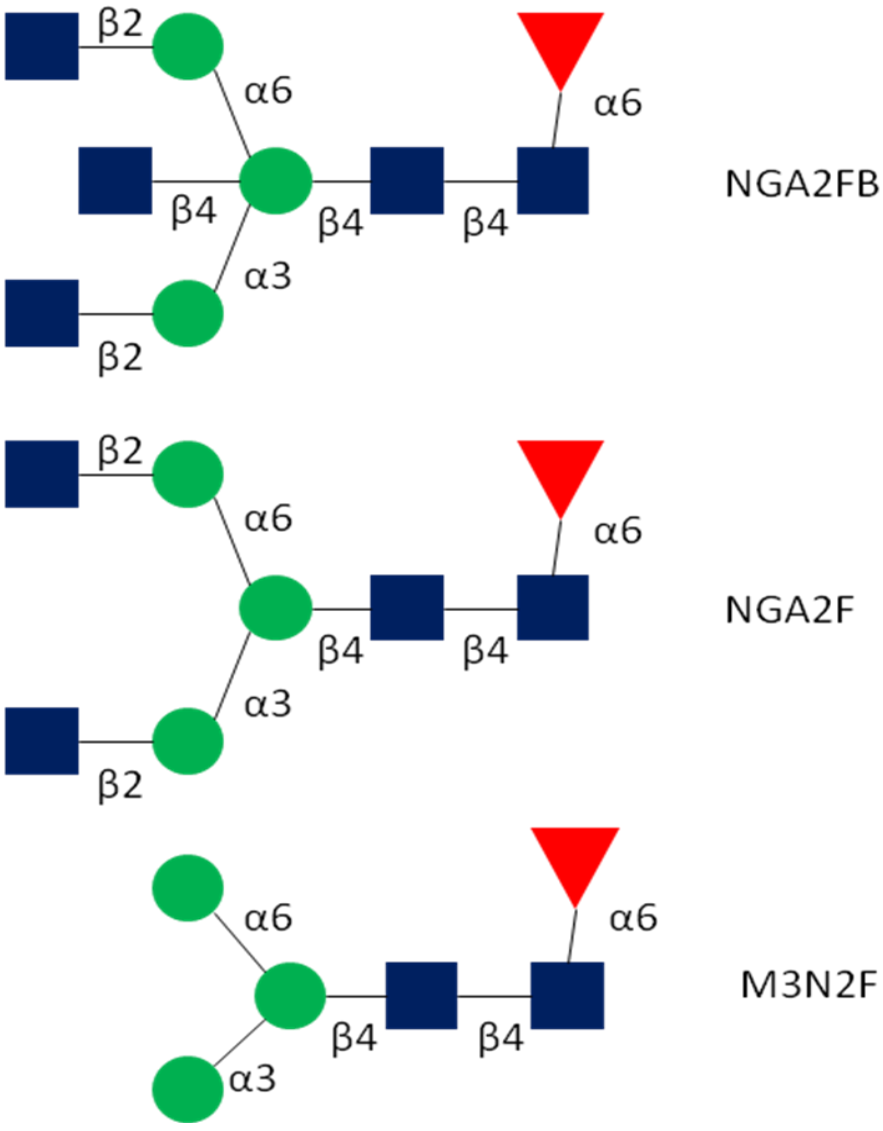

Figure 5.4: Structures of glycan standards

5.2.3 Glycan recovery

Samples were allowed to cool to room temperature, then 300 μL of ice-cold ethanol was added and the samples vortexed then cooled at -20 °C for one hour. Samples were then centrifuged for 20 minutes at 6,000 g and the supernatant transferred to a low bind tube. Samples were then dried down under nitrogen, and stored at -80 °C until derivatised.

5.2.4 Derivatisation of glycans – Rhodamine 110

To a microfuge tube containing cleaved, digested and extracted glycans, 10 μL of Rhodamine 110 solution (5 mM, 1:19 acetic acid:methanol) and 10 μL sodium cyanoborohydride solution (0.1 M in methanol) was added. Samples were vortexed to reconstitute dried down glycans, then incubated overnight at 37 °C. Samples were cooled to room temperature, then 10 μL potassium hexacyanoferrate (III) solution (0.2 M in water) was added and allowed to react for 30 minutes at room temperature. Samples were dried down under nitrogen, then reconstituted in 50 μL water for analysis by LC-MS. The derivatisation reaction is shown in figure 5.5.

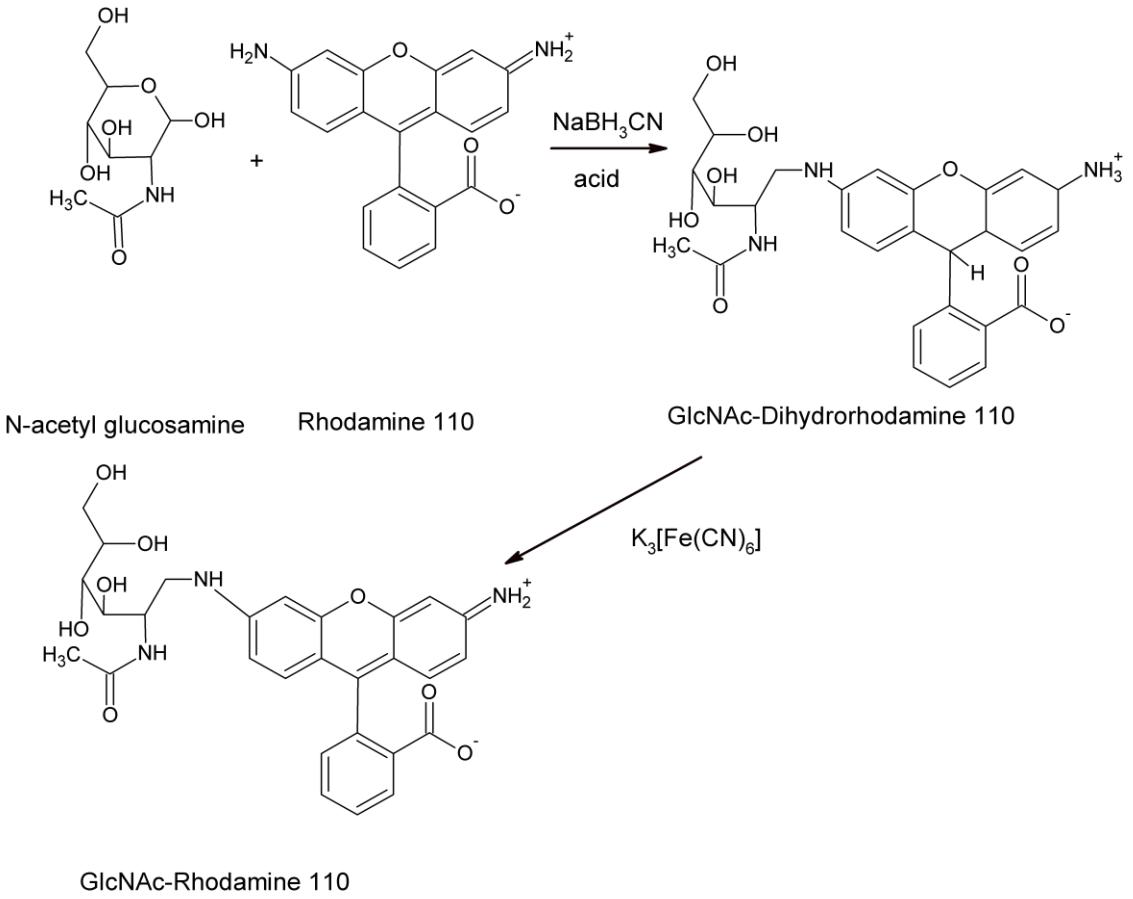

Figure 5.5: Reductive amination of N-acetylglucosamine with rhodamine 110, and restoration to a fluorescent product with potassium hexacyanoferrate (III)

5.2.5 Derivatisation of glycans – APTS

To a microfuge tube containing cleaved, digested and extracted glycans, 10 μL of sodium cyanoborohydride (0.2 M in THF) and 10 μL of APTS (40 mM in 15% acetic acid) were added. Samples were vortexed to reconstitute dried down glycans, then incubated in the dark at room temperature overnight. Samples were dried down under nitrogen, then reconstituted in 50 μL water for analysis by LC-MS. The derivatisation reaction is shown in figure 5.6.

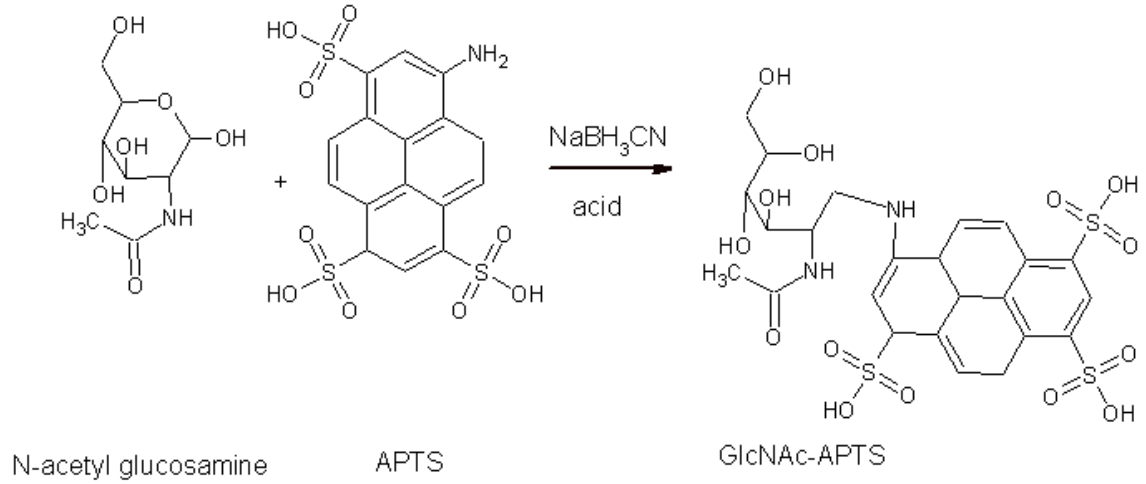

Figure 5.6: Reductive amination of N-acetylglucosamine with APTS.

5.2.6. LC-MS analysis of derivatised glycans

Recombinant EPO and IgG which had been digested for 12 hours after a second addition of enzymes were analysed using an Acquity UPLC system and Orbitrap mass spectrometer. Recombinant EPO and IgG which had been digested for 20 hours after the second addition of enzymes were, due to machine availability, analysed using a Thermo Accela HPLC system and Orbitrap.

HPLC solvents were A: water and 0.1% formic acid and B: acetonitrile and 0.1% formic acid. LC was carried out at a flow rate of 200 μL/minute. A gradient elution was carried out, starting at 95% A, and increasing linearly to 57% A at 15 minutes. 10 μL of sample was injected on column.

Mass spectrometer conditions were (positive/negative ion mode): Sheath gas flow 60 arbitrary units (a.u.); auxillary gas flow 10 a.u.; Spray voltage 4.0/3.0 kV; Capillary temperature 250 °C; Capillary voltage 92.5/-95.0 V; Tube lens voltage 165/-145 V; Skimmer voltage 44/-32 V; Heater temperature 300 °C. Scans were carried out between 350 and 2,000 m/z.

Rhodamine derivatised samples were analysed in positive ion mode. APTS derivatised samples were analysed in both positive and negative ion mode.

Samples from the time series digest of IgG and rEPO, and the digested huEPO standard, were analysed using a Q-Exactive mass spectrometer. HPLC was carried out using the same column, solvents and flow rates as previously. The mass spectrometer was operated in the positive mode, using the following conditions:
Resolution 35,000; Number of microscans 1; Maximum inject time 30; Sheath gas flow rate (arbitrary units) 70; auxillary gas flow rate 10 A.U.; sweep gas flow rate 0 A.U; spray voltage 3.75 kV; capillary temperature 320 °C; S-lens RF level 55.0; heater temperature 350 °C.
Samples were injected three times, to ensure that any detected differences in retention time were not down to method variability.

5.2.7 Use of superchargers to enhance detection of derivatised glycans

Rhodamine 110 derivatised glycans from rEPO were analysed as in 5.2.6, except that 1% sulfolane (v/v) was added to the LC solvents.

5.2.8 CE-LIF analysis of derivatised glycans

APTS-labelled glycans from long and short digests of IgG and rEPO were analysed using CE-LIF. Analysis was carried out using a Beckman Coulter PA 800 Plus Pharmaceutical Analysis System. A 488 nm laser (Ar^{+}) was used for fluorescent excitation, with a 520 nm emission filter. Samples were separated in a 100 mM acetate buffer, pH 4.75 using a Beckman Coulter N-CHO coated capillary, 60 cm total length, effective length 50 cm, 75 μm internal diameter. Samples were pressure injected for 10 seconds and were kept at 10 °C in the sample tray. Separation was carried out over 15 minutes, in reverse polarity at a maximum voltage of 30 kV. Capillary was conditioned between each sample injection by washing for 1 minute with 0.1 N NaOH (aq). An APTS-labelled glucose ladder was used to evaluate the size of glycans detected.

5.2.9 Extraction, digestion and derivatisation of EPO from urine samples

Extraction of EPO from blank urine samples (20 mL) was carried out using MAIIA immunoaffiity monolithic cartridges, according to the kit instructions. Positive and negative control urines were also made up, by filtering urine samples through a 30 kDa centrifugal filter, and then spiking samples with huEPO (standard 67/343) or rEPO (BRP-EPO batch 3) at a concentration of 1 mIU/mL, and these were extracted in the same way. Final elution from the columns was into a volume of 50 μL. Samples were then transferred to an Ultra-10 Amicon centrifugal filter and dialysed and recovered in the same manner as Epiao EPO in 5.2.2.

Cleavage of glycans with PNGase, exoglycosidase digestion, recovery of glycans and derivatisation with Rhodamine 110 was carried out as in 5.2.2, 5.2.3 and 5.2.4. Samples were analysed using an Acquity UPLC system and Orbitrap mass spectrometer.

5.3 Results and discussion

5.3.1 Rhodamine 110 derivatisation of glycans from standards

Glycans digested for 24 hours and then for 12 further hours after addition of more enzymes were derivatised with rhodamine 110. Extracted ion chromatograms (EICs) for m/z 366.1389, produced to identify glycan containing regions, are shown in figure 5.7.

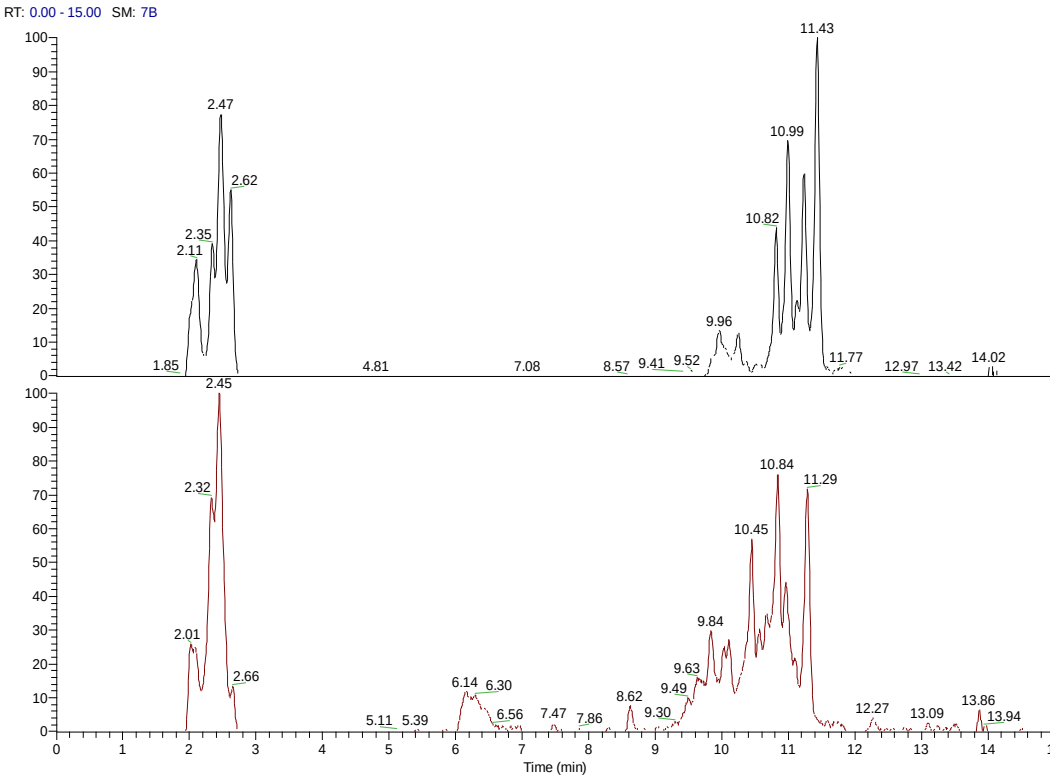

Figure 5.7 EIC of m/z 366.1389 from IgG (top) and rEPO derivatised glycan digests

Two main regions of glycan elution are seen. The first, between approximately 2 minutes and 2.7 minutes, consists of underivatised glycans. Spectra from these regions, shown in figure 5.8, show that the glycans found are fucosylated pentasaccharide core glycans, with none (m/z 1,057.39), one (m/z/ 1,260.47) or two (m/z 1,463.37) GlcNAc attached.

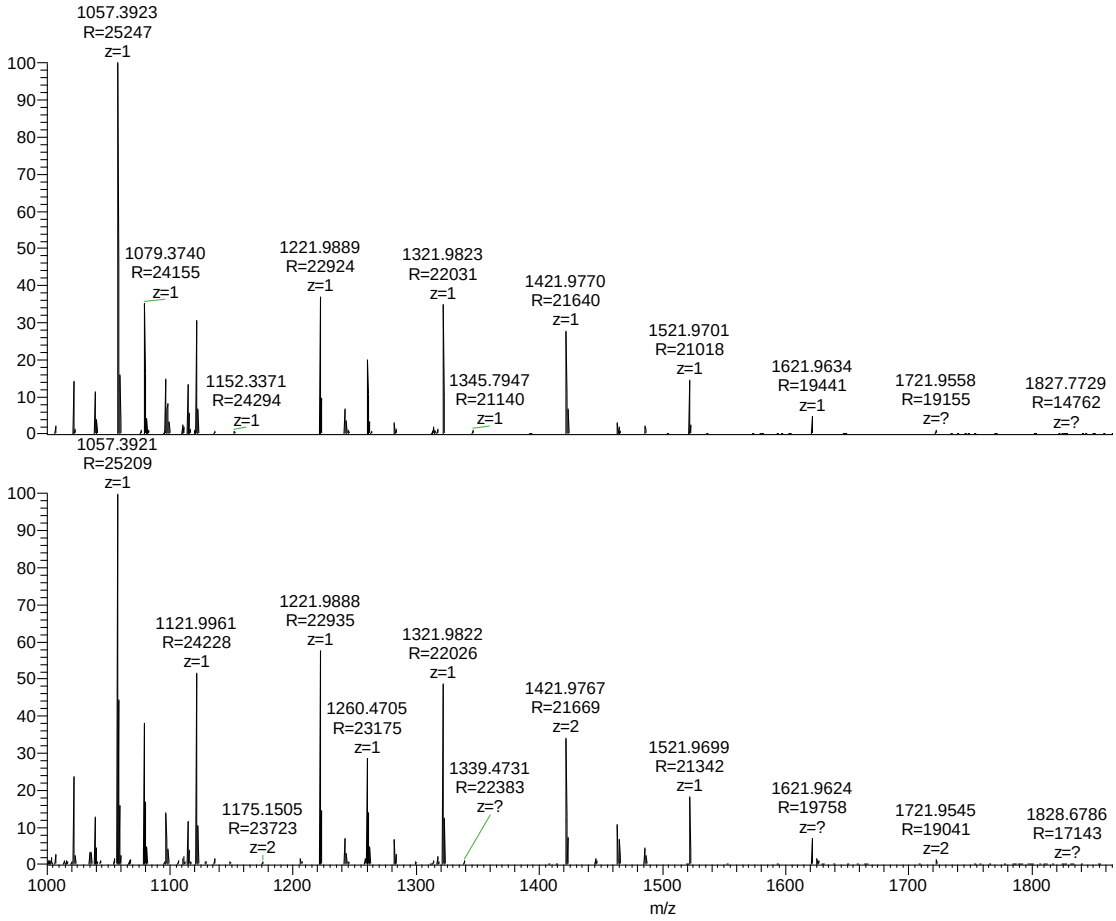

Figure 5.8 Mass spectra from early eluting glycan region of chromatogram, demonstrating presence of underivatised glycans. Spectra also contains several peaks approximately 100 m/z apart from instrument calibration solution. Top – IgG, bottom - rEPO.

The intensity of the signal from these peaks suggests that a significant amount of glycans remain underivatised by the current method. In turn, this would mean that sensitivity gains could be made by improving the efficiency of the derivatisation.

Mass spectra from the time 9.3 minutes to 11.5 minutes are shown in figure 5.9.

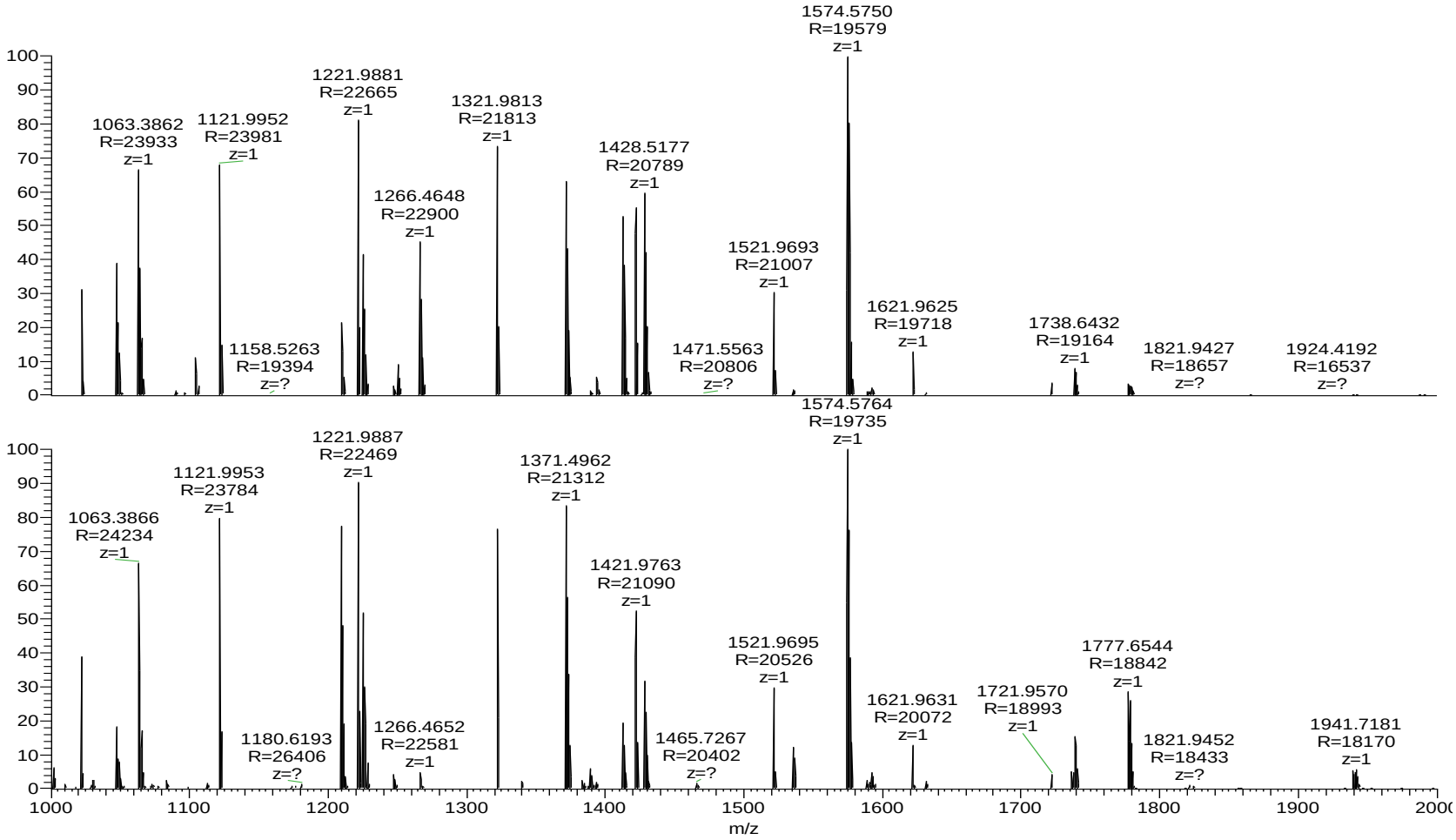

Figure 5.9 Mass spectra from 9.3 minutes to 11.5 minutes of chromatograms in figure 5.6. Top – IgG, bottom - rEPO

The derivatised glycans found match the underivatised glycans which elute earlier. Again, they consist of fucosylated pentasaccharide core glycans, with no (m/z 1,371.49), one (m/z 1,574.57) and two (m/z 1,777.65) GlcNAc residues attached. Glycans without fucose attached are also detected, at m/z 1,225.4345 and 1,428.52, corresponding to pentasaccharide core glycans with none and one GlcNAc residues.

LC-MS analysis resulted in double peaks in extracted ion chromatograms which corresponded in mass to either the rhodamine 110 derivative, or to the dihydrorhodamine derivative, if the glycan ring, shown open in figure 5.4, subsequently closed again. If it was the latter, this failure of the derivatisation method would prevent analysis using CE-LIF. To check that the oxidation with potassium hexacyanoferrate (III) was successful, the derivatisation process was repeated without glycans. The results, shown in figure 5.10, show that rhodamine 110 does indeed form dihydrorhodamine when incubated with sodium cyanoborohydride, but that this reaction is reversed when potassium hexacyanoferrate (III) is added. Furthermore, only one peak is seen with either rhodamine 110 or dihydrorhodamine. Therefore, it is likely that the double peaks correspond to glycan isomers, derivatised with rhodamine 110, although it is not clear what isomers these would be. Alternatively, the oxidation step may not be as effective once the rhodamine 110 is attached to the glycan; the double peak could then be due to the presence of both the oxidised and reduced form of rhodamine 110.

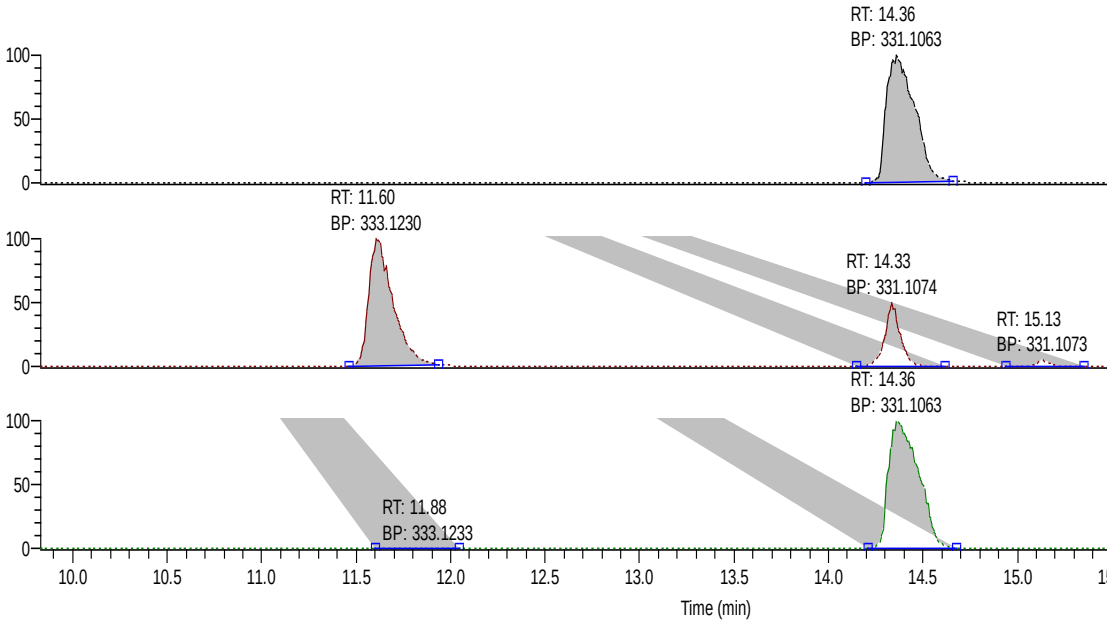

Figure 5.10 Base peak chromatograms from rhodamine 110 (top), rhodamine 110 reduced with sodium cyanoborohydride to give dihydrorhodamine (middle) and rhodamine 110 reduced and then oxidised with potassium hexacyanoferrate (III) (bottom)

Extracted ion chromatograms for the derivatised oligosaccharides showed that they had the same retention times regardless of whether they came from IgG or rEPO, with one exception, that for m/z 1,574.57. This corresponds to the fucosylated pentasaccharide core with one GlcNAc attached. The retention time for this glycan from rEPO was slightly shorter than that for the glycan from IgG, as shown in figure 5.11. Mixing the two derivatised digests confirmed that two sets of peaks were present. Since IgG consists largely of glycans containing a bisecting GlcNAc, and since β-N-acetylglucosaminidase is much less active in cleaving bisecting sugars, it is a reasonable hypothesis that the separation of the peaks is due to the position of this sugar.

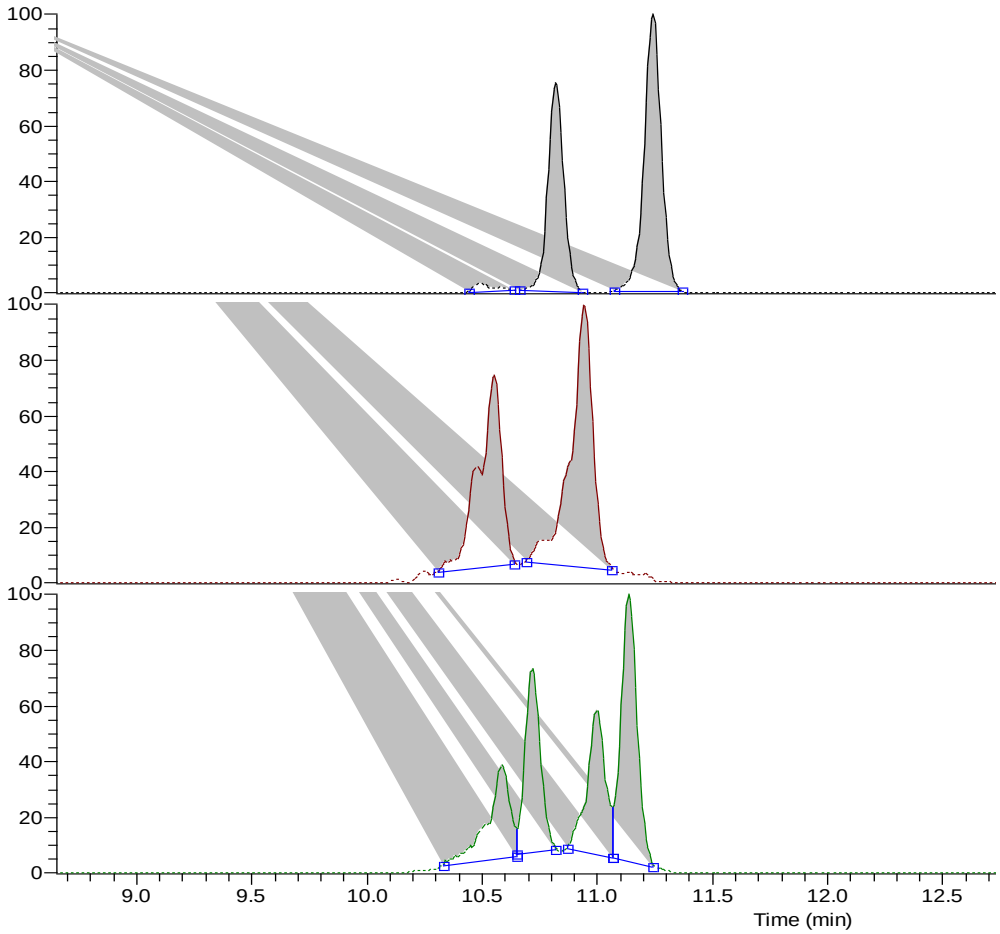

Figure 5.11: Extracted ion chromatograms of of m/z 1,574.57 - Rhodamine 110 derivatised sugars, Exoglycosidase digested. From top: IgG, rEPO, IgG/rEPO.

Digestion of glycans for an additional 20 hours after the addition of extra enzymes resulted in different glycan profiles. Extracted ion chromatograms of m/z 1,574.57 showed that very little was detected in the rEPO digest, although it was still easily detected in the IgG digest, as shown in figure 5.12.

Extracted ion chromatograms of m/z 1,371.49, shown in figure 5.13, show that in rEPO, after 20 hours the glycans have been nearly entirely digested back to the fucosylated pentasaccharide core. With IgG, although this peak is large, a significant amount is still present with a single GlcNAc residue attached.

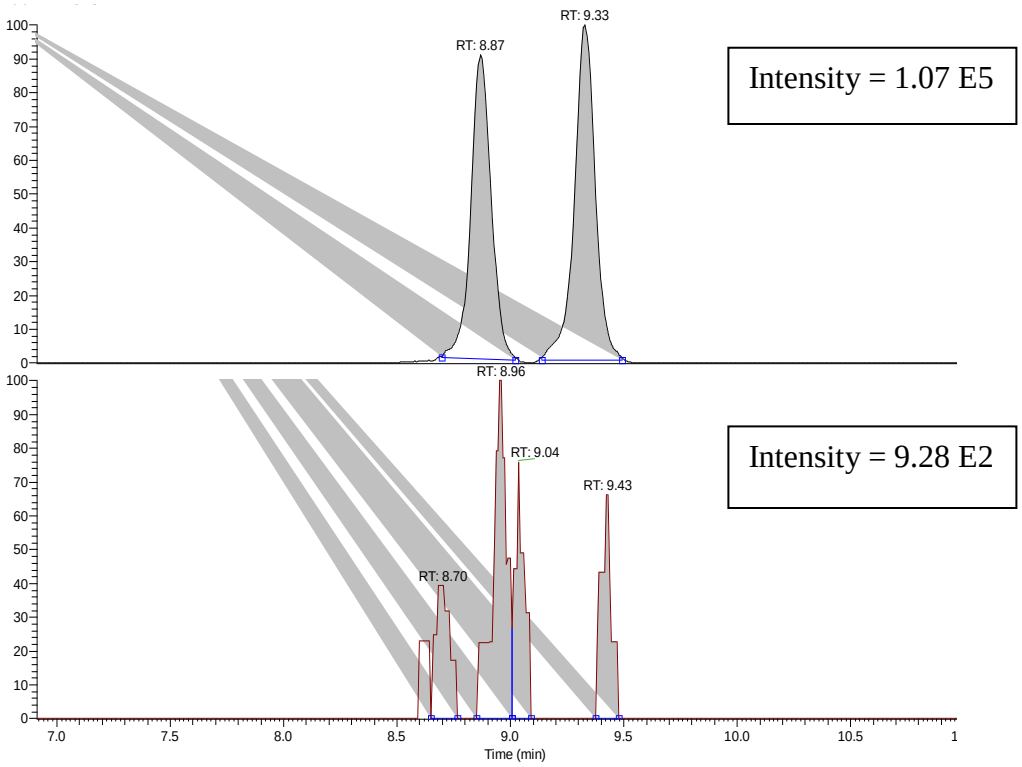

Figure 5.12 EICs of m/z 1,574.57 from rhodamine 110 derivatised IgG (top) and rEPO digests, 20 hours after addition of extra exoglycosidase enzymes

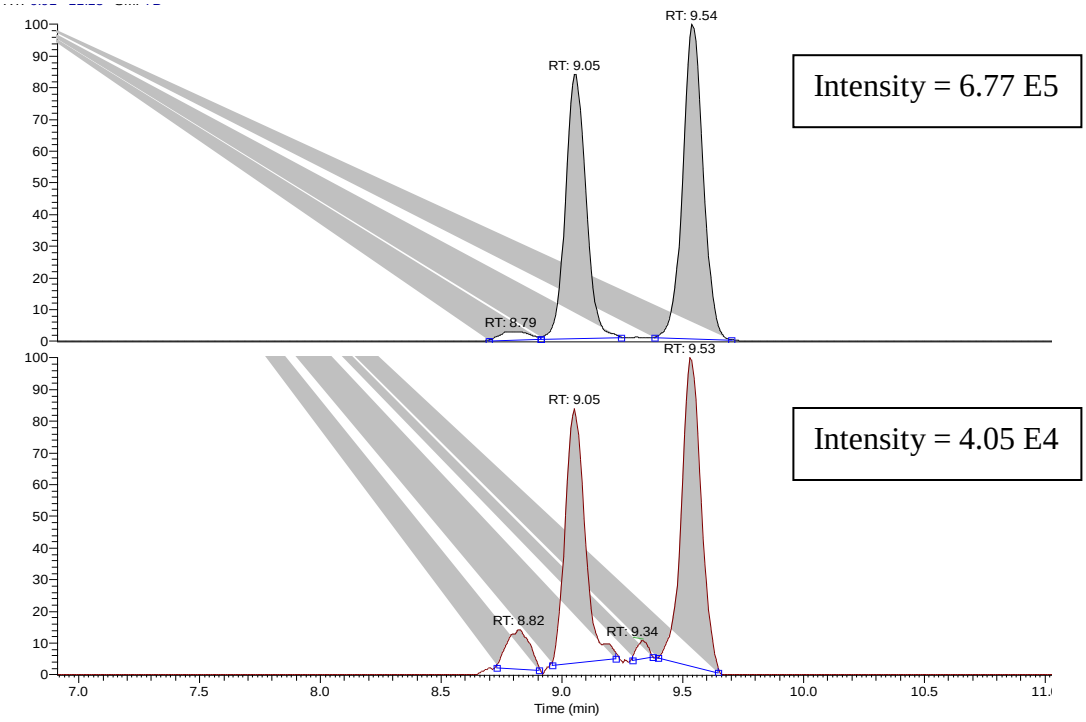

Figure 5.13 EICs of m/z 1,371.49 from rhodamine 110 derivatised IgG (top) and rEPO digests, 20 hours after addition of extra exoglycosidase enzymes

With IgG, the ratio of peak areas for glycans with a single GlcNAc attached to the pentasaccharide core to those without the residue is approximately 1:5.7. For rEPO, the ratio is about 1:47. If oligosaccharides with two GlcNAc residues attached to the pentasaccharide core are included with those with one attached, the difference is even more pronounced. None were detected in the rEPO digest, but the ratio in the IgG digest changes to 1:3.9.

5.3.2 APTS derivatisation of glycans from standards

In comparison with the good LC-MS results observed with the rhodamine 110 derivatised N-glycans, those from APTS derivatised glycans were poor. Although EICs for m/z 366.1389 detected only very small peaks from underivatised glycans in the IgG and rEPO digests, suggesting the derivatisation is more efficient than with rhodamine 110, peaks from derivatised glycans were also hard to detect. Figures 5.14 and 5.15 show the EICs for glycans with no, one and two remaining N-acetylglucosamines for the IgG and rEPO digest, respectively.

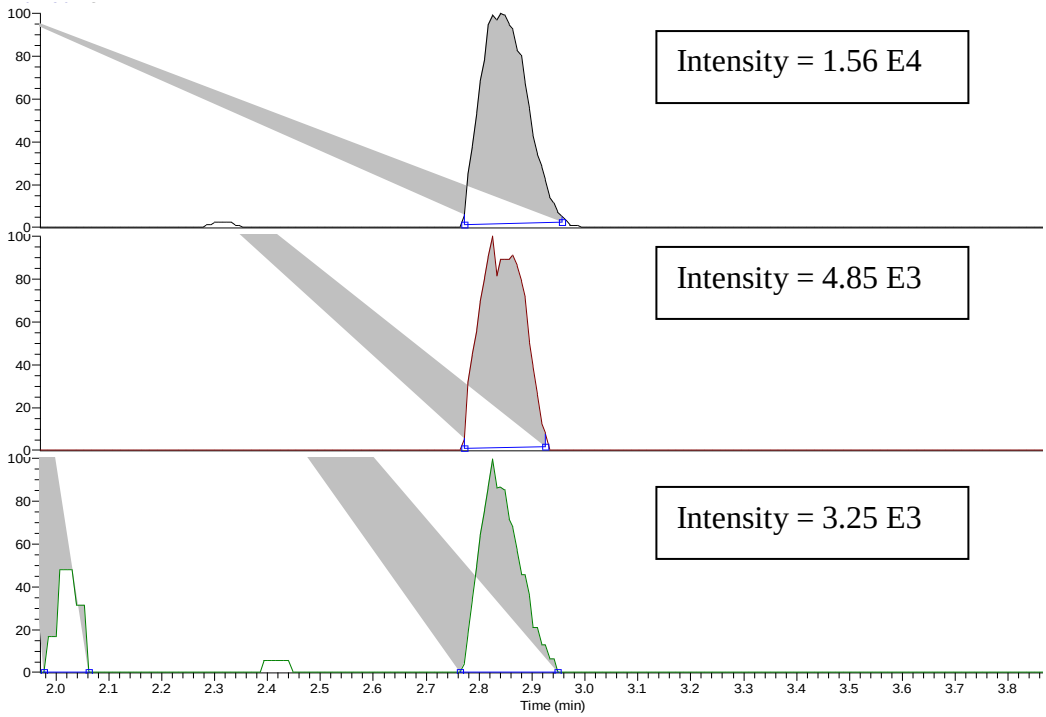

Figure 5.14 EICs from APTS derivatised IgG digest for (from top) m/z 747.67, 849.21, and 950.75 , corresponding to no, one and two remaining GlcNAc residues.

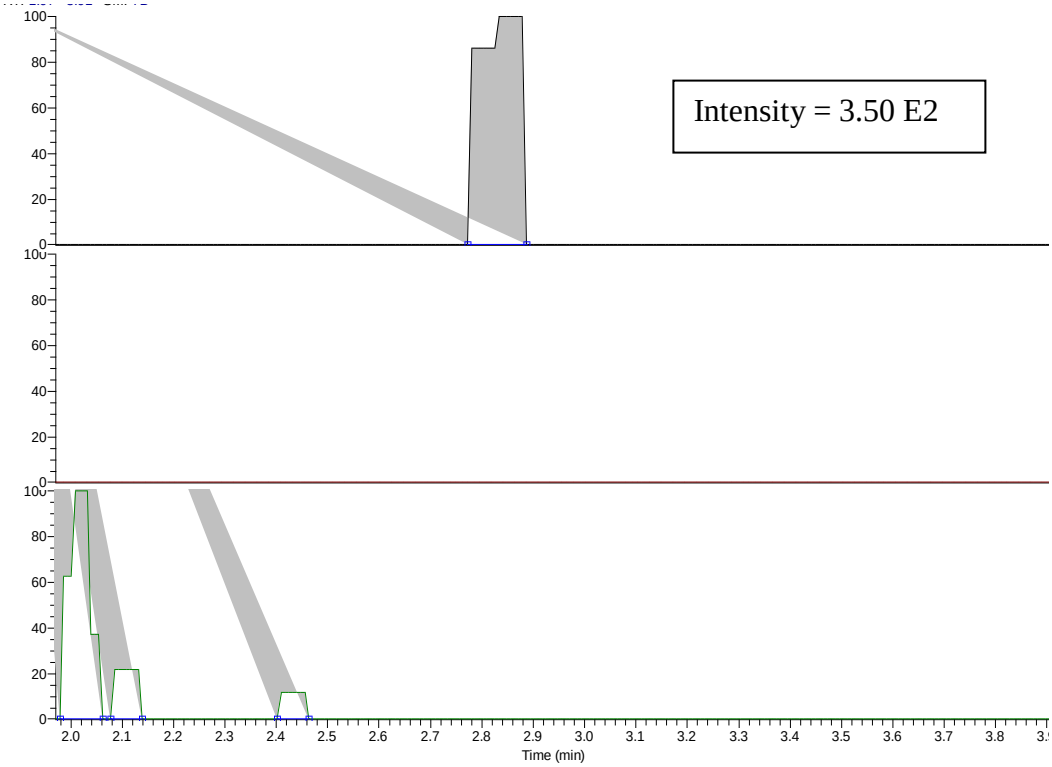

Figure 5.15 EICs from APTS derivatised rEPO digest for (from top) m/z 747.67, 849.21, and 950.75, corresponding to no, one and two remaining N-acetylglucosamine residues.

Retention was much reduced with APTS derivatisation, and the separation of different glycans seen with rhodamine 110 derivatisation did not occur. Since peaks co-eluted, accurate quantitative analysis of peak areas is not possible. However, the peak area ratio for IgG of glycans with and without GlcNAc residues attached to the pentasaccharide core was 1: 2.2, so it is in the same region as that obtained with rhodamine 110. With rEPO, only the pentasaccharide core structure was detected. It is not clear why the peak seen for this glycan was so much smaller in the rEPO digest than in that of IgG with APTS derivatisation, when the peaks were closer in size with rhodamine 110 derivatisation.

5.3.3 Comparison of digests from rEPO, IgG and huEPO with glycan standards at different time points

Glycan standards NGA2FB, NGA2F and M3N2F were derivatised with Rhodamine 110, and analysed using LC-MS. EICs from these samples are shown in figure 5.16.

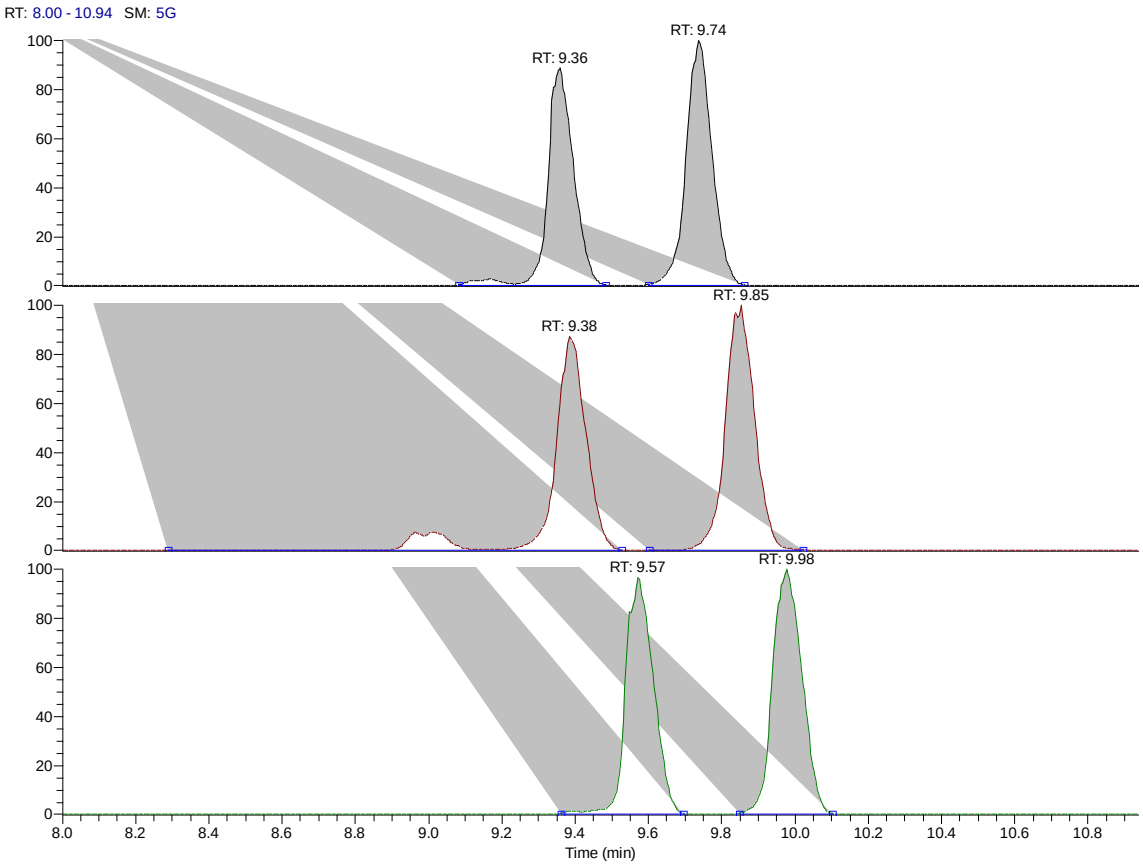

Figure 5.16 EICs of Rhodamine 110 derivatised glycan standards. From top, glycans are NGA2FB, NGA2F and M3N2F

The reduction in the hydrophilic nature of the derivatised glycans as the size of the glycans is reduced results in an increasing retention time. Mass spectra from these peaks are shown in figures 5.17-5.19.

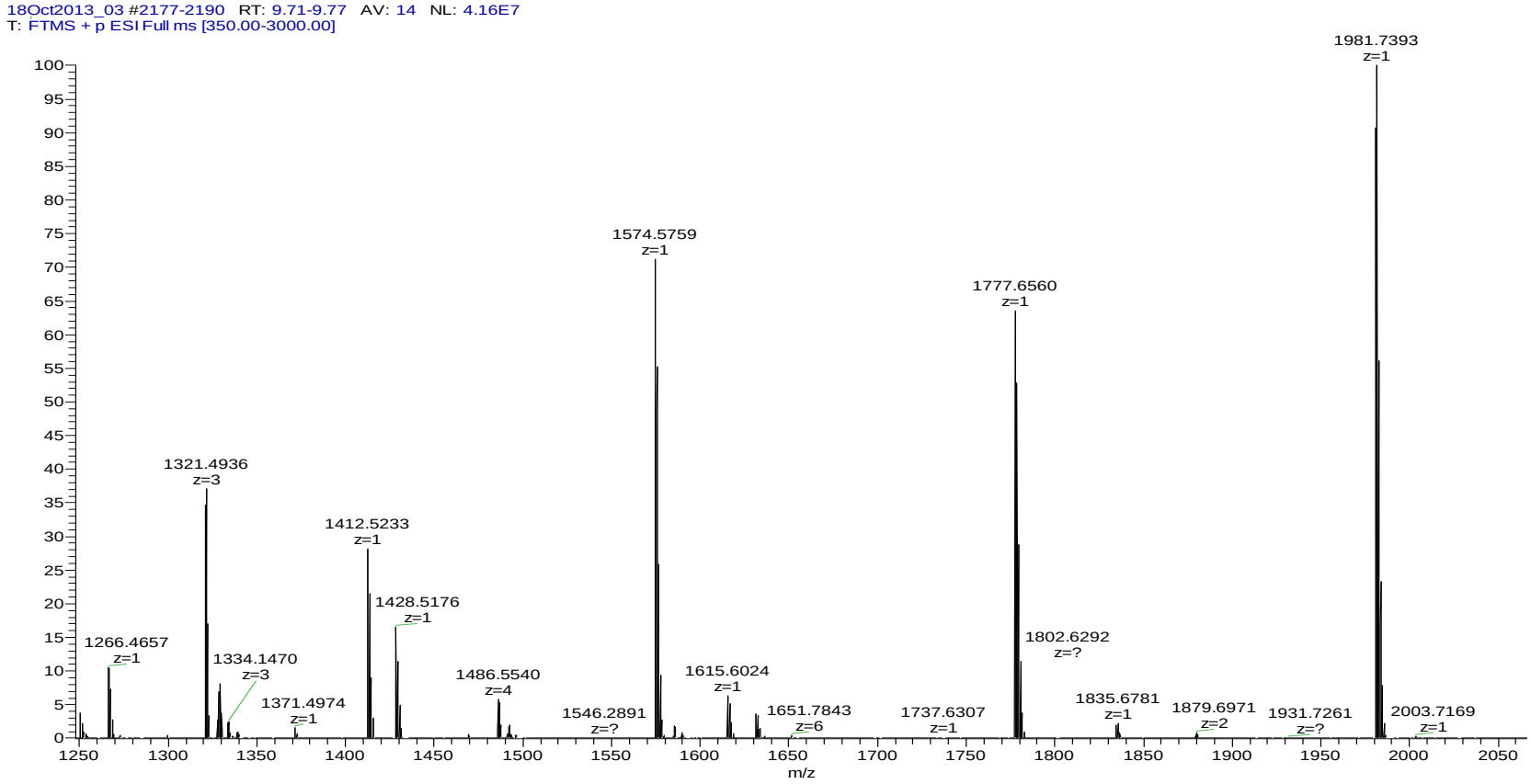

Figure 5.17 – Mass spectrum from NGA2FB peak in figure 5.16

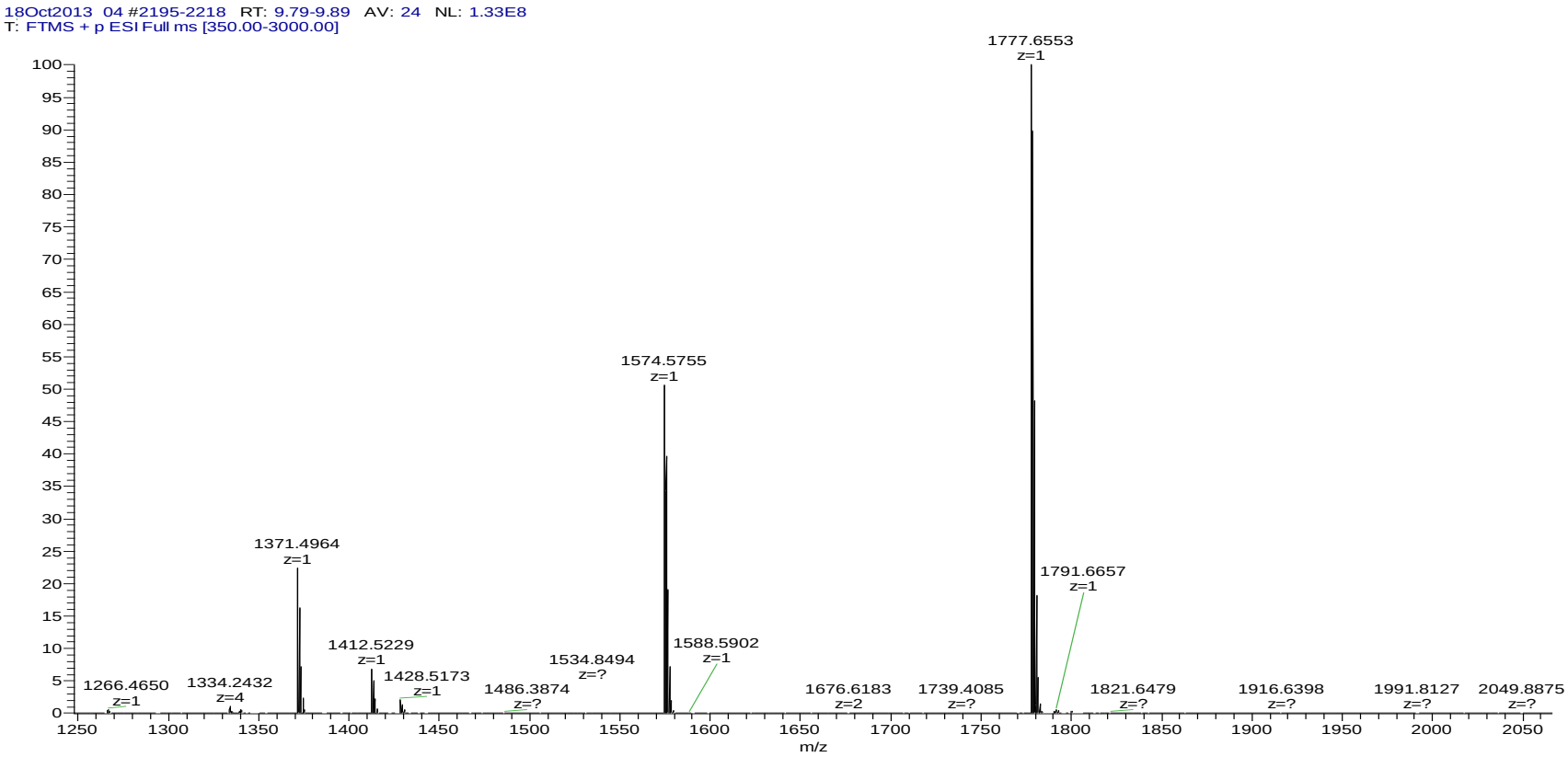

Figure 5.18 – Mass spectrum from NGA2F peak in figure 5.16

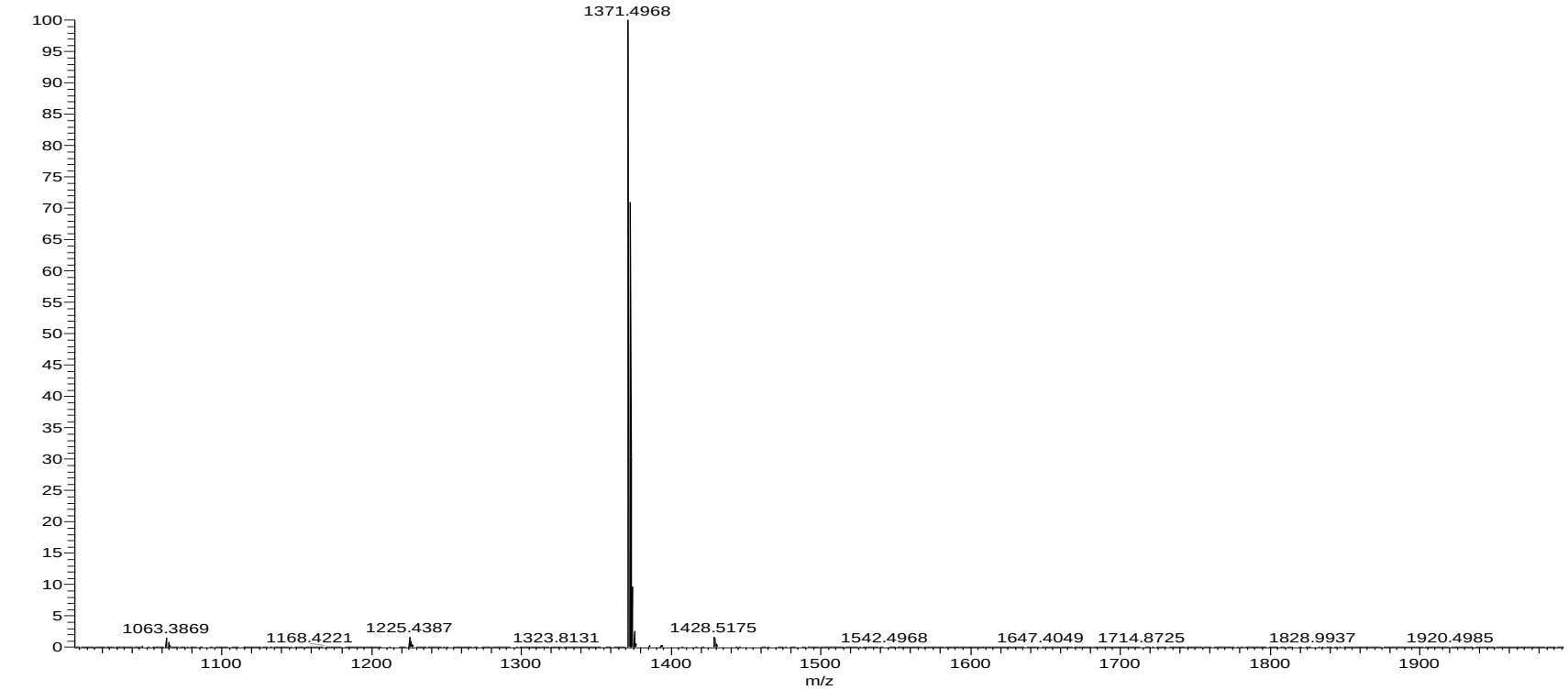

Figure 5.19 – Mass spectrum from M3N2F peak in figure 5.16

EICs of m/z 366.1384 (used to identify glycan containing peaks) from the rEPO digest at 0, 3, 6, 12 and 24 hours are shown in Figure 5.20. The inital chromatogram shows a very broad peak, presumably due to the large variety in glycans present at the start. Over time, this broad peak resolves itself into more distinct peaks, presumably as this variety is reduced by sequential cleavage of sugar residues by exoglycosidases. The final chromatogram shows only a few overlapping, but partially resolved peaks.

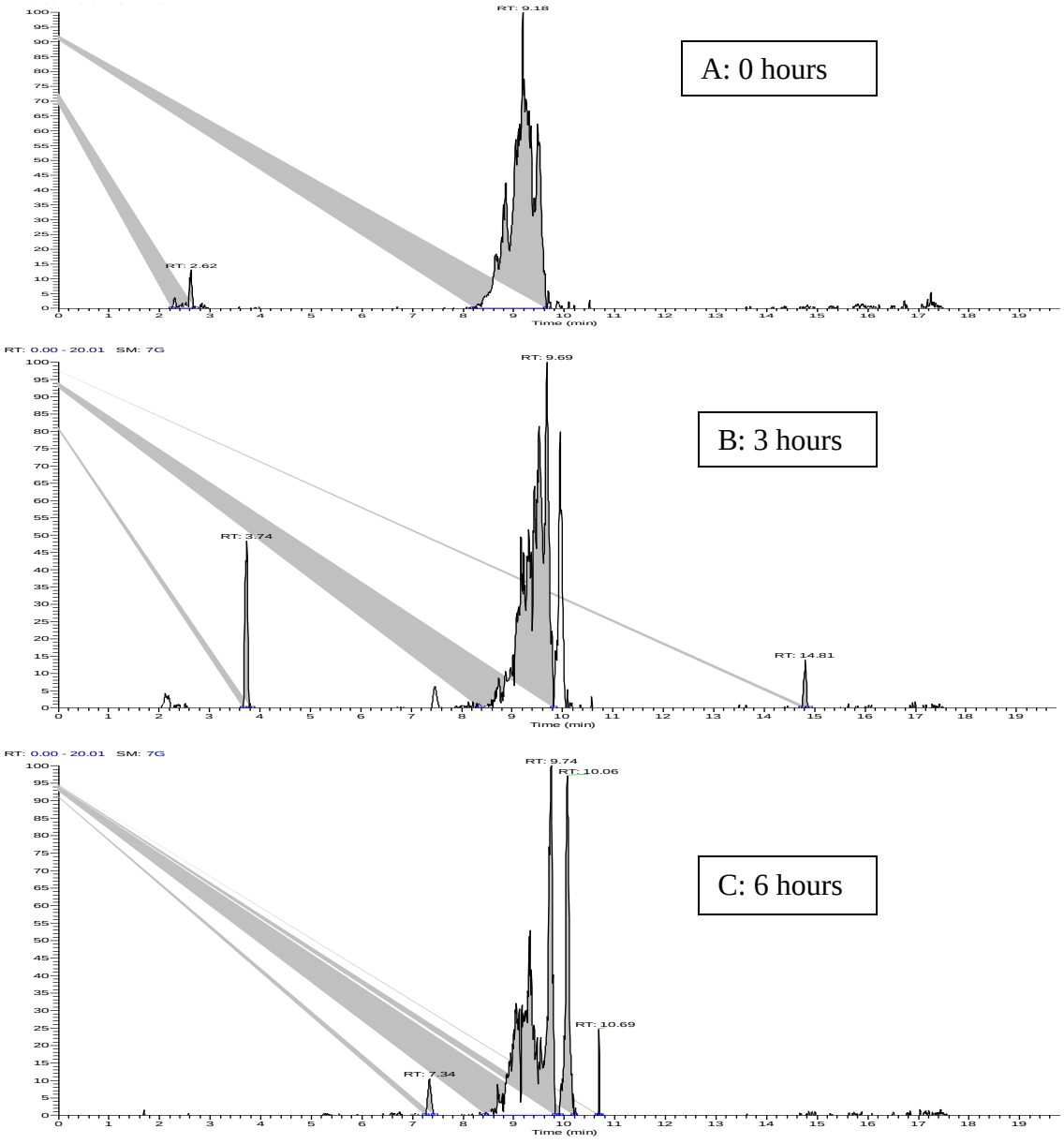

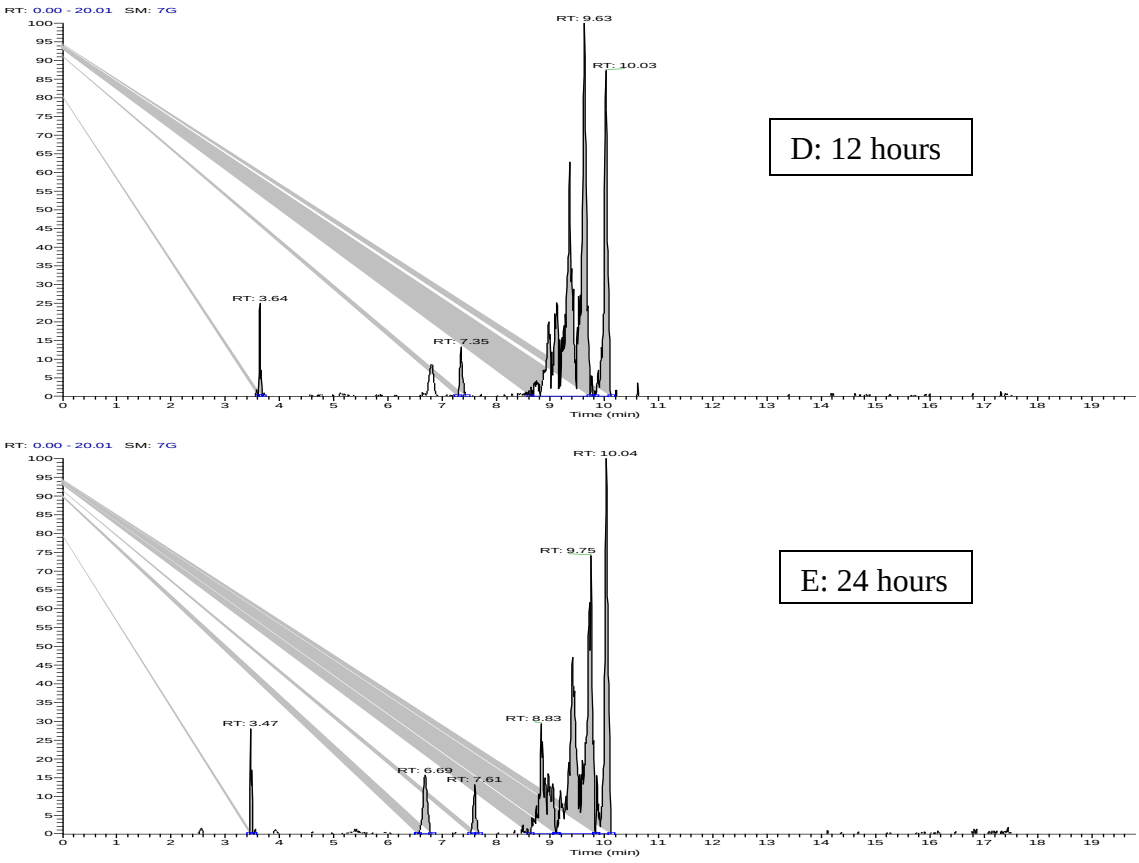

Figure 5.20: EICs of m/z 366.1384 from rEPO digest at – A: 0 hours, B: 3 hours, C: 6 hours, D: 12 hours, E: 24 hours

The mass spectrum from this final chromatogram between 9 and 10 minutes is shown in figure 5.21. This shows that after 24 hour digestion glycans consisting of the fucosylated pentasaccharide core with one (m/z 1574.58), two (m/z 1777.66 or 889.33) and three (m/z 990.87) GlcNAc residues attached are detected, but the predominant glycan detected is the fucosylated pentasaccharide core with no other residues attached (m/z 1371.49).

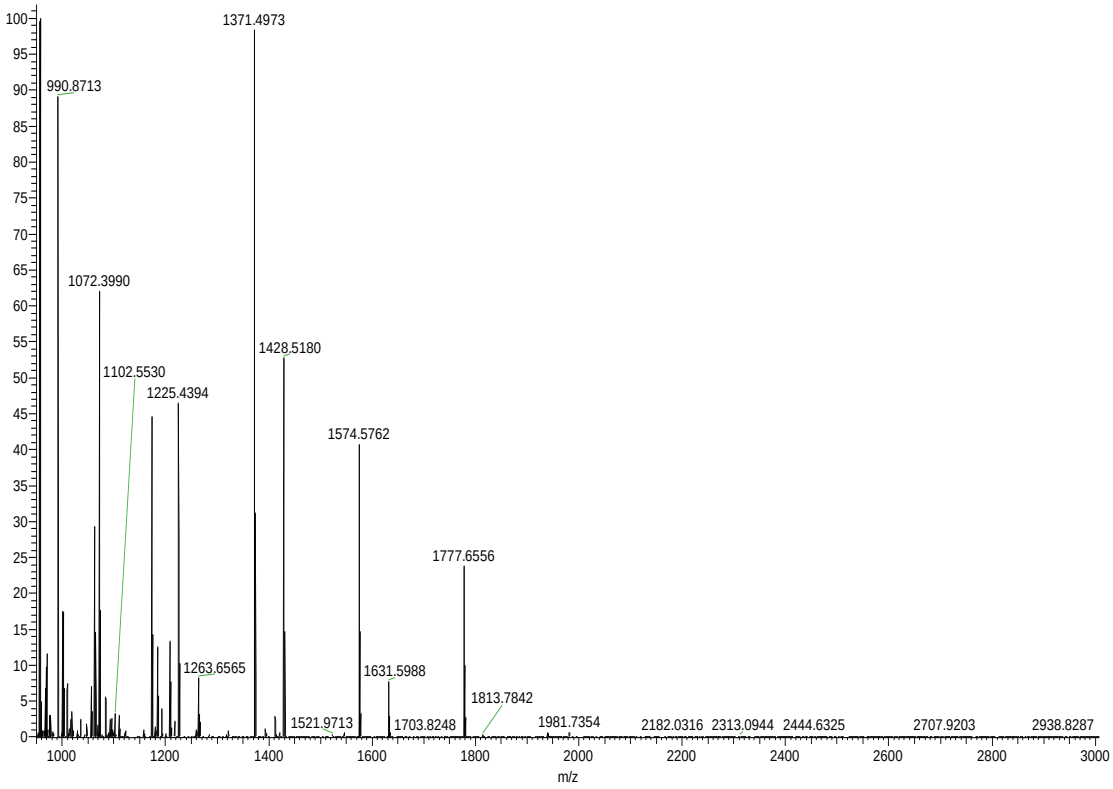

Figure 5.21 Mass spectrum from 9 to 9.5 minutes from chromatogram E, figure 5.20

For reference, the spectrum from the same time in the chromatogram from the starting point of the digest (A in figure 5.20) is shown in figure 5.22, below. Interestingly, there is evidence of a glycan with m/z 1574.58 in this sample, although it is possible this is formed by in-source fragmentation.

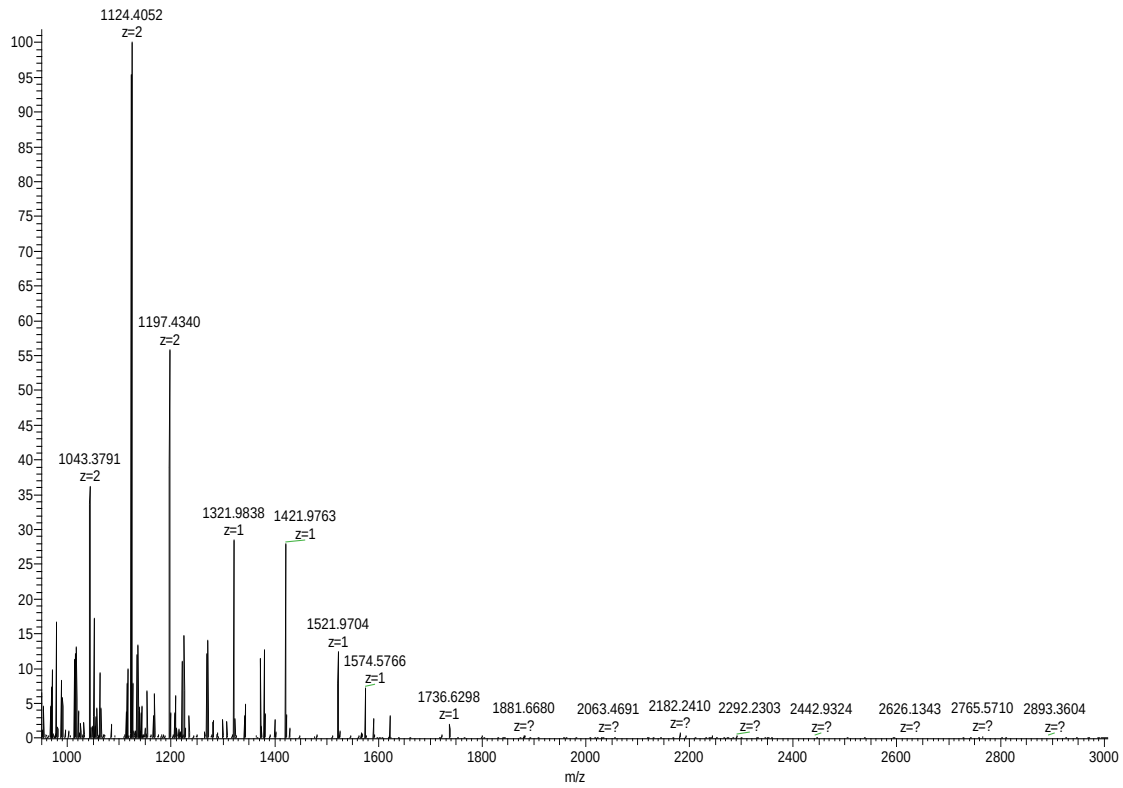

Figure 5.22 Mass spectra from 9 to 9.5 minutes from chromatogram A, figure 5.20

Comparison of the digest of IgG, rEPO and the glycan standard of NGA2FB showed that in the rEPO and IgG digest after 24 hours, a glycan corresponding in mass to a fucosylated pentasaccharide core with one attached GlcNAc residue was present, but that it had a different retention time in the two digests (see Figure 5.23) The retention time of the glycan present in IgG matched that of the same glycan in NGA2FB, the bisected standard. This was true for all three injections of the samples. This adds more weight to the proposal that the two can be separated because of the position of the GlcNAc residue.

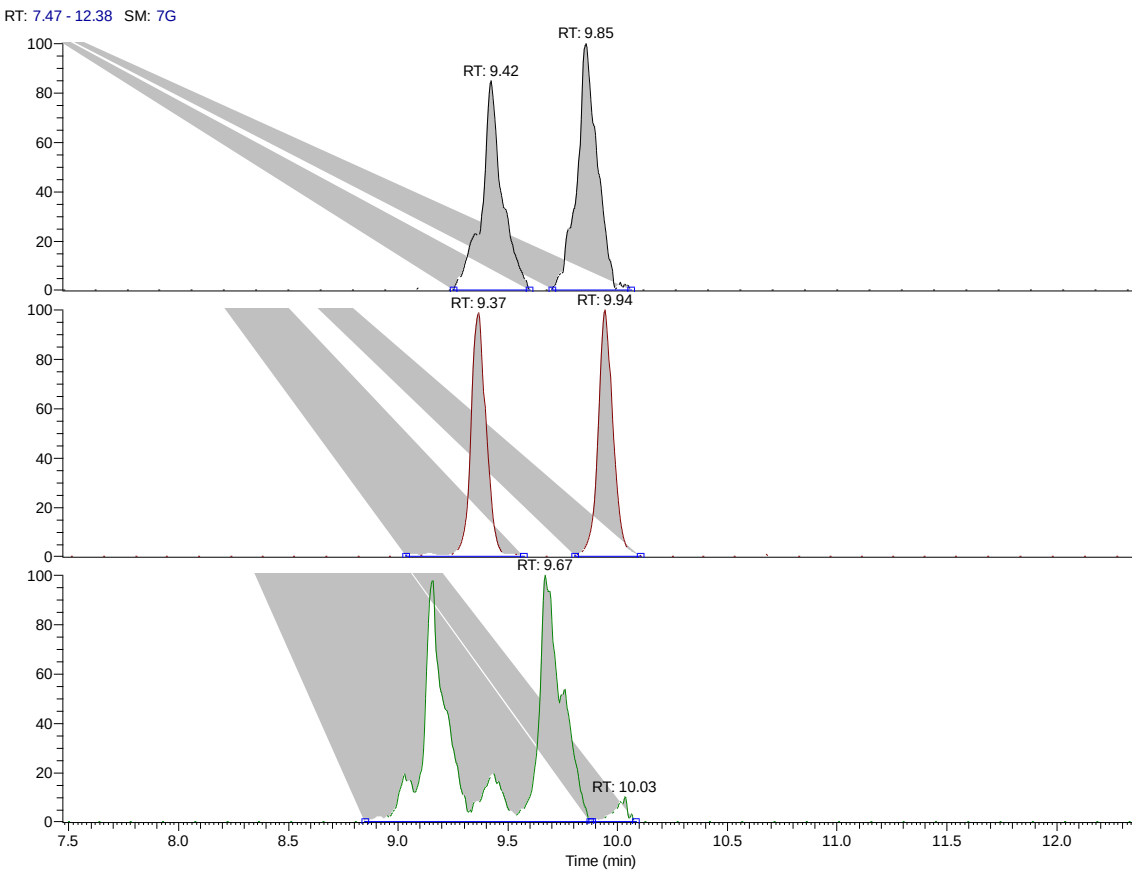

Figure 5.23 EICs of m/z 1574.57 from digests after 24 hours. From top: IgG, NGA2FB, rEPO

Unfortunately, attempts to see if the retention time of the same glycan from the digest of huEPO matched that from the digest of IgG or rEPO were not successful, as no glycan with this m/z was detected in the huEPO digest. However, a peak was found in the huEPO electropherogram with an m/z the same as that of the intact glycan standard NGA2FB. EICs of this m/z from LC analysis of this standard as well as 24 hour digests of rEPO, IgG, huEPO (all derivatised with Rhodamine 110) are shown in figure 5.24. They show that there is partial resolution of the peaks found with NGA2FB, IgG and huEPO from those found in rEPO. This was especially true of the first of the two peaks in the chromatogram, where there is near baseline resolution. This resolution was seen in all three repeat injections of the samples.

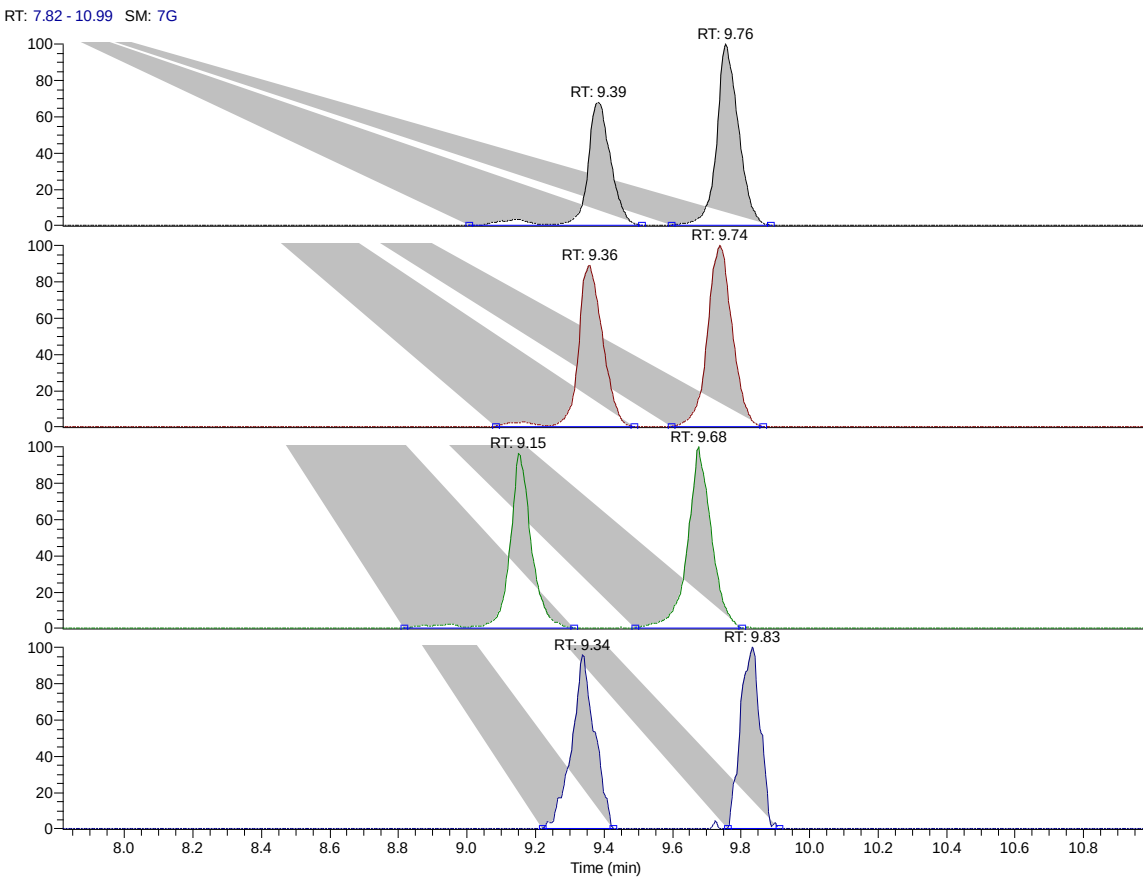

Figure 5.24 EICs of m/z 990.87 (2+ ion). From top, 24 hour digest of IgG, NGA2FB standard, 24 hour digest of rEPO, 24 hour digest of huEPO

These results suggest that there is a real and detectable difference in the core structures of glycans from IgG, rEPO and the huEPO standard. Specifically, it suggests that the bisected glycan NGA2FB is the same structure found at the core of glycans from IgG (as has been previously reported) and also at the core of glycans from the huEPO standard (as suggested by Christian Reichel). This glycan structure is not, however, found in rEPO. As such, glycans with the same mass found in rEPO digests must consist of the fucosylated pentasaccharide core with three GlcNAc residues, all of which are attached to the α-linked mannose residues. As shown in the chromatograms in Figure 5.24, these different core glycans can be resolved on a C18 column after derivatisation with Rhodamine 110.

5.3.4. Use of superchargers to enhance detection of derivatised glycans

Extracted ion chromatograms for m/z 1,574.57 from samples of derivatised glycans from rEPO analysed with and without sulfolane in the LC solvent are shown in figure 5.25.

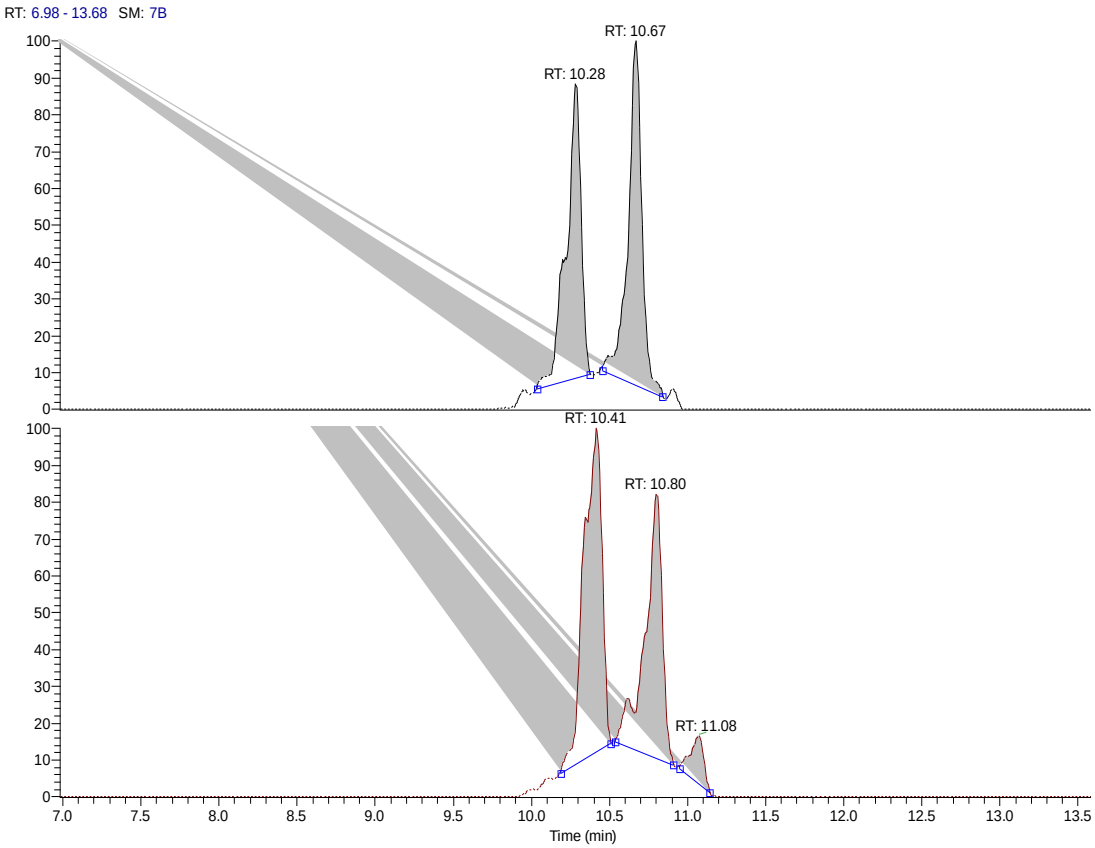

Figure 5.25 EIC of m/z 1574.57 from analysis of derivatised glycans from rEPO, with (bottom) and without addition of 1% sulfolane to the LC solvent

The addition of sulfolane causes a (very slight) increase in retention time. As can be seen in the mass spectra from these chromatograms (figure 5.26), it also causes an increase in peak height. Samples were run twice, and mean increase in peak height for the 1,574.57 ion was 2.2 times.

EICs for m/z 1,371.49 and mass spectra focusing on this m/z are shown in figures 5.27 and 5.28. Again, as well as a slight increase in retention time, an increase in signal is seen; mean increase this time was 2.7 times.

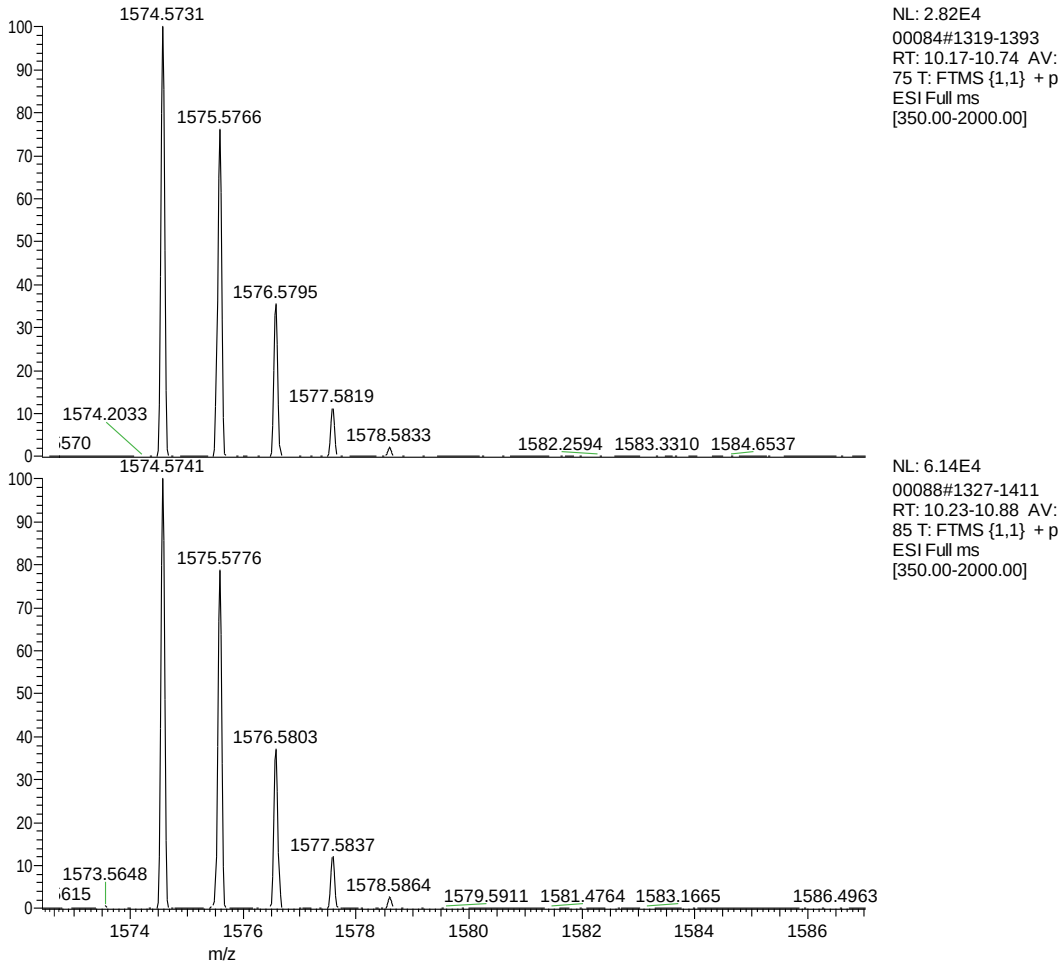

Figure 5.26 Mass spectra from peaks in EICs in figure 5.25. Top, without sulfolane; bottom, with 1% sulfolane in LC solvent

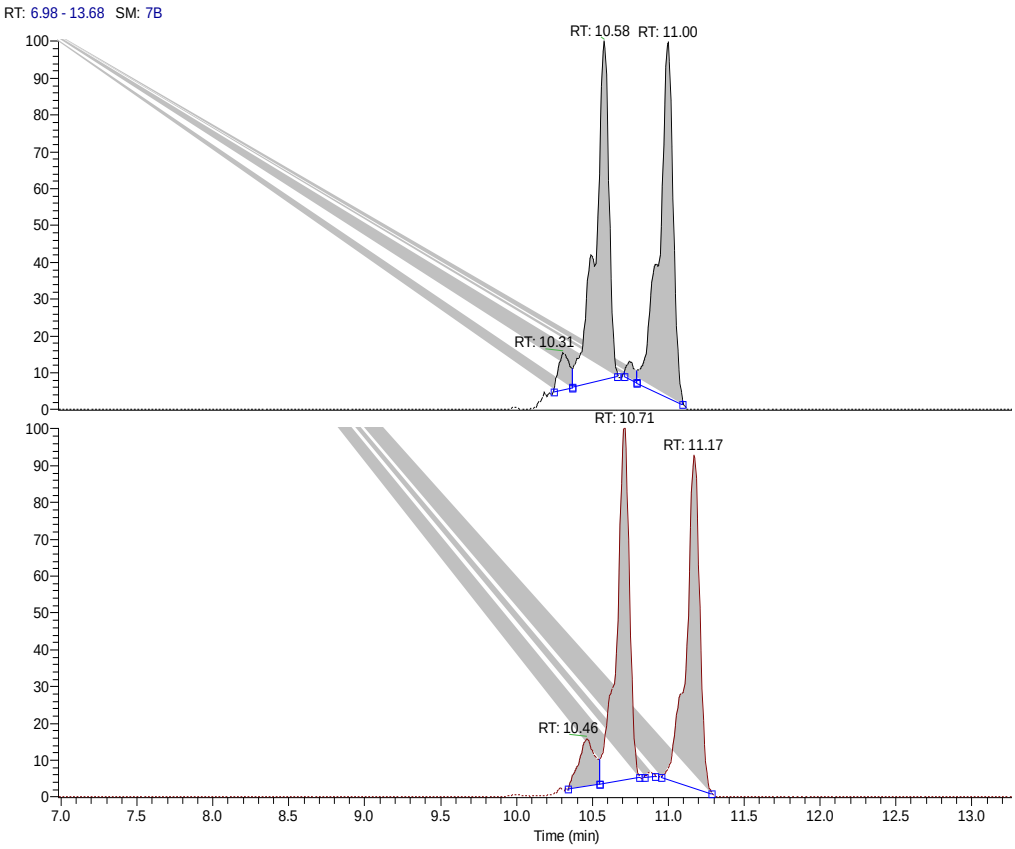

Figure 5.27 EIC of m/z 1,371.49 from analysis of derivatised glycans from rEPO, with (bottom) and without addition of 1% sulfolane to the LC solvent

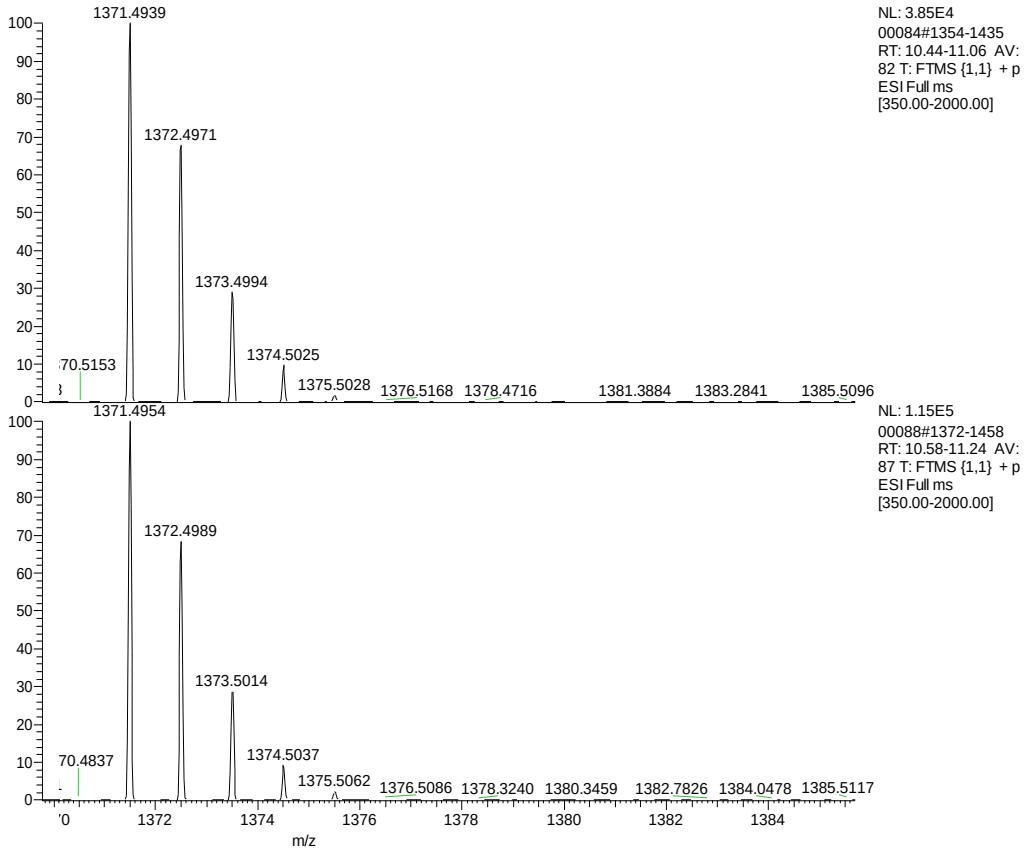

Figure 5.28 Mass spectra from peaks in EICs in figure 5.27. Top, without sulfolane; bottom, with 1% sulfolane in LC solvent

5.3.5 CE-LIF analysis of glycans

CE-LIF analysis of APTS labelled glycans was less suggestive of a difference between rEPO and IgG after short digestion. Figure 5.29 shows the electropherogram of the shorter digests of rEPO and IgG, zoomed in on the region between 4 and 10 on the glucose ladder. The only major peak for rEPO is at approximately 11.6 minutes, which is about 6 glucose units in size and probably corresponds to the fucosylated pentasaccharide core. There is no obvious peak which would correspond to this core plus a single (non-bisecting) GlcNAc. In the IgG electropherogram, as well as this core structure, other peaks are seen which could correspond to the core plus one, two and three additional GlcNAc moieties.

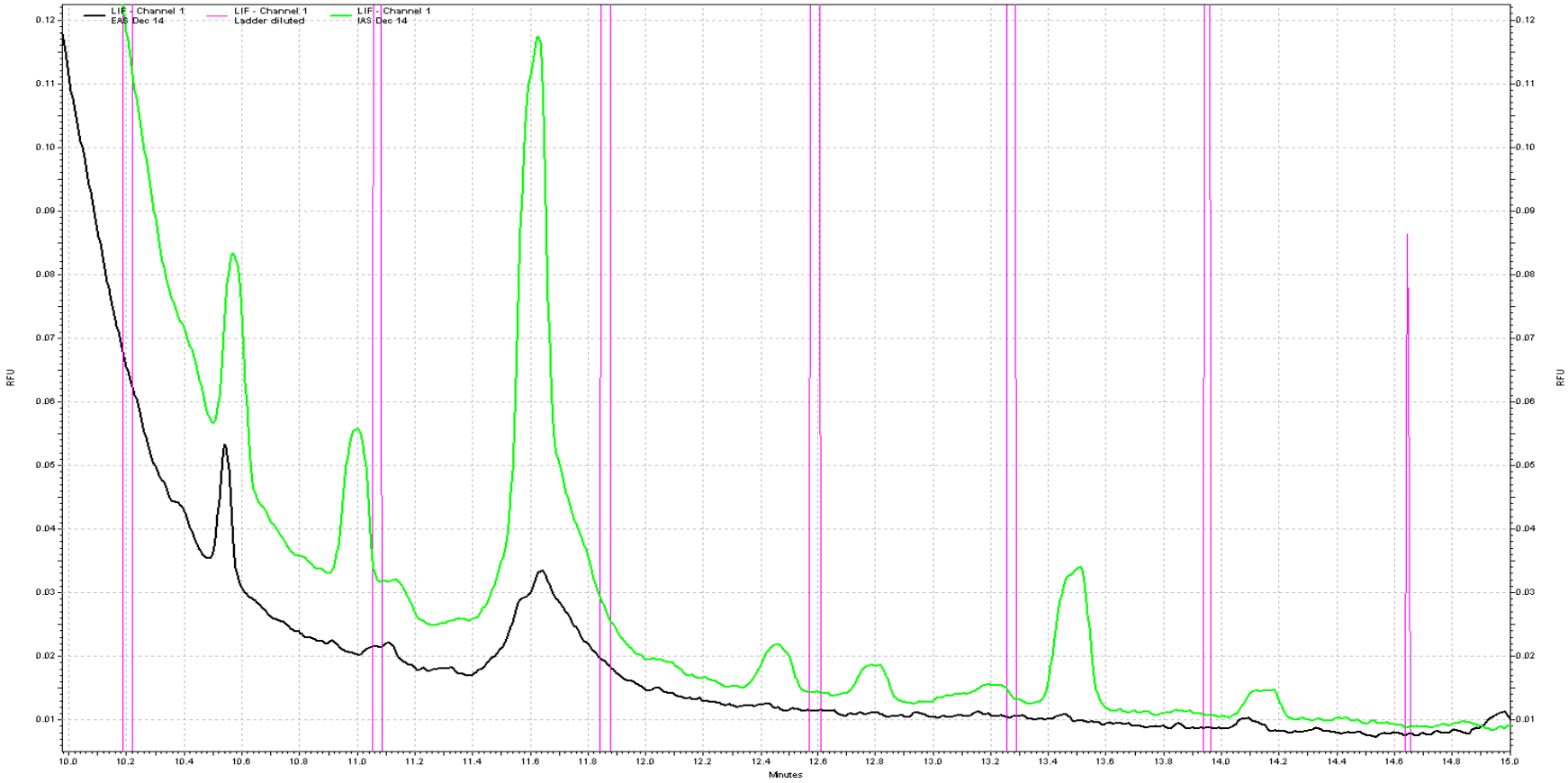

Figure 5.29 Electropherogram of APTS labelled glycans from rEPO (black) and IgG (green) after the shorter digestion. Pink peaks are from glucose ladder, 4-10 residues long

Figure 5.30 shows the electropherograms from CE-LIF analysis of the longer digests. At about five glucose units long, there are two peaks found in both digests, corresponding to the positional isomers of the fucosylated pentasaccharide core with one mannose removed. It is not clear how this is formed, since no mannosidases were present in the digest. It could be that some of the enzymes used have some secondary mannosidase activity, and that as a result of the longer digest, some of this glycan is formed. A small third peak is also seen in the IgG digest; potentially, this could be the pentasaccharide core with two mannose residues removed and a bisecting GlcNAc present, although this has not been confirmed.

At six glucose residues long, the large fucosylated pentasaccharide peak is again observed. This peak seems to be split in the IgG trace; again, it is not clear why this is. Then, at seven residues long, there are two peaks seen in both IgG and rEPO digests; one peak (at approximately 12.7 minutes) is seen in both; however, a peak is present in the IgG electropherogram at 12.4 minutes, and at 12.5 minutes in the rEPO electropherogram. It is possible that the peak present in IgG is the fucosylated pentasaccharide core with a bisecting GlcNAc residue. Certainly, at eight residues long, there are three peaks present in the digest of IgG, and one (or possibly two) present in the digest of rEPO, which corresponds to the positional isomers possible respectively with and without a bisecting GlcNAc residue present.

If the peaks from 7-residue long glycans are those from the fucosylated core structure with bisecting or non-bisecting GlcNAc residues, then the ratios of the peaks may provide a way to discriminate between endogenous and recombinant EPO. However, the sensitivity of this approach still needs to be determined. Due to time constraints, it was not possible to run a dilution series to estimate the limit of detection of this method. This would need to be addressed to see if it is a viable approach.

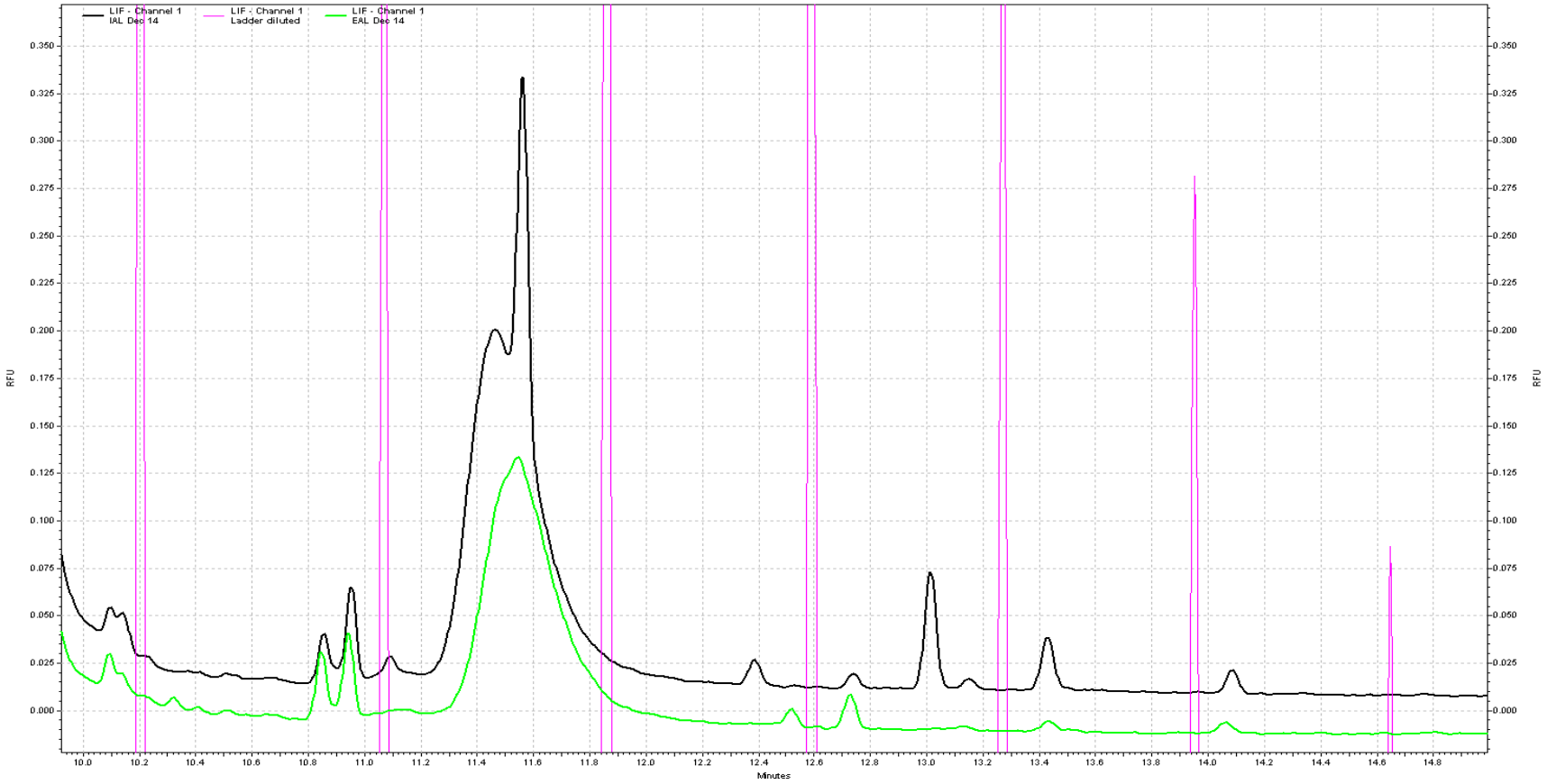

Figure 5.30 Electropherogram of APTS labelled glycans from IgG (black) and rEPO (green) after the longer digestion. Pink peaks are from glucose ladder, 4-10 residues long.

5.3.6 Extraction, digestion and derivatisation of EPO from urine samples

The method presented here does not have the sensitivity to detect glycans from EPO at the level it is found in urine. However, samples were nonetheless extracted using MAIIA cartridges, digested and derivatised and then analysed in the same manner as standards. EICs for m/z 1,574.57 and 1,371.49 did not detect any peaks in these samples. This does at least demonstrate that there are not compounds present at much higher levels than EPO which could give false positive results, although obviously it does not preclude them being present at similar levels to EPO.

5.4 Conclusions

There is evidence that IgG and rEPO behave differently when digested at approximately equimolar concentrations (of glycans) by exoglycosidases. IgG, which has been reported to consist mostly of glycans carrying a bisecting GlcNAc, was digested by the combination of enzymes used here to two main structures after 36 hours: a fucosylated pentasaccharide core, and the same core structure with a single GlcNAc residue attached.

These are also the structures detected when rEPO is digested by the same process for the same length of time. However, there are two key differences, depending on the length of the digestion. With a shorter digest time, both structures were detected in significant amounts. EICs of the mass corresponding to the glycan with the single GlcNAc residue attached showed that peaks from rEPO eluted in a shorter time than peaks from IgG. This suggests that the peaks are isomers. Since IgG is predominantly bisected, it is reasonable to suggest that the peaks seen could be from glycans with a single bisecting GlcNAc residue remaining, whereas those seen in rEPO (which is not thought to contain a bisecting GlcNAc) have a remaining GlcNAc attached to the α3 or α6 linked mannose residues. The detection in sufficient quantities of this latter glycan may provide a way of detecting rEPO in the presence of endogenous EPO.

A second difference is seen when the digestion is carried on for longer. After 20 hours, the glycans from the rEPO digest had been digested almost entirely to the fucosylated

pentasaccharide core. This was not the case with the glycans from IgG, which still contained a large amount of the glycan containing an additional GlcNAc. This would tally with this residue being bisecting; the N-acetylglucosaminidase used in the digests shows less activity at cleaving bisecting residues. As a result, after 20 hours, there was still a relatively large amount of it left. This could provide a second approach for discriminating between endogenous and rEPO; after a sufficiently lengthy digest, the ratio of m/z 1,574.57 to 1,371.49 ions would be higher with endogenous EPO than with rEPO; in the digests carried out here, the ratios were 1:5.7 for IgG, and 1:47 for rEPO.

Experiments using a purified standard of glycan NGA2FB provided additional evidence for the idea that the presence of a bisecting GlcNAc can enable glycans to be separated on a C18 column after derivatisation with Rhodamine 110. As stated, glycans from digested rEPO could be separated from isobaric glycans from IgG. Exoglycosidase digestion of the NGA2FB standard showed that the retention time of glycans from IgG was the same as the retention time of glycans from the bisected standard.

Unfortunately, this difference was not able to provide a way to distinguish between huEPO and rEPO, as the glycan with m/z 1,574.57 was not detected in the digest of the huEPO standard. However, a glycan corresponding in mass to the bisected standard NGA2FB (m/z 990.87, 2+ ion) was detected in this digest. A glycan with this mass was also detected in 24 hour digests of rEPO and IgG. The retention time of this glycan was the same in the digests of IgG and huEPO, and matched the retention time of the NGA2FB standard. However, the retention time in rEPO of this glycan was different. This could be because in the three former glycans, one of the GlcNAc residues is bisecting; in the latter, it is not.

At present this approach has not been demonstrated with sufficient sensitivity to be tested on real antidoping samples. However, the technology may already exist to provide sufficient sensitivity. Digests of rEPO (which were split to enable derivatisation with both rhodamine 110 and APTS) were run at a final concentration of 200 μg/mL on the Exactive, and had a signal:noise ratio of 223, which increased to 687 when sulfolane was added to the LC solvent. Using a minimum signal:noise ratio of 3:1, this would imply a limit of detection of 291 ng/mL. Assuming a not unreasonable 50% recovery from the MAIIA cartridges and reconstituting in 20 μL after derivatisation, real doping

samples would be expected to have a concentration in the region of 5 ng/mL. Although this would appear to be a long way from the limit of detection of the method presented here, a change from a 2.1 mm column to a 75 μm capillary column would theoretically increase sensitivity by up to 784 times. Changing to the more sensitive Q-Exactive improved detection; samples were made up at 2 μg/mL, but still displayed high signal:noise values. It is worth mentioning, however, that although at relatively low concentrations, 100 ng of huEPO was still used in the digest; this is the amount found in 10 litres of urine, and dropping down to lower absolute amounts may result in much higher proportional losses.

It also needs pointing out that even if the difference in the chromatograms of digested and derivatised rEPO and huEPO standards is due to the absence and presence respectively of a glycan containing bisecting GlcNAc, it does not necessarily follow that this bisected glycan is present in huEPO, only that it is present in the standard. It is possible that the standard also contains other glycoproteins, which may themselves contain a glycan with a bisecting GlcNAc. Tryptic digest of the huEPO standard followed by LC-MS/MS identification of the peptides present may enable this to be checked.

CE-LIF analysis was only carried out on APTS labelled glycans, due to time and equipment constraints. It may be valuable to check the sensitivity and separation seen with CE-LIF analysis of rhodamine 110 labelled glycans as well.

The data that was obtained did not entirely tally with that from the LC-MS analysis, although the two analyses were carried out on differently derivatised samples. The long digests of rEPO and IgG resulted in electropherograms in which peaks were present which could correspond to 7-residue glycans without and with bisecting GlcNAc residues. The equivalent peaks from LC-MS analysis of rhodamine 110 labelled glycans were very small, if present, in the long rEPO digest.

The short digest of rEPO did not result in detectable peaks in CE-LIF that would correspond to glycans of this size, although they were detected in LC-MS analysis of this digest. Glycans of this size were detected in both the CE-LIF analysis and LC-MS analysis of the short digest of IgG. It is not clear where this discrepancy in the data comes from. It is possible that the derivatisation process causes some changes to the

glycan structures found, although this would not necessarily be a problem if any effects are reproducible and affect different glycan structures equally. However, the CE-LIF work was severely time constrained. Although it perhaps provides complementary data to that obtained by LC-MS, it needs to be repeated before too much weight should be attached to it.

It would also be useful to provide more time points through the digest than just two. In particular, a profile of the digest at, or near, time zero could be helpful. Analysis of a digestion progression may better demonstrate how the glycans from the two glycoproteins are sequentially digested, and the differences that arise between the two profiles as a result. In this way, digestion could be optimised to maximise the detectable differences. As mentioned above, this work was partly carried out using LC-MS; it suggested that after 24 hours, the digests of rEPO and IgG could be distinguished by the retention times of glycans consisting of the fucosylated pentasaccharide core with 3 GlcNAc residues attached. The retention time of this glycan from a huEPO digest matched that from IgG and differed from that from rEPO. Unfortunately, machine availability issues meant that analysis of the samples gathered at different time points through a digest could not be carried out using CE-LIF; there was also no opportunity to examine digested huEPO. Since improved resolution might be expected with capillary electrophoresis, use of this approach may provide further evidence of the structural differences claimed here.

5.5 References

Albrecht, S., H. A. Schols, et al. (2010). "CE-LIF-MSn profiling of oligosaccharides in human milk and feces of breast-fed babies." Electrophoresis **31**(7): 1264-1273.

Boucher, S., A. Kane, et al. (2012). "Qualitative and quantitative assessment of marketed erythropoiesis-stimulating agents by capillary electrophoresis." Journal of Pharmaceutical and Biomedical Analysis **71**(0): 207-213.

Chen, F.-T. A. and R. A. Evangelista (1998). "Profiling glycoprotein N-linked oligosaccharide by capillary electrophoresis." Electrophoresis **19**(15): 2639-2644.

Costell, C., J. Contado-Miller, et al. (2007). "A glycomics platform for the analysis of permethylated oligosaccharide alditols." Journal of the American Society for Mass Spectrometry **18**(10): 1799-1812.

Galuska, S. P., H. Geyer, et al. (2012). "Glycomic strategy for efficient linkage analysis of di-, oligo- and polysialic acids." Journal of Proteomics **75**(17): 5266-5278.

Gennaro, L. A. and O. Salas-Solano (2008). "On-Line CE−LIF−MS Technology for the Direct Characterization of N-Linked Glycans from Therapeutic Antibodies." Analytical Chemistry **80**(10): 3838-3845.

Guttman, A., F.-T. A. Chen, et al. (1996). "Separation of 1-aminopyrene-3,6,8-trisulfonate-labelled asparagine-linked fetuin glycans by capillary gel electrophoresis." Electrophoresis **17**(2): 412-417.

Guttman, A. and T. Pritchett (1995). "Capillary gel electrophoresis separation of high-mannose type oligosaccharides derivatized by 1-aminopyrene-3,6,8-trisulfonic acid." Electrophoresis **16**(1): 1906-1911.

Huang, Y., X. Shi, et al. (2011). "Improved Liquid Chromatography-MS/MS of Heparan Sulfate Oligosaccharides via Chip-Based Pulsed Makeup Flow." Analytical Chemistry **83**(21): 8222-8229.

Huhn, C., L. R. Ruhaak, et al. (2012). "Alignment of laser-induced fluorescence and mass spectrometric detection traces using electrophoretic mobility scaling in CE-LIF-MS of labelled N-glycans." Electrophoresis **33**(4): 563-566.

Hurum, D. C. and J. S. Rohrer (2011). "Five-minute glycoprotein sialic acid determination by high-performance anion exchange chromatography with pulsed amperometric detection." Analytical Biochemistry **419**(1): 67-69.

Ijiri, S., K. Todoroki, et al. (2011). "Highly sensitive capillary electrophoresis analysis of N-linked oligosaccharides in glycoproteins following fluorescence derivatization with rhodamine 110 and laser-induced fluorescence detection." Electrophoresis **32**(24): 3499-3509.

Lee, Y. C. (1996). "Carbohydrate analyses with high-performance anion-exchange chromatography." Journal of Chromatography A **720**(1-2): 137-149.

Liu, J., O. Shirota, et al. (1991). "Separation of fluorescent oligosaccharide derivatives by microcolumn techniques based on electrophoresis and liquid chromatography." Journal of Chromatography A **559**(1–2): 223-235.

NIBSC. (2012) "Biological Reference Materials Product Catalogue." Retrieved 08/11/12, from http://www.nibsc.ac.uk/products/biological_reference_materials/product_catalogue/detail_page.aspx?catid=67/343.

Pabst, M., J. S. Bondili, et al. (2007). "Mass + Retention Time = Structure: A Strategy for the Analysis of N-Glycans by Carbon LC-ESI-MS and Its Application to Fibrin N-Glycans." Analytical Chemistry **79**(13): 5051-5057.

Pabst, M., J. Grass, et al. (2012). "Isomeric analysis of oligomannosidic N-glycans and their dolichol-linked precursors." Glycobiology **22**(3): 389-399.

Raju, T. S., J. B. Briggs, et al. (2000). "Species-specific variation in glycosylation of IgG: evidence for the species-specific sialylation and branch-specific galactosylation and importance for engineering recombinant glycoprotein therapeutics." Glycobiology **10**(5): 477-486.

Reichel, C. (2011). "The overlooked difference between human endogenous and recombinant erythropoietins and its implication for sports drug testing and pharmaceutical drug design." Drug Testing and Analysis **3**(11-12): 883-891.

Staples, G. O., M. J. Bowman, et al. (2009). "A chip-based amide-HILIC LC/MS platform for glycosaminoglycan glycomics profiling." Proteomics **9**(3): 686-695.

Townsend, R. R., M. R. Hardy, et al. (1989). "Separation of branched sialylated oligosaccharides using high-pH anion-exchange chromatography with pulsed amperometric detection." Anal Biochem **182**(1): 1-8.

Varki, A., R. Cummings, et al., Eds. (2009). Essentials of Glycobiology. Cold Spring Harbor (NY), Cold Spring Harbor Laboratory Press.

Zhang, Z., N. M. Khan, et al. (2012). "Complete Monosaccharide Analysis by High-Performance Anion-Exchange Chromatography with Pulsed Amperometric Detection." Analytical Chemistry **84**(9): 4104-4110.

Chapter 6: Discussion, conclusions and future work

Erythropoietins (EPOs) are available as the original Amgen recombinant material and, since the expiration of the patent, as a plethora of biosimilars produced in laboratories around the world with differing post-translational isoform structures.

The current methods for identification of the misuse of EPOs and related drugs (isoelectric focusing or SDS/Sarcosyl-PAGE and immunoblotting) abused for performance enhancing purposes are both time and labour intensive, albeit that they can detect very small concentrations of epoietins. The results they produce are subjective and it is suspected that they result in a large number of false negatives, as their lack of specificity means that the criteria for a positive test need to be set more tightly than is perhaps desirable.

Alternative methods developed with the intention of tackling this problem either fail to identify all the isoforms, lack sufficient sensitivity to be used in anti-doping tests, or have not been validated with real anti-doping samples.

The original aim of this PhD was to develop a mass spectrometry-based method for the detection of rEPO in anti-doping samples. Mass spectrometry based methods which had been previously tried had failed due to a lack of sensitivity; this in turn was due to the low levels at which EPO is present in urine (~10 ng/L), combined with the extensive variation in the glycosylation found. At the start of the PhD, recently published research (Groleau, Desharnais et al. 2008) had been able to detect and identify the three most prominent glycoforms of Asn_{24} and Asn_{38} using 100 ng of rEPO after desialylation, at a concentration of 500 μg/mL. Partial assignment of the glycan structures on these glycopeptides was possible, including the identification of N-acetyl lactosamine repeat units. With the fully sialylated glycopeptides, detection of the three most abundant isoforms of Asn_{24} was possible with 100 ng of material, but identification of repeat units and therefore structural assignment was not.

Efforts to improve on these results and enable the use of mass spectrometry as a detection method at endogenous EPO levels were split broadly into two approaches. Firstly, there were attempts to improve the recovery of EPO from urine and to do so in a method amenable to analysis by LC-MS. Secondly, efforts were focused on improving

detection in LC-MS; specifically, on improving the signal from sialylated glycopeptides from enzymatically digested EPO, and on detecting differences in the glycosylation which could enable endogenous EPO and rEPO to be distinguished.

The first method investigated for the extraction of EPO from urine samples was the use of antibody activated magnetic beads. At the time, the only WADA approved method for the extraction of EPO was the use of repeated ultrafiltration. This required several time consuming steps, and resulted in an end product which was viscous, difficult to apply to the IEF gels used for analysis, and not suitable for analysis by LC-MS. Experience with antibody activated magnetic beads had shown that they could efficiently and rapidly bind proteins from biological samples. Their use had been demonstrated previously for the extraction of EPO from blood using polyclonal antibodies and tosyl activated beads (Skibeli, Nissen-Lie et al. 2001). The use of protein G coated beads to bind monoclonal antibodies promised a more efficient and rapid way of producing beads with more uniform and reproducible extraction results.

Initial results were disappointing. Modification of beads with anti-EPO clone AE7A5 did not result in any binding of EPO from solution, even in buffer. This, it is suspected, is because when this antibody is used to bind EPO on an IEF gel, the EPO has previously been denatured. However, modification of the beads with anti-EPO clone 9C21D11 produced beads which rapidly and effectively bound EPO from buffered solution. Analysis using mass spectrometry found a mean recovery of approximately 69% from urine which had been filtered to remove all naturally occurring EPO, then spiked at a known concentration. Analysis using IEF and immunoblotting showed that although some isoform selectivity may be seen, it would not be enough to confuse results.

Unfortunately, attempts to extract EPO from real urine samples did not succeed. Extraction of EPO by ultrafiltration following incubation with magnetic beads showed that in complete urine samples, the beads failed to bind EPO. Spiking urine samples after ultrafiltration and then extracting them showed that the inhibiting substance was likely to be a large compound, possibly a protein to which the 9C21D11 clone showed

cross-reactivity. Work could be done to try to elucidate what this protein (or proteins) is. Elution of the bound protein from the beads, followed by tryptic digest and sequencing of proteins by LC-MS/MS could provide an answer. However, this is of limited value, as since the work was started, monolithic antibody activated cartridges which bind EPO from urine have become commercially available from MAIIA Diagnostics. These are easy to use, efficient and bind EPO rapidly from solution. They were initially expensive, so that the magnetic bead approach could have been better at least in terms of cost. However, their price has now come down to a competitive one. As such, although a useful technique for the rapid extraction of proteins from biological fluids, the use of immunomagnetic beads to bind EPO from urine does not appear to be a valuable path to continue down.

One key aspect of the development of this new tool from MAIIA Diagnostics is the time it took them to come to market; the product was in development for several years. Although it is not known for sure what aspect of the development process took so long, the results presented here demonstrate the necessity and difficulty of finding the right antibody, with sufficient affinity, avidity and specificity to effectively bind EPO from a complex matrix.

Attempts were also made to produce modified silica with phenylboronic acid functionality. This functional group has been shown in the past to reversibly bind cis-diol groups, such as are found in saccharides and therefore in glycoproteins. Binding and release are pH dependent, which suggested a theoretically simple and efficient way of selectively binding glycoproteins and glycopeptides from complex solutions before releasing them for analysis.

Again, however, results were not as hoped. None of the silicas produced, by three different (published) methods, was successful at binding saccharides, glycopeptides or glycoproteins. Replication of two of these methods was problematic, and did not appear to result in a functionalised product; the third method, although analysis by FTIR and

ICP-MS suggested it resulted in silica modified with phenylboronic acid, still did not result in silica capable of binding glycan groups in solution.

It is not entirely clear why these results were obtained. Efforts to contact the authors of the original papers were not successful. Similarly, attempts to obtain some of the (self-produced) silica as was used by the authors failed, and the authors themselves have published nothing else utilising the same methods since.

It is also possible that there were problems elsewhere in the methods. To check if non-specific binding to the microfuge tubes used in the experiments was distorting the results, experiments were carried out at different pH transferring a glycoprotein digest between multiple tubes, and seeing how the peak heights of different glycopeptides were affected. However, at the concentrations involved, only one glycopeptide was significantly affected by non-specific binding, and this was excluded from the assay as a result.

Measurements of the surface area, and perhaps most importantly, pore size of the silica used before and after modification were not carried out. As stated above, analysis by ICP-MS of HF digests of the modified silica demonstrated an increase in boron concentration, which was also suggested by the FTIR data. However, the location of these boronic acid groups is not determined by these methods. Measurement of the pore size (and particle size) could potentially show if modification is primarily confined to the inside of the pores, which could be out of reach of the large glycopeptides, providing an explanation for their failure to bind. However, binding was seen with commercially available boronic acid functionalised material, which had much smaller pores than those on the unmodified silica, suggesting that steric hindrance should not be a problem.

Modification of polymeric beads resulted in another hard-to-explain phenomenon. The beads were shown to bind both mannitol and glycopeptides from solution; however, recovery from these beads by adjustment to an acidic pH was unsuccessful, and the beads seemed to bind both glycosylated and non-glycosylated peptides. This continued

to be the case even after an attempt was made to block the non-specific binding by incubation with insulin.

In short, it is not clear why the production and use of boronic acid functionalised materials was not successful. There is also the question of the usefulness of the technique, when combined with LC-MS. When MALDI is used as the ionisation method, the presence of non-glycosylated proteins or peptides significantly suppresses ionisation of glycosylated ones. This is also seen when a mixture of glycosylated and non-glycosylated compounds is infused into a mass spectrometer via ESI. However, although boronic acid functionalised silica, had it behaved as had been hoped, could have been useful as a trapping column, the separation of glycosylated and non-glycosylated compounds can also be carried out by efficient LC; HILIC stationary phases in particular are very effective at separating the two types of compound.

Enhancement of MS signal by the introduction of 'superchargers' into LC solvents was investigated. This was shown to be effective with small molecules, particularly in negative ion mode. Although superchargers have generally been shown to increase the average charge on large molecules, the results here showed that they could also increase (and decrease) the signal from small, singly charged molecules. The results obtained did not provide a full picture on what caused this effect. Signal intensity was not directly correlated with the effect of superchargers on electrospray droplet surface tension or temperature. Further work could look at isolating these factors further, as well as other potential influencing factors such as gas phase basicity, to try to elucidate the exact method of their effect. Since different superchargers appear to have different effects on different analytes, a proper understanding of the mechanism of their action may enable a better selection of additives for improved signal strength.

The use of superchargers as an LC additive for the analysis of sialylated glycopeptides was also examined. An increase in average charge was seen, and it is probable that this is responsible for an increase in the detection of oxonium ions from in-source fragmentation of glycopeptides. As a result, the addition of superchargers resulted in

improved identification of glycopeptides from a digest of fetuin. The mechanism which results in the increase in charging is also yet to be fully identified. A proposed mechanism, which involves the partial desorption of large molecules from electrospray droplets, could be involved. The validity of this mechanism could be examined relatively easily, as it should mean that glycopeptides with more hydrophobic peptide portions would be more affected by the presence of superchargers. Isocratic elutions of glycopeptides such as those from tryptically digested HRP, which vary in peptide sequence but are fairly uniform in glycosylation could provide useful information.

Finally, the cleavage, digestion and derivatisation of N-glycans to identify bisected and non-bisected structures as a way to discriminate between rEPO and huEPO was examined. Ovine IgG, which has been reported to be mostly bisected, was used as a model for huEPO, due to the shortage of analytical standards for the latter glycopeptide. Its suitability as a model has yet to be demonstrated. Since the bisecting N-acetyl glucosamine (GlcNAc) in huEPO was proposed as a result of data obtained by SDS-PAGE analysis of sequential exoglycosidase digestions of huEPO, it would be logical to repeat this work with ovine IgG, to demonstrate that it follows the same pattern of digestion.

LC-MS analysis of exoglycosidase digests of cleaved N-glycans from ovine IgG and rEPO suggested that the presence or absence of a bisecting GlcNAc results in a detectable difference. After a short digest period, both digests were found to contain glycans containing a fucosylated pentasaccharide core structure, with a single GlcNAc residue attached. However, these structures were resolved by LC, suggesting they are positional isomers of each other. It is suggested that the glycan predominantly found in the IgG digest is that with a bisecting residue. If this is so, and the same is found in huEPO, it could provide a way of distinguishing the presence of rEPO in urine.

After a longer digest, the levels of this glycan in rEPO digests became nearly undetectable; however, in the IgG digest they remained high, due to the much lower activity of the N-acetylglucosaminidase enzyme used in cleaving bisecting residues. In

the rEPO digest, nearly all the glycans found had been digested back to the fucosylated pentasaccharide core. As such, an alternative method for distinguishing rEPO and huEPO could rely on the ratio of the fucosylated pentasaccharide core to the same glycan with an extra GlcNAc residue.

CE-LIF analysis of the same digests (though derivatised by a different process), however, gave slightly different results. They seemed to suggest that a detectable difference, that of the presence or absence of the bisecting GlcNAc, was detectable after the longer digest process, but not after the short one. However, these results still need to be repeated to check their accuracy and rule out any derivatisation specific effects. Even so, although the results from the CE-LIF analysis do not fully tally with those from LC-MS, they do suggest that a detectable difference can be found, but that optimisation of the digest process may be key.

The use of a still shorter digest process found that the presence of a bisecting GlcNAc may also enable those glycans with the residue to be distinguished from those without. After a 24 hour incubation with exoglycosidases, a fucosylated pentasaccharide core glycan with 3 GlcNAc residues attached was detected in digests of IgG, rEPO and huEPO standard. The retention time of this glycan in the IgG and huEPO digests matched that of the bisected glycan standard, NGA2FB. The retention time of the glycan found in the rEPO digest, however, was different. This provides further backing for the proposal that huEPO contains a bisecting GlcNAc residue, although it is possible that the glycan is found on another glycoprotein also present in the standard.

There is still a significant amount of work to do to fully develop this method. Optimisation of the enzyme digest to reduce reaction time is necessary to make the method a viable alternative to the current testing process. This is also necessary to optimise the extent of digestion, enabling the difference between the glycans of rEPO and huEPO to be most easily distinguished. It would be useful to carry out analysis of a huEPO digest at different time points, including at time zero, to understand how the glycan profiles change through the digestion.

It is not yet known what the limit of sensitivity is of the analysis by CE-LIF. This needs to be checked, and it would also be useful to analyse samples labelled with rhodamine 110, not only to check if the data tallies with that obtained by LC-MS, but also to see what the limits of detection found with that approach are.

As stated in Chapter 5, the development of a nanoflow LC method, coupled to a sensitive mass spectrometer, is needed to provide the sensitivity required to work at the concentrations and amounts found in anti-doping samples. If this is achieved, it will also be necessary to check that there are no other compounds present in urine which would interfere with the results. This would have to be carried out with a large range of normal blank urines, ideally from athletes from different disciplines and different ethnic backgrounds. It would also have to be carried out with so-called 'effort' and 'active' urines, both of which have proved problematic under the current testing process. The experiments presented here would also need to be repeated with other rEPOs, including biosimilars, and ideally with NESP and CERA as well to demonstrate that the glycans of these drugs can also be distinguished from those of endogenous EPO.

However, despite the volume of work still to be done, at present the results obtained suggest that the method may provide an alternative way of detecting the use of rEPO as a performance enhancing drug at the levels found in anti-doping urine samples.

References

Groleau, P. E., P. Desharnais, et al. (2008). "Low LC-MS/MS detection of glycopeptides released from pmol levels of recombinant erythropoietin using nanoflow HPLC-chip electrospray ionization." J Mass Spectrom **43**(7): 924-35.

Skibeli, V., G. Nissen-Lie, et al. (2001). "Sugar profiling proves that human serum erythropoietin differs from recombinant human erythropoietin." Blood **98**(13): 3626-3634